## MODIFICATION OF BACKSCATTERING OF A LOOP BY IMPEDANCE LOADING

Thesis for the Degree of Ph. D. MICHIGAN STATE UNIVERSITY JUANG-LU LIN 1967



### This is to certify that the

#### thesis entitled

Modification of Backscattering of a Loop by Impedance Loading

## presented by

Juang-Lu Lin

has been accepted towards fulfillment of the requirements for

Ph. D. degree in E. E.

Major protessor

Date May 5, 1967

**Q**-169

#### ABSTRACT

## MODIFICATION OF BACKSCATTERING OF A LOOP BY IMPEDANCE LOADING

## by Juang-Lu Lin

In this thesis the modification of the backscattering of a loop by the impedance loading method is investigated theoretically and experimentally.

First of all, the resonant phenomena of a loop when illuminated by an electromagnetic wave is studied. Next, the backscattering of a circular conducting loop is considered and the impedance loading method is applied to minimize its backscatter. Finally, the minimization of the backscattering of a rectangular loop is investigated.

In the theoretical analysis, a new me thod based on a differential equation for the loop current is developed for the case of a circular loop. For the case of a rectangular loop an existing method is applied with slight modification. Throughout the entire analysis, the principle of superposition is applied to simplify the problem of an illuminated loaded loop to the combination of an illuminated solid loop and a radiating loop. The major objectives of the theoretical analysis are to determine the induced current on a loaded loop, the scattered field from a loaded loop and the optimum impedance which, when loaded on the loop, makes the backscatter of the loop vanish.

Extensive experimental study was also conducted. The resonant phenomena of a solid loop was investigated carefully. The impedance loading technique was then applied to the circular and the rectangular

loops to minimize their backscatters. In the course of this experiment, the backscatter of a loop was successfully minimized to the noise level.

The major finding of this study is to show theoretically that the backscatter of a conducting loop can be eliminated by a properly chosen impedance loading, and to verify experimentally that indeed the backscatter of a loop can be minimized by a practical arrangement of the impedance loading technique. This investigation should prove significant in the understanding of the scattering phenomena of a conducting loop and in the practice of radar camouflage.

# MODIFICATION OF BACKSCATTERING OF A LOOP BY IMPEDANCE LOADING

Ву

Juang-Lu Lin

## A THESIS

Submitted to
Michigan State University
in partial fulfillment of the requirements
for the degree of

DOCTOR OF PHILOSOPHY

Department of Electrical Engineering

### ACKNOWLEDGMENT

The author is grateful to his major professor Dr. K. M. Chen for his guidance and encouragement in the course of this research. He also wishes to thank the members of his guidance committee, Dr. J. A. Strelzoff, Dr. L. W. Von Tersch, Dr. Y. Tokad and Dr. N. Hills, for reading the thesis and valuable suggestions. The help extended by J. W. Hoffman of the Division of Engineering Research is also appreciated. The research reported in this thesis was supported by the Air Force Cambridge Research Laboratories under contract AF19(628)-5732.

## TABLE OF CONTENTS

			Page
Acknowle	doment		ii
			vi
List of Fi	igures		VI
Introducti	ion		1
Chapter I	. Backs	cattering of a Solid Loop	3
1.1.	Definitio	on of Backscattering Cross Section	3
1.2.	Experim	nent	4
	1.2.1.	Description of the experimental	•
	1.2.2.	arrangement and the measuring technique Measurement of the backscattering cross	4
	1 3 4	section of a circular loop	6
	1.2.3.	Measurement of the backscattering cross section of square loops	7
	1.2.4.	Measurement of the resonance of loops	11
1.3.	Theory		16
	1.3.1.	Backscattering from a solid circular loop	18
	(A)	Geometry of problem	18
	(B) (C)	Differential equation for loop current Solution for loop current	20 23
	(D)	Backscattering cross section	24
	(E)	Determination of $\Phi_{\alpha}^{S}$ and $\Phi_{i}^{S}$	27
	(F')	Numerical results	30
	1.3.2.	Scattering from a solid rectangular loop	34
	(A)	Formulation of problem	34
	(B) (C)	Integral equations for loop currents  Zeroth order solutions for loop currents	34 43
	(D)	First order solutions for loop currents	47
	(E)	Evaluation of particular integrals $\mathcal{O}_{4}^{(s)}(y)$	
		and $\theta_1^{\infty}(r)$	59
	(F`)	Backscatt wing cross section of a solid	,
	<b>(</b> G)	rectangular loop Expansion paremeter $\Phi_{_{f S}}$	68 74
	(日)		75
	//	Evaluation of $\mathbf{J}_1$ and $\mathbf{J}_2$	1 3

## TABLE OF CONTENTS (continued)

			Page
Chapter	II. Minin Loop	nization of Backscattering of a Circular	7.8
2.1.	Introduc	etion	78
2. 2.	Theo ry		79
	2. 2. 1. 2. 2. 2.	Scattering from a solid circular loop Radiation from a circular loop	81 81
	(A) (B)	Differential equation for loop current Solution for loop current	83 86
	2. 2. 3. 2. 2. <b>4</b> .	Total current and total back scattered field Optimum impedance for zero back	88
	2 2 5	scattering	89
	2. 2. 5.	Determination of $\Phi_{\mathbf{q}}^{\mathbf{r}}$ and $\Phi_{\mathbf{i}}^{\mathbf{r}}$	90
	2.2.6.	Numerical examples	93
2.3.	Experin	nent	97
	2.3.1.	Experimental setup and measuring	
		technique	97
	2. 3. 2.	Experimental results	99
2.4.	Compar	ison Between Theory and Experiment	100
Chapter	III. Minii	mization of Backscattering of a Loaded	
	Rectang	ular Loop	118
3.1.	Introduc	etion	118
3. 2.	Theory		118
	3.2.1.	Scattering from a solid rectangular loop	119
	3. 2. 2.	Radiation from a rectangular loop	133
	(A)	Geometry of Problem	123
	(B)	Integral equations for loop currents	123
	(C)	Zeroth order solutions for loop currents	1 31
	(D) (E)	First order solutions for loop currents Evaluation of particular integrals $\theta f(y)$	136
	• •	and $\theta_1^x(\mathbf{x})$	1-1-1
	(F)	Expansion parameter, $\Phi_r$	157
3. 3.	Total Lo	oon Currents	1.58

## TABLE OF CONTENTS (concluded)

				Page
3.4	<del>1</del> .	Total B	ackscattered Field	162
		3.4.1.	Total backscattered field based on first order currents	162
		3.4.2.	Total backscattered field based on sub-first order currents	165
		3.4.3.	Evaluation of $K_1$ and $K_2$	167
3.	5.	Optimu	m Impedance for Zero Backscattering	169
		3. 5. 1.	zero backscattering	169
		3. 5. 2.	Sub-first order optimum impedance for zero backscattering	170
3.6	<b>6.</b>	Numeri	cal Examples	170
3. 7	7.	Experin	nent	172
		3.7.1.	1	1.7.2
		3.7.2.	measuring technique Experimental results	172 172
Refer	ence	e <b>s</b>		187

## LIST OF FIGURES

Figure		Page
1.1.	Experimental Setup and Circuit Diagram	. 5
1.2.	A Circular Loop if Illuminated by a Plane Wave at either Normal or Horizontal Incidence	8
1.3.	Backscattering Cross Section of Circular Loops Illuminated by a Plane Wave at Normal Incidence	9
1.4.	Backscattering Cross Section of Circular Loops Illuminated by a Plane Wave at Horizontal Incidence	10
1.5.	Backscattering Cross Section of Square Loops Illuminated by a Plane Wave at Normal Incidence	12
1.6.	Backscattering Cross Section of Square Loops Illuminated by a Plane Wave at Horizontal Incidence	13
1.7.	Scattering Cross Sections of Loops as Functions of Loop Sizes (First Resonance Curves)	15
1.8.	Scattering Cross Sections of Loops as Functions of Loop Sizes (Second Resonance Curves)	17
1.9.	Geometry of Solid Circular Loop	19
1.10.	Geometry for the Calculation of Radiation Field of a Solid Circular Loop	26
1.11.	$\Phi_{q}^{s}$ as a Function of $\beta_{0}b$ $(\frac{a^{2}}{b^{2}} = 0.00179)$	31
1.12.	$\Phi_i^s$ as a Function of $\beta_0 b$ ( $\frac{a^2}{b^2}$ = 0.00179)	32
1.13.	Comparison Between Theory and Experiment for Circular Loops Illuminated by Plane Wave at Normal Incidence	33
1.14.	Geometry for Solid Rectangular Loop	35
1.15.	Geometry for the Calculation of Radiation Field of a Solid Rectangular Loop	69

## LIST OF FIGURES (continued)

Figure		Page
1.16.	Comparison Between Theory and Experiment for a Square Loop Illuminated by a Plane Wave at Normal Incidence	72
2.1.1.	A Loaded Loop is the Sum of a Scattering Loop and a Radiating Loop	. 80
2.1.2.	Geometry of a Radiating Loop	82
2. 2.	$\Phi_q^r$ as a Function of $\beta_0 b$ $(\frac{a^2}{b^2} = 0.00179)$	94
2. 3.	$\Phi_i^r$ as a Function of $\beta_0 b$ ( $\frac{a^2}{b^2}$ = 0.00179)	95
2.4.	Optimum Impedance for Zero Backscattering $\left(\frac{a^2}{b^2} = 0.00179\right)$	96
2.5.	Experimental Setup and Circuit Diagram	98
2.6.	Backscattering Cross Section of a Loaded Loop as a Function of Loading Impedance (f = 1.61 GC)	102
2.7.	Backscattering Cross Section of a Loaded Loop as a Function of Loading Impedance (f = 1.71 GC)	103
2.8.	Backscattering Cross Section of a Loaded Loop as a Function of Loading Impedance (f = 1.75 GC)	104
2.9.	Backscattering Cross Section of a Loaded Loop as a Function of Loading Impedance (f = 1.80 GC)	105
2.10.	Backscattering Cross Section of a Loaded Loop as a Function of Loading Impedance (f = 1.85 GC)	106

## LIST OF FIGURES (continued)

Figure		Page
2.11.	Backscattering Cross Section of a Loaded Loop as a Function of Loading Impedance (f = 1.90 GC)	107
2.12.	Backscattering Cross Section of a Loaded Loop as a Function of Loading Impedance (f = 1.95 GC)	108
2.13.	Backscattering Cross Section of a Loaded Loop as a Function of Loading Impedance (f = 2.00 GC)	109
2.14.	Backscattering Cross Section of a Loaded Loop as a Function of Loading Impedance (f = 2.05 GC)	110
2.15.	Backscattering Cross Section of a Loaded Loop as a Function of Loading Impedance (f = 2.10 GC)	111
2.16.	Backscattering Cross Section of a Loaded Loop as a Function of Loading Impedance (f = 2.15 GC)	112
2.17.	Backscattering Cross Section of a Loaded Loop as a Function of Loading Impedance (f = 2.20 GC)	113
2.18.	Backscattering Cross Section of a Loaded Loop as a Function of Loading Impedance (f = 2.30 GC)	114
2.19.	Backscattering Cross Section of a Loaded Loop as a Function of Loading Impedance (f = 2.40 GC)	115
2. 20.	Backscattering Cross Section of a Loaded Loop as a Function of Loading Impedance (f = 2.50 GC)	116
2. 21.	Optimum Impedance for Minimum Backscattering from a Circular Loop Illuminated by a Plane Wave at Normal Incidence	117

## LIST OF FIGURES (continued)

Figure		Page
3. 1.	A Loaded Loop is the Sum of a Scattering Loop and a Radiating Loop	120
3. 2.	Geometry of a Radiating Loop	122
3. 3.	Geometry for the Calculation of the Radiation Field of a Radiating Rectangular Loop	163
3.4.	$\Phi_{r}$ as a Function of $\beta_{o}h$ ( $\frac{a}{h} = 0.0388$ )	171
3.5.	Optimum Impedance for Zero Backscattering $(\frac{a}{h} = 0.0388)$	173
3.6.	Backscattering Cross Section of a Loaded Square Loop as a Function of Loading Impedance (f = 1.61 GC)	175
3.7.	Backscattering Cross Section of a Loaded Square Loop as a Function of Loading Impedance (f = 1.7 GC)	176
3.8.	Backscattering Cross Section of a Loaded Square Loop as a Function of Loading Impedance (f = 1.8 GC)	177
3. 9.	Backscattering Cross Section of a Loaded Square Loop as a Function of Loading Impedance (f = 1.9 GC)	178
3. 10.	Backscattering Cross Section of a Loaded Square Loop as a Function of Loading Impedance (f = 2 GC)	179
3.11.	Backscattering Cross Section of a Loaded Square Loop as a Function of Loading Impedance (f = 2.1 GC)	180
3.12.	Backscattering Cross Section of a Loaded Square Loop as a Function of Loading Impedance (f = 2.2 GC)	181
3. 13.	Backscattering Cross Section of a Loaded Square Loop as a Function of Loading Impedance (f = 2.3 GC)	182

## LIST OF FIGURES (concluded)

Figure		Page
3.14.	Backscattering Cross Section of a Loaded Square Loop as a Function of Loading Impedance (f = 2.4 GC)	183
3. 15.	Backscattering Cross Section of a Loaded Square Loop as a Function of Loading Impedance (f = 2.5 GC)	184
3.16.	Backscattering Cross Section of a Loaded Square Loop as a Function of Loading Impedance (f = 2.55 GC)	185
3.17.	Optimum Reactive Impedance for Minimum Backscattering from a Square Loop	186

#### INTRODUCTION

In recent years much research has been conducted on reducing the radar cross sections of metallic objects. The conventional techniques include the use of radar absorbing material and the method of reshaping the body. Recently the impedance loading method has been found to be especially effective in reducing the radar cross sections of metallic objects with dimensions of the order of a wavelength. In this thesis, the minimization of the backscattering of a conducting loop, both circular and rectangular, by an impedance loading method is investigated.

Historically, Kouyoumjian and Weston are the first ones who investigated the backscattering cross sections of a thin solid circular loop with a result of fairly good agreement with the experiment. The methods employed by them are quite complicated and involved tedious computation. For our purpose, a mathematically simpler method has been developed. Our theoretical results also agree with experimental results quite satisfactorily. For the case of the solid rectangular loop, the method used by Chen and King was adopted in obtaining first-order solution for current distribution. Experimental results and those of theory appear to be in good agreement.

In solving the problem, the principle of superposition is employed. Based on the superposition principle, an illuminated loaded loop can be considered as the combination of an illuminated solid loop and a radiating loop. In this study, the two cases are solved separately and then combined together to yield the final solution for an illuminated loop.

For the minimization of the backscattering of a circular loop, a consideration is given to the perfectly conducting loop which is loaded symmetrically with two identical lumped impedances and is assumed to be illuminated by a plane wave at normal incidence. The induced current on the loaded loop is determined as a function of loop dimensions and loading impedance. The backscattered field produced by the loaded circular loop is calculated as a function of the loading impedance among other parameters. It is then possible to find an optimum impedance which makes the back scattered field equal to zero. An explicit expression for the optimum impedance for zero backscattering is obtained as a function of loop dimensions. Some numerical examples are included. The theory is later verified by an experiment.

A theory on the minimization of the backscatter of a conducting rectangular loop by the impedance loading method is developed in the last chapter. A rectangular loop loaded symmetrically with two identical lumped impedances at the centers of the long sides of the loop is assumed to be illuminated by a plane wave at normal incidence. The zeroth order and the first-order solutions of the induced current are evaluated as functions of the loop dimensions and the loading impedance. Based on the induced current, the backscattered field can be calculated. An optimum impedance which leads to zero backscattering from the rectangular loop is then found as a function of loop dimensions. Some numerical examples are included. An experiment was performed for the case of a square loop loaded with two identical reactive impedances and illuminated by a plane wave with vertical polarization at normal incidence. The experimental results indicate that it is possible to reduce the backscatter of a conducting, square loop to the noise level if the loading impedance is properly chosen.

#### CHAPTER I

#### BACKSCATTERING OF A SOLID LOOP

### 1.1. Definition of Backscattering Cross Section

An electromagnetic wave incident upon a metallic object will induce time-varying distributions of oscillating charges and currents in the object. The induced charges and currents will, in turn, maintain an electromagnetic field which is known as the scattered field. To characterize the reradiating properties of an object, total scattering cross section  $\sigma$  is defined as

$$\sigma = \frac{P^s}{s^i}$$

Where P<sup>S</sup> is the total scattered power and S<sup>i</sup> is the scalar magnitude of the real part of the incident complex Poynting vector at the location of the object. In radar, transmitter and receiver are installed at the same location so that only the power scattered by the object in the direction of the transmitter-receiver is observed. In this sense, backscattering cross section of an object is defined as a measure to characterize the quantity of the power scattered back toward the source by the object. In symbol, the backscattering cross section of an object is defined as

$$\sigma_{B} = \lim_{R \to \infty} 4\pi R^{2} \frac{\left|E^{s}\right|^{2}}{\left|E^{i}\right|^{2}}$$

where E<sup>s</sup> is the magnitude of the backscattered field and E<sup>i</sup> is that of the incident electric field.

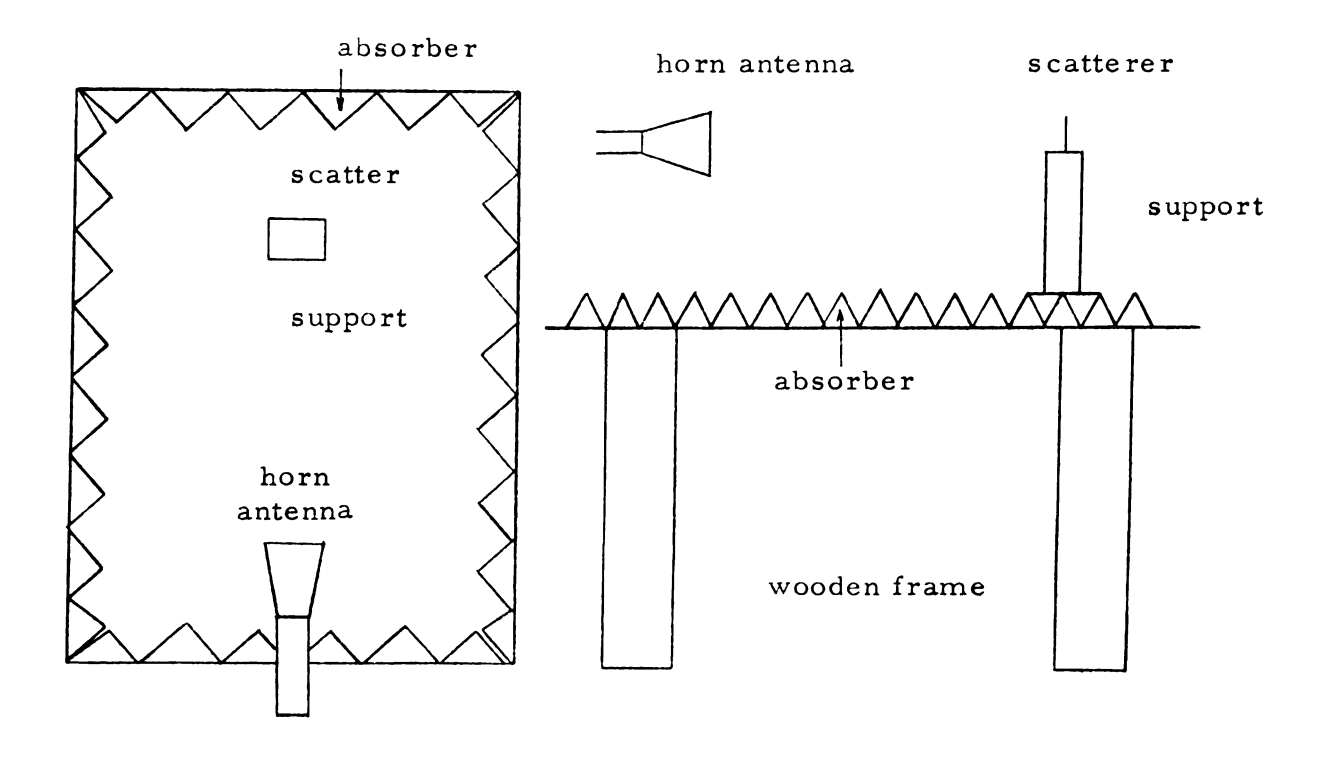
## 1.2. Experiment

A number of methods are available for measuring the backscattering cross section of an object. In this research the cancellation
method was used. The prinicple of this method is to cancel the signal
received by the receiving antenna when the scatterer is absent. After
this the scatterer is put in place. The signal received by the receiving
antenna with the scatterer present will then represent the scattered
field by the scatterer.

In this section experimental arrangement and the measuring technique of the backscattering cross section of rectangular and circular loops are discussed. The loops are illuminated by a plane wave for the cases of normal and horizontal incidence. Resonant phenomena of loops are also investigated.

## 1.2.1. Description of the Experimental Arrangement and the Measuring Technique

The experimental setup is shown in Figure 1.1. The experiment was conducted inside of an anechoic chamber (0.8 m x 1.4 m x 0.7 m in size) which is firmly mounted on a wooden frame. A horn antenna (HP X890A) is projected into the anechoic chamber through one of the narrow sides of the chamber. A cellular plastic column made of styrofoam is used as scatterer support. The support is placed in the far zone of the horn antenna and its height is so chosen that the scatterer on the support is on the axis of the antenna. The circuit diagram of the experiment is also shown in Figure 1.1. The klystron generator (F X R type X760A) modulated by a 1 KC square wave generator (HP 715A) is used as the R.F. source. The isolator (Polytechnic Res. and Dev. Co. type 1203) is used to protect the possible



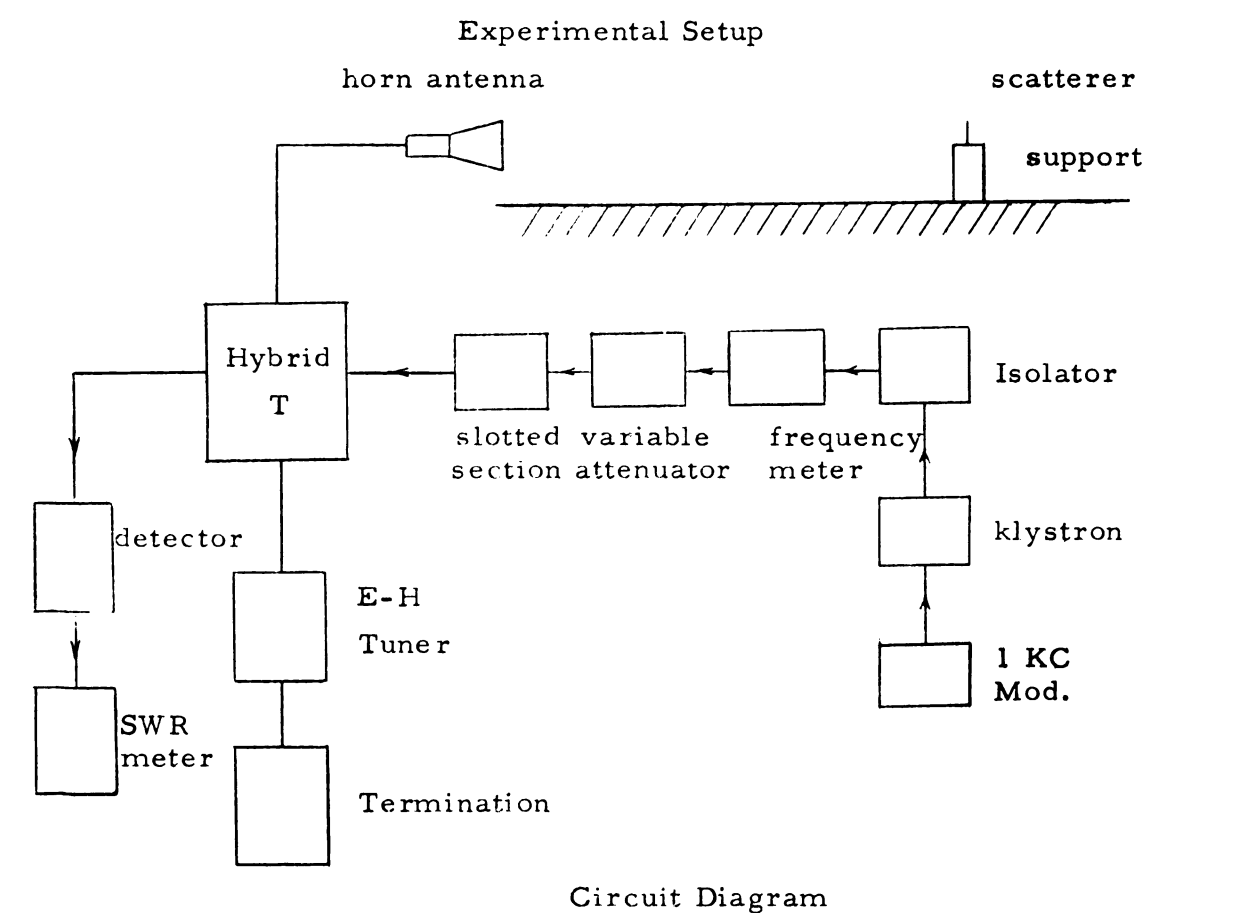


Figure 1.1. Experimental setup and circuit diagram.

backward energy from damaging the R.F. generator. Frequency is measured by a frequency meter (HP X532A). A variable attenuator (HP X375A) and slotted section (HP X810B) are used to control and probe the wave from the source. A hybrid T (HP X845A) is used to separate the incident wave to the antenna and the reflected wave back from the antenna. Two other terminals of the Hybrid T are connected to a matched load through an E-H tuner (HP X880A) and to a detector. The output of the detector is then measured by a SWR meter (HP 415B). The horn antenna in this experiment serves both as the radiating element and the receiving probe. In the experiment, a series of measurements have been made with various sizes of loops.

By the arrangement mentioned above, a plane wave with vertical polarization can be made to illuminate the loop either normally or horizontally. When the scatterer is absent, the reading of the SWR meter can be set to zero by adjusting the E-H tuner. After this balancing process is completed, the scatterer is introduced. The reading of the SWR meter will then indicated the back scattered field by the scatterer.

## 1.2.2. Measurement of the Backscattering Cross Section of Circular Loops

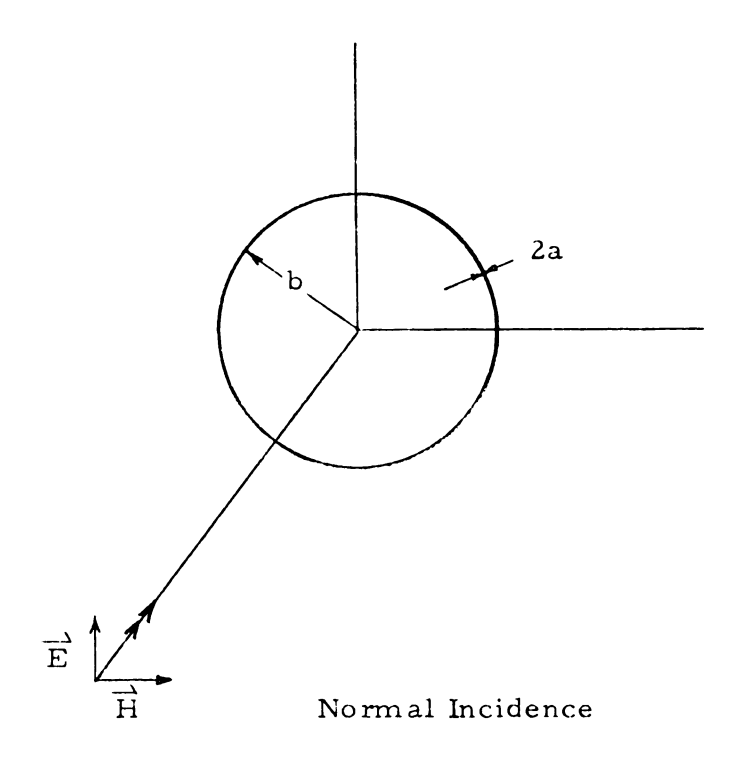
To measure the backscattering cross section of metallic circular loops, a total of 35 circular loops with radius ranging from 0.3 cm to 3.5 cm were constructed as experimental models. The diameter of the wire is 0.1 cm. The frequency of 9.61 GC was used. The loops are mounted upright on the support which is located 26 cm ( $\approx 8\lambda$ ) away from the horn antenna. The loops are, therefore, considered to be in the far zone of the radiating element. Theoretically,

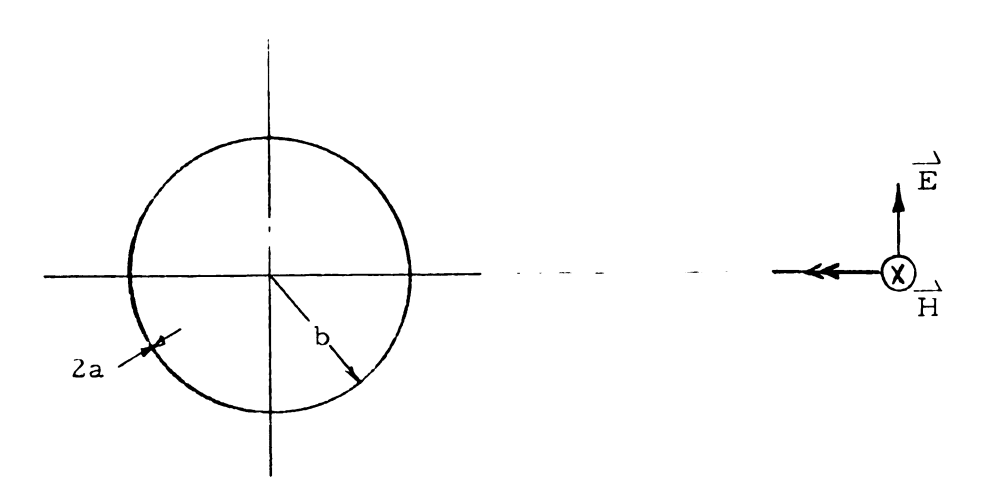
the distance between the antenna and the scatterer should be made as great as possible. However, to obtain a detectable scattered field from the scatterer one has to compromise for a finite distance. The radiated wave from the horn antenna at the location of the scatterer is then approximately a plane wave with a vertical E field.

In the experiment the plane of the loop is first oriented parallel to the horn aperture so that the loop is illuminated by a plane wave with vertical polarization at normal incidence. For the case of horizontal incidence, the loop is turned 90° from the vertical incidence position making its plane perpendicular to the horn aperture. The geometries of these two cases are shown in Figure 1.2. In Figure 1.3 and 1.4, relative backscattering cross section of the circular loops  $\sigma$  are plotted as functions of loop dimension  $\beta_0$ b where  $\beta_0$  is the wave number and b is the radius of the loop. Figure 1.3 shows the backscattering cross section of the circular loop illuminated by a plane wave at normal incidence and Figure 1.4 shows that of horizontal incidence case. It is observed from these two figures that the first resonances for both cases occur when the half of the loop periphery is near  $\frac{1}{2}$  wavelength (i.e., when  $\beta_0 b = 1$ ). The first resonant peak in the case of normal incidence appears to be higher than that of the horizontal incidence case.

## 1.2.3. Measurement of the Backscattering Cross Section of Square Loops

The same technique used for the circular loops was adopted to measure the backscattering cross sections of the square loops. A number of square loops ranging from 0.5 cm x 0.5 cm to 3.5 cm x 3.5 cm in size were constructed as experimental models. The diameter of the metallic wire is 0.06 cm. The experiment was





Horizontal Incidence

Figure 1.2. A circular loop is illuminated by a plane wave at either normal or horizontal incidence.

: :

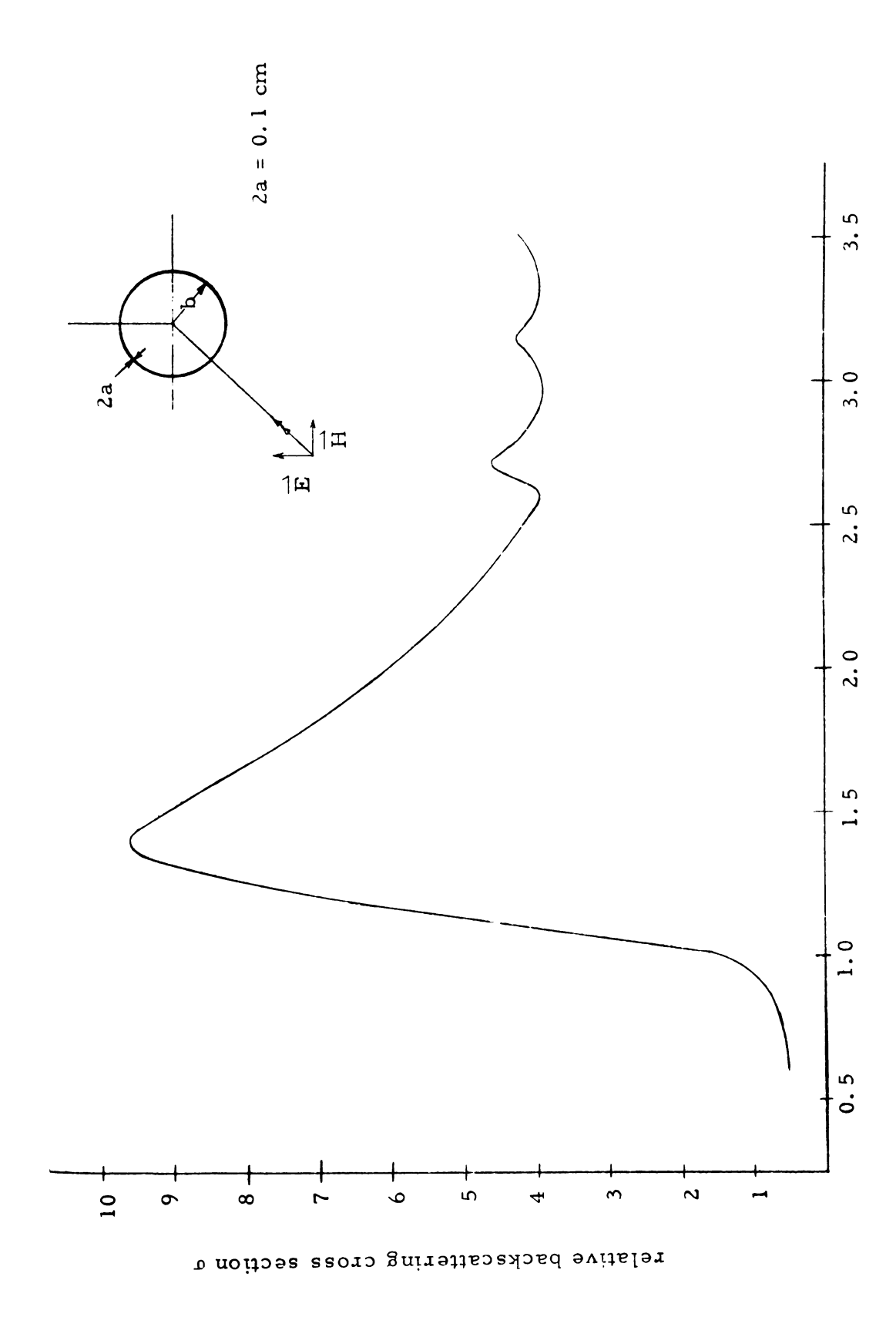
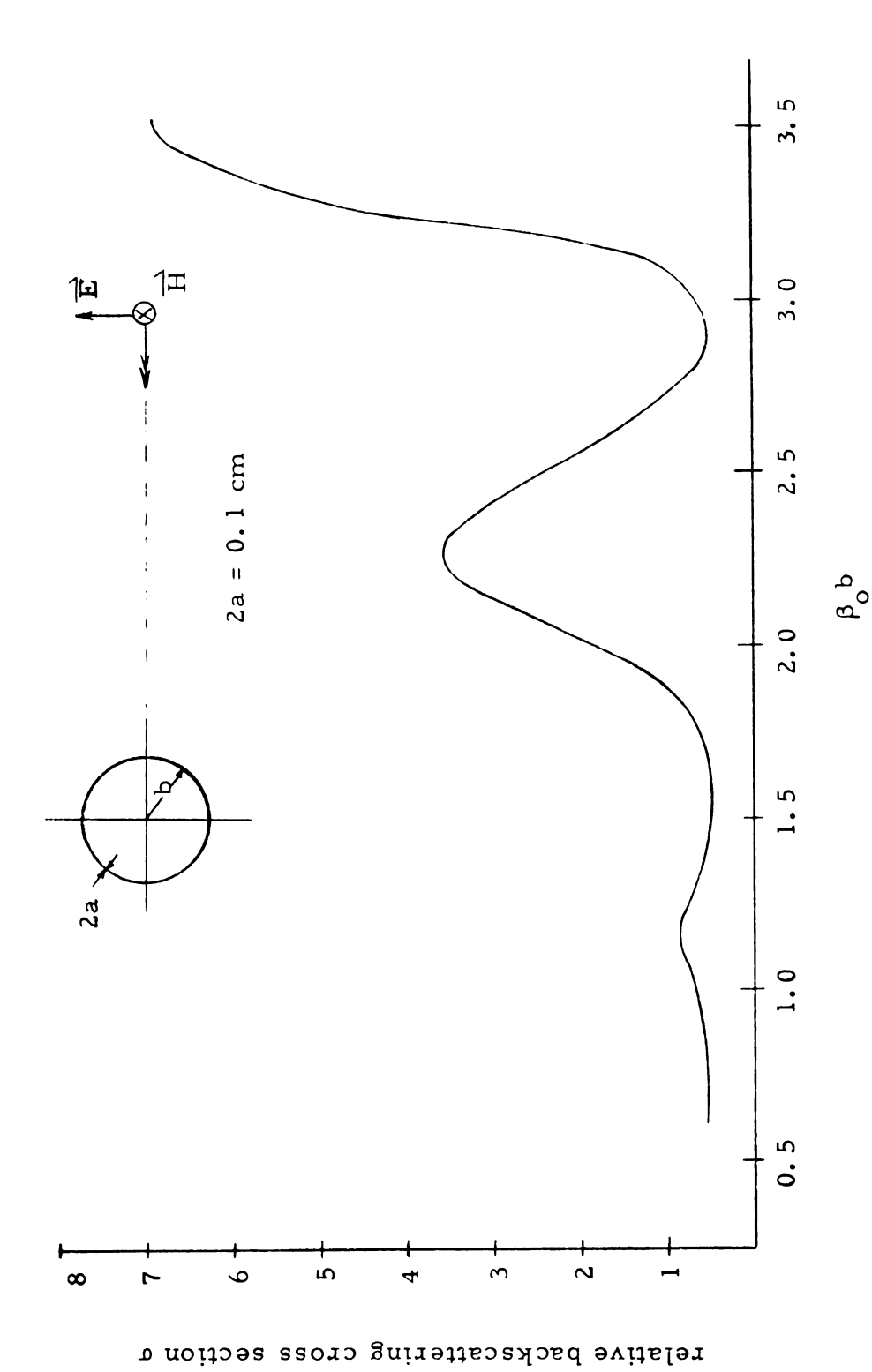


Figure 1.3. Backscattering cross section of circular loops illuminated by a plane wave at normal incidence.

 $\beta_{o}^{b}$ 



Backscattering cross section of circular loops illuminated by a plane wave at horizontal incidence. Figure 1.4.

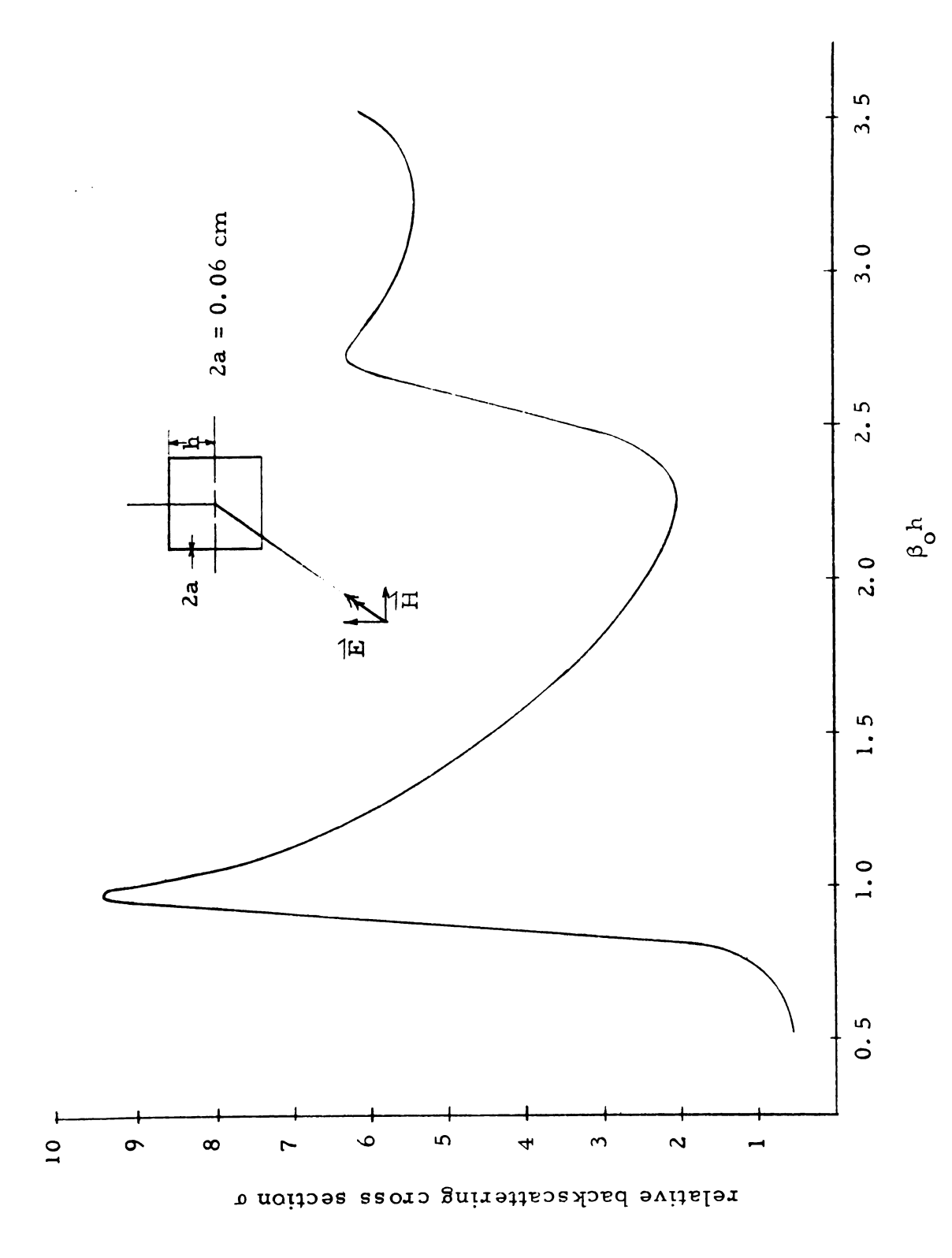
conducted with the same setup described in previous sections and at the same frequency.

The backscattering cross sections of square loops are plotted as functions of loop dimensions  $\beta_0$ h (where 2h = one side of the square loop) in Figures 1.5 and 1.6. Figure 1.5 shows the backscattering cross section of square loops illuminated by the plane wave at normal incidence, and Figure 1.6 shows the backscattering cross section for the case of horizontal incidence.

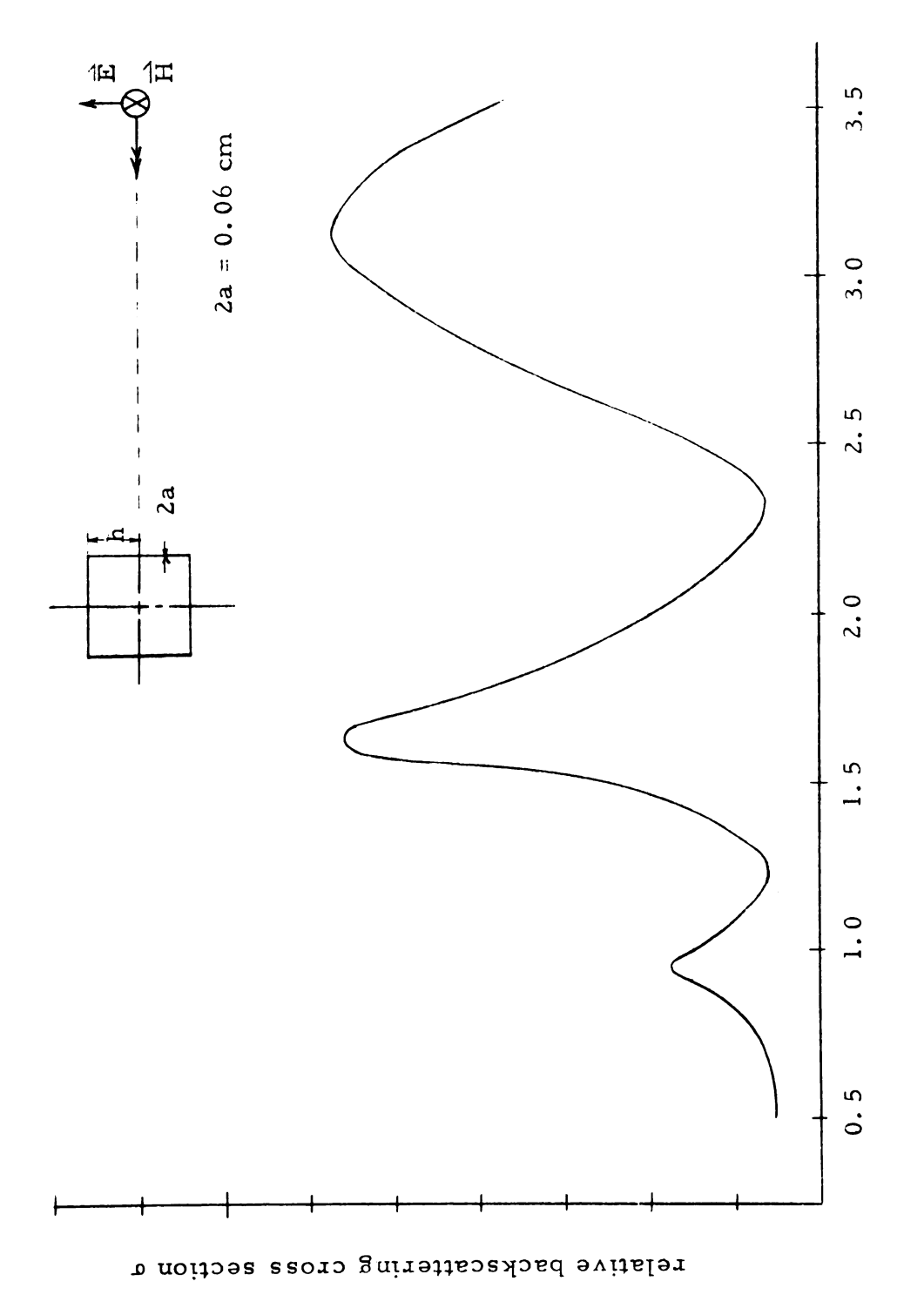
Once again it is observed that the first resonances of both normal and horizontal cases occur when half of the loop periphery is near  $\frac{1}{2}$  wavelength (i.e., when  $\beta_0 h = 0.8$ ).

## 1.2.4. Measurement of the Resonances of Loops

The backscattering cross sections of a circular and a square loop described in the last two sections have a common nature that the first resonance tends to occur when the half of the loop periphery is near  $\frac{1}{2}$  wavelength and the second resonance at  $\frac{3}{2}$  wavelength and so on. At these resonant conditions the induced currents on the loops are maximum and likewise the scattered fields. However, it is anticipated that the loops with the same periphery but different geometrical shapes may have different resonant sizes. To testify these conjectures five kinds of rectangular loops were constructed. The five kinds of rectangular loops have the ratio of  $h_1/h_2$  equal to 1, 1.5, 2.0, 2.5, and 3.0 where  $h_1$  and  $h_2$  are the short and the long side of the loop. The loops are illuminated by a plane wave with vertical polarization at normal incidence. The experiment was conducted inside of an anechoic chamber at the frequency of 9.61 GC with the same experimental setup mentioned previously.



Backscattering cross section of square loops illuminated by a plane wave at normal incidence. Figure 1.5.



Backscattering cross section of square loops illuminated by a plane wave at horizontal incidence. Figure 1.6.

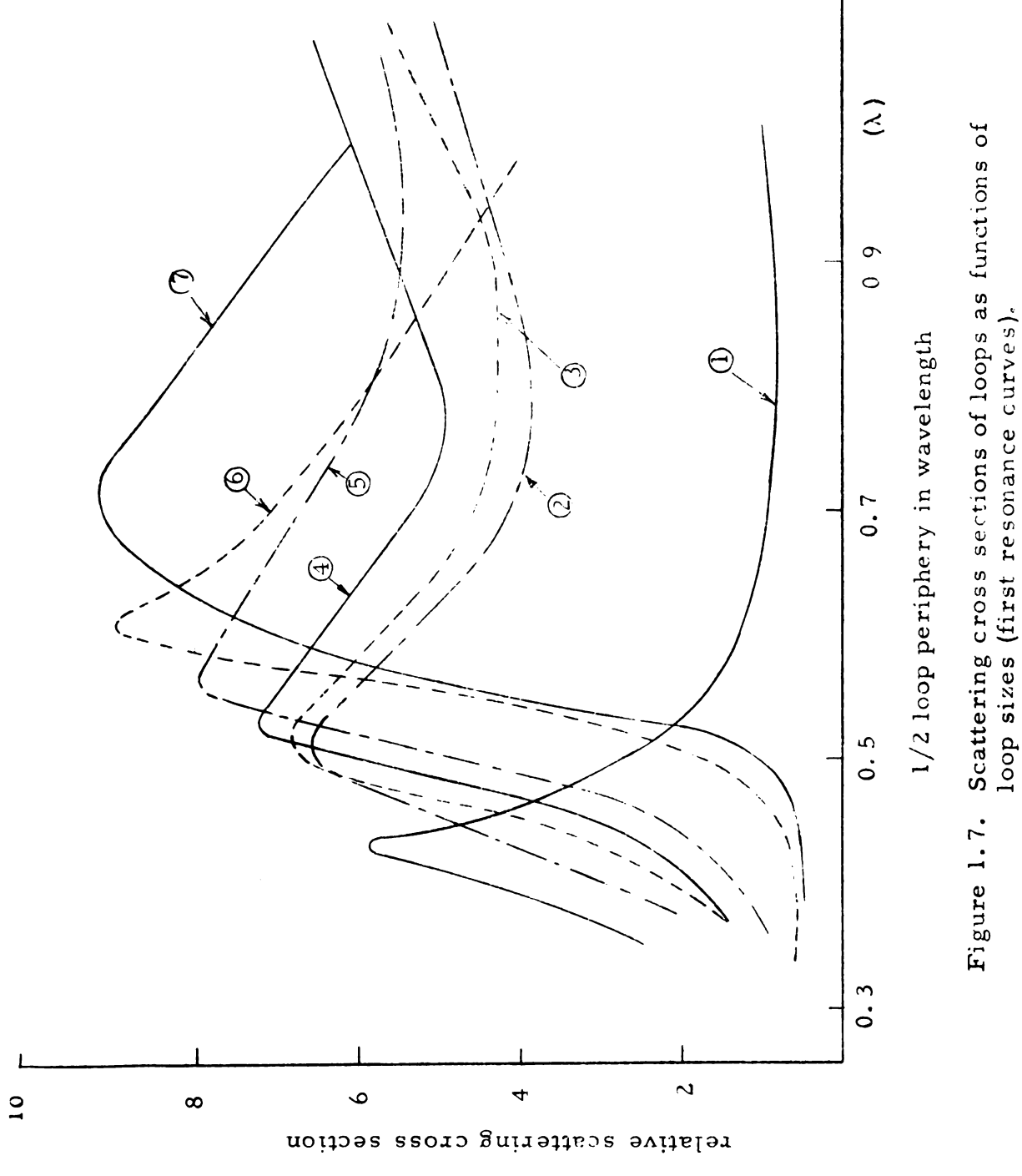
The experimental results are shown in Figures 1.7 and 1.8. Figure 1.7 shows the first resonance curves of the loops. The resonant curve of a straight wire which corresponds to a loop with  $h_1/h_2 = 0$  is also included in the figure. The scattering cross sections of the loops are plotted as functions of the loop sizes. From the peak of the curve the resonant size of the loop is determined.

It is observed that the first resonances of the loops with various shapes indeed occur when the half peripheries of loops are near  $\frac{1}{2}$  wavelength. It is also seen that the first resonant size of a loop is dependent of its geometrical shape. These phenomena are summarized in Table 1.1. It is true that the first resonant size of a loop tends to increase as the loop becomes broader or the ratio of  $h_1/h_2$  becomes larger.

Table 1.1.

	first resonant
Loop Geometry	size* $(\frac{1}{2} \text{ periphery})$
straight wire $(h_1/h_2 = 0)$	0.433λ
rectangular loop $(h_1/h_2 = \frac{1}{3})$	0.513λ
rectangular loop $(h_1/h_2 = \frac{1}{1.25})$	0.516λ
rectangular loop $(h_1/h_2 = \frac{1}{2})$	0.53 λ
rectangular loop $(h_1/h_2 = \frac{1}{1.5})$	0.561λ
rectangular loop $(h_1/h_2 = \frac{1}{1})$	0.61 λ
circular loop	0.705λ

<sup>\*</sup> For the wire  $\frac{1}{2}$  periphery corresponds to the total length For rectangular loop  $\frac{1}{2}$  periphery =  $2(h_1 + h_2)$  For circular loop  $\frac{1}{2}$  periphery =  $\pi b$  where b = radius Radius of wire of which the loops are made of = a = 0.01 $\lambda$ 



I straight wire  $(h_1/h_2 = 0)$  5 rectangular loop  $(h_1/h_2 = 1/1.5)$  5 rectangular loop  $(h_1/h_2 = 1/3)$  6 rectangular loop  $(h_1/h_2 = 1/3)$  7 circular loop  $(h_1/h_2 = 1/3)$  3 rectangular loop  $(h_1/h_2 = 1/2.5)$  7 circular loop  $(h_1/h_2 = 1/3)$  4. rectangular loop  $(h_1/h_2 = 1/3)$  7 circular loop  $(h_1/h_2 = 1/3)$  8.

The second resonance curves of the loops are shown in Figure 1.8. It is observed that the second resonance peaks are not clearly observable in the loops with large ratio of  $h_1/h_2$ . The second resonances of the loops occur when the half peripheries of loops are in the neighborhood of  $\frac{3}{2}$  wavelength. The second resonant sizes of the loops are summarized in Table 1.2.

Table 1.2.

Loop Geometry	Second resonant size $(\frac{1}{2}$ periphery)
straight wire $(h_1/h_2 = 0)$	1.44λ
rectangular loop $(h_1/h_2 = \frac{1}{3})$	) 1.67λ
rectangular loop $(h_1/h_2 = \overline{1})$	$\frac{1}{.25}$ ) 1.68 $\lambda$
rectangular loop $(h_1/h_2 = \frac{1}{2})$	1.58λ
rectangular loop $(h_1/h_2 = \frac{1}{1.})$	$\frac{1}{5}$ ) not clear
rectangular loop $(h_1/h_2 = \frac{1}{1})$	) 1.73λ
circular loop	not clear

### 1.3. Theory

A theory is presented here to calculate the backscattering cross section of a solid circular loop and a solid rectangular loop when they are illuminated by a plane wave with vertical polarization at normal incidence.

Some numerical results are obtained and are compared with the experimental results in Section 1. 2.

3

)\_

••

k

7.2

•

4

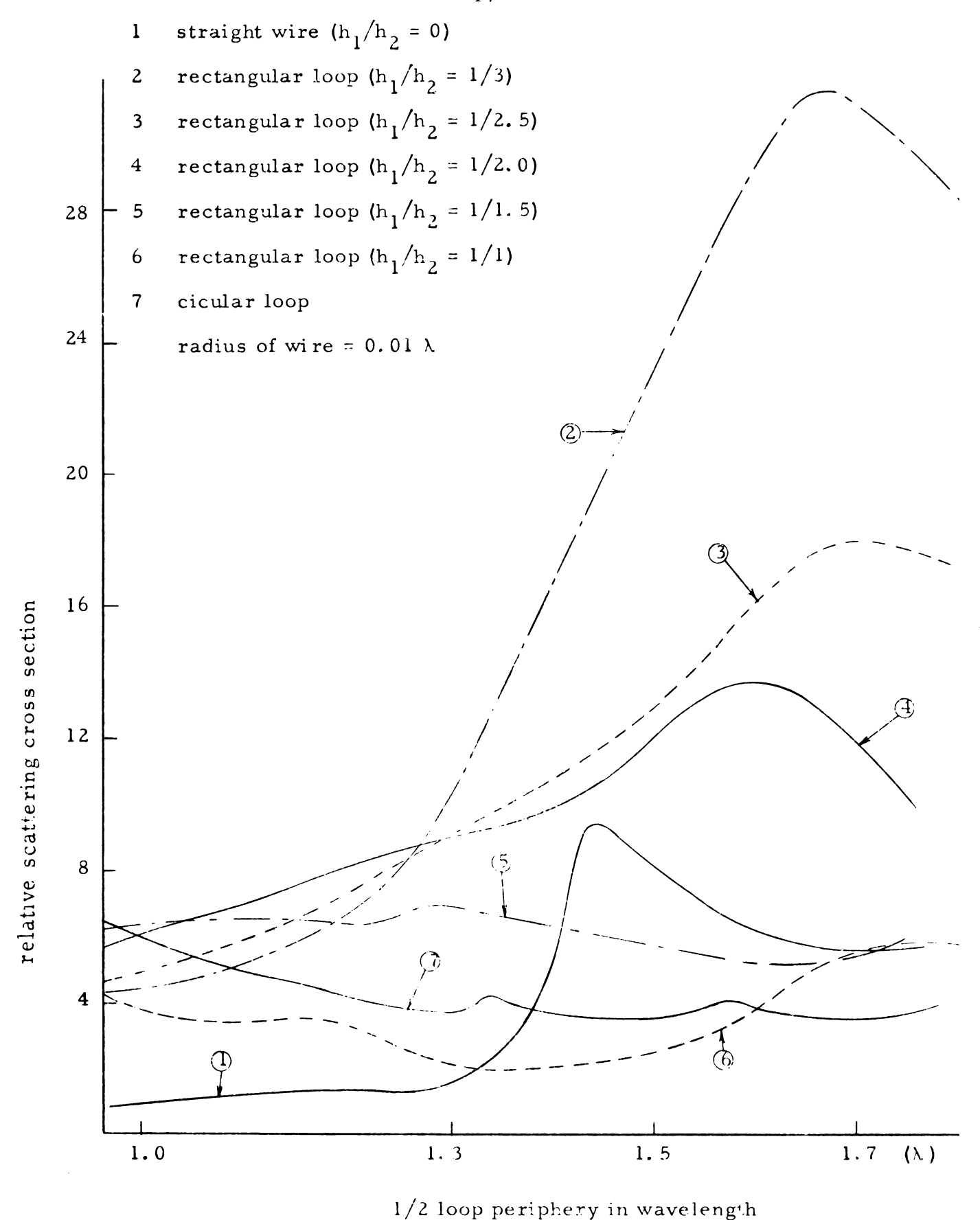


Figure 1.8. Scattering cross sections of loops as functions of loop sizes (second resonance curves)

### 1.3.1. Backscattering from a Solid Circular Loop

The backscattering cross section of a circular metallic loop was first explored by Kouyoumjian<sup>1</sup> who used a variational method to determine approximate formulas for the backscattering cross sections of thin wire loops. Numerically he was able to calculate the backscattering cross sections of a circular loop illuminated by a plane wave at either normal or horizontal incidence. A good agreement between the theory and the experiment was obtained in this study. The weakness of this method is the tedious computation. Later Weston<sup>2</sup> investigated the same case by solving the wave equation in toroidal coordinates to obtain general expressions for the electromagnetic field. Numerical values for an arbitrary incident angle were determined and his analysis is deemed as a generalization of earlier work by Kouyoumjian.

These two methods are too complicated to serve our purpose of solving the case of a loaded circular loop developed in the next chapter. A mathematically simpler method has been developed in this research.

### (A) Geometry of Problem

The geometry of the problem is as shown in Figure 1.9.

A loop of radius b is assumed to be made of perfectly conducting metallic wire of radius a. A plane electromagnetic wave with the E field parallel to the plane of the loop is incident normally upon the loop. The dimensions of interest are

$$a^2 << b^2$$
 ,  $\beta_0^2 a^2 << 1$ 

where  $\beta_0$  is the wave number. We assume that the wire is thin enough so that only the  $\theta$  component of current is induced.

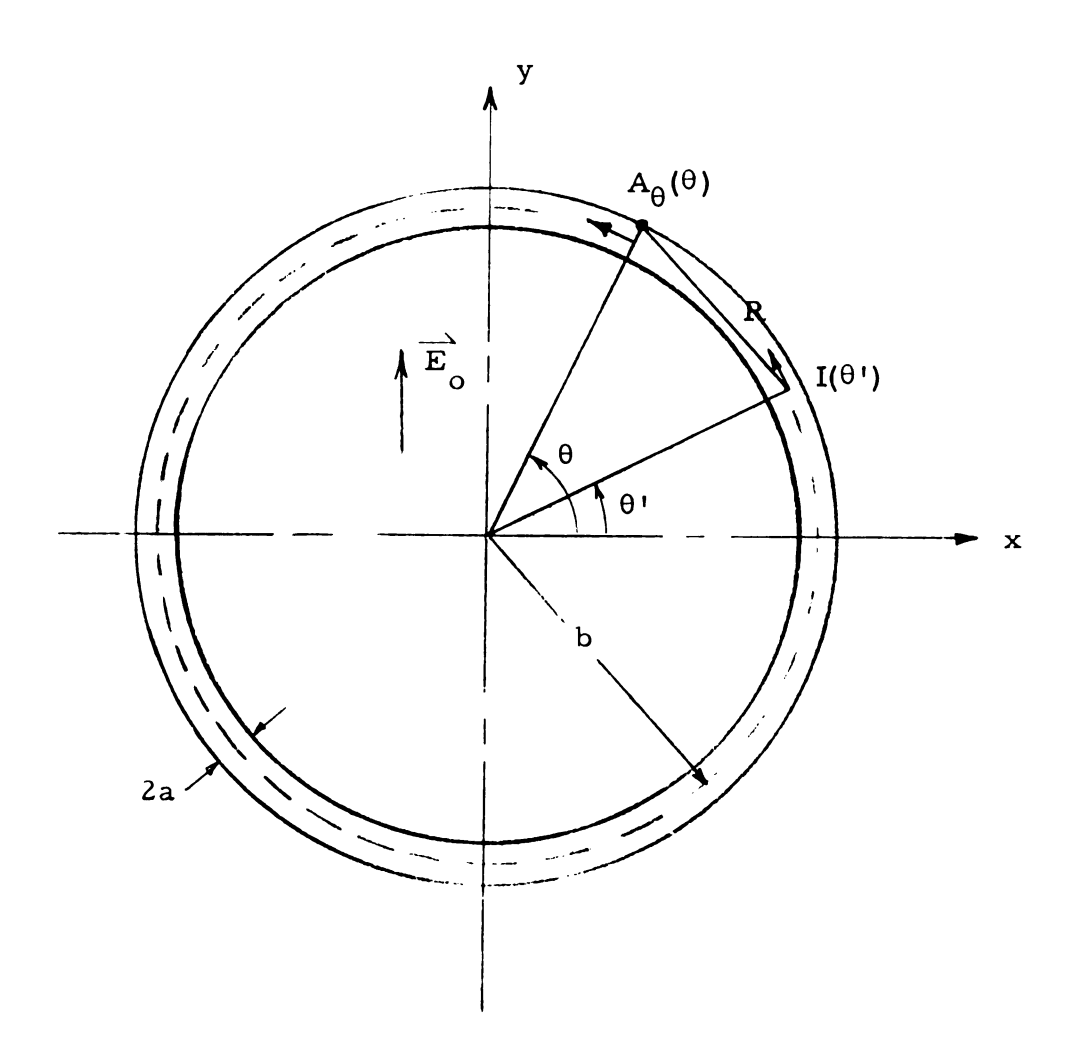


Figure 1.9. Geometry of solid circular loop.

## (B) Differential Equation for Loop Current

Since the tangential electric field should vanish at the surface of the loop, the following equation is valid:

$$E_t^{i} + E_t^{a} = 0 for -\pi \le \theta \le \pi (1.1)$$

where  $E_t^a$  is the tangential electric field maintained by the current and the charge on the loop,  $E_t^i$  is the tangential electric field of the incident wave.

The symmetry of the geometry gives

$$I_{\theta}^{s}(\theta) = -I_{\theta}^{s}(\pi - \theta)$$

$$I_{\theta}^{s}(\pm \frac{\pi}{2}) = 0$$
(1.2)

where  $I^s(\theta)$  is the induced current in the loop. The tangential component of the incident E field along the loop is

$$E_t^{i} = E_0 \cos \theta \tag{1.3}$$

where E is a constant electric field.

The current and the charge on the loop maintain a tangential electric field at the surface which can be expressed as

$$E_{t}^{a} = -(\nabla \phi^{s})_{\theta} - j\omega A_{\theta}^{s} \qquad (1.4)$$

where  $\phi^s$  is the scalar potential maintained by the charge on the loop and  $A^s_{\theta}$  is the tangential component of the vector potential maintained by the current on the loop.  $\phi^s$  can be expressed as

$$\phi^{\mathbf{s}}(\theta) = \frac{1}{4\pi\epsilon_{0}} \int_{-\pi}^{\pi} q^{\mathbf{s}}(\theta') \frac{e^{-j\beta_{0}R}}{R} b d\theta' \qquad (1.5)$$

where  $q^{\mathbf{S}}(\theta^{\,\prime})$  is the density of charge induced on the loop at  $\theta$  =  $\theta^{\,\prime}$  , and

$$R = b \sqrt{4 \sin^2 \frac{\theta - \theta'}{2} + \frac{a^2}{b^2}} = b \sqrt{2 - 2 \cos (\theta - \theta') + \frac{a^2}{b^2}}$$
(1.6)

Assume  $\phi^{s}(\theta)$  can be approximated as

$$\phi^{S}(\theta) = \frac{\Phi_{q}^{S}}{4\pi\epsilon_{Q}} \quad q^{S}(\theta)$$
 (1.7)

where  $\Phi_{\mathbf{q}}^{\mathbf{s}}$  is the ratio between scalar potential to charge density and can be defined as

$$\Phi_{\mathbf{q}}^{\mathbf{s}} = 4 \pi \epsilon_{\mathbf{O}} \frac{\Phi^{\mathbf{s}}(\theta)}{\mathbf{q}^{\mathbf{s}}(\theta)}$$
 (1.8)

With (1.8)

$$(\nabla \phi^{\mathbf{s}})_{\theta} \Big|_{\mathbf{r} = \mathbf{b}} = \frac{\Phi_{\mathbf{q}}^{\mathbf{s}}}{4\pi\epsilon_{0}} \quad \frac{1}{\mathbf{b}} \quad \frac{q^{\mathbf{s}}(\theta)}{\partial \theta}$$
 (1.9)

From the equation of continuity

$$q^{s}(\theta) = j\frac{1}{\omega} \nabla \cdot \overrightarrow{I^{s}} = j\frac{1}{\omega b} \frac{\partial I_{\theta}^{s}(\theta)}{\partial \theta}$$
 (1.10)

it leads to

$$(\nabla \phi^{\mathbf{s}})_{\theta} = \frac{\Phi_{\mathbf{q}}^{\mathbf{s}}}{4\pi\epsilon_{0}} \frac{\mathbf{j}}{\omega b^{2}} \frac{\partial^{2} \mathbf{I}_{\theta}^{\mathbf{s}}(\theta)}{\partial \theta^{2}}$$

$$(1.11)$$

Writing  $A_{\theta}^{s}$  in terms of the induced current  $I_{\theta}^{s}(\theta)$  on the loop, we have

$$\mathbf{A}_{\Theta}^{\mathbf{S}}(\theta) = \frac{\mu_{o}}{4\pi} \int_{-\pi}^{\pi} I_{\theta}^{\mathbf{S}}(\theta') \frac{e^{-j\beta_{o}R}}{R} \cos(\theta - \theta') \, b \, d\theta' \qquad (1.12)$$

If  $\mathbf{A}_{\Theta}^{S}(\theta)$  is assumed to be proportional to  $I_{\theta}^{S}(\theta)$ , (1.12) can be rewritten as

$$A_{\theta}^{s}(\theta) = \frac{\mu_{O}\Phi_{i}^{s}}{4\pi} I_{\theta}^{s}(\theta) \qquad (1.13)$$

where  $\Phi_i^s$  is the ratio between the tangential component of vector potential to the current and is defined as

$$\Phi_{i}^{S} = \frac{4\pi}{\mu_{O}} \frac{A_{\theta}^{S}(\theta)}{I_{\Theta}^{S}(\theta)}$$
 (1.14)

With (1.11) and (1.13), (1.4) can be written as

$$-E_{t}^{a} = \frac{j \Phi_{q}^{s}}{4\pi \epsilon_{0} \omega b^{2}} \left[ \frac{\partial^{2} I_{\theta}^{s}(\theta)}{\partial \theta^{2}} + \beta_{0}^{2} b^{2} \alpha^{s} I_{\theta}^{s}(\theta) \right]$$
(1.15)

where

$$\alpha^{S} = \frac{\Phi_{i}^{S}}{\Phi_{q}^{S}} \tag{1.16}$$

The substitution of (1.3) and (1.15) in (1.1) gives

$$\left(\frac{\partial^2}{\partial \theta^2} + \beta_s^2 b^2\right) I_{\theta}^s(\theta) = K^s E_o \cos \theta \qquad (1.17)$$

for 
$$-\pi \le \theta \le \pi$$

where

$$\beta_{s}^{2} = \beta_{o}^{2} \alpha^{s} = \beta_{o}^{2} \frac{\Phi_{i}^{s}}{\Phi_{o}^{s}}$$
 (1.18)

$$K^{S} = -j \frac{4\pi \epsilon_{o} \omega b^{2}}{\Phi_{o}^{S}}$$
 (1.19)

# (C) Solution for Loop Current

The solution for  $I_{\theta}^{s}(\theta)$  can be expressed as

$$I_{\theta}^{s}(\theta) = C_{1}^{s} \cos \beta_{s} b \theta + C_{2}^{s} \sin \beta_{s} b \theta + P^{s}(\theta)$$
 (1.20)

where  $C_1^s$  and  $C_2^s$  are arbitrary constants, and  $P^s(\theta)$  is a particular integral.  $C_2^s$  is zero due to the symmetry and  $P^s(\theta)$  can be found to be

$$P^{s}(\theta) = \frac{K^{s} E_{o}}{\beta_{s}^{2} b^{2} - 1} \cos \theta$$
 (1.21)

Thus, (1.20) can be written as

$$I_{\theta}^{s}(\theta) = C_{1}^{s} \cos \beta_{s} b \theta + \frac{K^{s} E_{o}}{\beta_{s}^{2} b^{2} - 1} \cos \theta$$
 (1.22)

If the boundary condition of  $I_{\theta}^{s}(\frac{\pi}{2}) = 0$  is applied to (1.22), we obtain

$$C_1^s = 0$$
 (1.23)

The refore, the final solution for  $I_{\theta}^{s}(\theta)$  becomes

$$I_{\theta}^{s}(\theta) = \frac{K^{s} E_{o}}{\beta_{s} b^{2} - 1} \cos \theta \qquad (1.24)$$

for 
$$-\pi \le \theta \le \pi$$

# (D) Backscattering Cross Section

With the induced current found in (1.24), the vector potential in the direction of the incident wave and at the far zone of the loop can be calculated as

:

$$A_{y}^{s} = \frac{\mu_{o}}{4\pi} \int_{-\frac{\pi}{2}}^{\frac{\pi}{2}} 2I_{\theta}^{s}(\theta') \cos \theta' \frac{e^{-j\beta_{o}R_{1}}}{R_{1}} bd\theta'$$

$$= \frac{\mu_{o}}{4} \frac{e^{-j\beta_{o}R_{1}}}{R_{1}} b \frac{K^{s} E_{o}}{\beta_{s}^{2} b^{2} - 1}$$
 (1.25)

where  $R_1 = \sqrt{R_0^2 + b^2}$  and  $R_0$  is the distance between the center of the loop and an observation point on the axis of the loop as shown in Figure 1.10.

The back scattered field in the far zone is

$$E_{y}^{s} = -j \omega A_{y}^{s}$$

$$= -j \frac{\zeta_{o}}{4} \beta_{o} b \frac{e^{-j \beta_{o} R_{1}}}{R_{1}} \frac{K^{s} E_{o}}{\beta_{s}^{2} b^{2} - 1}$$
(1.26)

where  $\zeta_0 = \sqrt{\frac{\mu_0}{\epsilon_0}} = 120\pi$  and  $\beta_s$  is to be determined in a

following section.

The Poynting power density of the scattered field can be found to be

$$P = \frac{\left| E_{y}^{s} \right|^{2}}{2\zeta_{o}}$$

$$= \frac{\zeta_{o}}{32} (\beta_{o}^{b})^{2} \frac{E_{o}^{2}}{R_{1}^{2}} \left| \frac{K^{s}}{\beta_{s}^{2} b^{2} - 1} \right|^{2}$$
(1.27)

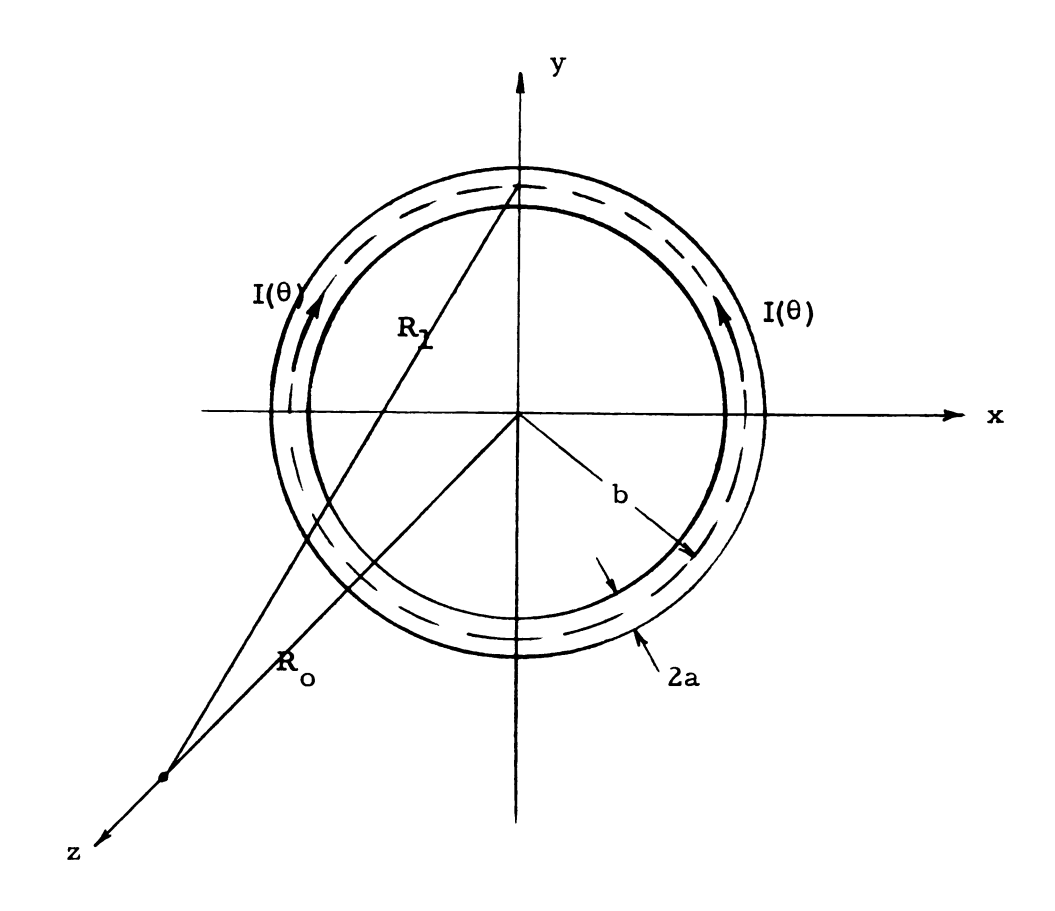


Figure 1.10. Geometry for the calculation of radiation field of a solid circular loop.

\$:

; ;; The backscattering cross section is then found to be

$$\sigma_{B} = \lim_{R_{1} \to \infty} 4\pi R_{1}^{2} \frac{\left|E_{y}^{s}\right|^{2}}{\left|E_{o}\right|^{2}}$$

$$= \frac{\pi \zeta_{o}^{2}}{4} (\beta_{o} b)^{2} \left|\frac{K^{s}}{\beta_{s}^{2} b^{2} - 1}\right|^{2}$$
(1.28)

Substitution of (1.19) in (1.28) yields

$$\sigma_{B} = 4\pi^{3} \zeta_{o}^{2} \epsilon_{o}^{2} \omega^{2} b^{4} (\beta_{o} b)^{2} \left| \frac{1}{\Phi_{q}^{s} (\beta_{s}^{2} b^{2} - 1)} \right|^{2}$$

$$= \lambda^{2} \pi (\beta_{0} b)^{6} \left| \frac{1}{\Phi_{q}^{s} (\beta_{s}^{2} b^{2} - 1)} \right|^{2}$$

or

$$\frac{\sigma_{B}}{\lambda^{2}} = \pi (\beta_{o} b)^{6} \left| \frac{1}{\Phi_{q}^{s} (\beta_{s}^{2} b^{2} - 1)} \right|^{2}$$
 (1.29)

where λ is the wavelength.

(E) Determination of  $\Phi_{
m q}^{
m s}$  and  $\Phi_{
m i}^{
m s}$ 

(i) Using the equation of continuity (1.10) and (1.24),  $\,q^s(\theta)\,$  can be found to be

$$q^{s}(\theta) = j \frac{1}{\omega b} \frac{\partial I^{s}(\theta)}{\partial \theta}$$

$$= -j \frac{1}{\omega b} \frac{K^s E_o}{\beta_s^2 b^2 - 1} \sin \theta \qquad (1.30)$$

for 
$$-\pi \leq \theta \leq \pi$$

With (1.5) and (1.30),  $\Phi_q^s$  defined in (1.8) is found as

$$\Phi_{\mathbf{q}}^{\mathbf{s}} = 4\pi \, \epsilon_{0} \quad \frac{\Phi_{0}^{\mathbf{s}}(\theta_{0})}{q^{\mathbf{s}}(\theta_{0})}$$

$$= \frac{\int_{-\pi}^{\pi} \sin \theta' \frac{e^{-j\beta_{o}R}}{R} b d\theta'}{\sin \theta_{o}}$$
(1.31)

where

$$R = b \sqrt{2 - 2 \cos (\theta_0 - \theta') + \frac{a^2}{b^2}}$$

 $Ch_{Oosing} \theta_{o} = \frac{\pi}{2}$ , the point of maximum charge density,  $\Phi_{q}^{s}$  becomes

$$\Phi_{\mathbf{q}}^{\mathbf{S}} = \int_{-\pi}^{\pi} \sin \theta' \frac{e^{-j\beta_{\mathbf{S}} \mathbf{b} \sqrt{2 - 2 \sin \theta' + \frac{\mathbf{a}^2}{\mathbf{b}^2}}}}{\sqrt{2 - 2 \sin \theta' + \frac{\mathbf{a}^2}{\mathbf{b}^2}}} d\theta'$$

$$= \int_{-\pi}^{\pi} \sin \theta' K_{1} \left( \theta', \frac{a^{2}}{b^{2}} \right) d\theta' \qquad (1.32)$$

where

$$K_{1}\left(\theta', \frac{a^{2}}{b^{2}}\right) = \frac{e^{-j\beta_{s} b \sqrt{2 - 2 \sin \theta' + \frac{a^{2}}{b^{2}}}}}{\sqrt{2 - 2 \sin \theta' + \frac{a^{2}}{b^{2}}}}$$
(1.33)

In actual calculation of  $\,\Phi_{q}^{\,s}$  ,  $\,\beta_{s}\,$  will be replaced by  $\beta_{o}$  as an approximation.

(ii) Similarly,  $\Phi_{\dot{i}}^{s}$  is obtained by making use of (1.12) and (1.14) as

$$\Phi_{i}^{s} = \frac{4\pi}{\mu_{o}} \frac{A_{\theta}^{s}(\theta_{o})}{I_{\theta}^{s}(\theta_{o})}$$

$$= \frac{\int_{-\pi}^{\pi} \cos \theta' \cos (\theta_{o} - \theta') \frac{e^{-j\beta_{s}R}}{R} b d \theta'}{\cos \theta_{o}}$$
 (1.34)

where

$$R = b \sqrt{2 - 2 \cos (\theta_0 - \theta') + \frac{a^2}{b^2}}$$

Choosing  $\theta_0 = 0$ , the point of maximum current,  $\Phi_i^s$  becomes

$$\Phi_{i}^{s} = \int_{-\pi}^{\pi} \cos^{2} \theta' \frac{e^{-j\beta_{s} b \sqrt{2 - 2 \cos \theta' + \frac{a^{2}}{b^{2}}}}}{\sqrt{2 - 2 \cos \theta' + \frac{a^{2}}{b^{2}}}} d\theta'$$

$$= 2 \int_{0}^{\pi} \cos^{2} \theta' K_{2}(\theta', \frac{a^{2}}{b^{2}}) d\theta'$$
(1.35)

where

$$K_2(\theta', \frac{a^2}{b^2}) = \frac{e^{-j\beta_s b \sqrt{2 - \cos \theta' + \frac{a^2}{b^2}}}}{\sqrt{2 - 2\cos \theta' + \frac{a^2}{b^2}}}$$
(1.36)

In actual calculation of  $\Phi_i^s$  ,  $\beta_s$  will be replaced by  $\beta_0$  as an approximation.

### (F) Numerical Results

To calculate the theoretical results of backscattering cross section,  $\Phi_q^s$  and  $\Phi_i^s$  are numerically calculated for the case of  $\frac{2}{b^2} = 0.00179$  as functions of  $\beta_0$ b. Numerical results of  $\Phi_q^s$  and  $\Phi_i^s$  are shown graphically in Figure 1.11 and Figure 1.12. It is observed that  $\Phi_q^s$  and  $\Phi_i^s$  vary only weakly over the range of interest. This agrees reasonably well with our original assumption of  $\Phi_q^s$  and  $\Phi_i^s$  being constant. The numerical result of backscattering cross section is plotted as functions of  $\beta_0$ b in Figure 1.13 in comparison with the perimental results.

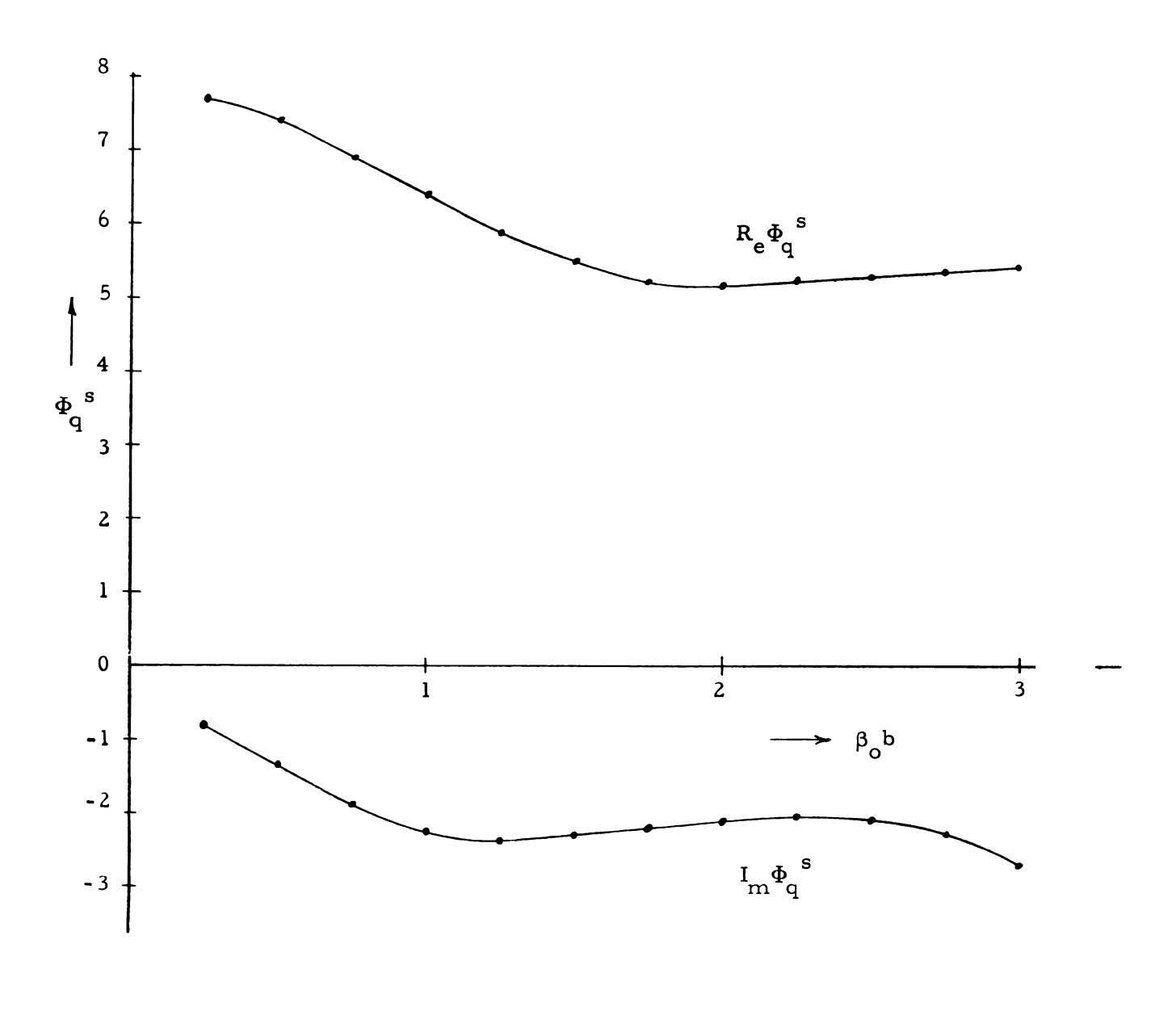


Figure 1.11.  $\Phi_q^s$  as a function of  $\beta_0 b$  ( $\frac{a^2}{b^2} = 0.00179$ ).

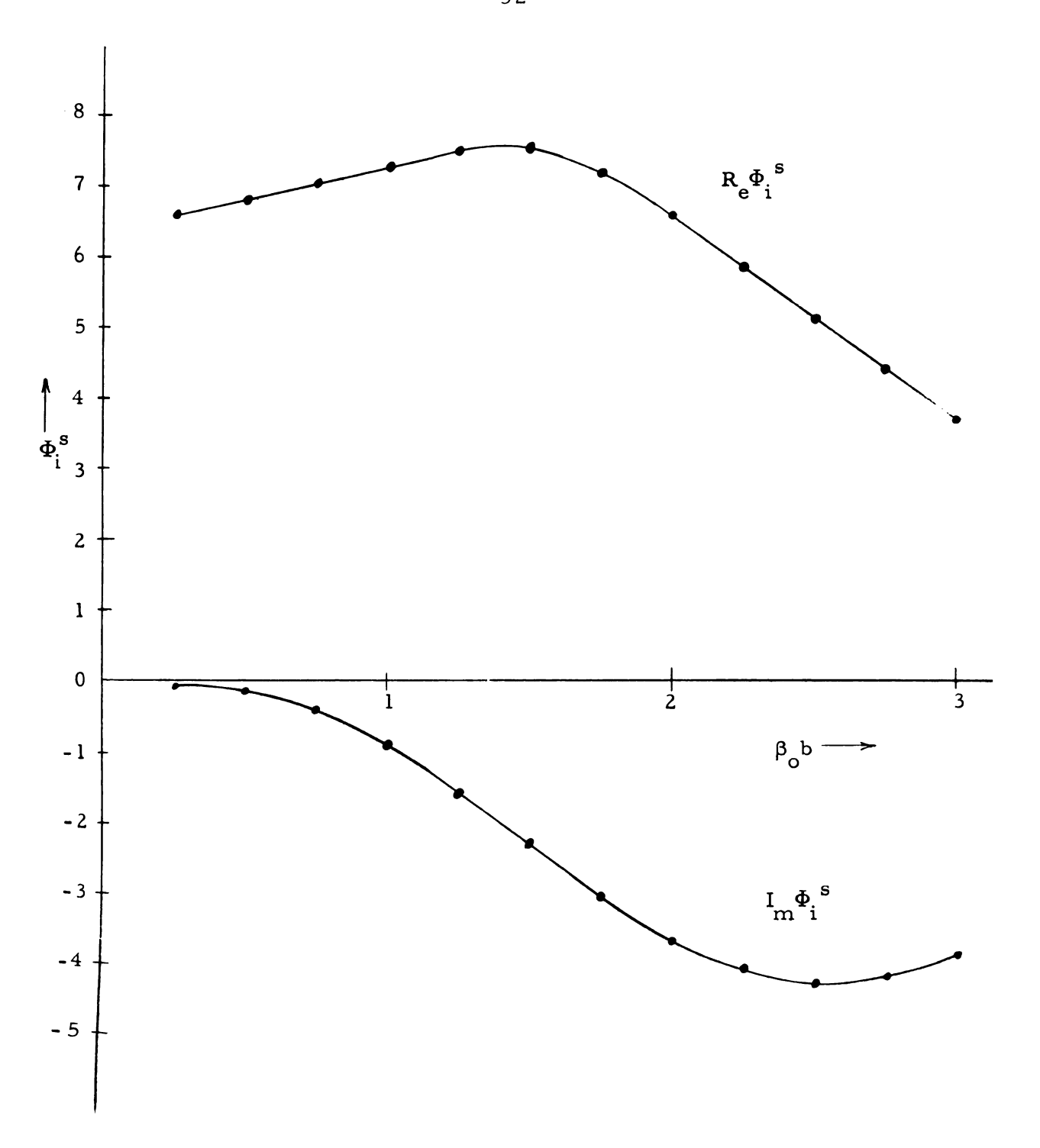


Figure 1.12.  $\Phi_i^s$  as a function of  $\beta_0^b (\frac{a^2}{b^2} = 0.00179)$ .

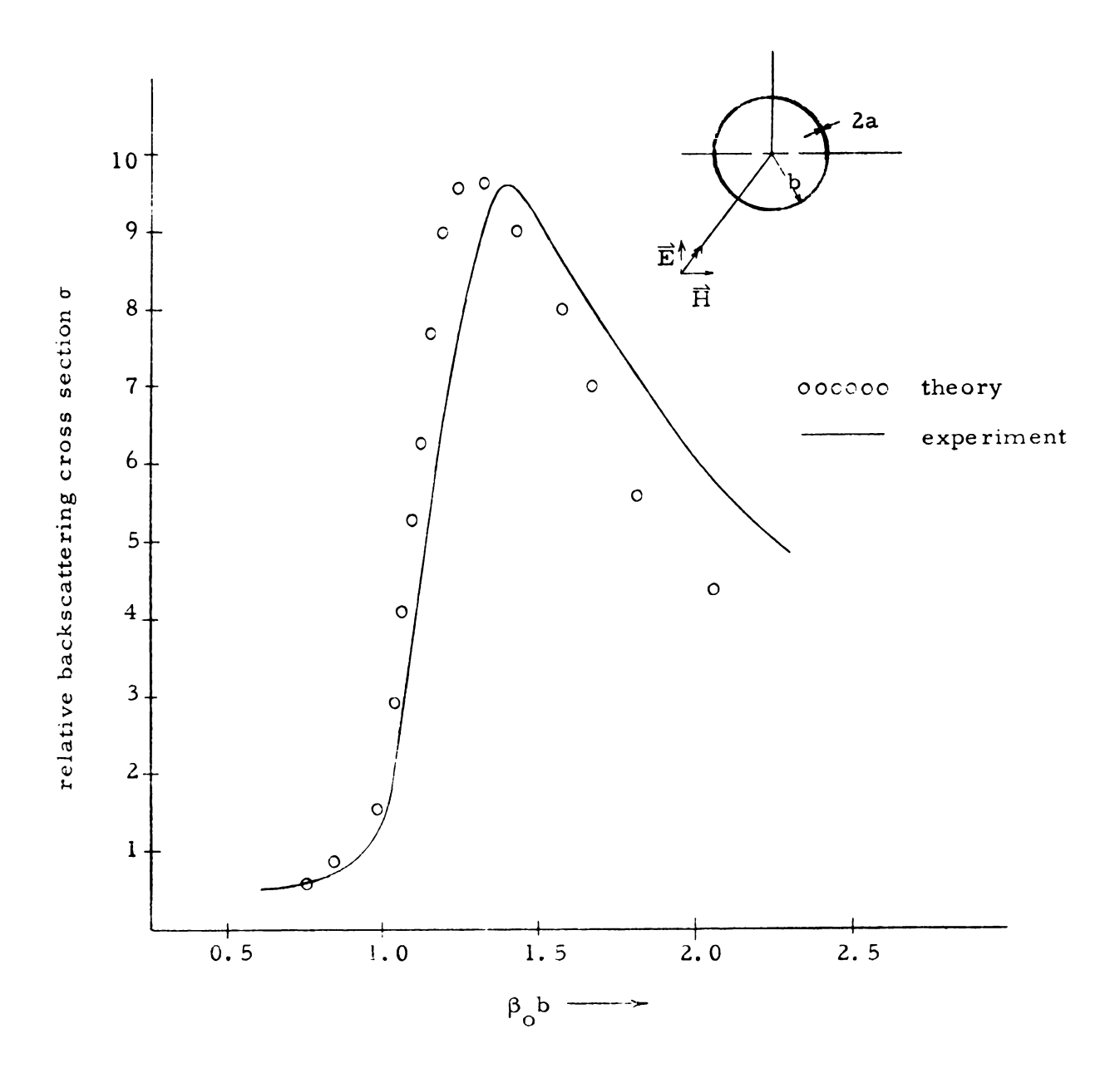


Figure 1.13. Comparison between theory and experiment for circular loops illuminated by plane wave at normal incidence.

The theory predicts fairly well for the loops with  $\beta_0$  b smaller than 1.5 which is the range of interest. For a larger loop the present theory fails to give accurate solution. A refined theory would give better results but we find the present theory adequate for further theoretical development.

### 1.3.2. Scattering from a Solid Rectangular Loop

To study the backscattering from a solid rectangular loop an approach which is different from that used for a circular loop will be used. The first order solution will be obtained by using the method developed by Chen and King.

#### (A) Formulation of Problem

The geometry of the problem is as shown in Figure 1.14. A rectangular loop with short side  $2h_1$  and long side  $2h_2$  is assumed to be made of perfectly conducting metallic wire of radius a. A plane electromagnetic wave with the E field parallel to the plane of the loop is incident normally to the loop. The dimensions of interest are

$$a^2 << h_1^2 \text{ and } h_2^2$$
 ,  $\beta_0^2 a^2 << 1$ 

where  $\beta_0$  is the wave number. We assume that the wire is thin enough so that only the tangential component of current is induced.

## (B) Integral Equations for Loop Currents

Since the tangential electric field should be continuous at the surface of the loop, we obtain the following equation:

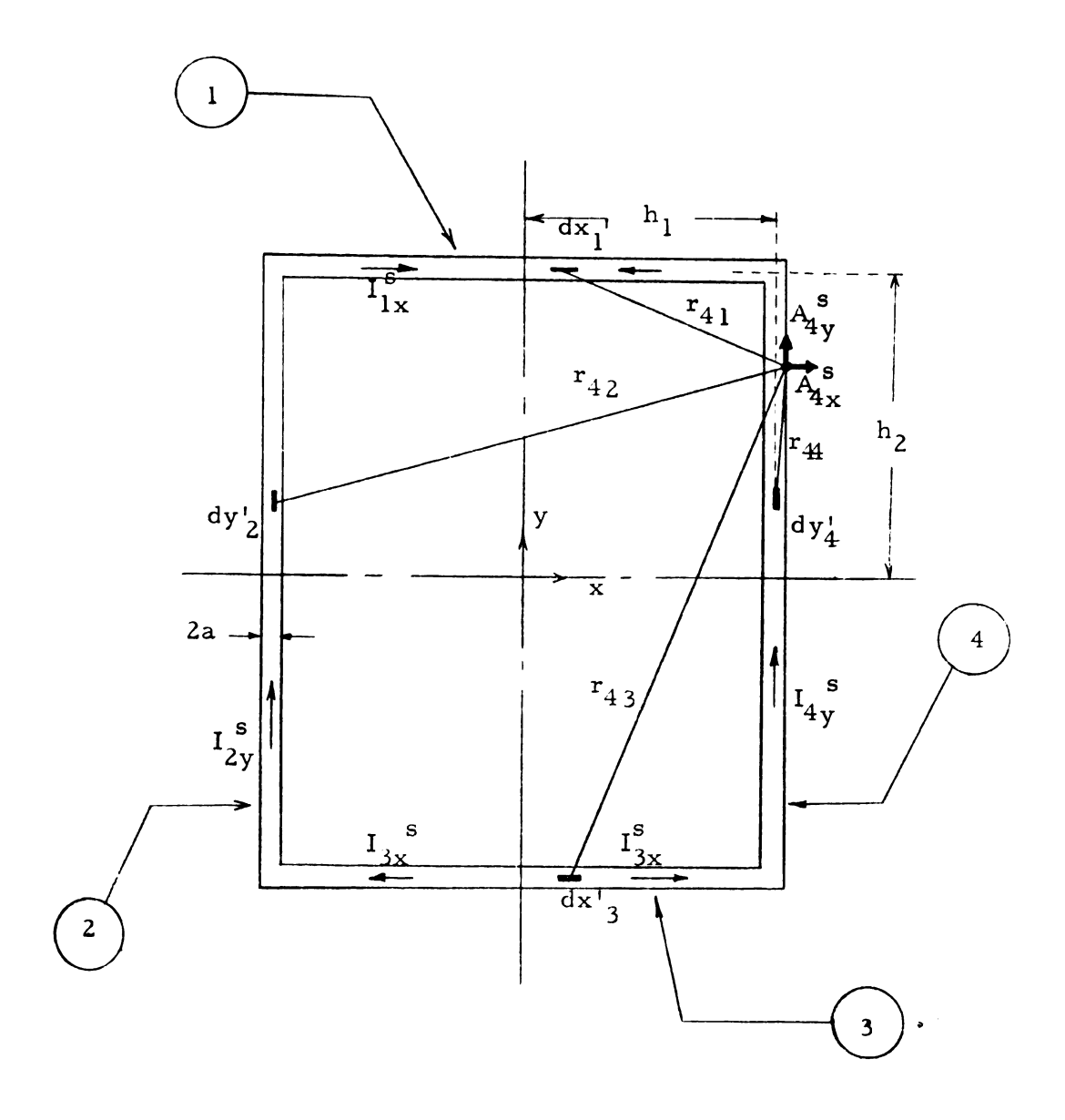


Figure 1.14. Geometry for solid rectangular loop.

For side 4

$$E_{4t}^{i} + E_{4t}^{a} = 0 (1.37)$$

$$E_{4t}^{i} = E_{0}$$
 (1.38)

where  $E_{4t}^{i}$  is the tangential electric field of the incident wave and  $E_{4t}^{a}$  is the tangential E field at the surface of side 4 maintained by the induced current and charge on the loop.

Due to symmetrical configuration, it follows that

$$I_{2y}^{s}(y) = I_{4y}^{s}(y)$$
 (1.39)

$$I_{1x}^{s}(x) = -I_{3x}^{s}(x)$$
 (1.40)

$$q_2^s(y) = q_4^s(y)$$
 (1.41)

$$q_1^s(x) = -q_3^s(x)$$
 (1.42)

where  $I_{4y}^{s}$  (y) is the induced current in side 4 and  $I_{1x}^{s}$  (x) is that in side 1, etc., whereas  $q_{i}^{s}$  denotes the induced charge on side i, i = 1, 2, 3, and 4.  $E_{4t}^{a}$  can be expressed as

$$E_{4t}^{a} = - \left( \nabla \phi_{4}^{s} \right)_{y} - j \omega \left( \overline{A}_{4}^{s} \right)_{y}$$
 (1.43)

where  $A_4^s$  is the vector potential at the surface of side 4 contributed by the induced current in the loop;  $\phi_4^s$  is the scalar potential at the

surface of side 4 maintained by the induced charges on the loop. In symbols,  $\overrightarrow{A_4}^s$  and  $\phi_4^s$  can be expressed as

$$\overrightarrow{A}_{4}^{S} = A_{4x}^{S} \hat{x} + A_{4y}^{S} \hat{y}$$
 (1.44)

$$\phi_4^s = \phi_{41}^s + \phi_{42}^s + \phi_{43}^s + \phi_{44}^s \tag{1.45}$$

 $\phi_{4i}^{s}$  is the scalar potential at the surface of side 4 maintained by the induced charges on side i, i = 1, 2, 3, and 4.  $A_{4y}^{s}$  can be expressed in terms of current by Helmholtz integrals as

$$A_{4y}^{s}(y) = \frac{\mu_{o}}{4\pi} \int_{h_{2}}^{h_{2}} I_{4y}^{s}(y') \frac{e^{-j\beta_{o} r_{44}}}{r_{44}} dy'$$

$$+\frac{\mu_{o}}{4\pi} \int_{-h_{2}}^{h_{2}} I_{2y}^{s}(y') \frac{e^{-j\beta_{o}r_{42}}}{r_{42}} dy'$$

$$= \frac{\mu_{O}}{4\pi} \int_{-h_{2}}^{h_{2}} I_{4y}^{s} (y') K_{IA} (y, y') dy'$$
(1.46)

where

$$K_{1A}(y, y') = \frac{e^{-j\beta_0 r_{44}}}{r_{44}} + \frac{e^{-j\beta_0 r_{42}}}{r_{42}}$$
 (1.47)

$$r_{44} = \sqrt{(y' - y)^2 + a^2}$$
 (1.48)

$$r_{42} = \sqrt{(y' - y)^2 + 4h_1^2}$$
 (1.49)

With (1.44) and (1.45), (1.43) can be rewritten as

$$E_{4t}^{a} = -\frac{\partial}{\partial y} (\phi_{42}^{s} + \phi_{44}^{s}) - j \omega A_{4y}^{s} - \frac{\partial}{\partial y} (\phi_{41}^{s} + \phi_{43}^{s})$$
 (1.50)

By the Lorentz condition, it follows that

$$\phi_{42}^{s} + \phi_{44}^{s} = \frac{j\omega}{\beta_{0}^{2}} \quad \nabla \cdot (\overrightarrow{A}_{42}^{s} + \overrightarrow{A}_{44}^{s}) = \frac{j\omega}{\beta_{0}^{2}} \quad \frac{\partial A_{4y}^{s}(y)}{\partial y}$$
 (1.51)

After substituting (1.51) in (1.50) and after rearranging, (1.50) becomes

$$E_{4t}^{a} = \frac{-j\omega}{\beta_0^2} \left(\frac{\partial^2}{\partial y^2} + \beta_0^2\right) A_{4y}^{s}(y) - \frac{\partial}{\partial y} (\phi_{41}^{s} + \phi_{43}^{s})$$
 (1.52)

Substitution of (1.38) and (1.52) in (1.37) gives

$$\left(\frac{\partial^2}{\partial y^2} + \beta_0^2\right) A_{4y}^s(y) = -\frac{j\beta_0^2}{\omega} E_{\zeta} + \frac{j\beta_0^2}{\omega} \frac{\partial}{\partial y} (\phi_{41}^s + \phi_{43}^s) \quad (1.53)$$

Similarly, the differential equation for the vector potential at side 1 can be obtained as follows:

For side 1

$$E_{1t}^{i} + E_{1t}^{a} = 0 (1.54)$$

$$E_{1t}^{i} = 0$$
 (1.55)

where  $E_{lt}^{i}$  is the tangential E field of the incident wave and  $E_{lt}^{a}$  is the tangential E field at the surface of side 1 maintained by the induced current and charge on the loop.

E<sub>1t</sub> can be expressed as

$$E_{lt}^{a} = - (\nabla \phi_{l}^{s})_{x} - j \omega (\overrightarrow{A}_{l}^{s})_{x}$$
 (1.56)

where  $\phi_l^s$  is the scalar potential at the surface of side 1 maintined by the induced charges on the loop and  $\overrightarrow{A}_l^s$  is the vector potential at the surface of side 1 contributed by the induced currents in the loop. In symbols,  $\overrightarrow{A}_l^s$  and  $\phi_l^s$  can be expressed as

$$\frac{\Delta}{A_1} = A_{1x} + A_{1y} + A_{1y}$$
 (1.57)

$$\phi_1^s = \phi_{11}^s + \phi_{12}^s + \phi_{13}^s + \phi_{14}^s$$
 (1.58)

where  $A_{lx}^{s}$  is the vector potential at the surface of side 1 contributed by the induced currents in sides 1 and 3; while  $A_{ly}^{s}$  is that contributed by the induced currents in sides 2 and 4.  $\phi_{li}^{s}$  is the scalar potential

at the surface of side 1 maintained by the induced charges on side i, i = 1, 2, 3 and 4.

 $A_{lx}^{s}$  can be expressed in terms of current as

$$A_{1x}^{s}(x) = \frac{\mu_{o}}{4\pi} \int_{-h_{1}}^{h_{1}} I_{1x}^{s}(x') \frac{e^{-j\beta_{o}r_{11}}}{r_{11}} dx'$$

$$+ \frac{\mu_{o}}{4\pi} \int_{-h_{1}}^{h_{1}} I_{3x}^{s}(x') \frac{e^{-j\beta_{o}r_{13}}}{r_{13}} dx'$$

$$= \frac{\mu_{o}}{4\pi} \int_{-h_{1}}^{h_{1}} I_{1x}^{s}(x') K_{2A}(x, x') dx' \qquad (1.59)$$

where

$$K_{2A}(x, x') = \frac{e^{-j\beta_0 r_{11}}}{r_{11}} - \frac{e^{-j\beta_0 r_{13}}}{r_{13}}$$
 (1.60)

$$r_{11} = \sqrt{(x - x')^2 + a^2}$$
 (1.61)

$$r_{13} = \sqrt{(x' - x)^2 + 4h_2^2}$$
 (1.62)

With (1.57) and (1.58), (1.56) can be rewritten as

$$E_{1t}^{a} = -\frac{\partial}{\partial x} \left( \phi_{11}^{s} + \phi_{13}^{s} \right) - j \omega A_{1x}^{s} - \frac{\partial}{\partial x} \left( \phi_{12}^{s} + \phi_{14}^{s} \right)$$
 (1.63)

By the Lorentz condition, we have

$$\phi_{11}^{s} + \phi_{13}^{s} = \frac{j\omega}{\beta_{0}^{2}} \nabla \cdot (\overrightarrow{A}_{11}^{s} + \overrightarrow{A}_{13}^{s}) = \frac{j\omega}{\beta_{0}^{2}} \frac{\partial A_{1x}^{s}}{\partial x}$$
 (1.64)

Substituting (1.64) in (1.63), we can rearrange (1.63) as

$$E_{1t}^{a} = -\frac{j\omega}{\beta_{o}^{2}} \left( \frac{\partial^{2}}{\partial x^{2}} + \beta_{o}^{2} \right) A_{1x}^{s} - \frac{\partial}{\partial x} \left( \phi_{12}^{s} + \phi_{14}^{s} \right)$$
 (1.65)

With (1.55) and (1.65), (1.54) can be rewritten as

$$\left(\frac{\partial^{2}}{\partial x^{2}} + \beta_{0}^{2}\right) A_{1x}^{s}(x) = \frac{j\beta_{0}^{2}}{\omega} \frac{\partial}{\partial x} \left(\phi_{12}^{s} + \phi_{14}^{s}\right)$$
(1.66)

Due to symmetry, we note that

$$A_{4y}^{s}(y) = A_{4y}^{s}(-y)$$
 (1.67)

and

$$A_{1x}^{s}(x) = -A_{1x}^{s}(-x)$$
 (1.68)

With (1.67), the general solution for  $A_{4v}^{s}(y)$  in (1.53) is then

$$A_{4y}^{s}(y) = \frac{-j}{v_o} \left[ C_4^{s} \cos \beta_0 y + \theta_4^{s}(y) \right]$$
 (1.69)

where  $C_4^s$  is an arbitrary constant,  $v_0$  is the velocity of light in free space and  $\theta_4^s(y)$  is a particular integral which can be found as

$$\theta_4^{s}(y) = \frac{E_0}{\beta_0} - \int_0^y \frac{\partial}{\partial s} \left[ \phi_{41}^{s}(s) + \phi_{43}^{s}(s) \right] \sin \beta_0(y - s) ds \qquad (1.70)$$

Similarly, with (1.68) the general solution for  $A_{lx}^{s}(x)$  in (1.66) can be expressed as

$$A_{1x}^{s}(x) = \frac{-j}{v_{o}} \left[ C_{1}^{s} \sin \beta_{o} x + \theta_{1}^{s}(x) \right]$$
 (1.71)

where  $C_{\hat{l}}^{\ \ \ \ }$  is an arbitrary constant and  $\theta_{\hat{l}}^{\ \ \ \ \ }(x)$  is a particular integral which can be found as

$$\theta_1^s(x) = -\int_0^x \frac{\partial}{\partial s} \left[ \phi_{12}^s(s) + \phi_{14}^s(s) \right] \sin \beta_0(x - s) ds$$
 (1.72)

With (1.46) and (1.69), it follows that

$$\frac{4\pi}{\mu_0} A_{4y}^{s}(y) = \int_{-h_2}^{h_2} I_{4y}^{s}(y') K_{1A}(y, y') dy'$$

$$= -\frac{j4\pi}{\zeta_0} \left[ C_4^s \cos \beta_0 y + \theta_4^s (y) \right]$$
 (1.73)

Similarly, with (1.59) and (1.66), we obtain

$$\frac{4\pi}{\mu_0} A_{1x}^{s}(x) = \int_{-h_1}^{h_1} I_{1x}^{s}(x') K_{2A}(x, x') dx'$$

$$= -\frac{j4\pi}{\zeta_0} \left[ C_1^s \sin \beta_0 x + \theta_1^s(x) \right]$$
 (1.74)

## (C) Zeroth Order Solutions for Loop Currents

For the first approximation, we assume that

$$\frac{A_{4y}^{s}(y)}{I_{4y}^{s}(y)} = \frac{\mu_{o}}{4\pi} \Phi_{s}(y)$$
 (1.75)

and

$$\frac{A_{1x}^{s}(x)}{I_{1x}(x)} = \frac{\mu_{0}}{4\pi} \Phi_{s}(x) \qquad (1.76)$$

where  $\Phi_{_{\mathbf{S}}}(\mathbf{y})$  and  $\Phi_{_{\mathbf{S}}}(\mathbf{x})$  are defined respectively as

$$\Phi_{s}(y) = \frac{4\pi}{\mu_{o}} \frac{A_{4y}^{s}(y)}{I_{4y}^{s}(y)}$$
 (1.77)

and

$$\Phi_{s}(x) = \frac{4\pi}{\mu_{o}} \frac{A_{1x}^{s}(x)}{I_{1x}(x)}$$
 (1.78)

Substituting (1.75) in (1.73), we obtain

$$I_{4y}^{s}(y) = \frac{-j4\pi}{\zeta_{0}\Phi_{s}(y)} \left[ C_{4}^{s} \cos \beta_{0} y + \theta_{4}^{s} (y) \right]$$
 (1.79)

Similarly, the substitution of (1.76) in (1.74) gives

$$I_{1x}^{s}(x) = \frac{-j4\pi}{\zeta_{0}\Phi_{s}(x)} \left[ C_{1}^{s} \sin \beta_{0} x + \theta_{1}^{s}(x) \right]$$
 (1.17)

By looking closely at (1.46) and (1.59), we note that the more contributions to  $A_{4y}^{-s}(y)$  and  $A_{1x}^{-s}(x)$  are due to the current elements located at y'=y and x'=x respectively. It is then reasonable to assume that  $\Phi_s(y)$  and  $\Phi_s(x)$  are constant over the entire commutar except at the corners. For simplicity, we assume that

$$\Phi_{s}(y) = \Phi_{s}(x) = \Phi_{s}$$
 (1.51)

To determine  $C_4^{\ \ s}$  and  $C_1^{\ \ s}$  , the following boundary conditions will be used.

(a) Current at the corners being continuous.

i.e., 
$$I_{4y}^{s}(y : h_2) = -1_{1x}^{s}(x = h_1)$$
 (1.82)

(b) Charge around the corners being continuous.

i.e., 
$$q_4^{s}(x = h_2) = q_1^{s}(x = h_1)$$
 (1.48)

The substitution of (1.79), (1.89) and (1.81) in (1.84) yields

$$C_4^s \cos \beta_0 h_2 + \theta_4^s (h_2) = C_1^s \sin \beta_0 h_1 - \theta_1^s (h_1)$$
 (1.13)

 $q_4^{(s)}(y)$  and  $q_1^{(s)}(x)$  can be found as follows by using the equation of continuity.

$$q_4^s(y) = \frac{j}{\omega} \frac{\partial}{\partial y} I_{4y}^s(y)$$

$$= \frac{j}{\omega} \frac{-j4\pi}{\zeta_0 \Phi_s} \left[ -C_4^s \beta_0 \sin \beta_0 y + \frac{\partial \theta_4^s(y)}{\partial y} \right]$$
 (1.85)

$$q_1^s(x) = \frac{j}{\omega} \frac{\partial}{\partial x} I_{1x}^s(x)$$

$$= \frac{j}{\omega} \qquad \frac{-j4\pi}{\zeta_0 \Phi_s} \left[ C_1^s \beta_0 \cos \beta_0 x + \frac{\partial \theta_1^s(x)}{\partial x} \right] \qquad (1.86)$$

Combining (1.85) and (1.86) with boundary condition (1.83), we have

$$-C_{4}^{s}\beta_{0}\sin\beta_{0}h_{2} + \frac{\partial\theta_{4}^{s}(y)}{\partial y} \bigg|_{y=h_{2}} = C_{1}^{s}\beta_{0}\cos\beta_{0}h_{1} + \frac{\partial\theta_{1}^{s}(x)}{\partial x} \bigg|_{x=h_{1}}$$

$$(1.87)$$

Solving (1.84) and (1.87) for  $C_4^s$  and  $C_1^s$ , we obtain

$$C_{4}^{s} = \frac{1}{\beta_{o} \left[\cot \beta_{o} h_{1} \cos \beta_{o} h_{2} - \sin \beta_{o} h_{2}\right]} \left[ \frac{\partial \theta_{1}^{s}(x)}{\partial x} \right|_{x = h}$$

$$-\frac{\partial \theta_4^{s}(y)}{\partial y}\bigg|_{y=\underline{h}_2} + \frac{1}{\tan \beta_0 h_1 \sin \beta_0 h_2 - \cos \beta_0 h_2} \times$$

$$\theta_1^{s}(h_1) + \theta_4^{s}(h_2)$$
(1.88)

$$C_{1}^{s} = \frac{1}{\beta_{o} \left[ \sin \beta_{o} h_{1} \tan \beta_{o} h_{2} - \cos \beta_{o} h_{1} \right]} \quad x$$

$$\cdot \left[ \frac{\partial \theta_{1}^{s}(x)}{\partial x} \right|_{x = h_{1}} - \frac{\partial \theta_{4}^{s}(y)}{\partial y} \right|_{y = h_{2}}$$

$$- \beta_{0} \tan \beta_{0}h_{2} \left[ \theta_{1}^{s}(h_{1}) + \theta_{4}^{s}(h_{2}) \right]$$
(1.89)

For the zeroth order solutions, we assume that  $\theta_4^{s}(y)$  in (1.70) and  $\theta_1^{s}(x)$  in (1.72) can be approximated respectively as

$$\left[\theta_4^{s}(y)\right]_0 = \frac{E_0}{\beta_0} \tag{1.90}$$

$$\begin{bmatrix} \theta_1^{\mathbf{s}}(\mathbf{y}) \\ 0 \end{bmatrix} = 0 \tag{1.91}$$

With (1.90) and (1.91) substituted in (1.88) and (1.89), we obtain

$$\begin{bmatrix} C_4^{s} \end{bmatrix}_0 = -\frac{E_0}{\beta_0} \frac{\cos \beta_0 h_1}{\cos \beta_0 (h_1 + h_2)}$$
 (1.92)

Consequently, the zeroth order solutions for the currents are obtained as

$$\begin{bmatrix}
I_{4y}(y) \end{bmatrix}_{0} = \frac{-j4\pi}{\zeta_{o}\Phi_{s}} \left\{ -\frac{E_{o}}{\beta_{o}} \frac{\cos \beta_{o}h_{1}}{\cos \beta_{o}(h_{1} + h_{2})} \cos \beta_{o}y + \theta_{4}^{s}(y) \right\} \tag{1.94}$$

$$\begin{bmatrix}
I_{1x}(x) \\
0
\end{bmatrix} = \frac{-j4\pi}{\zeta_0 \Phi_s} \left\{ \frac{E_o}{\beta_o} \frac{\sin \beta_o h_2}{\cos \beta_o (h_1 + h_2)} \sin \beta_o x + \theta_1^s(x) \right\}$$
(1.95)

If (1.90) and (1.91) are applied to (1.94) and (1.95), we have

$$\begin{bmatrix}
I_{4y}^{s}(y) \\
I_{00} = \frac{j_{4\pi}}{\zeta_{0}\Phi_{s}}
\end{bmatrix} \xrightarrow{E_{0}} \frac{\cos \beta_{0}h_{1} \cos \beta_{0}y - \cos \beta_{0}(h_{1} + h_{2})}{\cos \beta_{0}(h_{1} + h_{2})} \qquad (1.96)$$

$$\left[I_{1x}^{s}(y)\right]_{00} = \frac{-j4\pi}{\zeta_{o}\Phi_{s}} \frac{E_{o}}{\beta_{o}} \frac{\sin\beta_{o}h_{2}}{\cos\beta_{o}(h_{1}+h_{2})} \sin\beta_{o}x \tag{1.97}$$

## (D) First Order Solutions for Loop Currents

To obtain the first order solutions for the currents, the method used by Chen and King is adopted.

The following equations are needed:

From (1.69) and (1.71)

$$A_{4y}^{s}(y) = \frac{-j}{v_0} \left[ C_4^{s} \cos \beta_0 y + \theta_4^{s}(y) \right]$$

$$A_{1x}^{s}(x) = \frac{-j}{v_{0}} \left[ C_{1}^{s} \sin \beta_{0} x + \theta_{1}^{s}(x) \right]$$

From (1.75) and (1.76), we have

$$\left[I_{4y}(y)\right]_{0} = \frac{-j4\pi}{\zeta_{0}\Phi_{s}} \left[C_{4}^{s} \cos \beta_{0} y + \theta_{4}^{s}(y)\right]$$

$$\left[I_{lx}^{s}(x)\right]_{0} = \frac{-j4\pi}{\zeta_{o}\Phi_{s}}\left[C_{l}^{s} \sin \beta_{o}x + \theta_{l}^{s}(x)\right]$$

From (1.85) and (1.86) we have

$$\left[q_4^{s}(y)\right]_0 = \frac{4\pi}{\omega\zeta_0\Phi_s} \left[ -C_4^{s} \beta_0 \sin \beta_0 y + \frac{\partial \theta_4^{s}(y)}{\partial y} \right]$$

$$\left[q_{1}^{s}(x)\right]_{0} = \frac{4\pi}{\omega \zeta_{0} \Phi_{s}} \left[C_{1}^{s} \beta_{0} \cos \beta_{0} x + \frac{\partial \theta_{1}^{s}(x)}{\partial x}\right]$$

First order currents are formulated as follows:

$$\begin{bmatrix} \mathbf{I_{4y}^{s}}(y) \end{bmatrix}_{1} = \begin{bmatrix} \mathbf{I_{4y}^{s}}(y) \end{bmatrix}_{0} + \frac{4\pi}{\mu \underbrace{\Phi_{o}^{s}}} \left\{ \mathbf{A_{4y}^{s}} - \frac{\mu_{o}^{s}}{4\pi} \right\}$$

$$\cdot \int_{h_{2}}^{h_{2}} \left[ I_{4y}^{s}(y') \right]_{0} K_{1A}(y, y') dy'$$
 (1.98)

$$\begin{bmatrix} I_{1x}(x) \end{bmatrix} = \begin{bmatrix} I_{1x}(x) \end{bmatrix}_0 + \frac{4\pi}{\mu_0 \Phi_s} \left\{ A_{1x}^s - \frac{\mu_0}{4\pi} \right\}$$

$$\cdot \int_{-h_1}^{n_1} \left[ I_{1x}(x') \right]_0 K_{2A}(x, x') dx'$$
 (1.99)

In effect, (1.98) and (1.99) can be rewritten as

$$\begin{bmatrix}
I_{4y}^{s}(y)
\end{bmatrix}_{1}^{2} = 2 \begin{bmatrix}
I_{4y}^{s}(y)
\end{bmatrix}_{0} - \frac{1}{\Phi_{s}} \int_{-h_{2}}^{h_{2}} \begin{bmatrix}
I_{4y}^{s}(y')
\end{bmatrix}_{0} K_{1A}(y, y') dy' \qquad (1.100)$$

$$\begin{bmatrix}
\mathbf{I}_{1\mathbf{x}}(\mathbf{x})
\end{bmatrix}_{1} \cong 2 \begin{bmatrix}
\mathbf{I}_{1\mathbf{x}}(\mathbf{x})
\end{bmatrix}_{0} - \frac{1}{\Phi_{\mathbf{s}}} \qquad \int_{-h_{1}}^{h_{1}} \begin{bmatrix}
\mathbf{I}_{1\mathbf{x}}(\mathbf{x}')
\end{bmatrix}_{0} K_{2\mathbf{A}}(\mathbf{x}, \mathbf{x}') d\mathbf{x}' \qquad (1.101)$$

The substitution of the zeroth order solutions in (1.100) and (1.101) yields

$$\begin{split} \begin{bmatrix} I_{4y}^{s}(y) \end{bmatrix}_{1} &= \frac{-j4\pi}{\zeta_{0}\Phi_{s}} \left\{ 2 \left[ C_{4}^{s} \cos \beta_{0} y + \theta_{4}^{s}(y) \right] \right. \\ &\left. - \frac{C_{4}^{s}}{\Phi_{s}} \int_{-h_{2}}^{h_{2}} \cos \beta_{0} y' K_{1A}(y, y') dy' \right. \\ &\left. - \frac{1}{\Phi_{s}} \int_{-h_{2}}^{h_{2}} \theta_{4}^{s}(y') K_{1A}(y, y') dy' \right\} \\ &= \frac{-j4\pi}{\zeta_{0}\Phi_{s}} \left\{ C_{4}^{s} \left[ 2 \cos \beta_{0} y - \frac{T_{ca}(y)}{\Phi_{s}} \right] + 2 \theta_{4}^{s}(y) - \frac{n_{1}^{s}(y)}{\Phi_{s}} \right\} \\ &= \frac{-j4\pi}{\zeta_{0}\Phi_{s}} \left\{ C_{4}^{s} L_{1}^{s}(y) + 2 \theta_{4}^{s}(y) - N_{1}^{s}(y) \right\} \end{split}$$

$$(1.102)$$

where

$$L_1^{s}(y) = 2 \cos \beta_0 y - \frac{T_{ca}(y)}{\Phi_s}$$
 (1.103)

$$N_1^s(y) = \frac{n_1^s(y)}{\Phi_s}$$
 (1.104)

$$T_{ca}(y) = \int_{-h_2}^{h_2} \cos \beta_0 y' K_{1A}(y, y') dy'$$
 (1.105)

$$n_1^s(y) = \int_{-h_2}^{h_2} \theta_4^s(y') K_{1A}(y, y') dy'$$
 (1.106)

$$\left[I_{lx}(x)\right]_{l} = \frac{-j4\pi}{\zeta_{o}\Phi_{s}} \left\{ 2\left[C_{l}^{s} \sin \beta_{o}x + \theta_{l}^{s}(x)\right] - \frac{C_{l}^{s}}{\Phi_{s}} \right\}$$

$$\int_{-h_{1}}^{h_{1}} \sin \beta_{0} x' K_{2A}(x, x') dx' - \frac{1}{\Phi_{s}} \int_{-h_{1}}^{h_{1}} \theta_{1}^{s}(x') K_{2A}(x, x') dx'$$

$$= \frac{-j4\pi}{\zeta_0 \Phi_s} \left\{ C_1^s \left[ 2 \sin \beta_0 x - \frac{T_{s*d}(x)}{\Phi_s} \right] + 2\theta_1^s(x) - \frac{d_1^s(x)}{\Phi_s} \right\}$$

$$= \frac{-j4\pi}{\zeta_0 \Phi_s} \left\{ C_1^s M_1^s(x) + 2\theta_1^s(x) - D_1^s(x) \right\}$$
 (1.107)

$$M_1^{s}(x) = 2 \sin \beta_0 x - \frac{T_{s*d}(x)}{\Phi_s}$$
 (1.108)

$$D_1^s(x) = \frac{d_1^s(x)}{\Phi_s}$$
 (1.109)

$$T_{s*d}(\mathbf{x}) = \int_{-h_1}^{h_1} \sin \beta_0 \mathbf{x}' K_{2A}(\mathbf{x}, \mathbf{x}') d\mathbf{x}'$$
 (1.110)

$$d_1^s(x) = \int_{h_1}^{h_1} \theta_1^s(x') K_{2A}(x, x') dx'$$
 (1.111)

The scalar potentials  $\varphi_{41}^{\ \ s}$  and  $\varphi_{43}^{\ \ s}$  in (1.45) can be expressed in terms of the charges as

$$\phi_{41}^{s} + \phi_{43}^{s} = \frac{1}{4\pi\epsilon_{o}} \int_{-h_{1}}^{h_{1}} q_{1}^{s}(x') \frac{e^{-j\beta_{o}r_{41}}}{r_{41}} dx'$$

$$+ \frac{1}{4\pi\epsilon_{o}} \int_{-h_{1}}^{h_{1}} q_{3}^{s}(x') \frac{e^{-j\beta_{o}r_{43}}}{r_{43}} dx'$$

$$= \frac{1}{4\pi\epsilon_{0}} \int_{h_{1}}^{h_{1}} q_{1}^{s}(x') K_{1B}(y, x') dx'$$
 (1.112)

$$K_{1B}(y, x') = \frac{e^{-j\beta_0 r_{41}}}{r_{41}} - \frac{e^{-j\beta_0 r_{43}}}{r_{43}}$$
 (1.113)

$$r_{41} = \sqrt{(h_2 - y)^2 + (h_1 - x')^2}$$
 (1.114)

$$r_{43} = \sqrt{(h_2 + y)^2 + (h_1 - x')^2}$$
 (1.115)

Similarly,

$$\phi_{12}^{s} + \phi_{14}^{s} = \frac{1}{4\pi\epsilon_{0}} \int_{-h_{2}}^{h_{2}} q_{2}^{s}(x') \frac{e^{-j\beta_{0}r_{12}}}{r_{12}} dy'$$

$$+\frac{1}{4\pi\epsilon_{0}}\int_{-h_{2}}^{h_{2}}q_{4}^{s}(x')\frac{e^{-j\beta_{0}r_{14}}}{r_{14}}dy'$$

$$= \frac{1}{4\pi\epsilon_0} \int_{-h_2}^{h_2} q_4^{s}(x^2) K_{2B}(x, y^2) dy^2$$
(1.116)

$$K_{2B}(x, y') = \frac{e^{-j\beta_0 r_{12}}}{r_{12}} + \frac{e^{-j\beta_0 r_{14}}}{r_{14}}$$
 (1.117)

$$r_{12} = \sqrt{(h_2 - y')^2 + (h_1 + x)^2}$$
 (1.118)

$$r_{14} = \sqrt{(h_2 - y')^2 + (h_1 - x)^2}$$
 (1.119)

With (1.51) and (1.112), (1.45) can be rewritten as

$$\phi_4^s = \phi_{44}^s + \phi_{42}^s + \phi_{41}^s + \phi_{43}^s$$

$$= \frac{j \omega}{\beta_0^2} \frac{\partial A_{4y}^{s}(y)}{\partial y} + \frac{1}{4\pi\epsilon_0} \int_{-h_1}^{h_1} q_1^{s}(x') K_{1B}(y, x') dx'$$
(1.120)

Similarly, with (1.64) and (1.116), (1.58) becomes

$$\phi_1^s = \phi_{11}^s + \phi_{13}^s + \phi_{12}^s + \phi_{14}^s$$

$$= \frac{j\omega}{\beta_0^2} - \frac{\partial A_{1x}^s}{\partial x} + \frac{1}{4\pi\epsilon_0} - \int_{-h_2}^{h_2} q_4^s(y') K_{2B}(x, y') dy'$$
(1.121)

If we substitute the zeroth order solutions in (1.120) and (1.121) we obtain

$$\phi_4^s(y) = \frac{j\omega}{\beta_0^2} \frac{-j}{v_0} \left[ -C_4^s \sin \beta_0 y + \frac{\partial_4 \theta_s^s(y)}{\partial y} \right]$$

$$+\frac{1}{4\pi\epsilon_0}\int_{-h_1}^{h_1}\left[q_1^s(x')\right]_0K_{1B}(y,x')dx'$$

$$= -C_4^s \sin \beta_0 y + \frac{1}{\beta_0} \frac{\partial \theta_4^s(y)}{\partial y} + \frac{C_1^s}{\Phi_s} \int_{-h_1}^{h_1} \cos \beta_0 x' K_{1B}(y, x') dx'$$

$$+\frac{1}{\Phi_{s}\beta_{o}}\int_{-h_{1}}^{h_{1}}\frac{\partial\theta_{1}^{s}(\mathbf{x}')}{\partial\mathbf{x}'} K_{1B}(\mathbf{y},\mathbf{x}') d\mathbf{x}'$$

$$= -C_4^s \sin \beta_0^{\prime} y + \frac{1}{\beta_0^{\prime}} \frac{\partial \theta_4^{\prime s}(y)}{\partial y} + C_1^s \frac{T_{cd}(y)}{\Phi_s} + \frac{f_1^{\prime s}(y)}{\Phi_s}$$

$$= -C_4^{s} (\sin \beta_0 y + \frac{1}{\beta_0}) - \frac{\partial \theta_4^{s}(y)}{\partial y} + C_1^{s} L_2^{s}(y) + F_1^{s}(y)$$
(1.122)

$$L_2^{s}(y) = \frac{T_{cd}(y)}{\Phi_s}$$
 (1.123)

$$F_1^s(y) = \frac{f_1^s(y)}{\Phi_s}$$
 (1.124)

$$T_{cd}(y) = \int_{-h_1}^{h_1} \cos \beta_0 x' K_{lB}(y, x') dx'$$
 (1.125)

$$f_1^s(y) = \frac{1}{\beta_0} \int_{-h_1}^{h_1} \frac{\partial \theta_1^s(\mathbf{x}')}{\partial \mathbf{x}'} K_{1B}(y, \mathbf{x}') d\mathbf{x}'$$
 (1.126)

$$\phi_1^s(x) = \phi_{11}^s + \phi_{13}^s + \phi_{12}^s + \phi_{14}^s$$

$$= \frac{j\omega}{\beta_0^2} \frac{\partial A_{1x}^s}{\partial x} + \frac{1}{4\pi \epsilon_0} \int_{-h_2}^{h_2} q_4^s(y') K_{2B}(x, y') dy'$$

$$= \frac{j\omega}{\beta_0^2} \frac{-j}{v_0} \left\{ C_1^s \beta_0 \cos \beta_0 x + \frac{\partial \theta_1^s(x)}{\partial x} \right\}$$

+ 
$$\frac{1}{4\pi\epsilon_0}$$
  $\int_{-h_2}^{h_2} \left[q_4^s(y')\right]_0 K_{2B}(x, y')dy'$ 

$$= C_1^s \cos \beta_0 x + \frac{1}{\beta_0} \frac{\partial \theta_1^s(x)}{\partial x} - \frac{C_4^s}{\Phi_s} T_{s*a}(x) + \frac{f_2^s(x)}{\Phi_s}$$

$$= C_1^{s} \cos \beta_0 x + \frac{1}{\beta_0} \frac{\partial \theta_1^{s}(x)}{\partial x} - C_4^{s} M_2^{s}(x) + F_2^{s}(x)$$
(1.127)

$$M_2^{s}(x) = \frac{T_{s*a}(x)}{\Phi_s}$$
 (1.128)

$$F_2^s(x) = \frac{f_2^s(x)}{\Phi_s}$$
 (1.129)

$$T_{s*a}(x) = \int_{-h_2}^{h_2} \sin \beta_0 y' K_{2B}(x, y') dy'$$
 (1.130)

$$f_2^s(x) = \frac{1}{\beta_0} \int_{-h_2}^{h_1} \frac{\partial \theta_4^s(y^i)}{\partial y^i} K_{2B}(x, y^i) dy^i$$
 (1.131)

The boundary conditions to be used for the first order solutions are:

(a) Current at the corners being continuous

i.e.,

$$I_{4y}^{s}(y = h_2) = -I_{1x}^{s}(x = h_1)$$
 (1,132)

(b) Scalar potential at the corners being continuous

i.e.,

$$\phi_4^{s}(y = h_2) = \phi_1^{s}(x = h_1)$$
 (1.133)

Substitution of (1.102) and (1.107) in (1.132) gives

$$C_{4}^{s}L_{1}^{s}(h_{2}) + 2\theta_{4}^{s}(h_{2}) - N_{1}^{s}(h_{2})$$

$$= -\left[C_{1}^{s}M_{1}^{s}(h_{1}) + 2\theta_{1}^{s}(h_{1}) - D_{1}^{s}(h_{1})\right] \qquad (1.134)$$

With (1.122) and (1.127), (1.133) becomes

$$-C_{4}^{s} \sin \beta_{0}h_{2} + \frac{1}{\beta_{0}} \frac{\partial \theta_{4}^{s}(y)}{\partial y} + C_{1}^{s}L_{2}^{s}(h_{2}) + F_{1}^{s}(h_{2})$$

$$= C_{1}^{s} \cos \beta_{0} h_{1} + \frac{1}{\beta_{0}} \frac{\partial \theta_{1}^{s}(x)}{\partial x} \bigg|_{x = h_{1}} - C_{4}^{s} M_{2}^{s}(h_{1}) + F_{2}^{s}(h_{1})$$
(1.135)

Solving (1.134) and (1.135) for  $C_4^{\ \ s}$  and  $C_1^{\ \ s}$  , we obtain

$$C_{4}^{s} = \frac{\left[2\theta_{4}^{s}(h_{2}) + 2\theta_{1}^{s}(h_{1}) - N_{1}^{s}(h_{2}) - D_{1}^{s}(h_{1})\right] \left[\cos\beta_{0}h_{1} - L_{2}^{s}(h_{2})\right]}{H_{1}^{s}(h_{1})\left[\frac{1}{\beta_{0}} \frac{\partial\theta_{4}^{s}(y)}{\partial y}\right] - \frac{1}{\beta_{0}} \frac{\partial\theta_{1}^{s}(x)}{\partial x}\right] + F_{1}^{s}(h_{2}) - F_{2}^{s}(h_{1})}{x = h_{1}}$$

$$C_{4}^{s} = \frac{M_{1}^{s}(h_{1})\left[\sin\beta_{0}h_{2} - M_{2}^{s}(h_{1})\right] - L_{1}^{s}(h_{2})\left[\cos\beta_{0}h_{1} - L_{2}^{s}(h_{2})\right]}{(1.136)}$$

$$C_{1}^{s} = \frac{\begin{bmatrix} \overline{2\theta_{4}^{s}}(h_{2}) + 2\theta_{1}^{s}(h_{1}) - N_{1}^{s}(h_{2}) - D_{1}^{s}(h_{1}) \end{bmatrix} [\sin \beta_{0}h_{2} - M_{2}^{s}(h_{1})]}{H_{1}^{s}(h_{2}) \left[ \frac{1}{\beta_{0}} \frac{\partial \theta_{4}^{s}(y)}{\partial y} \right] - \frac{1}{\beta_{0}} \frac{\partial \theta_{1}^{s}(x)}{\partial x} + F_{1}^{s}(h_{2}) - F_{2}^{s}(h_{1}) \end{bmatrix}} + F_{1}^{s}(h_{2}) - F_{2}^{s}(h_{1}) \right]} C_{1}^{s} = \frac{M_{1}^{s}(h_{1}) \left[ \sin \beta_{0}h_{2} - M_{2}^{s}(h_{1}) \right] - L_{1}^{s}(h_{2}) \left[ \cos \beta_{0}h_{1} - L_{2}^{s}(h_{2}) \right]}{(1.137)}$$

For the first approximation, we assume that

$$\theta_4^{s}(y) \simeq \left[\theta_4^{s}(y)\right]_0 = \frac{E_0}{\beta_0}$$
 (1.138)

$$\theta_1^{s}(\mathbf{x}) \simeq \begin{bmatrix} \theta_1^{s}(\mathbf{x}) \\ 0 \end{bmatrix}_0 = 0$$
 (1.139)

Then, (1.106), (1.109), (1.124) and (1.129) can be rewritten as

$$N_1^{s}(y) = \frac{\frac{E_o}{\beta_o}}{\Phi_s} \int_{-h_2}^{h_2} K_{1A}(y, y') dy' = \frac{E_o}{\Phi_s \beta_o} T_{ea}(y)$$
 (1.140)

where

$$T_{ea}(y) = \int_{-h_2}^{h_2} K_{1A}(y, y') dy'$$
 (1.141)

$$D_1^{s}(x) = 0$$
 (1.142)

$$\mathbf{F_1}^{s}(y) = 0$$
 (1.143)

$$\mathbf{F}_{2}^{S}(\mathbf{x}) = 0$$
 (1.144)

With (1.138) and (1.139), (1.136) and (1.137) can be simplified respectively as follows if only the terms with the order of  $\frac{1}{\Phi_s}$  are retained in both numerator and denominator:

$$\begin{bmatrix} C_4^s \\ 1 \end{bmatrix}_1 = -\frac{E_0}{\beta_0} \frac{\cos \beta_0 h_1 + \frac{1}{\Phi_s} B^s}{\cos \beta_0 (h_1 + h_2) + \frac{1}{\Phi_s} G}$$
(1.145)

$$C_{1}^{s} = \frac{E_{o}}{\beta_{o}} \frac{\sin \beta_{o}h_{2} + \frac{1}{\Phi_{s}}}{\cos \beta_{o}(h_{1} + h_{2}) + \frac{1}{\Phi_{s}}} G$$
 (1.146)

$$B^{s} = -\frac{1}{2} \left[ 2 T_{cd}(h_{2}) + T_{ea}(h_{2}) \cos \beta_{o} h_{1} \right]$$
 (1.147)

$$G = \frac{1}{2} \left[ T_{s*d}(h_1) \sin \beta_0 h_2 + 2T_{s*a}(h_1) \sin \beta_0 h_1 \right]$$

$$-T_{ca}(h_2) \cos \beta_0 h_1 - 2T_{cd}(h_2) \cos \beta_0 h_2$$
 (1.148)

$$H^{s} = -\frac{1}{2} \left[ T_{ea}(h_{2}) \sin \beta_{0} h_{2} + 2T_{s*a}(h_{1}) \right]$$
 (1.149)

Substituting (1.81), (1.145) and (1.146) in (1.79) and (1.80), we obtain

$$I_{4y}^{s}(y) = \frac{-j4\pi}{\zeta_{o}\Phi_{s}} \left\{ -\frac{E_{o}}{\beta_{o}} - \frac{\cos \beta_{o}h_{1} + \frac{1}{\Phi_{s}}}{\cos \beta_{o}(h_{1} + h_{2}) + \frac{1}{\Phi_{s}}} \cos \beta_{o}y + \theta_{4}^{s}(y) \right\} (1.150)$$

$$\begin{bmatrix} I_{1x}(x) \end{bmatrix}_{1} = \frac{-j4\pi}{\zeta_{0}\Phi_{s}} \left\{ \begin{array}{c} E_{0} \\ \overline{\beta_{0}} \end{array} \right. \frac{\sin \beta_{0}h_{2} + \frac{1}{\Phi_{s}} H^{s}}{\cos \beta_{0}(h_{1} + h_{2}) + \frac{1}{\Phi_{s}}} \sin \beta_{0}x + \theta_{1}^{s}(x) \right\} (1.151)$$

(E) Evaluation of Particular Integrals  $\theta_4^s(y)$  and  $\theta_1^s(x)$ .

Integration by parts enables us to rewrite  $\theta_4^s(y)$  and  $\theta_1^s(x)$  in (1.70) and (1.72) respectively as

$$\theta_4^s(y) = \frac{E_o}{\beta_o} - \int_0^y \frac{\partial}{\partial s} \left[ \phi_{41}^s(s) + \phi_{43}^s(s) \right] \sin \beta_o(y - s) ds$$

$$= \frac{E_o}{\beta_o} + \left[\phi_{41}^{s}(0) + \phi_{43}^{s}(0)\right] \sin \beta_o y$$

$$+\beta_0 \int_0^y \left[\phi_{41}^s(s) + \phi_{43}^s(s)\right] \cos\beta_0(y-s) ds$$

$$= \frac{E_{o}}{\beta_{o}} + \beta_{o} \int_{0}^{y} \left[ \phi_{41}^{s}(s) + \phi_{43}^{s}(s) \right] \cos \beta_{o}(y - s) ds$$
 (1.152)

Equation (1.152) is arrived due to the condition of

$$\phi_{41}^{s}(0) = -\phi_{43}^{s}(0)$$
 (1.153)

Similarly

$$\theta_1^s(x) = -\int_0^x \frac{\partial}{\partial s} \left[ \phi_{12}^s(s) + \phi_{14}^s(s) \right] \sin \beta_0(x - s) ds$$

$$= \left[ \phi_{12}^{s}(0) + \phi_{14}^{s}(0) \right] \sin \beta_{0} x + \beta_{0} \int_{0}^{x} \left[ \phi_{12}^{s}(0) + \phi_{14}^{s}(0) \right] \cos \beta_{0}(x - s) ds$$

$$= 2\phi_{12}^{s}(0)\sin\beta_{0}x + \beta_{0} \int_{0}^{x} \left[\phi_{12}^{s}(s) + \phi_{14}^{s}(s)\right] \cos\beta_{0}(x-s)ds$$
(1.154)

Equation (1.154) is obtained because

$$\phi_{12}^{s}(0) = \phi_{14}^{s}(0)$$
 (1.155)

For the first approximation, we substitute (1.138) and (1.139) in (1.85). and (1.86).

$$q_4^s(y) = -\frac{4\pi\epsilon_0}{\Phi_s} C_4^s \sin \beta_0 y$$
 (1.156)

$$q_1^s(x) = \frac{4\pi\epsilon_0}{\Phi_s} C_1^s \cos \beta_0 x \qquad (1.157)$$

The substitution of (1.157) in (1.112) yields

$$\phi_{41}^{s}(y) + \phi_{43}^{s}(y) = \frac{C_{1}^{s}}{\Phi_{s}} \int_{-h_{1}}^{h_{1}} \cos \beta_{0} x' K_{1B}(y, x') dx'$$

$$= \frac{C_{1}^{s}}{\Phi_{s}} T_{cd}(y)$$
(1.158)

Similarly, with (1.156), (1.116) can be rewritten as

$$\phi_{12}^{s}(x) + \phi_{14}^{s}(x) = \frac{-C_{4}^{s}}{\Phi_{s}} \int_{-h_{2}}^{h_{2}} \sin \beta_{0} y' K_{2B}(x, y') dy'$$

$$= \frac{-C_{4}^{s}}{\Phi_{s}} T_{s*a}(x) \qquad (1.159)$$

With (1.155), (1.159) yields

$$2\phi_{12}(0) = \frac{-C_4^s}{\Phi_s} T_s *a(0)$$
 (1.160)

Substituting (1.158) in (1.152), we obtain

$$\theta_4^s(y) = \frac{E_0}{\beta_0} + \frac{C_1^s \beta_0}{\Phi_s} \int_0^y T_{cd}(s) \cos \beta_0(y - s) ds$$
 (1.161)

Similarly, with (1.158) and (1.159), (1.154) becomes

$$\theta_1^s(x) = -\frac{C_4^s}{\Phi_s} T_{s*a}(0) \sin \beta_0 x - \frac{C_4^s \beta_0}{\Phi_s} \int_0^x T_{s*a}(s) \cos \beta_0 (x-s) ds$$
(1.162)

With (1.146), (1.161) becomes

$$\left[\theta_{4}^{s}(y)\right]_{1} = \frac{E_{o}}{\beta_{o}} + \frac{\sin \beta_{o}h_{2} + \frac{1}{\Phi_{s}} H^{s}}{\cos \beta_{o}(h_{1} + h_{2}) + \frac{1}{\Phi_{s}} G} \xrightarrow{\beta_{o}} \frac{\beta_{o}}{\Phi_{s}} \xrightarrow{E_{o}}$$

$$\cdot \int_0^y T_{cd}(s) \cos \beta_0(y - s) ds$$

$$= \frac{E_{o}}{\beta_{o}} \left[ 1 + \frac{\beta_{o}}{\Phi_{s}} \frac{\sin \beta_{o} h_{2} + \frac{1}{\Phi_{s}} H^{s}}{\cos \beta_{o} (h_{1} + h_{2}) + \frac{1}{\Phi_{s}} G} t_{cd}(y) \right]$$
(1.163)

where

$$t_{cd}(y) = \int_0^y T_{cd}(s) \cos \beta_0(y - s) ds$$
 (1.164)

Similarly, the substitution of (1.145) in (1.162) gives

$$\left[\theta_{1}^{s}(\mathbf{x})\right]_{1} = \frac{E_{o}}{\beta_{o}\Phi_{s}} \frac{\cos\beta_{o}h_{1} + \frac{1}{\Phi_{s}}B^{s}}{\cos\beta_{o}(h_{1} + h_{2}) + \frac{1}{\Phi_{s}}G}$$

$$\cdot \left[ T_{s*a}(0) \sin \beta_0 x + \beta_0 \int_0^x T_{s*a}(s) \cos \beta_0 (x - s) ds \right]$$

$$= \frac{E_{o}}{\beta_{o}} \frac{\cos \beta_{o} h_{1} + \frac{1}{\Phi_{s}} B^{s}}{\Phi_{s} \left[\cos \beta_{o} (h_{1} + h_{2}) + \frac{1}{\Phi_{s}} G\right]}$$

$$\cdot \left[ T_{s*a}(0) \sin \beta_{o} x + \beta_{o} t_{s*a}(x) \right]$$
 (1.165)

where

$$t_{s*a}(x) = \int_{0}^{x} T_{s*a}(s) \cos \beta_{o}(x - s) ds$$
 (1.166)

With (1.163), (1.150) becomes

$$\begin{bmatrix}
I_{4y}^{s}(y)
\end{bmatrix}_{ll} = \frac{j4\pi}{\zeta_{o}\Phi_{s}} \quad \frac{E_{o}}{\beta_{o}} \quad \mathbf{x}$$

$$\begin{bmatrix}
\cos \beta_0 h_1 \cos \beta_0 y - \cos \beta_0 (h_1 + h_2) \end{bmatrix} + \frac{1}{\Phi_s} \begin{bmatrix} B^s \cos \beta_0 y - \beta_0 \sin \beta_0 h_2 t_{cd}(y) - G \end{bmatrix}$$

$$- \frac{1}{\Phi_s^2} \beta_0 H^s t_{cd}(y)$$

$$\cos \beta_0 (h_1 + h_2) + \frac{1}{\Phi_s} G$$

$$= \frac{j4\pi}{\zeta_0 \Phi_s} \frac{E_0}{\beta_0}$$

$$\cdot \frac{\left[\frac{\cos \beta_{0}h_{1} \cos \beta_{0}y - \cos \beta_{0}(h_{1} + h_{2}) + \frac{1}{\Phi_{s}} P_{41}^{s}(y) + \frac{1}{\Phi_{2}} P_{42}^{s}(y)\right]}{\cos \beta_{0}(h_{1} + h_{2}) + \frac{1}{\Phi_{s}} G}$$
(1.167)

$$P_{41}^{s}(y) = B^{s} \cos \beta_{o} y - \beta_{o} \sin \beta_{o} h_{2} t_{cd}(y) - G$$
 (1.168)

$$P_{42}^{s}(y) = -\beta_0 H^{s}t_{cd}(y)$$
 (1.169)

Similarly, with (1.65), (1.51) becomes

$$\begin{bmatrix} I_{1x}^{s}(x) \end{bmatrix}_{11} = \frac{-j4\pi}{\zeta_{o}\Phi_{s}} \quad \frac{E_{o}}{\beta_{o}} \quad x$$

$$\cos \beta_0(h_1 + h_2) + \frac{1}{\Phi_s} G$$

$$= \frac{-j4\pi}{\zeta_0 \Phi_s} \frac{E_0}{\beta_0}$$

$$\frac{\sin \beta_{0} h_{2} \sin \beta_{0} x + \frac{1}{\Phi_{s}} P_{11}^{s}(x) + \frac{1}{\Phi_{s}^{2}} P_{12}^{s}(x)}{\cos \beta_{0}(h_{1} + h_{2}) + \frac{1}{\Phi_{s}} G}$$
(1.170)

$$P_{11}^{s}(x) = H^{s} \sin \beta_{o} x + \left[T_{s*a}(0) \sin \beta_{o} x + \beta_{o} t_{s*a}(x)\right] \cos \beta_{o} h_{1}$$
(1.171)

$$P_{12}^{s}(x) = B^{s} [T_{s*a}(0) \sin \beta_{o} x + \beta_{o} t_{s*a}(x)]$$
 (1.172)

 $\begin{bmatrix} I_{4y}(y) \end{bmatrix}_{11}$  and  $\begin{bmatrix} I_{1x}(x) \end{bmatrix}_{11}$  involve the double integrals which complicate the problem.

In order to avoid the double integrals, the following method is devised at the expense of decreasing the accuracy. First of all,

substituting (1.138) to (1.144)

in (1.102), we obtain

$$\begin{bmatrix}
I_{4y}^{s}(y) \\
I_{0}^{s}(y)
\end{bmatrix}_{10} = \frac{-j4\pi}{\zeta_{0}} \left\{ -\frac{E_{0}}{\beta_{0}} - \frac{\cos \beta_{0}h_{1} + \frac{1}{\Phi_{s}}}{\cos \beta_{0}(h_{1} + h_{2}) + \frac{1}{\Phi_{s}}} G \right\} \\
\left[ 2\cos \beta_{0}y - \frac{T_{ca}(y)}{\Phi_{s}} \right] + 2\frac{E_{0}}{\beta_{0}} - \frac{E_{0}}{\beta_{0}\Phi_{s}} T_{ea}(y) \right\}$$

$$= \frac{j4\pi}{\zeta_0 \Phi_s} \frac{E_0}{\beta_0} \times$$

$$2 \left[\cos \beta_{0}h_{1} \cos \beta_{0}y - \cos \beta_{0}(h_{1} + h_{2})\right] + \frac{1}{\Phi_{s}} \left[2 B^{s} \cos \beta_{0}y - 2G\right] \\
- \cos \beta_{0}h_{1} T_{ca}(y) + \cos \beta_{0}(h_{1} + h_{2}) T_{ea}(y) \\
+ \frac{1}{\Phi_{s}^{2}} \left[G T_{ea}(y) - B^{s} T_{ca}(y)\right]$$

$$\cos \beta_0(h_1 + h_2) \frac{1}{\Phi_s} G$$

$$= \frac{j4\pi}{\zeta_{o}\Phi_{s}} \frac{H_{o}}{\beta_{o}} \times \frac{2\left[\cos\beta_{o}h_{1}\cos\beta_{o}y - \cos\beta_{o}(h_{1} + h_{2})\right] + \frac{1}{\Phi_{s}}U_{41}^{s}(y) + \frac{1}{\Phi_{s}^{2}}U_{42}^{s}(y)}{\cos\beta_{o}(h_{1} + h_{2}) + \frac{1}{\Phi_{c}}G}$$

$$= \frac{2\left[\cos\beta_{o}h_{1}\cos\beta_{o}y - \cos\beta_{o}(h_{1} + h_{2})\right] + \frac{1}{\Phi_{s}}U_{41}^{s}(y) + \frac{1}{\Phi_{s}^{2}}U_{42}^{s}(y)}{\cos\beta_{o}(h_{1} + h_{2}) + \frac{1}{\Phi_{c}}G}$$

$$= \frac{2\left[\cos\beta_{o}h_{1}\cos\beta_{o}y - \cos\beta_{o}(h_{1} + h_{2})\right] + \frac{1}{\Phi_{s}}U_{41}^{s}(y) + \frac{1}{\Phi_{s}^{2}}U_{42}^{s}(y)}{\sin\beta_{o}(h_{1} + h_{2}) + \frac{1}{\Phi_{c}}G}$$

$$= \frac{1}{2}\left[\cos\beta_{o}h_{1}\cos\beta_{o}y - \cos\beta_{o}(h_{1} + h_{2})\right] + \frac{1}{\Phi_{s}}U_{41}^{s}(y) + \frac{1}{\Phi_{s}^{2}}U_{42}^{s}(y)$$

$$U_{41}^{s}(y) = 2B^{s} \cos \beta_{o} y - 2G - \cos \beta_{o} h_{1} T_{ca}(y) + \cos \beta_{o} (h_{1} + h_{2}) T_{ea}(y)$$
(1.174)

$$U_{42}^{s}(y) = G T_{ea}(y) - B^{s} T_{ca}(y)$$
 (1.175)

Similarly, the substitution of (1.138) to (1.144) in

(1.107) gives

$$\left[I_{1x}^{s}(x)\right]_{10} = \frac{-j4\pi}{\zeta_{o}\Phi_{s}} \left\{ \frac{E_{o}}{\beta_{o}} \frac{\sin\beta_{o}h_{2} + \frac{1}{\Phi_{s}}}{\cos\beta_{o}(h_{1} + h_{2}) + \frac{1}{\Phi_{s}}G} \left[2\sin\beta_{o}x - \frac{T_{s}*d(x)}{\Phi_{s}}\right] \right\}$$

$$= \frac{-j4\pi}{\zeta_0} \frac{E_0}{\beta_0} x$$

$$\frac{2 \sin \beta_{0}h_{2} \sin \beta_{0}x + \frac{1}{\Phi_{s}} \left[2H^{s} \sin \beta_{0}x - \sin \beta_{0}h_{2} T_{s*d}(x)\right] - \frac{g}{\Phi_{s}^{2}}T_{s*d}(x)}{\cos \beta_{0}(h_{1} + h_{2}) + \frac{1}{\Phi_{s}}G}$$

. . .

$$= \frac{-j4\pi}{\zeta_{o}\Phi_{s}} \frac{E_{o}}{\beta_{o}} \frac{2 \sin \beta_{o}h_{2} \sin \beta_{o}x + \frac{1}{\Phi_{s}} g_{11}^{s}(x) + \frac{1}{\Phi_{s}^{2}} g_{12}^{s}(x)}{\cos \beta_{o}(h_{1} + h_{2}) + \frac{1}{\Phi_{s}} G}$$
(1.176)

where

$$g_{11}^{s}(x) = 2H^{s} \sin \beta_{0} x - \sin \beta_{0} h_{2} T_{s*d}(x)$$
 (1.177)

$$g_{12}^{s}(x) = -H^{s} T_{s*d}(x)$$
 (1.178)

### (F) Backscattering Cross Section of a Solid Rectangular Loop

The vector potential, maintained by the induced current in the solid rectangular loop, at an arbitrary point on the axis of the loop and in the far zone of the loop (Fig. 1.15) can be expressed as

$$A^{s} = A_{y}^{s} = \frac{\mu_{o}}{4\pi} \int_{-h_{2}}^{h_{2}} 2 I_{4y}^{s}(y') \frac{e^{-j\beta_{o}R}}{R} dy'$$

$$\cong \frac{\mu_{o}}{2\pi} \quad \frac{e^{-j\beta_{o}R_{o}}}{R_{o}} \quad \int_{-h_{2}}^{h_{2}} \left[I_{4y}^{s}(y')\right]_{11} dy'$$
(1.179)

where

$$R = \sqrt{R_0^2 + y'^2 + h_1^2} \simeq R_0$$
 (1.180)

Substituting (1.167) in (1.179), we have

$$\begin{bmatrix} \mathbf{A}_{\mathbf{y}} \end{bmatrix}_{11} = \mathbf{j} \frac{2\mu_{o}}{\zeta_{o}\beta_{o}} \quad \mathbf{E}_{o} \quad \frac{e^{-\mathbf{j}\beta_{o}R_{o}}}{R_{o}} \quad \frac{\mathbf{J}_{1}}{\Phi_{s} \left[\cos\beta_{o}(\mathbf{h}_{1} + \mathbf{h}_{2}) + \frac{G}{\Phi_{s}}\right]}$$

$$(1.181)$$

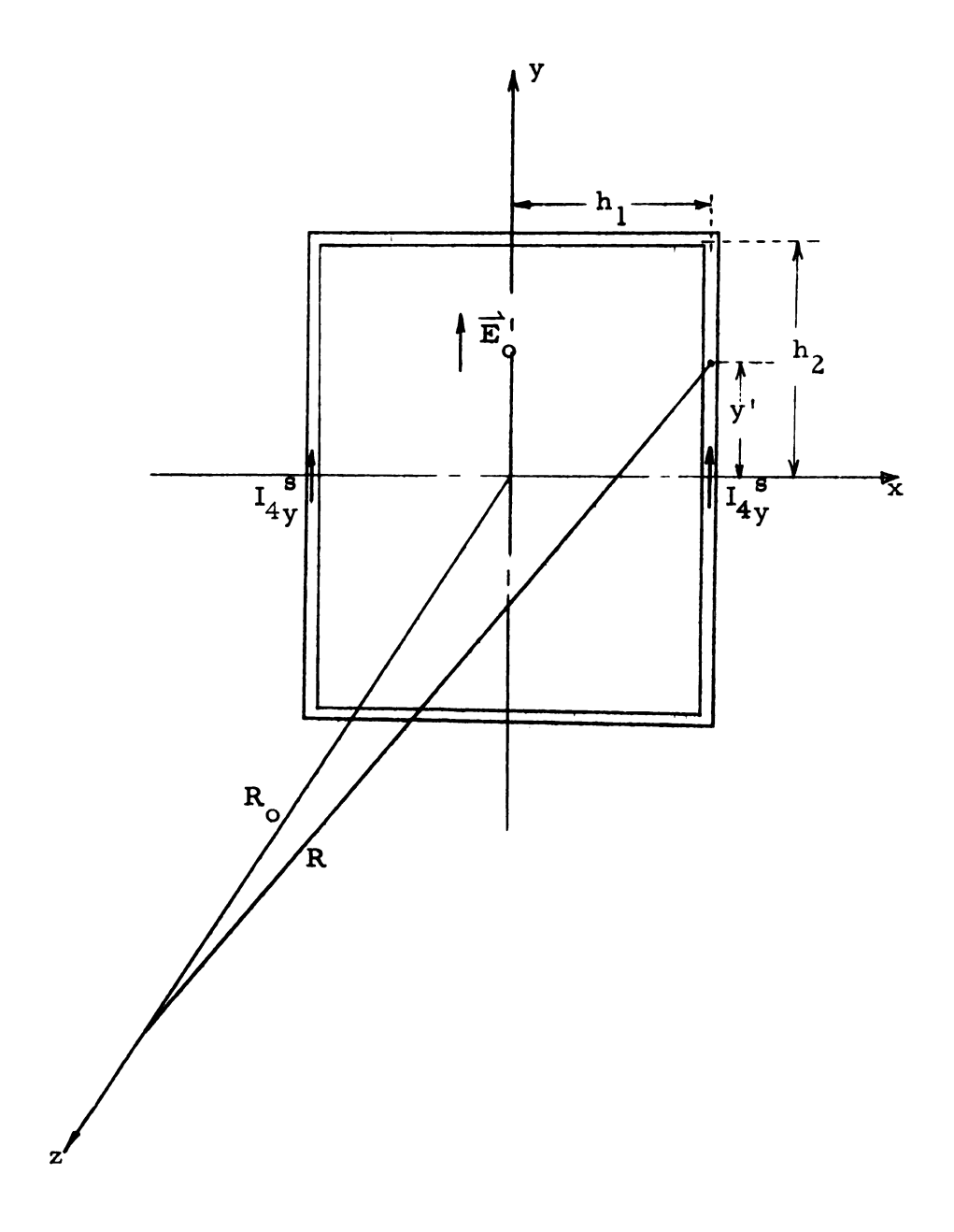


Figure 1.15. Geometry for the calculation of radiation field of a solid rectangular loop.

$$J_{1} = \int_{-h_{2}}^{h_{2}} \left[ \cos \beta_{0} h_{1} \cos y' - \cos \beta_{0} (h_{1} + h_{2}) + \frac{1}{\Phi_{s}} P_{41}^{s}(y') + \frac{1}{\Phi_{s}^{2}} P_{42}^{s}(y') \right] dy'$$

$$(1.182)$$

 $J_1$  will be evaluated later. Consequently the backscattered electric field due to the solid rectangular loop is

$$\begin{bmatrix} \mathbf{E}^{\mathbf{S}} \end{bmatrix}_{11} = \begin{bmatrix} \mathbf{E}_{\mathbf{y}}^{\mathbf{S}} \end{bmatrix}_{11} = -j\omega \begin{bmatrix} \mathbf{A}_{\mathbf{y}}^{\mathbf{S}} \end{bmatrix}_{11}$$

$$= 2\mathbf{E}_{o} \frac{e^{-j\beta_{o}R_{o}}}{R_{o}} \frac{J_{1}}{\Phi_{\mathbf{S}} \left[\cos\beta_{o}(h_{1} + h_{2}) + \frac{G}{\Phi_{\mathbf{S}}}\right]}$$

$$(1.183)$$

The backscattering cross section is found to be

$$\sigma_{\rm B} = \lim_{R_{\rm o} \to \infty} 4\pi R_{\rm o}^2 \frac{\left|E^{\rm s}\right|^2}{\left|E_{\rm o}\right|^2}$$

$$= 16\pi \left| \frac{J_1}{\Phi_s \left[ \cos \beta_0 (h_1 + h_2) + \frac{G}{\Phi_s} \right]} \right|^2$$
(1.184)

 $\sigma_B$  is plotted as the function of  $\beta_0$ h in Figure 1.16 to compare with the experimental results for the case of the square loop where

$$h_1 = h_2 = h = \frac{5.15}{2}$$
 cm and  $a = 0.03$  cm.

The agreement between the theory and the experiment is fairly good over the range where  $\beta$  h is small.

A simpler method in obtaining the backscattering cross section is also presented here. The vector potential at an arbitrary point on the axis of the loop and in the far zone of the loop is calculated on the basis of  $1_{4y}^{s}(y)$ .

$$A^{s} = A_{y}^{s} = \frac{\mu_{6}}{4\pi} \int_{-h_{2}}^{h_{2}} 2 I_{4y}^{s}(y') = \frac{-j\beta_{0}R}{R} dy'$$

$$\approx \frac{\mu_{o}}{2\pi} = \frac{e^{-j\beta_{o}R_{o}}}{R_{o}} \qquad \int_{-h_{2}}^{h_{2}} \left[I_{4y}^{s}(y')\right]_{10} dy'$$

$$(1.185)$$

Substituting (1.173) in (1.185), we have

$$\begin{bmatrix} A_{y} \\ J_{10} \end{bmatrix} = j \frac{2\mu_{o}}{\zeta_{o}\beta_{o}} E_{o} \frac{e^{-j\beta_{o}R_{o}}}{R_{o}} \frac{J_{2}}{\Phi_{s}[\cos\beta_{o}(h_{1}+h_{2})+\frac{G}{\Phi_{s}}]}$$
(1.186)

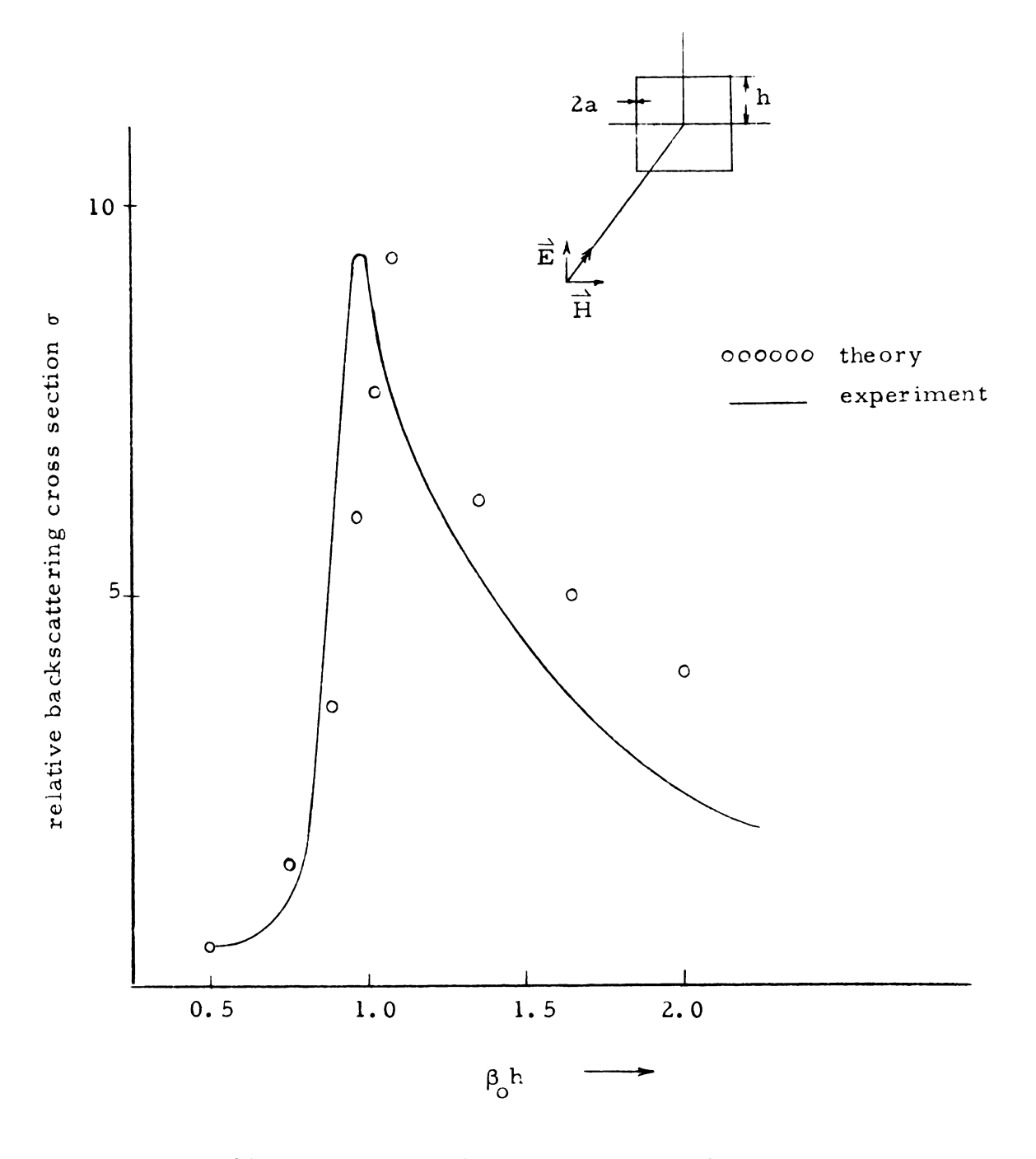


Figure 1.16. Comparison between theory and experiment for a square loop illuminated by a plane wave at normal incidence.

$$J_{2} = \int_{-h_{2}}^{h_{2}} \left[ 2 \cos \beta_{0} h_{1} \cos \beta_{0} y' - 2 \cos \beta_{0} (h_{1} + h_{2}) + \frac{U_{41}^{s}(y')}{\Phi_{s}} + \frac{U_{42}^{s}(y')}{\Phi_{s'}^{2}} \right] dy'$$

$$(1.187)$$

The evaluation of  $J_2$  will be presented later.

The backscattered electric field is, therefore, calculated as

$$\begin{bmatrix} \mathbf{E}^{\mathbf{S}} \end{bmatrix} = \begin{bmatrix} \mathbf{E}_{\mathbf{y}}^{\mathbf{S}} \end{bmatrix} = -\mathbf{j} \omega \begin{bmatrix} \mathbf{A}_{\mathbf{y}}^{\mathbf{S}} \end{bmatrix}$$

$$= 2E_o \frac{e^{-j\beta_o R_o}}{R_o} \frac{J_2}{\Phi_s \left[\cos \beta_o (h_1 + h_2) + \frac{G}{\Phi_s}\right]}$$
(1.188)

Based on (1.188), the backscattering cross section of a solid rectangular loop is found to be

$$\sigma_{\rm B} = \lim_{R_{\rm o} \to \infty} 4\pi R_{\rm o}^2 \frac{\left|E^{\rm s}\right|^2}{\left|E_{\rm o}\right|^2}$$

$$= 16\pi \left[\frac{J_2}{\Phi_{\rm s} \left[\cos \beta_{\rm o}(h_1 + h_2) + \frac{G}{\Phi_{\rm s}}\right]}\right]^2 \tag{1.189}$$

(G) Expansion Parameter  $\Phi_s$ From (1.77) we have

$$\Phi_{s}(y) = \frac{4\pi}{\mu_{o}} \frac{A_{4y}^{s}(y)}{I_{4y}^{s}(y)}$$

Considering the zeroth order current

$$I_{4y}^{s}(y) = \frac{j4\pi}{\zeta_{o s}} \frac{E_{o}}{\beta_{o}} \frac{\cos \beta_{o}h_{1} \cos \beta_{o}y - \cos \beta_{o}(h_{1} + h_{2})}{\cos \beta_{o}(h_{1} + h_{2})}$$

we obtain 
$$h_2$$

$$\int_{-h_2}^{h_2} \left[ \cos \beta_0 h_1 \cos \beta_0 y' - \cos \beta_0 (h_1 + h_2) \right] K_{1A}(y, y') dy'$$

$$\Phi_s(y) = \frac{\cos \beta_0 h_1 \cos \beta_0 y - \cos \beta_0 (h_1 + h_2)}{\cos \beta_0 h_1 \cos \beta_0 y - \cos \beta_0 (h_1 + h_2)}$$

$$= \frac{\cos \beta_{0} h_{1} T_{ca}(y) - \cos \beta_{0}(h_{1} + h_{2}) T_{ea}(y)}{\cos \beta_{0} h_{1} \cos \beta_{0} y - \cos \beta_{0}(h_{1} + h_{2})}$$

For a loop with  $\beta_0(h_1 + h_2) \le \frac{\pi}{2}$ , the point of maximum current is at y = 0. We can then set

$$\Phi_{s} = \left[\Phi_{s}(y)\right]_{y=0} = \frac{\cos \beta_{o} h_{1} T_{ca}(o) - \cos \beta_{o}(h_{1} + h_{2}) T_{ea}(o)}{\cos \beta_{o} h_{1} - \cos \beta_{o}(h_{1} + h_{2})}$$
(1.190)

For a loop with  $\beta_0(h_1+h_2)\geq \frac{\pi}{2}$  , the point of maximum current is at  $y=(h_1+h_2)-\frac{\lambda}{4}$  , so we set

$$\Phi_{s} = \left[\Phi_{s}(y)\right]$$

$$y = h_{1} + h_{2} - \frac{\lambda}{4}$$

$$= \frac{\cos \beta_{0} h_{1} T_{ca}(h_{1} + h_{2} - \frac{\lambda}{4}) - \cos \beta_{0}(h_{1} + h_{2}) T_{ea}(h_{1} + h_{2} - \frac{\lambda}{4})}{\cos \beta_{0} h_{1} \sin \beta_{0}(h_{1} + h_{2}) - \cos \beta_{0}(h_{1} + h_{2})}$$
(1.191)

(H) Evaluation of  $J_1$  and  $J_2$ 

Since

$$J_{1} = \int_{-h^{2}}^{h_{2}} \left[ \cos \beta_{0} h_{1} \cos \beta_{0} y' - \cos \beta_{0} (h_{1} + h_{2}) + \frac{1}{\Phi_{s}} P_{41}^{s}(y') \right]$$

$$+\frac{1}{\Phi_s} P_{42}(y') dy'$$

where

$$P_{41}^{s}(y) = B^{s} \cos \beta_{o} y - \beta_{o} \sin \beta_{o} h_{2} t_{cd}(y) - G$$

$$P_{42}^{s}(y) = -\beta_{o} H^{s} t_{cd}(y)$$

$$J_{1} = \frac{2}{\beta_{0}} \cos \beta_{0} h_{1} \sin \beta_{0} h_{2} - 2h_{2} \cos \beta_{0} (h_{1} + h_{2})$$

$$+ \frac{1}{\Phi_{s}} \left[ \frac{2B^{s}}{\beta_{0}} \sin \beta_{0} h_{2} - \beta_{0} \sin \beta_{0} h_{2} b_{cd} - 2h_{2}G \right]$$

$$-\frac{1}{\Phi_{s}^{2}}$$
  $\beta_{o}$  H<sup>s</sup> b<sub>cd</sub> (1.192)

$$b_{cd} = \int_{-h_2}^{h_2} t_{cd} (y') dy'$$

$$= \int_{-h_2}^{h_2} \left[ \int_{0}^{y'} T_{cd}(s) \cos \beta_0 (y' - s) ds \right] dy'$$
(1.193)

J<sub>1</sub> is difficult to evaluate because of the triple integral involved.

Equation (1.187) shows that

$$J_{2} = \int_{-h_{2}}^{h_{2}} \left[ 2 \cos \beta_{0} h_{1} \cos \beta_{0} y' - 2 \cos \beta_{0} (h_{1} + h_{2}) + \frac{U_{41}^{s}(y')}{\Phi} + \frac{U_{42}^{s}(y')}{\Phi^{2}} \right] dy'$$

$$U_{41}^{s}(y) = 2B^{s} \cos \beta_{0} y - 2G - \cos \beta_{0}h_{1} T_{ca}(y) + \cos \beta_{0}(h_{1} + h_{2}) T_{ea}(y)$$

$$U_{42}^{s}(y) = G T_{ea}(y) - B^{s} T_{ca}(y)$$

or

$$J_2 = \frac{4}{\beta_0} \cos \beta_0 h_1 \sin \beta_0 h_2 - 4h_2 \cos \beta_0 (h_1 + h_2)$$

$$+ \frac{1}{\Phi_s} \left[ \frac{4B^s}{\beta_o} \sin \beta_o h_2 - 4h_2 G - \cos \beta_o h_1 t_{ca} \right]$$

+ 
$$\cos \beta_0 (h_1 + h_2) t_{ea} + \frac{1}{\Phi_s} \left[ G t_{ea} - B^s t_{ca} \right]$$

(1.194)

where

$$t_{ea} = \int_{-h_2}^{h_2} T_{ca}(y') dy'$$
 (1.195)

$$t_{ca} = \int_{-h_2}^{h_2} T_{ea}(y') dy'$$
 (1.196)

#### CHAPTER II

#### MINIMIZATION OF BACKSCATTERING OF A CIRCULAR LOOP

#### 2.1. Introduction

The backscattering cross section of a metallic circular loop was studied in the previous chapter. It was found that when the loop is of resonant size, the induced current on the loop is maximum and likewise the backscattered field. In radar camouflage it is desirable to minimize the backscattering cross section of a loop, in particular, that of a resonant loop. Many investigations have been made in the recent years on the technique of minimizing the radar cross section of a metallic object. Two conventionally used techniques are to utilize radar absorbing material and to reshape the body to change the reflection patterns. Recently, a new method called the impedance loading method has been developed. This method was found to be especially effective in reducing the backscattering cross sections of metallic objects with dimensions of the order of a wavelength. Using this method Chen<sup>4-6</sup> and others<sup>7,8</sup> have investigated the minimization of the backscattering from a cylindrical object. Liepa and Senior have applied the same technique to reduce the radar cross section of a conducting sphere.

The basic principle of the impedance loading method is to control the amplitude and phase of the induced current on the metallic object by inseting appropriate impedances at appropriate points on the object in such a way that the backscatter maintained by the induced current is minimized.

In this chapter, the minimization of the backscattering of a conducting, circular loop by an impedance loading method is investigated.

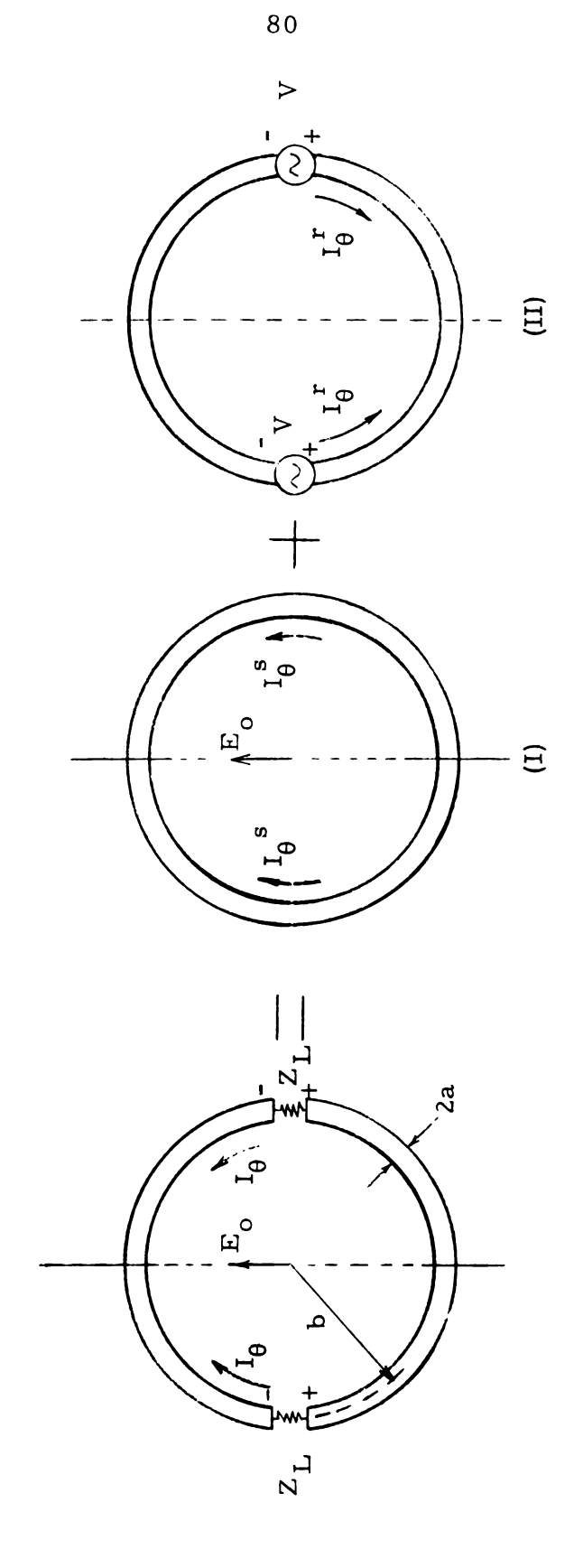
A perfectly conducting, circular loop which is loaded symmetrically with two identical lumped impedances, is assumed to be illuminated by a plane wave at normal incidence.

The induced current on the loaded loop is determined as a function of loop dimensions and loading impedance. The backscattered field maintained by the induced current in the loaded loop is calculated as a function of the loading impedance. It is then possible to find an optimum impedance which makes the back scattered field equal to zero. An explicit expression for the optimum impedance for zero backscattering is obtained as a function of loop dimensions. Some numerical examples are included.

Analytical study on the radiation of a loop is rare in the literature. Storer 10 studied a loop antenna using a method of Fourier series expansion based on a Hallan's integral equation. This method is too complicated for our problem. A new method which is simple enough for our purpose is developed in this research. This new method is based on a differential rather than on an integral equation. The theory is later verified by an experiment.

## 2.2. Theory

Based on the principle of superposition, a loaded circular loop illuminated by a plane wave at normal incidence can be considered as the combination of (A) a solid loop illuminated by a normally incident plane wave, and (B) a loop driven by two identical voltages at  $\theta = 0$  and  $\theta = \pi$ . The situation is shown graphically in Figure 2.1.1. Essentially, case (A) is the scattering of a solid circular loop and case (B) is the radiation of a circular loop antenna. The case (A) has already been solved in Chapter 1 and its results are rewritten here for further development. The problem of case (B) will be solved in this chapter.



A loaded loop is the sum of a scattering loop and a radiating loop. Figure 2.1.1.

After this the results of case (A) will be combined with that of case
(B) to produce the final solution for the problem of the scattering from a loaded loop.

## 2.2.1. Scattering from a Solid Circular Loop

The following equations from Chapter 1 are needed

$$I_{\theta}^{s}(\theta) = \frac{K^{s}E_{o}}{\beta_{s}^{2}b^{2} - 1} \cos \theta \qquad (1.24)$$

for 
$$-\pi \le \theta \le \pi$$

$$E_y^s = -j \frac{\zeta_o}{4} \beta_o b \frac{e^{-\beta_o R_1}}{R_1} \frac{K^s E_o}{\beta_s^2 b^2 - 1}$$
 (1.26)

where  $I_{\theta}^{\ \ s}(\theta)$  is the induced current on the solid circular loop and  $E_y^{\ \ s}$  is the backscattered field on the axis and in the far zone of the loop maintained by the induced current.

#### 2.2.2. Radiation from a Circular Loop

The geometry of the problem is as shown in Figure 2.1.2. The loop is driven by two identical voltages V at  $\theta=0$  and  $\theta=\pi$ . The dimensions of interest are

$$a^2 << b^2$$
 .  $\beta_0^2 a^2 << 1$ 

where  $\beta_0$  is the wave number. We assume that the wire is thin enough so that only the  $\theta$  component of current is induced.

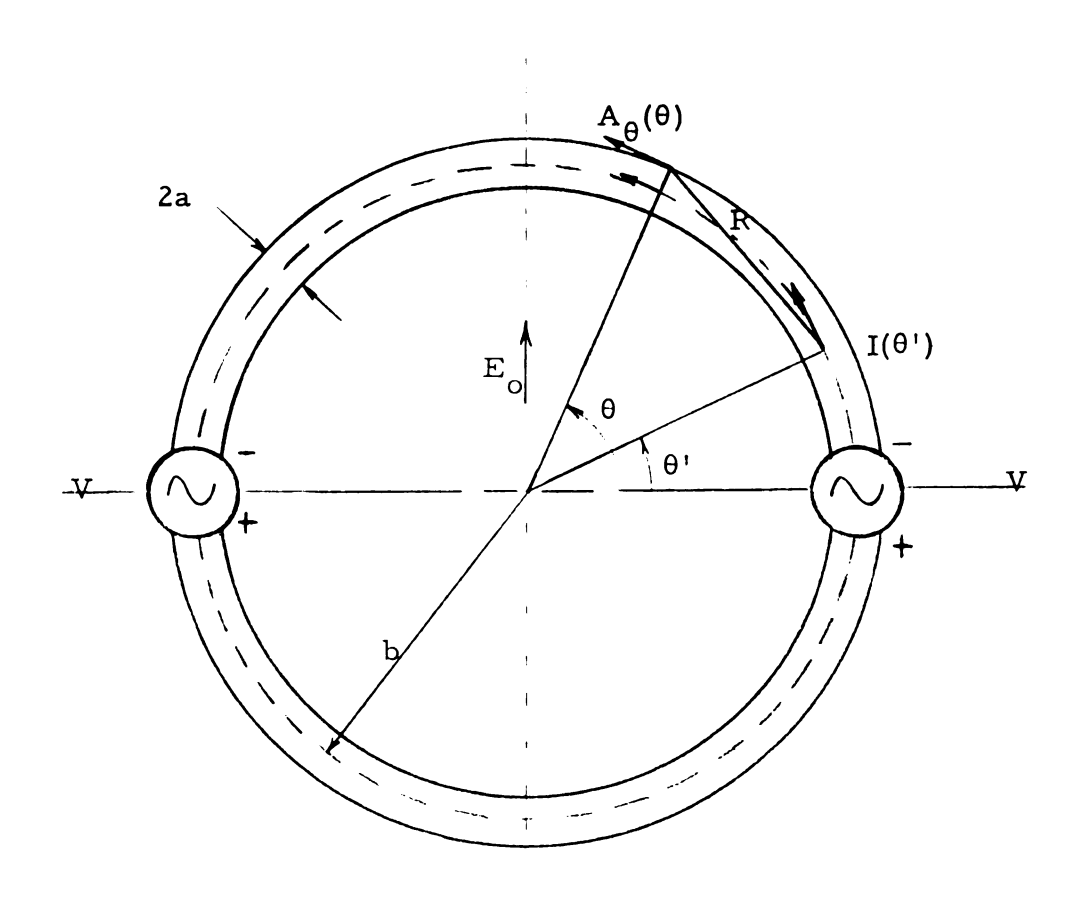


Figure 2.1.2. Geometry of a radiating loop.

## (A) Differential Equation for Loop Current

The total tangential electric field should vanish at the surface of the loop except at the gaps at  $\theta=0$  and  $\theta=\pi$  where voltages of V are maintained. Assuming that the gaps are very small, we obtain the following equation:

$$E_{t}^{a} = \frac{V}{b} \delta(\theta) - \frac{V}{b} \delta(\pi - \theta)$$
 (2.1)

for 
$$-\pi \le \theta \le \pi$$

where  $E_t^a$  is the tangential electric field at the surface of the loop and  $\delta(\theta)$  is a Dirac delta function. Due to the symmetrical configuration, the following conditions exist:

$$I_{\theta}^{r}(\theta) = -I_{\theta}^{r}(\pi - \theta)$$
 (2.2)

$$I_{\theta}^{r} \left(\pm \frac{\pi}{2}\right) = 0$$
 (2.3)

where  $I_{\theta}^{r}(\theta)$  is the current on the loop. This symmetry condition simplifies the problem and we only need to consider a half of the loop. In the right-half of the loop, (2.1) reduces to

$$E_{t}^{a} = \frac{V}{b} \delta(\theta)$$

$$for -\frac{\pi}{2} \le \theta \le \frac{\pi}{2}$$
(2.4)

The tangential electric field maintained by the current and the charge on the loop can be expressed as

$$E_{t}^{a} = -(\nabla \phi^{r})_{\theta} - j \omega A_{\theta}^{r}$$
 (2.5)

where  $\phi^r$  is the scalar potential maintained by the charge on the loop and  $A_{\theta}^{r}$  is the tangential component of the vector potential maintained by the current on the loop.  $\phi^r(\theta)$  can be expressed as

$$\phi^{\mathbf{r}}(\theta) = \frac{1}{4\pi \epsilon_{\mathbf{Q}}} \int_{-\pi}^{\pi} q^{\mathbf{r}}(\theta') \frac{e^{-j\beta_{\mathbf{Q}}R}}{R} bd\theta' \qquad (2.6)$$

where  $q^{r}(\theta)$  is the charge density induced on the loop at  $\theta$ , and

$$R = b\sqrt{4 \sin^2 \frac{\theta - \theta'}{2} + \frac{a^2}{b^2}}$$
 as mentioned in Chapter 1.

Assume that  $\phi^{r}(\theta)$  can be approximated as

$$\phi^{\mathbf{r}}(\theta) = \frac{\Phi^{\mathbf{r}}}{4\pi\epsilon_{0}} \quad q^{\mathbf{r}}(\theta)$$
 (2.7)

where  $\Phi_{\mathbf{q}}^{\mathbf{r}}$  is defined by

$$\Phi_{\mathbf{q}}^{\mathbf{r}} = 4\pi\epsilon_{\mathbf{0}} \frac{\Phi^{\mathbf{r}}(\theta)}{\Phi^{\mathbf{r}}(\theta)}$$
 (2.8)

 $\Phi_{\bf q}^{\bf r}$  is considered to be independent of  $\theta$  because  $\phi^{\bf r}(\theta)$  in (2.6) is mainly contributed by the induced charge  ${\bf q}^{\bf r}(\theta')$  in the vicinity of  $\theta'=\theta$ .

With (2.7), it leads to

$$(\nabla \phi^{\mathbf{r}})_{\theta} = \frac{\Phi_{\mathbf{q}}^{\mathbf{r}}}{4\pi\epsilon_{0}} = \frac{1}{b} = \frac{\partial q^{\mathbf{r}}(\theta)}{\partial \theta}$$
 (2.9)

By the equation of continuity,

$$q^{r}(\theta) = j \frac{1}{\omega} \nabla \cdot \overrightarrow{I}^{r} = j \frac{1}{\omega b} \frac{\partial I_{\theta}^{r}(\theta)}{\partial \theta}$$
 (2.10)

(2.9) can then be rewritten as

$$(\nabla \phi^{\mathbf{r}})_{\underline{\theta}} = \frac{\Phi_{\mathbf{q}}^{\mathbf{r}}}{4\pi\epsilon_{\mathbf{o}}} = \frac{\mathbf{d}^{\mathbf{r}}_{\mathbf{q}}}{4\omega\mathbf{b}^{2}} = \frac{\partial^{2} I_{\mathbf{\theta}}^{\mathbf{r}}(\theta)}{\partial \theta^{2}}$$
(2.11)

Relating  $A_{\theta}^{r}$  to the induced current  $I_{\theta}^{r}(\theta)$  on the loop, we have

$$A_{\theta}^{r}(\theta) = \frac{\mu_{o}}{4\pi} \int_{-\pi}^{\pi} I_{\theta}^{r}(\theta') \frac{e^{-j\beta_{o}R}}{R} \cos(\theta - \theta') bd\theta' \qquad (2.12)$$

where 
$$R = b \sqrt{4 \sin^2 \left(\frac{\theta - \theta'}{2}\right) + \frac{a^2}{b^2}}$$

Assume  $A_{\theta}^{r}(\theta)$  can be approximated as

$$A_{\theta}^{r}(\theta) = \frac{\mu_{o}}{4\pi} \Phi_{i}^{r} I_{\theta}^{r} (\theta)$$
 (2.13)

where  $\Phi_{i}^{\,\,\mathbf{r}}$  is defined by

$$\Phi_{i}^{r} = \frac{4\pi}{\mu_{o}} \frac{A_{\theta}^{r}(\theta)}{I_{\theta}^{r}(\theta)}$$
 (2.14)

 $\Phi_i^r$  here is presumed to be independent of  $\theta$  since (2.12) shows that main contribution to the vector potential at  $\theta$  is due to the current element located in the vicinity of  $\theta$ .

With (2.11) and (2.13), (2.5) can be rewritten as

$$E_{t}^{a} = \frac{-j\Phi_{q}^{r}}{4\pi\epsilon_{0}\omega b^{2}} \left[ \frac{\partial^{2}}{\partial\theta^{2}} + \beta_{0}b^{2}\alpha^{r} \right] I_{\theta}^{r}(\theta)$$
 (2.15)

$$\alpha^{r} = \frac{\Phi_{i}^{r}}{\Phi_{q}^{r}}$$
 (2.16)

The substitution of (2.15) in (2.4) gives

$$\left(\frac{\partial^{2}}{\partial \theta^{2}} + \beta_{r}^{2} b^{2}\right) I_{\theta}^{r}(\theta) = K^{r} \frac{V}{b} \delta(\theta)$$

$$for -\frac{\pi}{2} \le \theta \le \frac{\pi}{2}$$
(2.17)

where

$$\beta_{r}^{2} = \beta_{o}^{2} \alpha^{r} = \beta_{o}^{2} \frac{\Phi_{i}^{r}}{\Phi_{q}^{r}}$$
 (2.18)

$$K^{r} = j \frac{4\pi \epsilon_{o} \omega b^{2}}{\Phi_{q}^{r}}$$
 (2.19)

(B) Solution for Loop Current

The solution for  $I_{\theta}^{-r}(\theta)$  can be expressed as

$$I_{\theta}^{r}(\theta) = C_{1}^{r} \cos \beta_{r} b\theta + C_{2}^{r} \sin \beta_{r} b\theta + P^{r}(\theta)$$
 (2.20)

where  $C_1^r$  and  $C_2^r$  are arbitrary constants, and  $P^r(\theta)$  is a particular integral.  $C_2^r$  is zero due to the symmetry and  $P^r(\theta)$  can be found to be

$$P^{r}(\theta) = \frac{K^{r}V}{2\beta_{r}b^{2}} \sin \beta_{r}b |\theta| \qquad (2.21)$$

The application of the boundary condition of  $I_{\theta}^{r(\frac{\pi}{2})} = 0$  gives

$$C_1^r = \frac{-K^r V}{2\beta_r b^2} \tan \beta_r b \frac{\pi}{2}$$
 (2.22)

Finally, we have

$$I_{\theta}^{r}(\theta) = -\frac{K^{r}V}{2\beta_{r}b^{2}} \operatorname{sec} \beta_{r}b \frac{\pi}{2} \sin \beta_{r}b \left(\frac{\pi}{2} - |\theta|\right)$$
 (2.23)

for 
$$-\pi \le \theta \le \pi$$

The above expression for  $I_{\theta}^{r}(\theta)$  is extended to cover the whole range of  $-\pi \leq \theta \leq \pi$  by making use of the condition  $I_{\theta}^{r}(\theta) = -I_{\theta}^{r}(\pi - \theta)$ . With the current found in (2.23), the vector potential on the axis of the loop and in the far zone of the loop can be calculated as

$$A_{y}^{r} = \frac{\mu_{o}}{4\pi} \int_{-\frac{\pi}{2}}^{\frac{\pi}{2}} 2I_{\theta}^{r}(\theta') \cos \theta' \frac{e^{-j\beta_{o}R_{1}}}{R_{1}} \quad \text{bd} \theta'$$

$$= \frac{\mu_{o}}{4\pi} \frac{e^{-j\beta_{o}R_{1}}}{R_{1}} \frac{K^{r}V}{\beta_{r}^{2}b^{2}-1}$$
 (2. 24)

where  $R_1 = \sqrt{R_0^2 + b^2}$  and  $R_0$  is the distance between the center of the loop and an observation point on the axis of the loop.

The radiated electric field in the far zone of the loop is

$$E_{y}^{r} = -j \omega A_{y}^{r} = -j \omega \frac{\mu_{o}}{2\pi} \frac{e^{-j\beta_{o}R_{1}}}{R_{1}} \frac{K^{r}V}{\beta_{r}^{2}b^{2}-1}$$
 (2.25)

 $\boldsymbol{K}^{\boldsymbol{r}}$  and  $\boldsymbol{\beta}_{\boldsymbol{r}}$  are determined in a following section.

## 2.2.3. Total Current and Total Back Scattered Field

Total current can be obtained by superposing  $I_{\theta}^{\ s}(\theta)$  upon  $I_{\theta}^{\ r}(\theta)$  as follows:

$$I_{\theta}(\theta) = I_{\theta}(\theta) + I_{\theta}^{r}(\theta)$$

$$= \frac{K^{s} E_{o}}{\beta_{s}^{2} b^{2} - 1} \cos \theta$$

$$- \frac{K^{r} V}{2\beta_{r} b^{2}} \sec \beta_{r} b \frac{\pi}{2} \sin \beta_{r} b \left(\frac{\pi}{2} - |\theta|\right)$$
(2.26)

Based on the principle of superposition, V is found to be

$$V = \left[I_{\theta}^{s}(0) + I_{\theta}^{r}(0)\right] Z_{L}$$
 (2.27)

for  $-\pi \le \theta \le \pi$ 

With (1.24) and (2.23), V is determined as

$$V = \frac{2 \beta_r b^2}{2\beta_r b^2 + Z_L K^r \tan \beta_r b \frac{\pi}{2}} = \frac{Z_L K^s E_o}{\beta_s^2 b^2 - 1}$$
 (2.28)

The substitution of (2.28) in (2.26) yields a final expression for  $I_{\text{A}}(\theta)$  as

$$I_{\theta}(\theta) = \frac{K^{s}E_{o}}{\beta_{s}^{2}b^{2}-1} \left[ \cos \theta \right]$$

$$-\frac{Z_L K^r \sec \beta_r b \frac{\pi}{2}}{2 \beta_r b^2 + Z_L K^r \tan \beta_r b \frac{\pi}{2}} \sin \beta_r b \left(\frac{\pi}{2} - |\theta|\right)$$
(2.29)

for 
$$-\pi \le \theta \le \pi$$

Total E field in the far zone of the loop can be obtained as

$$E_{y} = E_{y}^{s} + E_{y}^{r}$$

$$= -j\omega \frac{\mu_{o}}{4\pi} \frac{e^{-j\beta_{o}R_{1}}}{R_{1}} \frac{K^{s}E_{o}b}{\beta_{s}^{2}b^{2}-1} \times$$

$$\left[ \pi + \frac{4 Z_{L} K^{r} \beta_{r} b}{(\beta_{r}^{2} b^{2} - 1) (2\beta_{r} b^{2} + Z_{L} K^{r} \tan \beta_{r} b \frac{\pi}{2})} \right]$$
(2.30)

# 2.2.4. Optimum Impedance for Zero Back Scattering

To minimize the backscattering to zero, total field in (2.30) is set equal to zero. This leads to

$$\pi + \frac{4Z_L K^r \beta_r b}{(\beta_r b^2 - 1) (2\beta_r b^2 + Z_L K^r \tan \beta_r b \frac{\pi}{2})} = 0$$
 (2.31)

Solving (2.31) for  $Z_L$ , we obtain the optimum impedance for zero back scattering as

With (2.19),  $\begin{bmatrix} z_1 \end{bmatrix}_0$  can be expressed as

- 2.2.5. Determination of  $\Phi_q^r$  and  $\Phi_i^r$
- (A) By making use of (2.23) and the equation of continuity, we have

$$q^{r}(\theta) = j \frac{1}{\omega b} \frac{\partial I_{\theta}^{r}(\theta)}{\partial \theta}$$

$$= \pm j \frac{1}{\omega b} \frac{K^{r}V}{2b} \sec \beta_{r} b \frac{\pi}{2} \cos \beta_{r} b \left(\frac{\pi}{2} - |\theta|\right)$$

$$- \text{for } -\pi \leq \theta \leq 0$$

$$(2.35)$$

+ for  $0 \le \theta \le \pi$ 

 $\Phi_{\mathbf{q}}^{\mathbf{r}}$  is then defined as

$$\Phi_{\mathbf{q}}^{\mathbf{r}} = \frac{-\int_{-\pi}^{0} \cos \beta_{\mathbf{r}} b \left(\frac{\pi}{2} + \theta'\right) \frac{e^{-j\beta_{o}R}}{R} b d\theta' + \int_{0}^{\pi} \cos \beta_{\mathbf{r}} b \left(\frac{\pi}{2} - \theta'\right) \frac{e^{-j\beta_{o}R}}{R} b d\theta'}{\cos \beta_{\mathbf{r}} b \left(\frac{\pi}{2} - \theta_{o}\right)}$$

$$\cos \beta_{\mathbf{r}} b \left(\frac{\pi}{2} - \theta_{o}\right)$$
(2.35)

where

$$R = b \sqrt{4 \sin^2 \left(\frac{\theta_0 - \theta^{\dagger}}{2}\right) + \frac{a^2}{b^2}}$$

Choosing  $\theta_0 = \frac{\pi}{2}$ , the point of maximum charge,  $\Phi_q^r$  becomes

$$\Phi_{\mathbf{q}}^{\mathbf{r}} = \int_{0}^{\pi} \cos \beta_{\mathbf{r}} b \left( \frac{\pi}{2} - \theta' \right) K_{3} \left( \theta', \frac{a^{2}}{b^{2}} \right) d\theta'$$
 (2.36)

where

$$K_{3}(\theta', \frac{a^{2}}{b^{2}}) = \frac{e^{-j\beta_{0}b\sqrt{2-2\sin\theta'+\frac{a^{2}}{b^{2}}}}}{\sqrt{2-2\sin\theta'+\frac{a^{2}}{b^{2}}}}$$

$$-j\beta_{0}b\sqrt{2+2\sin\theta'+\frac{a^{2}}{b^{2}}}$$

$$-\frac{e^{-j\beta_{0}b\sqrt{2+2\sin\theta'+\frac{a^{2}}{b^{2}}}}}{\sqrt{2+2\sin\theta'+\frac{a^{2}}{b^{2}}}}$$
(2.37)

In the actual calculation of  $\Phi_q^{\ r},\ \beta_r$  will be replaced by  $\beta_0$  as an approximation.

(B) Similarly,  $\Phi_{i}^{r}$  can be obtained by making use of (2.23) as

$$\Phi_{i}^{r} = \frac{4\pi}{\mu_{o}} \frac{A_{\theta}^{r}(\theta)}{I_{\theta}^{r}(\theta)}$$

$$= \frac{\int_{-\pi}^{\pi} \sin \beta_{r} b \left(\frac{\pi}{2} - |\theta'|\right) \cos (\theta_{o} - \theta') \frac{e^{-j\beta_{o} R}}{R} b d\theta'}{\sin \beta_{r} b \left(\frac{\pi}{2} - |\theta_{o}|\right)}$$
(2.38)

where

$$R = b \sqrt{4 \sin^2 \left(\frac{\theta - \theta'}{2}\right) + \frac{a^2}{b^2}}$$

Choosing

$$\theta_{o} = \begin{cases} 0 & \text{for } \beta_{r}b \leq 1 \\ \frac{\pi}{2} - \frac{\lambda}{4b} & \text{for } \beta_{r}b \geq 1 \end{cases}$$

where  $\boldsymbol{\theta}_{o}$  is the point of maximum current.  $\boldsymbol{\Phi}_{i}^{\;r}$  then becomes

$$\Phi_{i}^{r} = \begin{cases} \frac{1}{\sin \beta_{r} b \frac{\pi}{2}} \int_{-\pi}^{\pi} \sin \beta_{r} b \left(\frac{\pi}{2} - \left|\theta^{\dagger}\right|\right) \cos \theta^{\dagger} K_{4} \left(\theta^{\dagger}, \frac{a^{2}}{b^{2}}\right) d\theta^{\dagger} \\ & \text{for } \beta_{r} b \leq 1 \end{cases}$$

$$\int_{-\pi}^{\pi} \sin \beta_{r} b \left(\frac{\pi}{2} - \left|\theta^{\dagger}\right|\right) \sin \left(\frac{\lambda}{4b} + \theta^{\dagger}\right) K_{5} \left(\theta^{\dagger}, \frac{a^{2}}{b^{2}}\right) d\theta^{\dagger} \\ & \text{for } \beta_{r} b \geq 1 \end{cases} \tag{2.39}$$

where  $K_{4}(\theta^{1}, \frac{a^{2}}{b^{2}}) = \frac{e^{-j\beta_{0}b\sqrt{2-2\cos\theta^{1}+\frac{a^{2}}{b^{2}}}}}{\sqrt{2-2\cos\theta^{1}+\frac{a^{2}}{b^{2}}}}$ (2.40)

$$K_{5}\left(\theta', \frac{a^{2}}{b^{2}}\right) = \frac{e^{-j\beta_{0}b\sqrt{2-2\sin\left(\frac{\lambda}{4b}+\theta'\right)+\frac{a^{2}}{b^{2}}}}}{\sqrt{2-2\sin\left(\frac{\lambda}{4b}+\theta'\right)+\frac{a^{2}}{b^{2}}}}$$
(2.41)

In the actual calculation of  $\Phi_i^{\ r}$  ,  $\ \beta_r$  will be replaced by  $\beta_0$  as an approximation.

# 2.2.6. Numerical Examples

To show the theoretical results graphically,  $\Phi_q^{\ r}$  and  $\Phi_i^{\ r}$  are numerically calculated for the case of  $a^2/b^2=0.00179$  as function of  $\beta_0 b$ . The optimum impedance,  $\begin{bmatrix} Z_L \end{bmatrix}_0$ , is then calculated as a function of  $\beta_0 b$  for the case of  $a^2/b^2=0.00179$ . Numerical results of  $\Phi_q^{\ r}$  and  $\Phi_i^{\ r}$  are shown graphically in Figure 2.2 and 2.3 respectively. The numerical result of  $\begin{bmatrix} Z_L \end{bmatrix}_0$  is shown in Figure 2.4. In Figure 2.2 and 2.3,  $\Phi_q^{\ r}$  and  $\Phi_i^{\ r}$  vary only weakly over the range of interest. This agrees reasonably well with our original assumption of  $\Phi_q^{\ r}$  and  $\Phi_i^{\ r}$  being constant. In Figure 2.4 the following facts are observed:

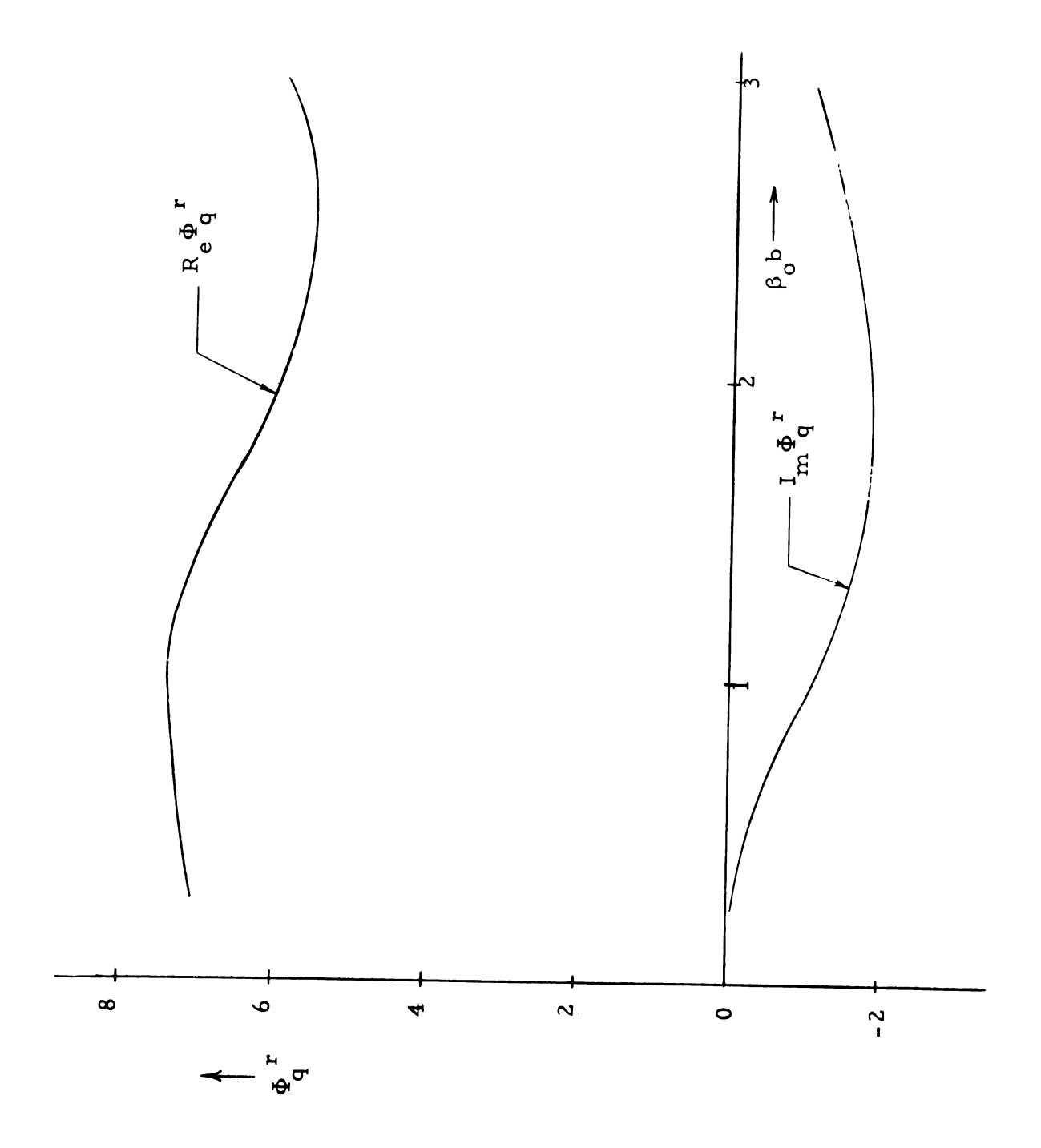


Figure 2.2.  $\Phi_{\mathbf{q}}$  as a function of  $\beta_{o}$  (a<sup>2</sup>/b<sup>2</sup> = 0.00179).

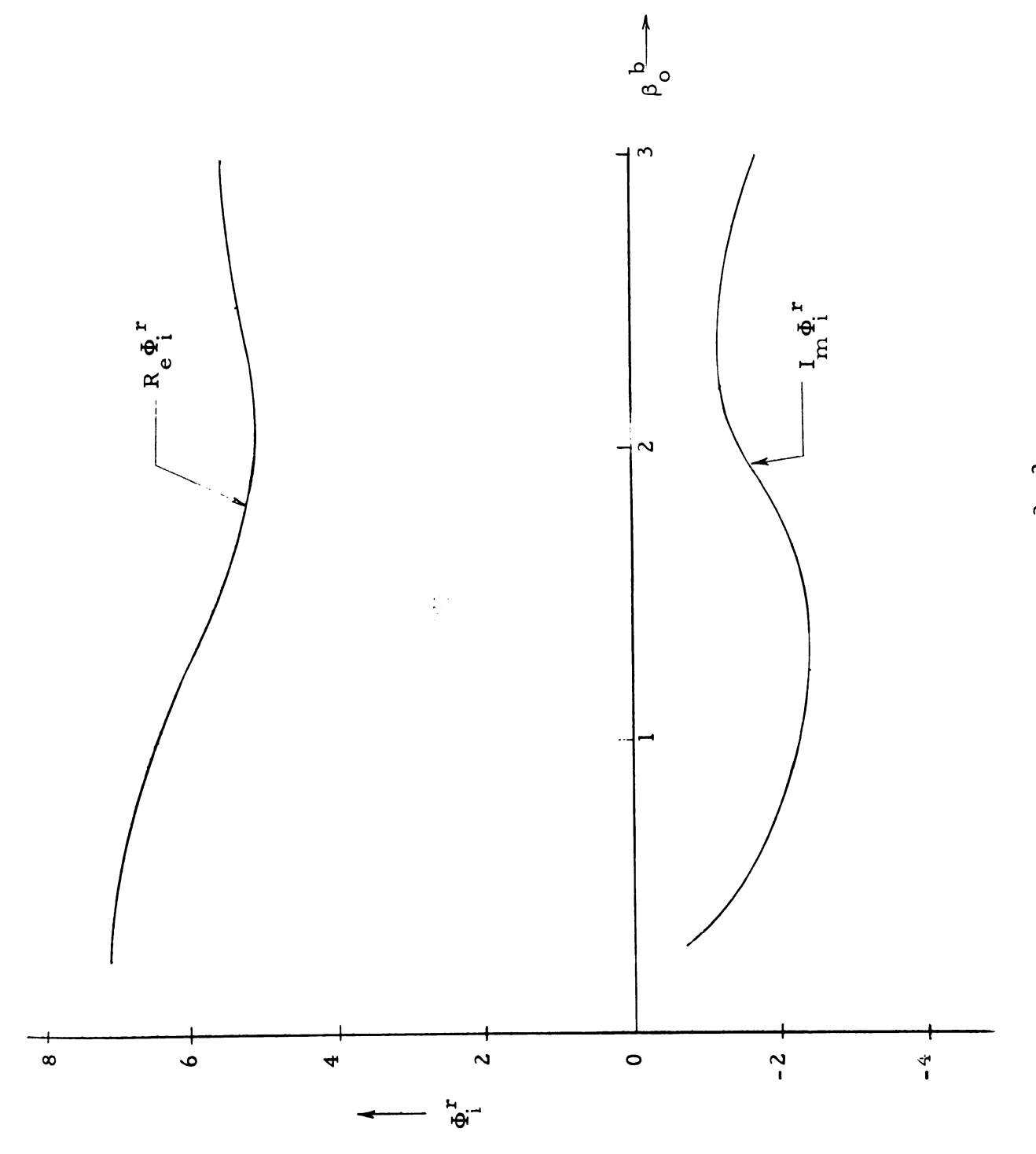


Figure 2.3.  $\Phi_{i}^{r}$  as a function of  $\beta_{o}^{b}$  ( $a^{2}/b^{2} = 0.00179$ ).

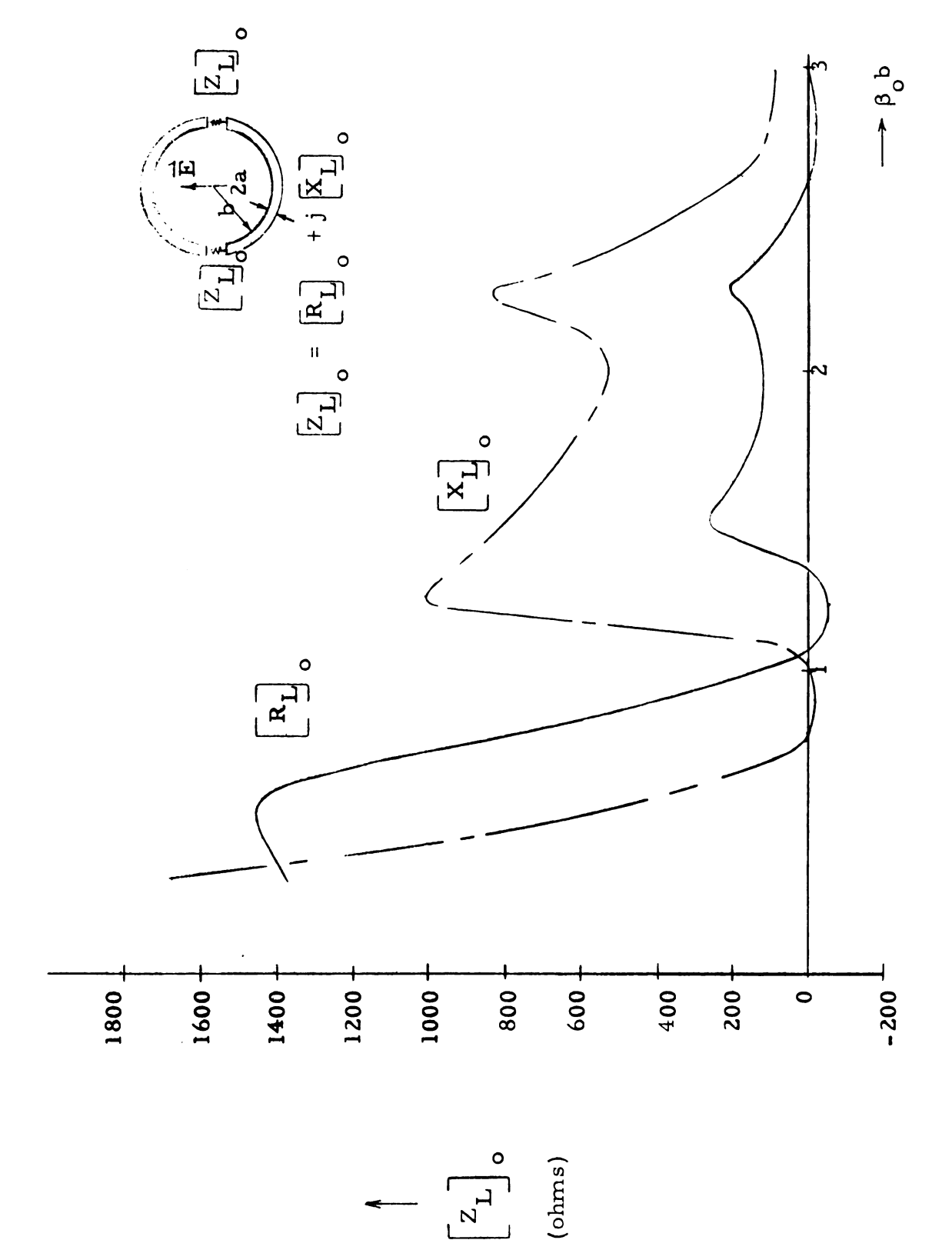


Figure 2.4. Optimum impedance for zero backscattering  $(a^2/b^2 = 0.00179)$ .

- (1) In general, the optimum impedance for zero back scattering needs both a resistive and a reactive component.
- (2) It requires a negative resistance around  $\beta_0 b = 1.25$ and a reactance with negative slope around  $\beta_0 b = 1$ .

### 2.3. Experiment

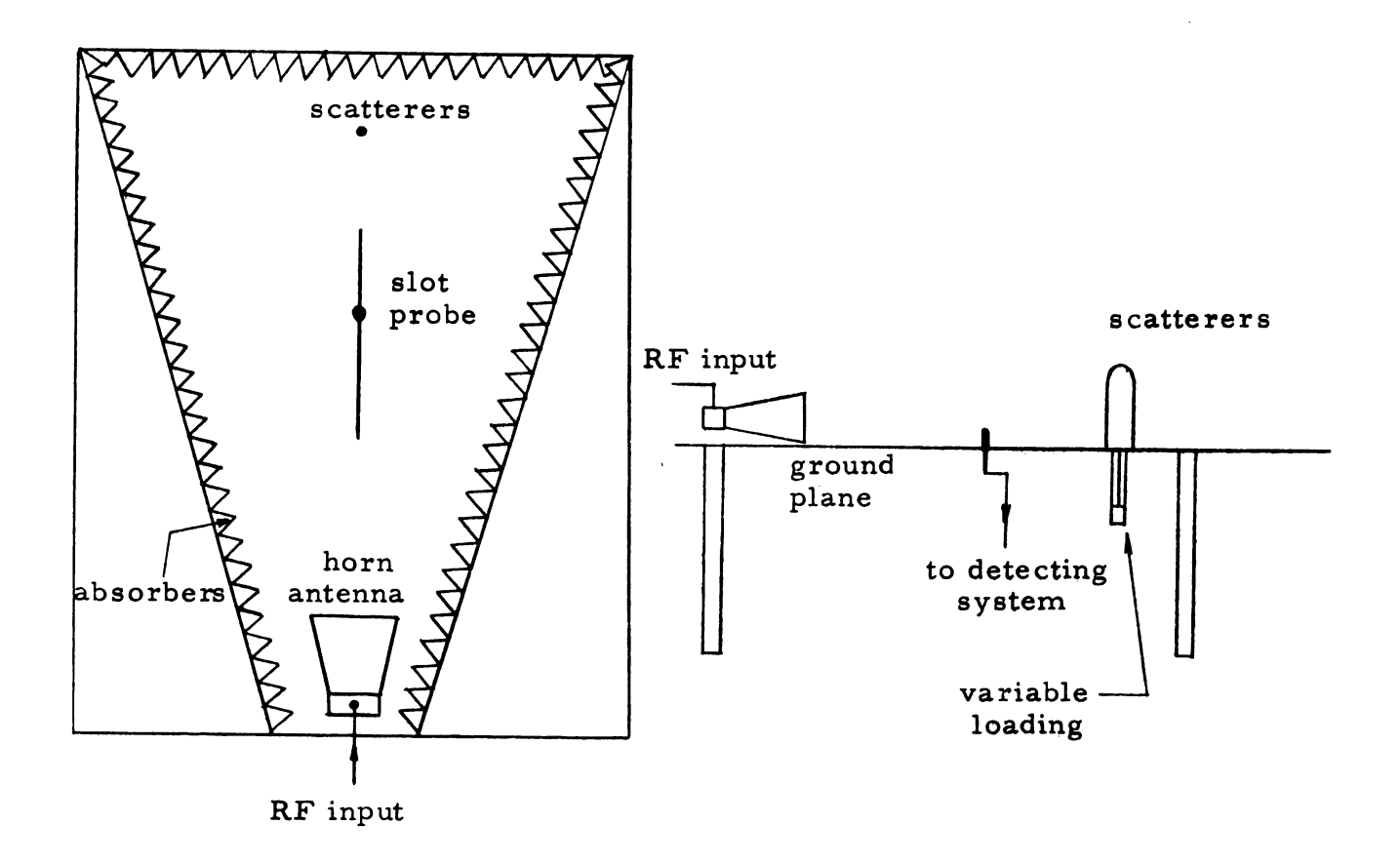
As mentioned in previous section, the optimum impedance for zero backscattering, in general, requires a negative resistance.

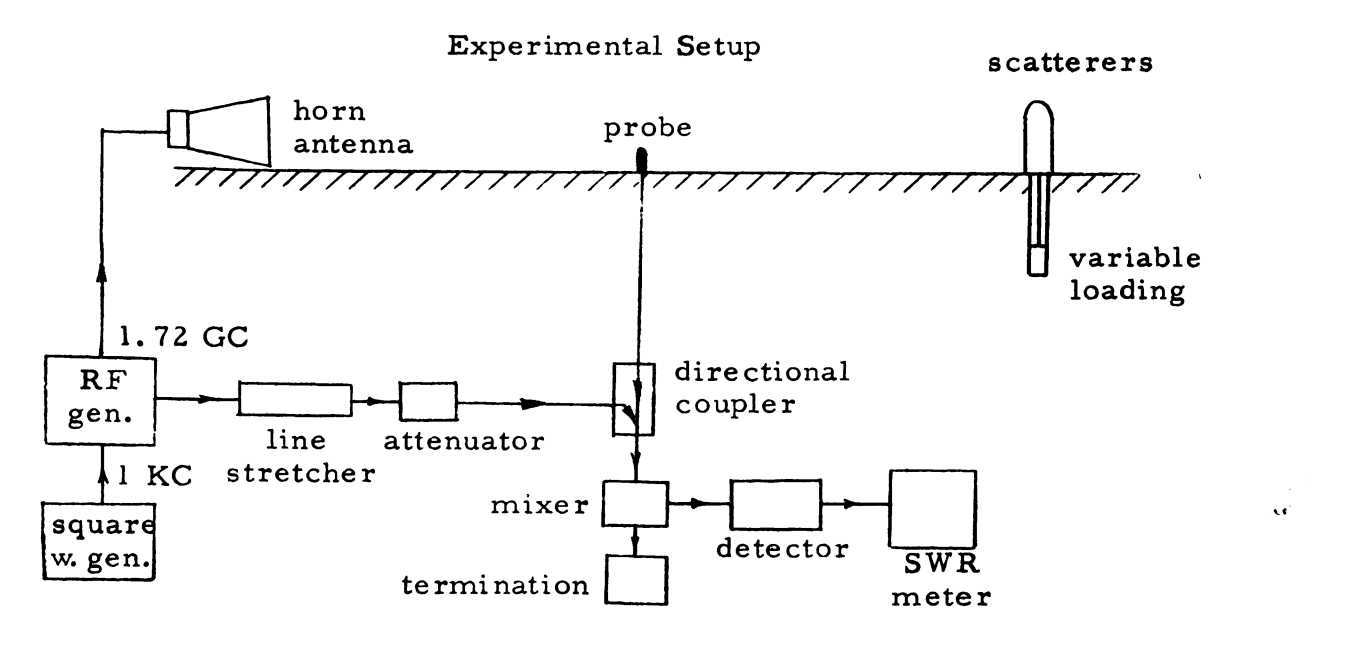
Practically, it is difficult to implement. To simplify the problem, an experiment was conducted for the case of a circular loop loaded with two purely reactive impedances.

In this section, experimental arrangement and experimental results are discussed. The comparison between the theory and the experimental results is also given.

# 2.3.1. Experimental Setup and Measuring Technique

The experimental setup is shown in Figure 2.5. The experiment was conducted inside of an anechoic chamber which is constructed on the top of an aluminum ground plane (10' x 12', 0.125" in thickness). In the experiment, the R.F. signal is radiated from a horn antenna (Scientic Atlanta model 12-1.7) located at one end of the ground plane and the circular loop is placed at the other end. With this arrangement, a plane wave is incident normally upon the loop. A slot is cut at the central part of the ground plane. A thin wire probe (Central Res. Lab. MX-1019/u) protruding out of the ground plane is movable along





Circuit Diagram

Figure 2.5. Experimental setup and circuit diagram.

the slot. The loop is loaded with a pair of identical coaxial lines (characteristic impedance  $Z_c = 50\,\mathrm{n}$ ) underneath the ground plane. This simple device provides a purely reactive loading to the loop. The approximate impedance of the coaxial cavity can be calculated from the well known expression  $Z_L = jZ_c \tan\beta_0 \ell$  where  $Z_c$  is the characteristic impedance of the coaxial cavity,  $\beta_0$  is the wave number and  $\ell$  is the length of the coaxial cavity.

The circuit diagram is also shown in Figure 2.5. The method of cancellation is employed in the experiment. The R.F. signal is generated from a microwave oscillator (GR 1360), modulated by a 1 KC square wave generator. The output of the R.F. oscillator is connected to the horn antenna. When the scatterer is absent, the signal received by the probe is cancelled by a reference signal from the R.F. oscillator through a line stretcher (GR874-LK20L) and an antenuator (ARRA 2414-20). The cancallation of the probe signal by the reference signal is accomplished by the combination of these two signals in a mixer after going through a directional coupler. After the cancellation process is completed, the loop is introduced. The output of the mixer or the reading of SWR meter will then represent the backscattered field by the loop.

# 2.3.2. Experimental Results

A circular loop (diameter = 5.15 cm) was constructed as as an experimental model using cylindrical wire of 0.1 cm radius. The experiment was performed at various frequencies (1.6 GC - 2.5 GC). Experimental results are shown in Figures 2.6 - 2.20 in which the backscattering cross sections of the loop wire plotted as functions of loading impedances at each specified frequency.

The backscattering cross section of the loaded loop is represented by a solid curve and that of the solid loop by a solid straight line. It is observed that if the loading impedance (or the length of the coaxial line) is properly adjusted, the backscatters of the loop can be minimized to the noise level. At each frequency about 15 db reduction in the back scattering cross section was obtained. It was also observed that the scattering in the off broadside direction was reduced when the backscatter in the broadside direction was minimized.

# 2.4. Comparison Between Theory and Experiment

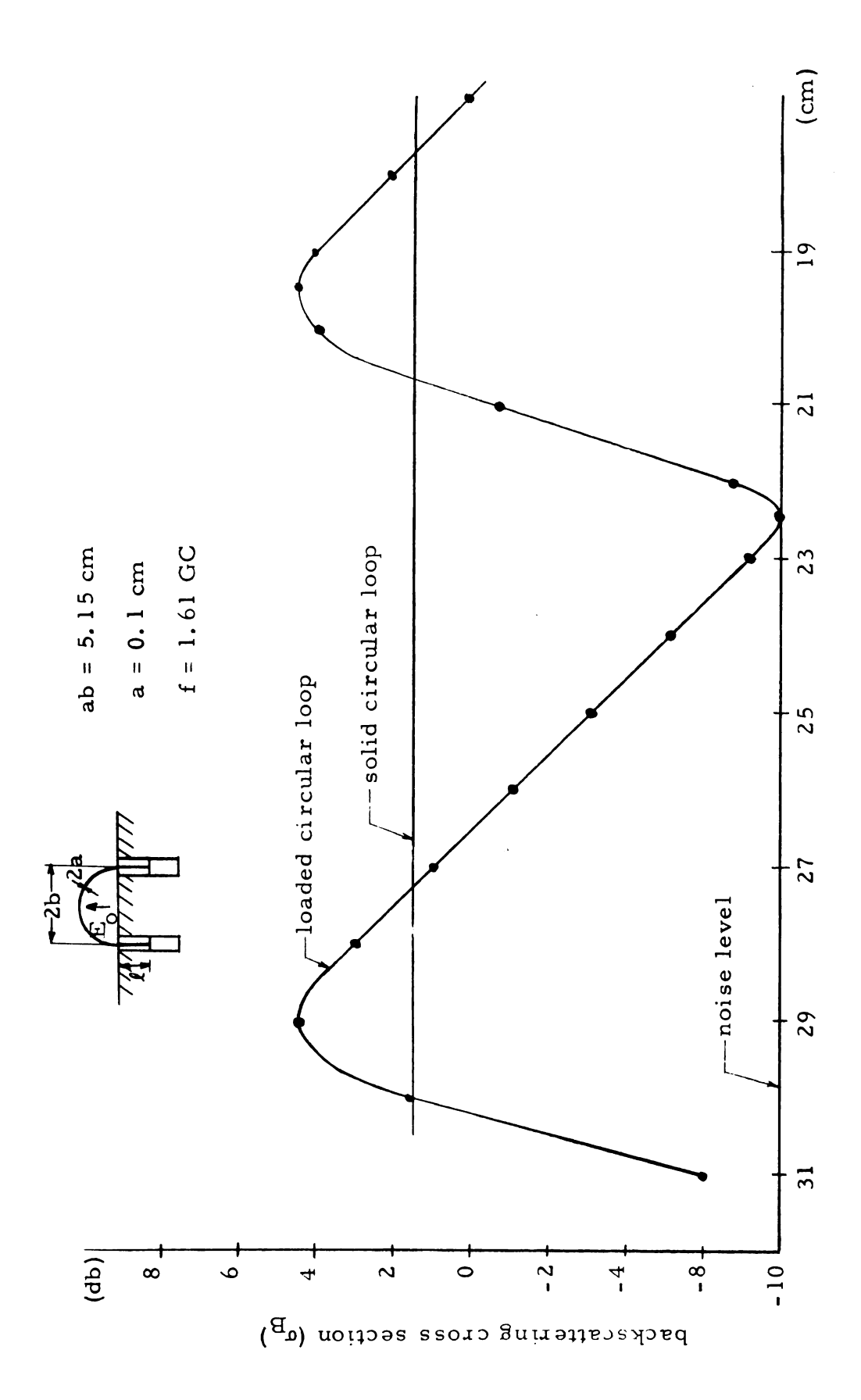
To check the accuracy of the theory, the optimum reactive impedance for the minimum backscattering was numerically calculated and then compared with the experimental results.

The theoretical value for the optimum reactive impedance is calculated as follows:

- (1) In the expression for the total back-scattered field, equation (2.30), the loading impedance  $Z_{L}$  is replaced by  $jX_{L}$ ,
- (2) An expression for the total backscattered field is numerically obtained for a particular frequency as the function of  $\boldsymbol{X}_{\text{T}}$ ,
- (3) A computer program is then set to calculate the particular value of  $\mathbf{X}_{L}$  which gives the minimum value of the total backscattered field,
- (4) Thus the optimum reactive impedance,  $X_L$ , is obtained as a function of  $\beta_0$ b.

The experimental value for the optimum reactive impedance was obtained by taking into account of the stray capacitance which exists at the end of the coaxial line.

The experimental and theoretical results of the optimum reactive impedance for the minimum backscattering are shown graphically in Figure 2.21. The dotted curve represents the experimental results and the solid curve represents that of the theory. The agreement between theory and experiment is reasonably good.



Backscattering cross section of a loaded loop as a function of loading impedance (f = 1.61 GC). Figure 2.6.

(1) length of coaxial line (loading impedance  $Z_L = jZ_c \tan \beta_o I$ )

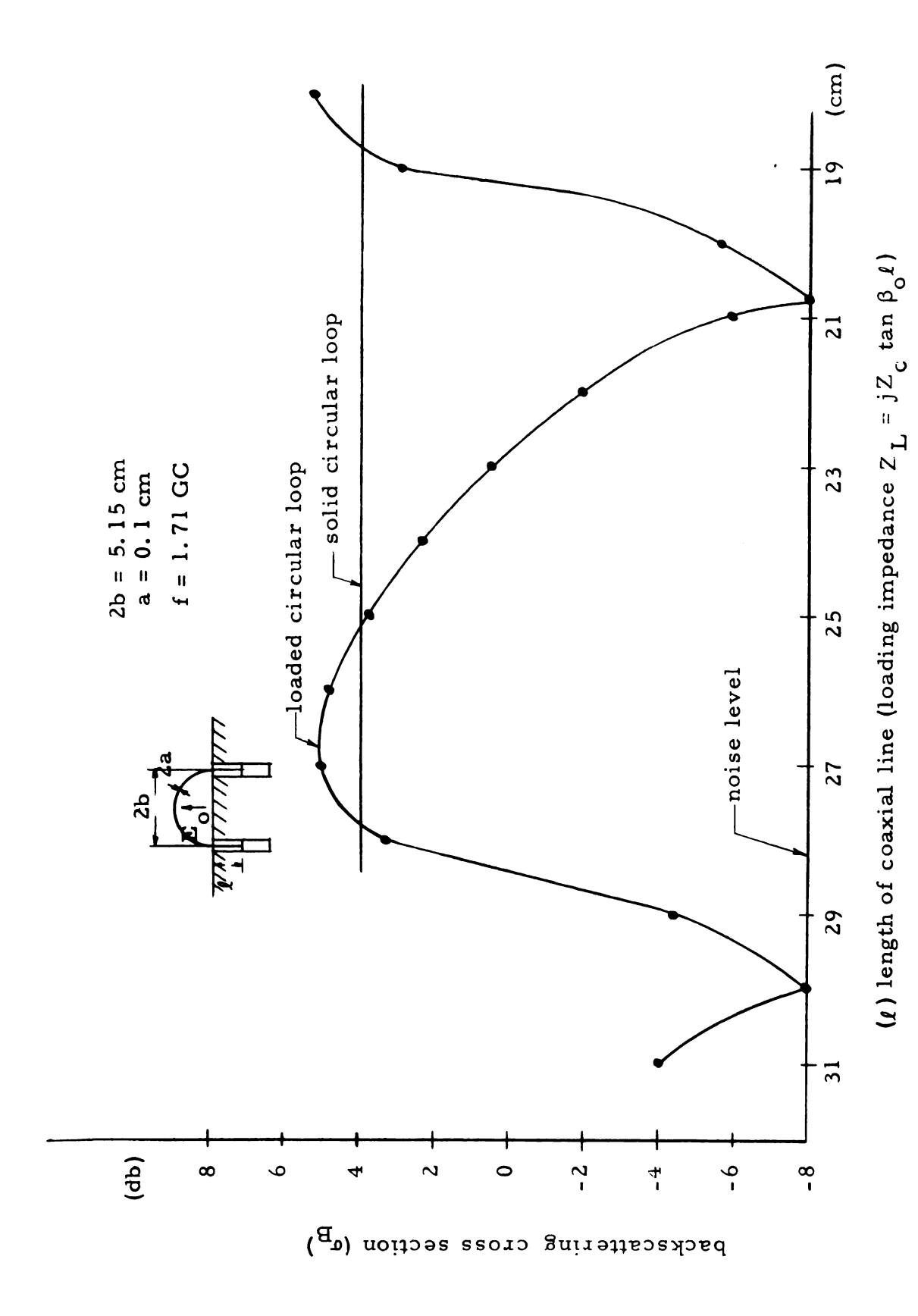
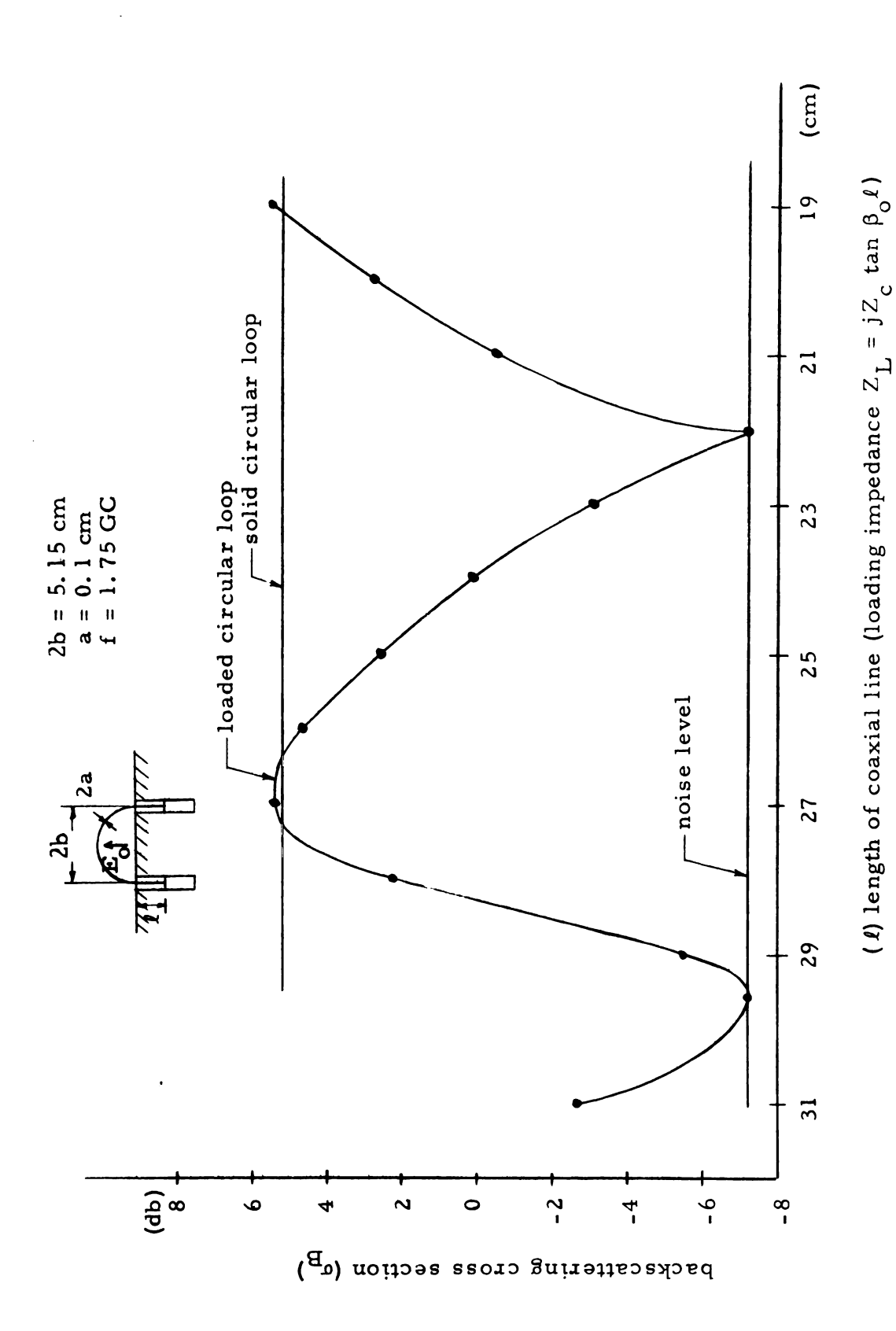
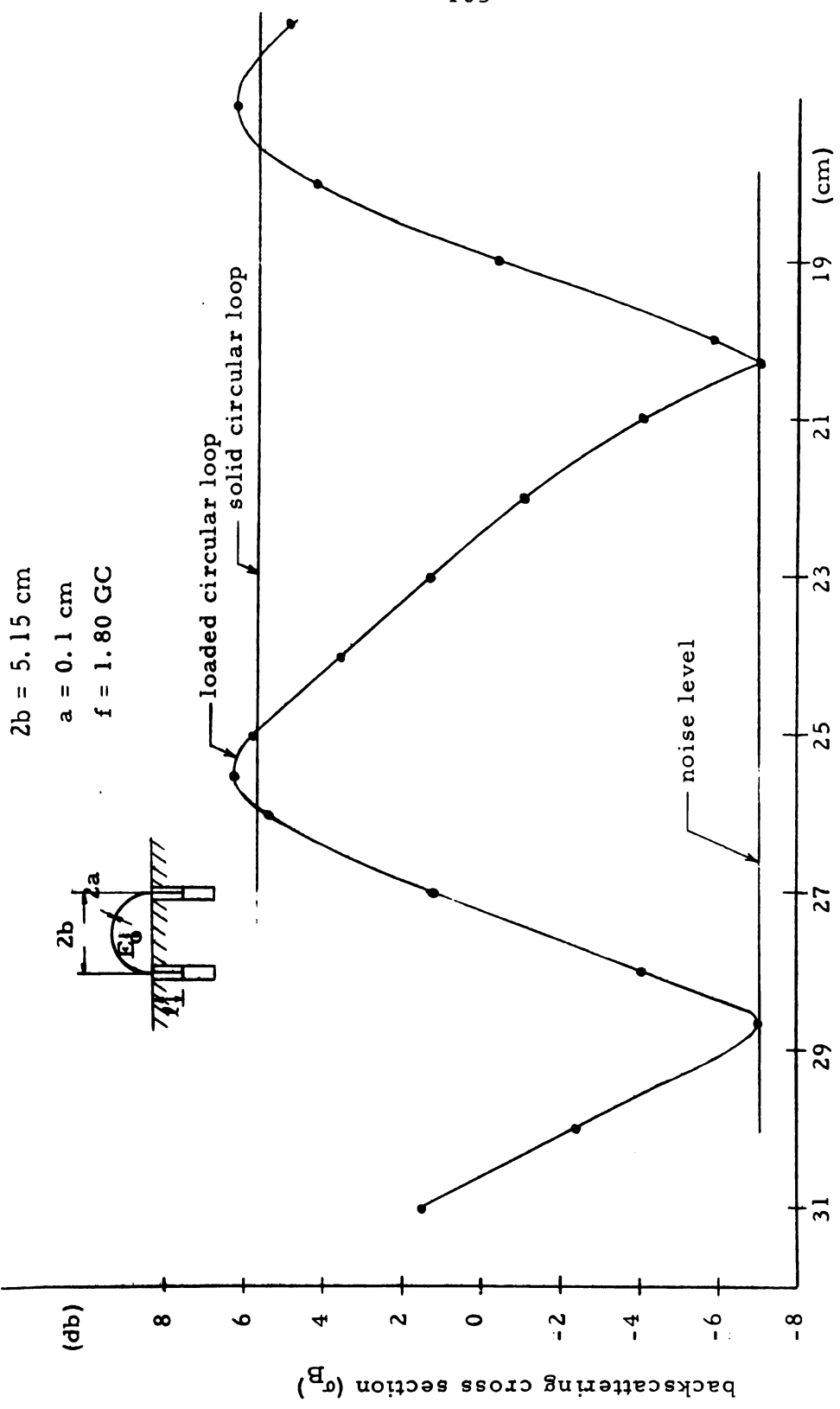


Figure 2.7. Backscattering cross section of a loaded loop as a function of loading impedance (f = 1.71 GC).



Backscattering cross section of a loaded loop as a function of loading impedance  $(f = 1.75 \, \text{GC})$ Figure 2.8.





Backscattering cross section of a loaded loop as a function of loading impedance (f = 1.80 GC). Figure 2.9.

(1) length of coaxial line (loading impedance  $Z_L = jZ_c \tan \beta_o I$ )

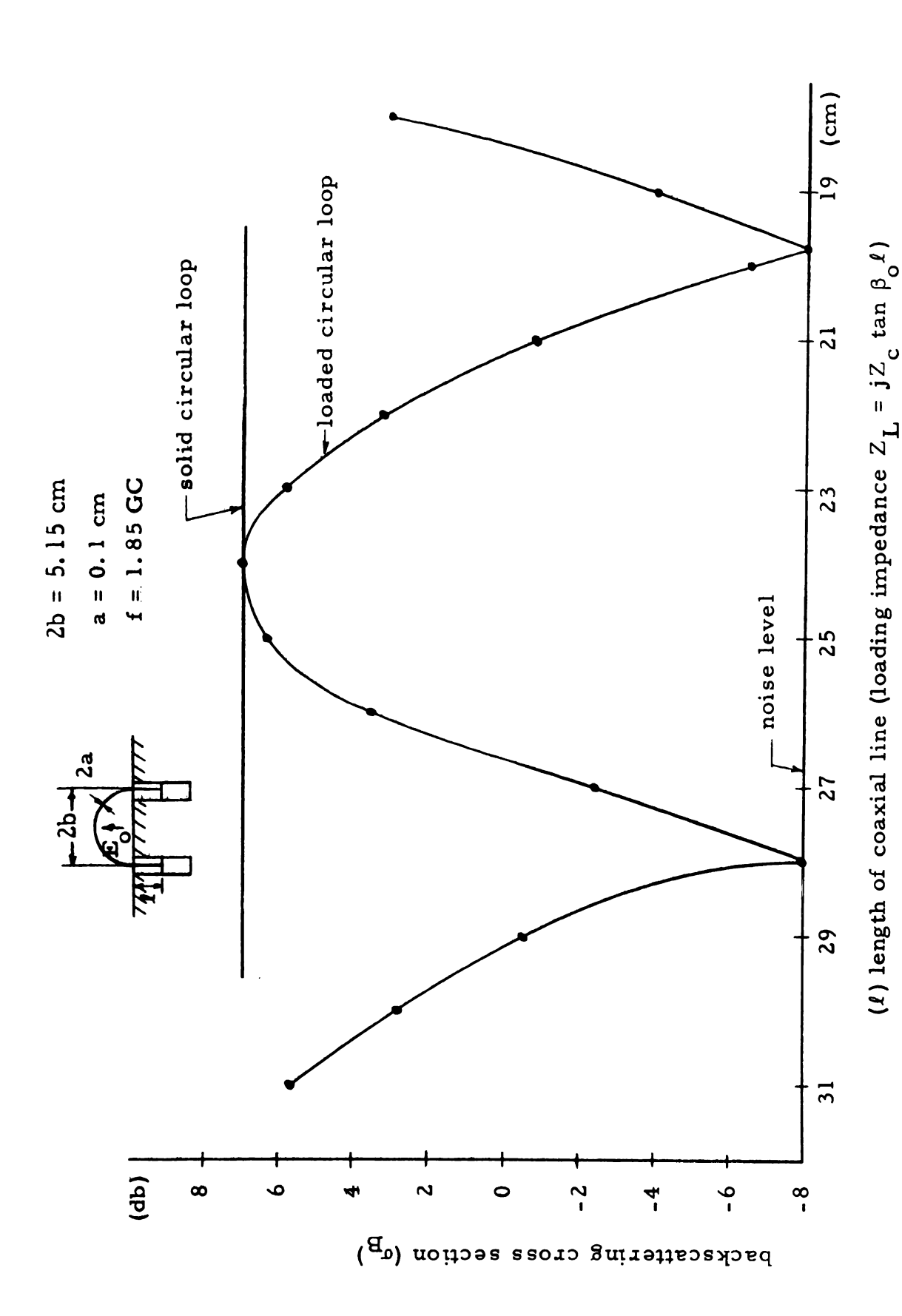


Figure 2.10. Backscattering cross section of a loaded loop as a function of loading impedance (f = 1.85 GC)

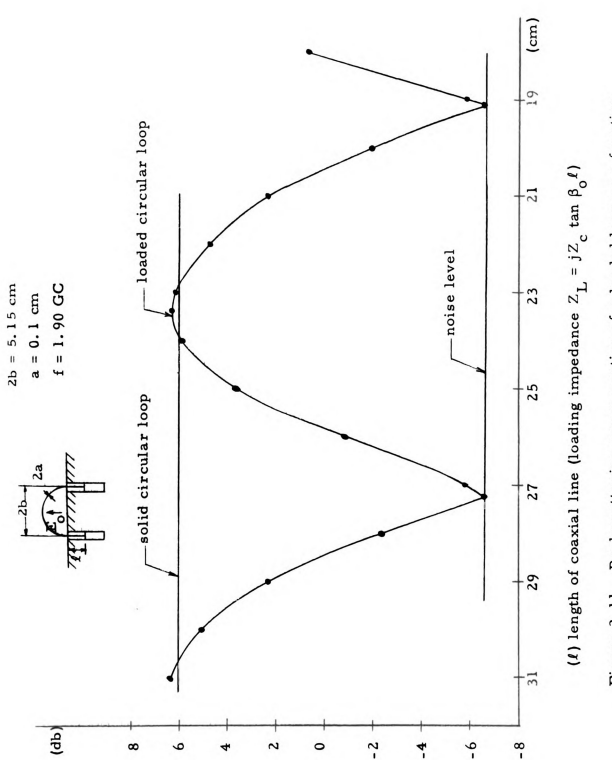


Figure 2.11. Backscattering cross section of a loaded loop as a function of loading impedance ( $f=1.90\ GC$ )

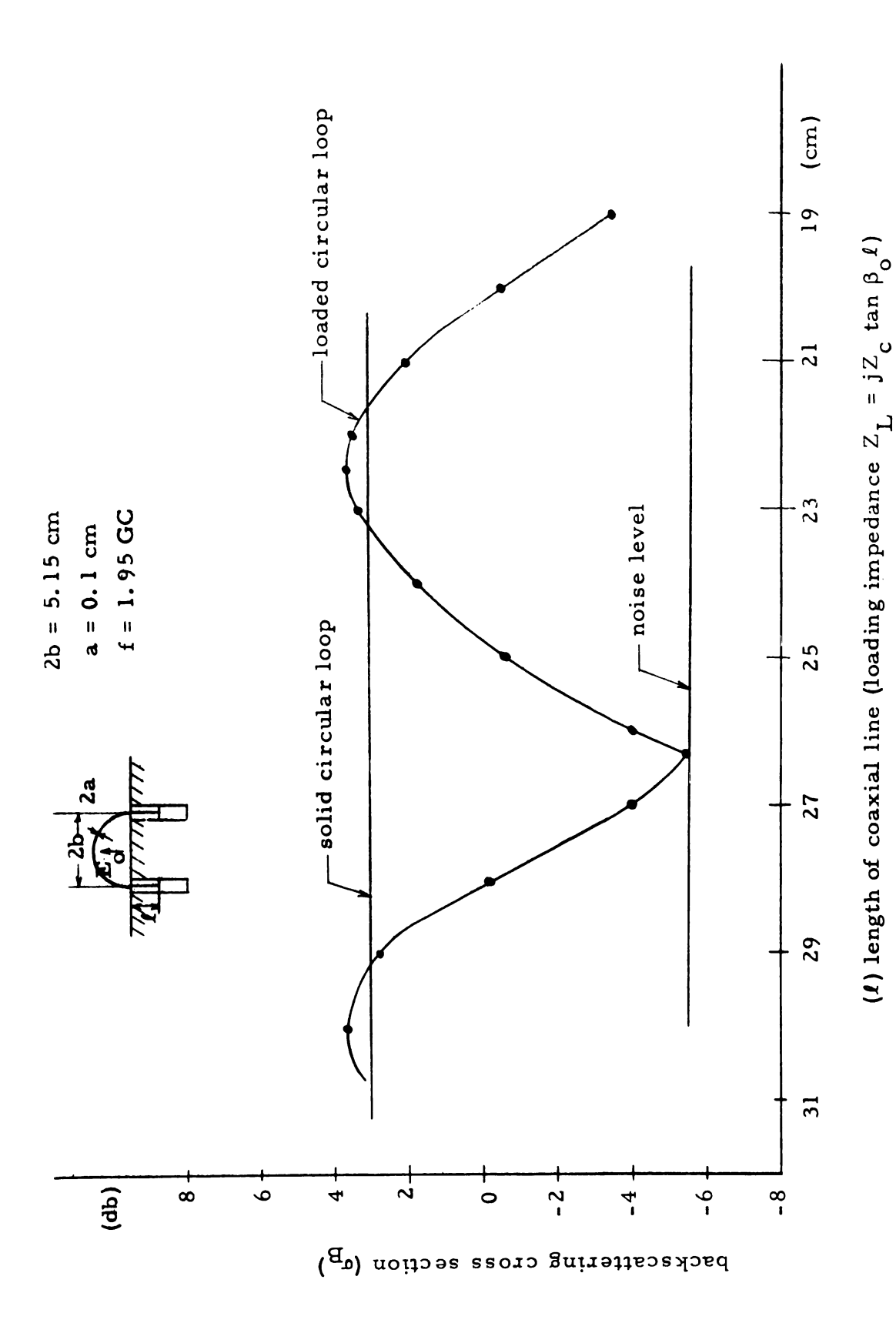


Figure 2.12. Backscattering cross section of a loaded loop as a function of loading impedance (f = 1.95 GC)

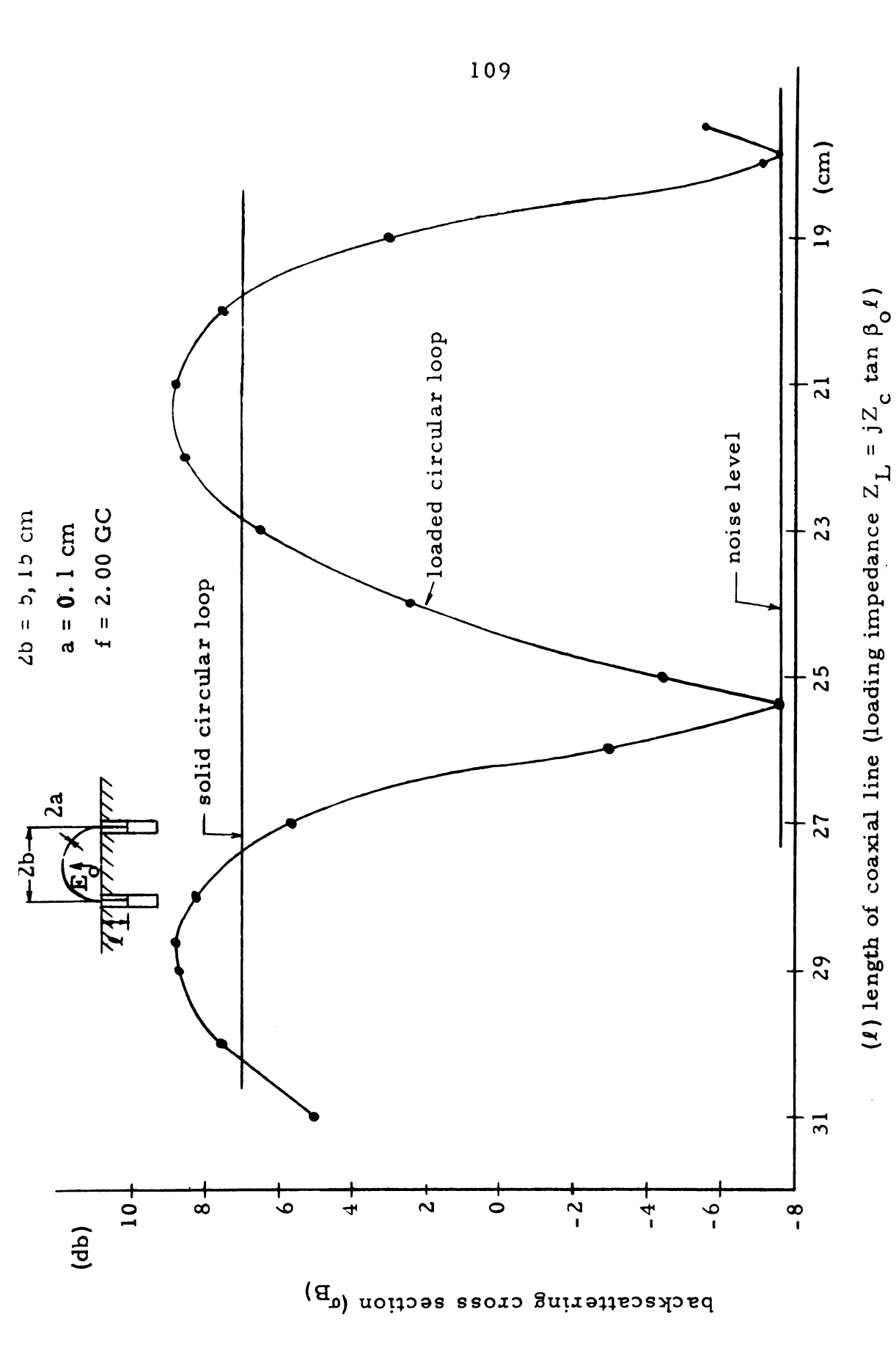


Figure 2.13. Backscattering cross section of a loaded loop as a function of loading impedance ( $f = 2.00 \, \text{GC}$ )

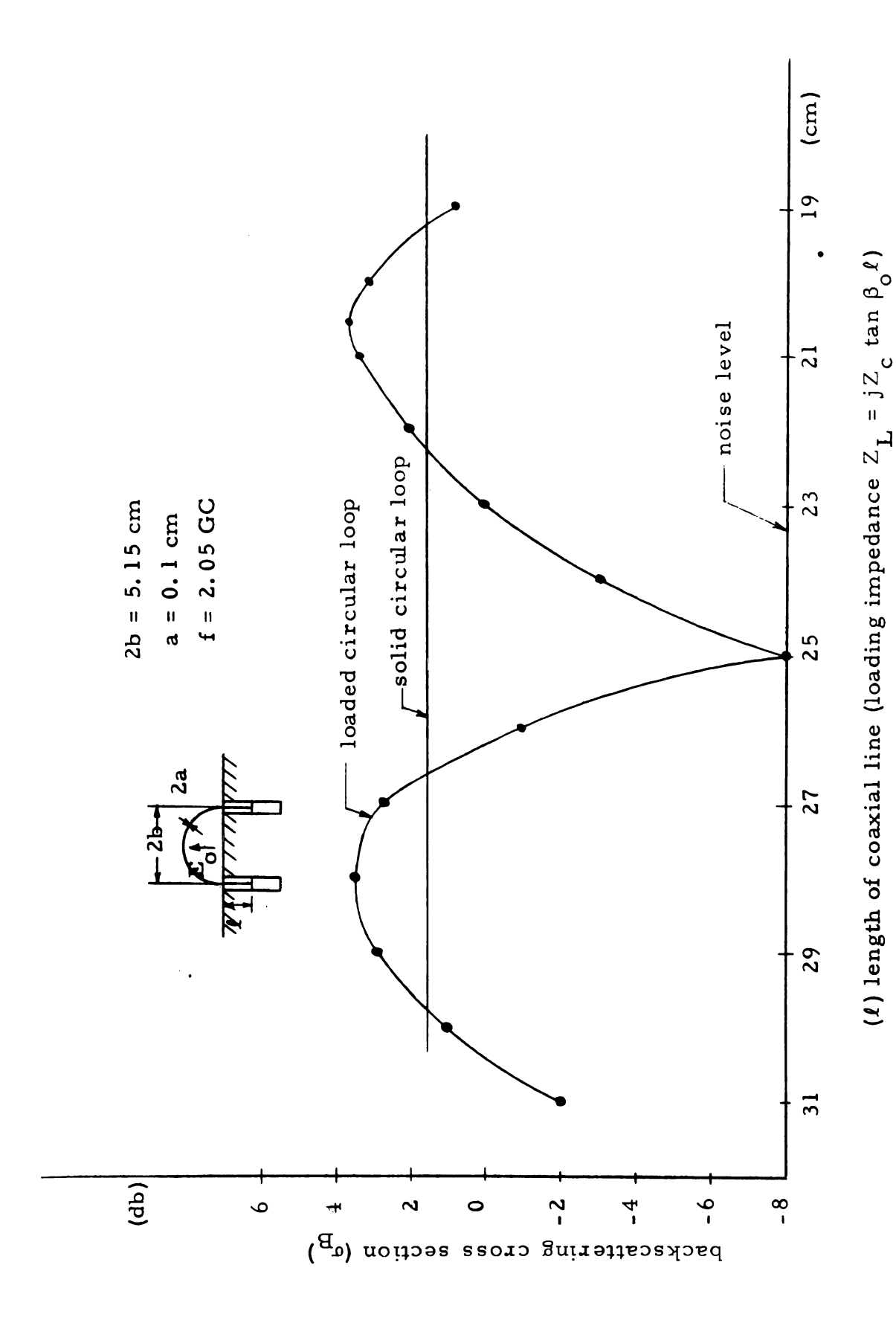


Figure 2. 14. Backscattering cross section of a loaded loop as a function of loading impedance (f = 2.05 GC)

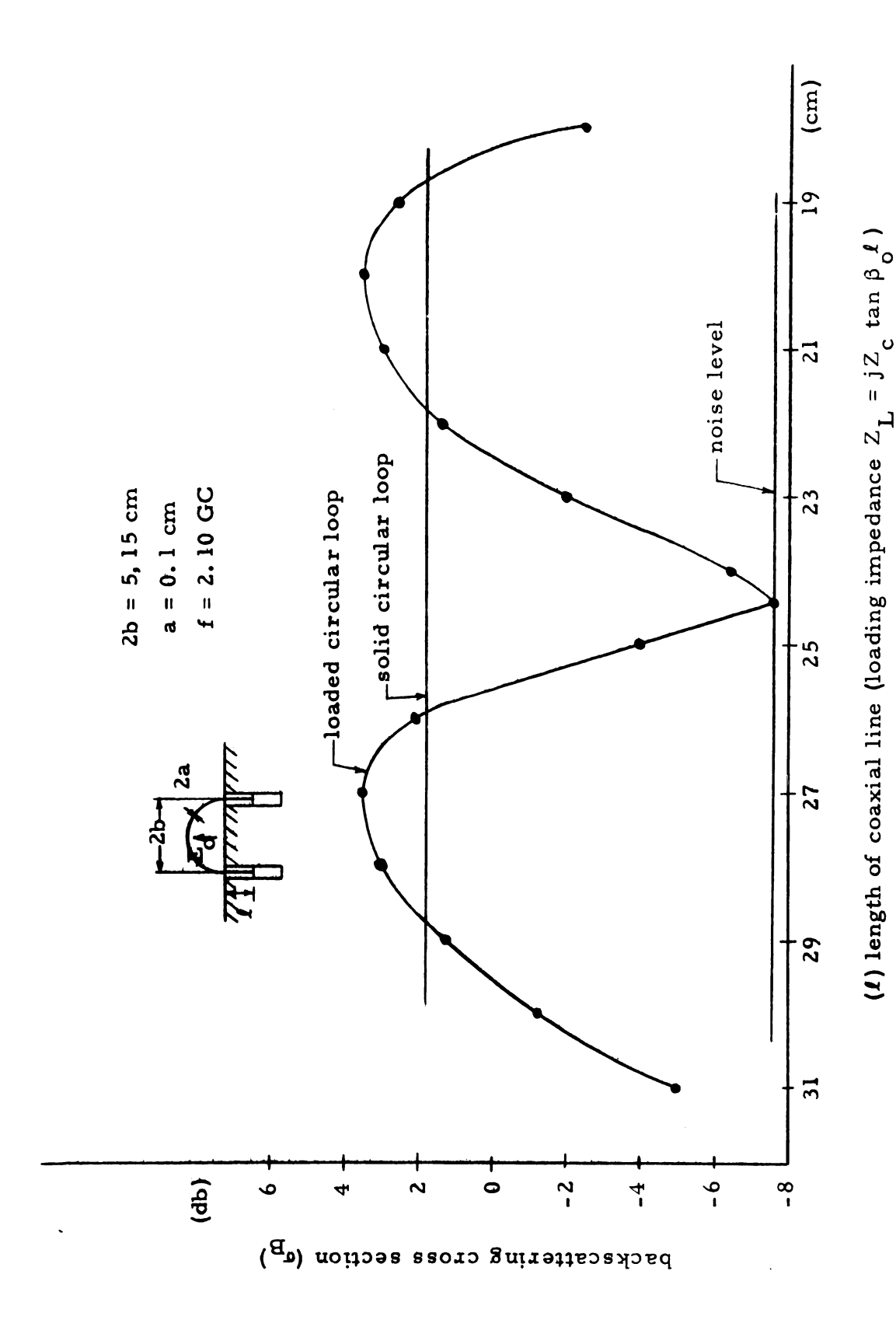
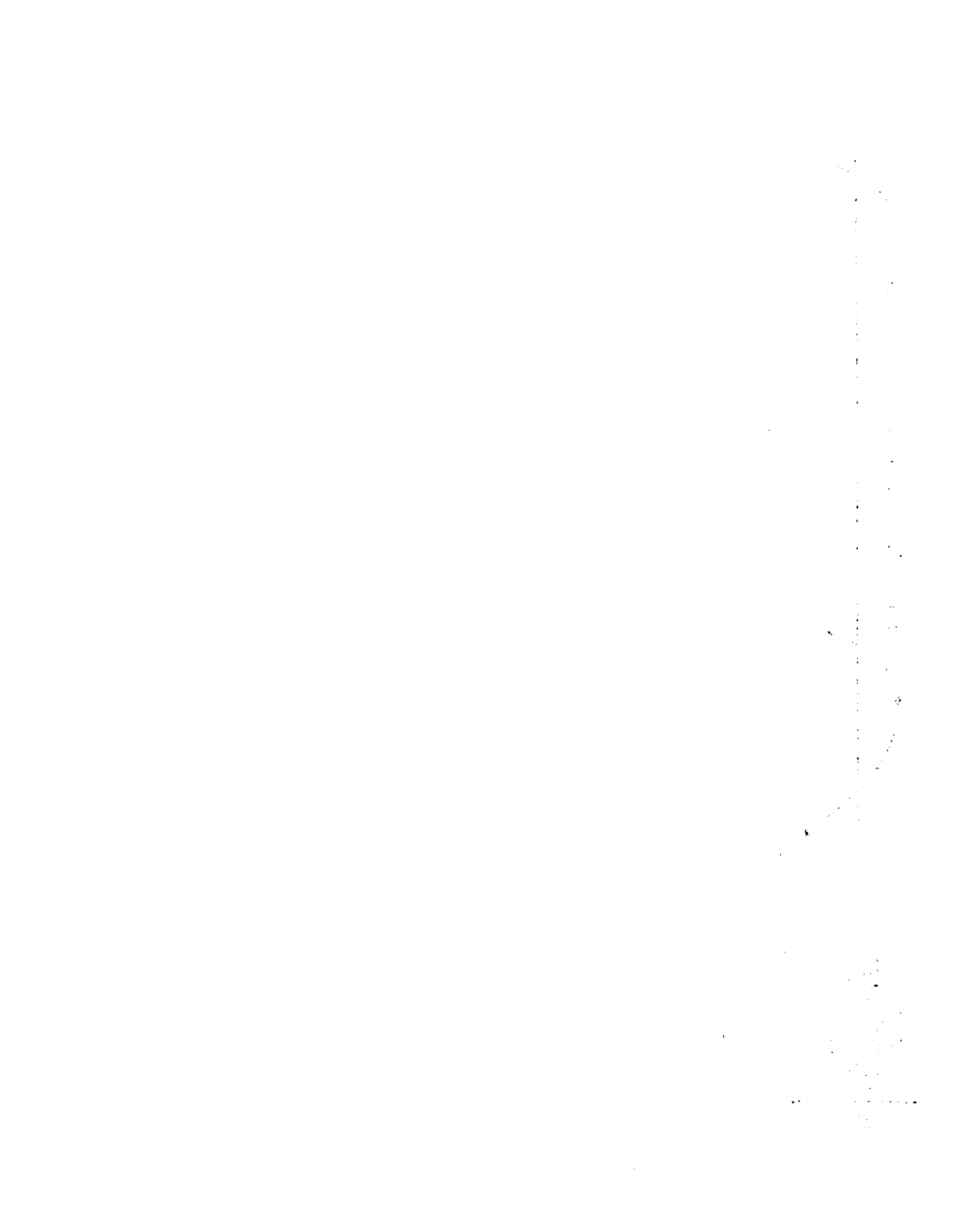


Figure 2.15. Backscattering cross section of a loaded loop as a function of loading impedance (f = 2.10 GC)



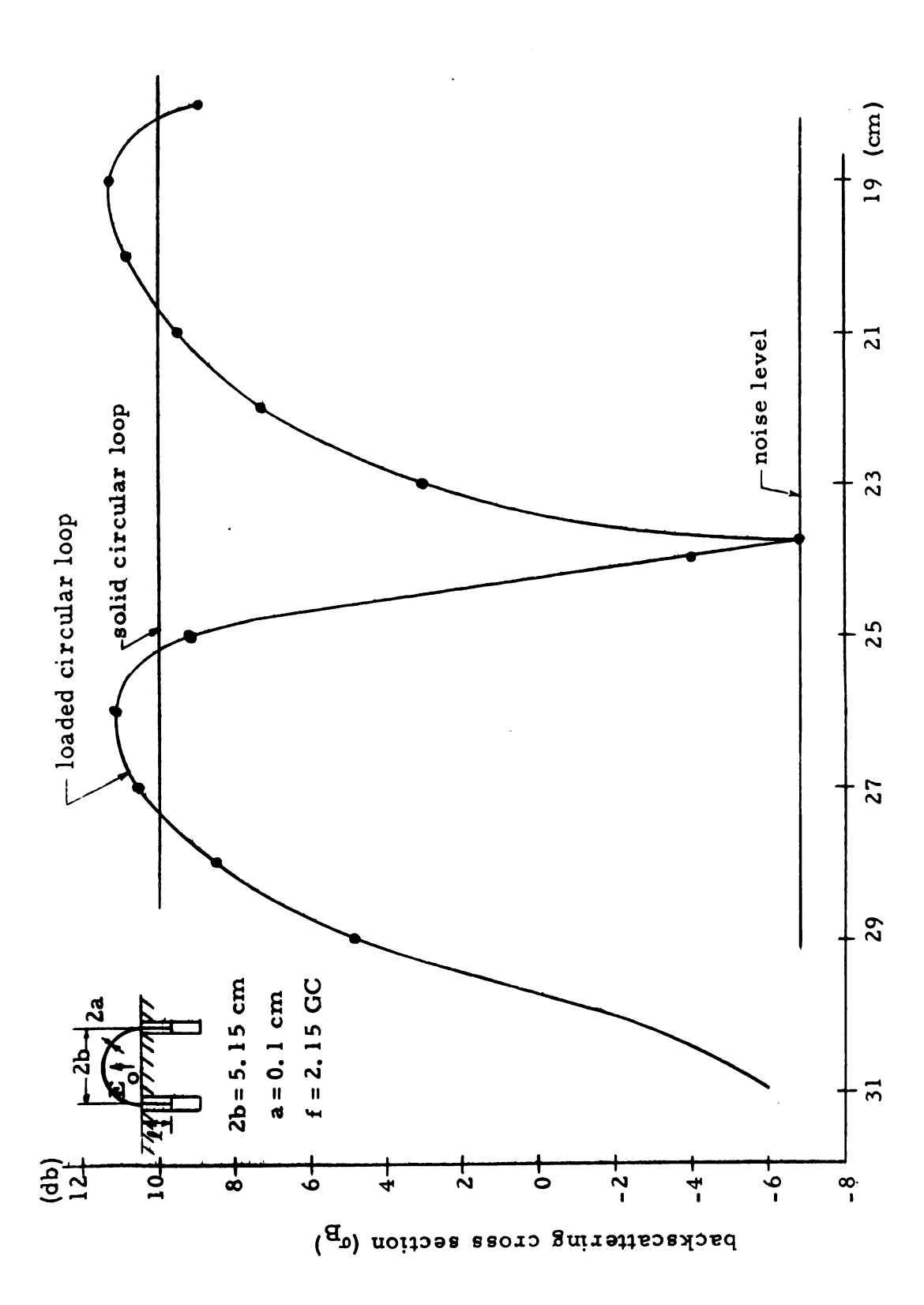


Figure 2. 16. Backscattering cross section of a loaded loop as a function of loading impedance ( $f = 2.15\,\mathrm{GC}$ )

(1) length of coaxial line (loading impedance  $Z_{
m L}={
m j}Z_{
m c}$  tan  $eta_{
m o}$ 1)

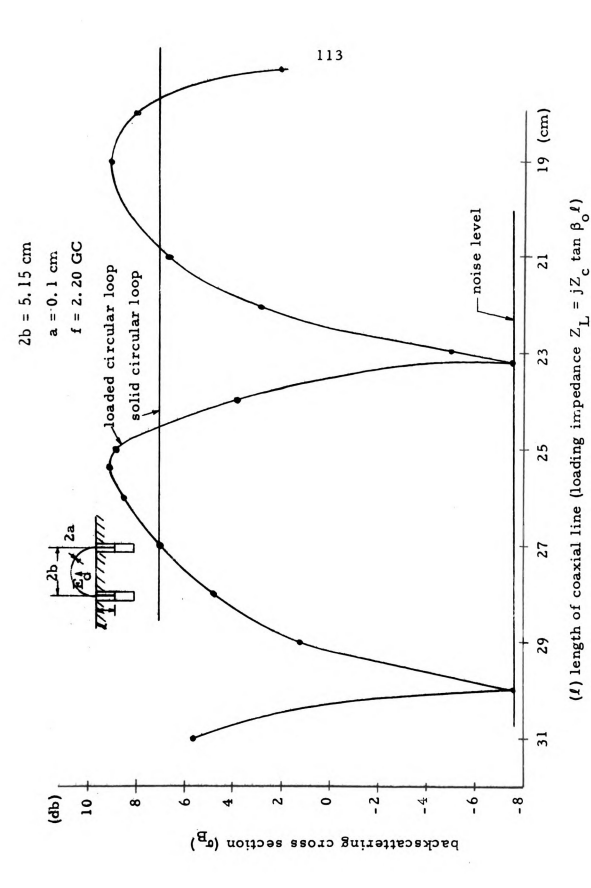


Figure 2.17. Backscattering cross section of a loaded loop as a function of loading impedance (f = 2.20 GC)

¢. 

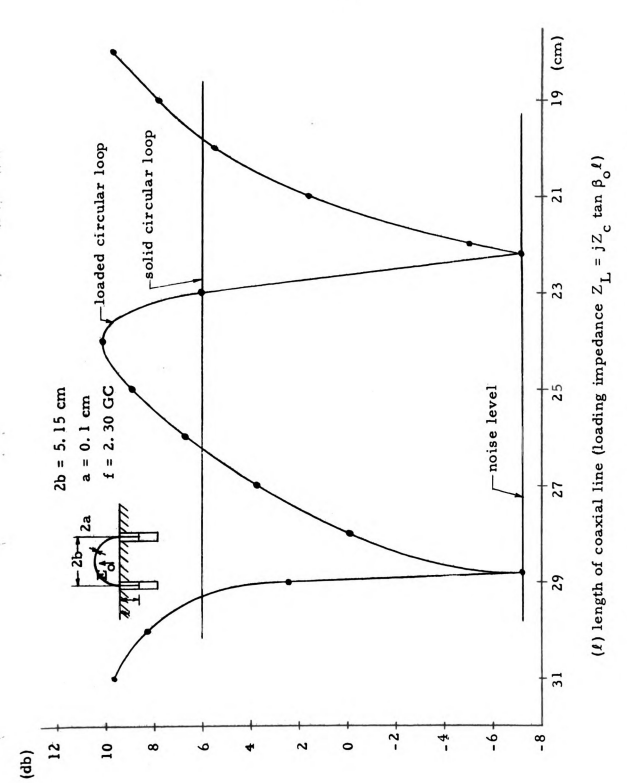


Figure 2.18. Backscattering cross section of a loaded loop as a function of loading impedance (f = 2.30 GC)

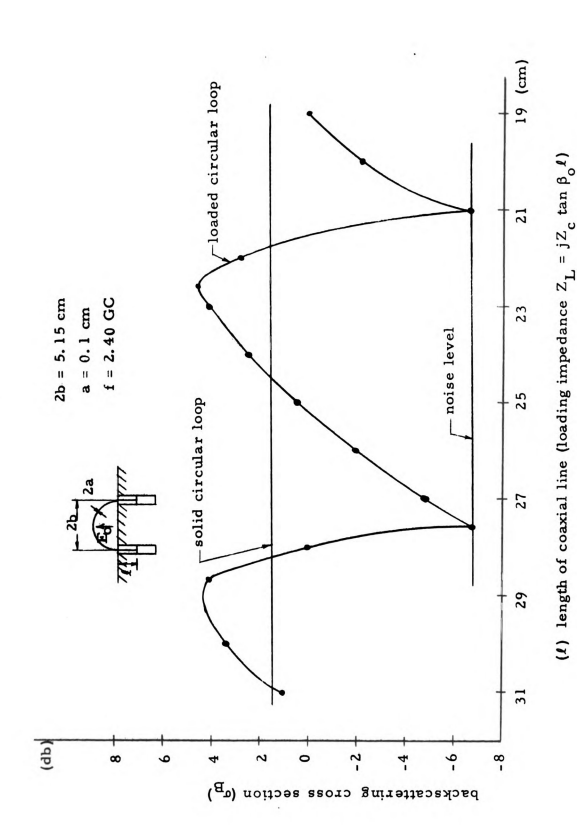
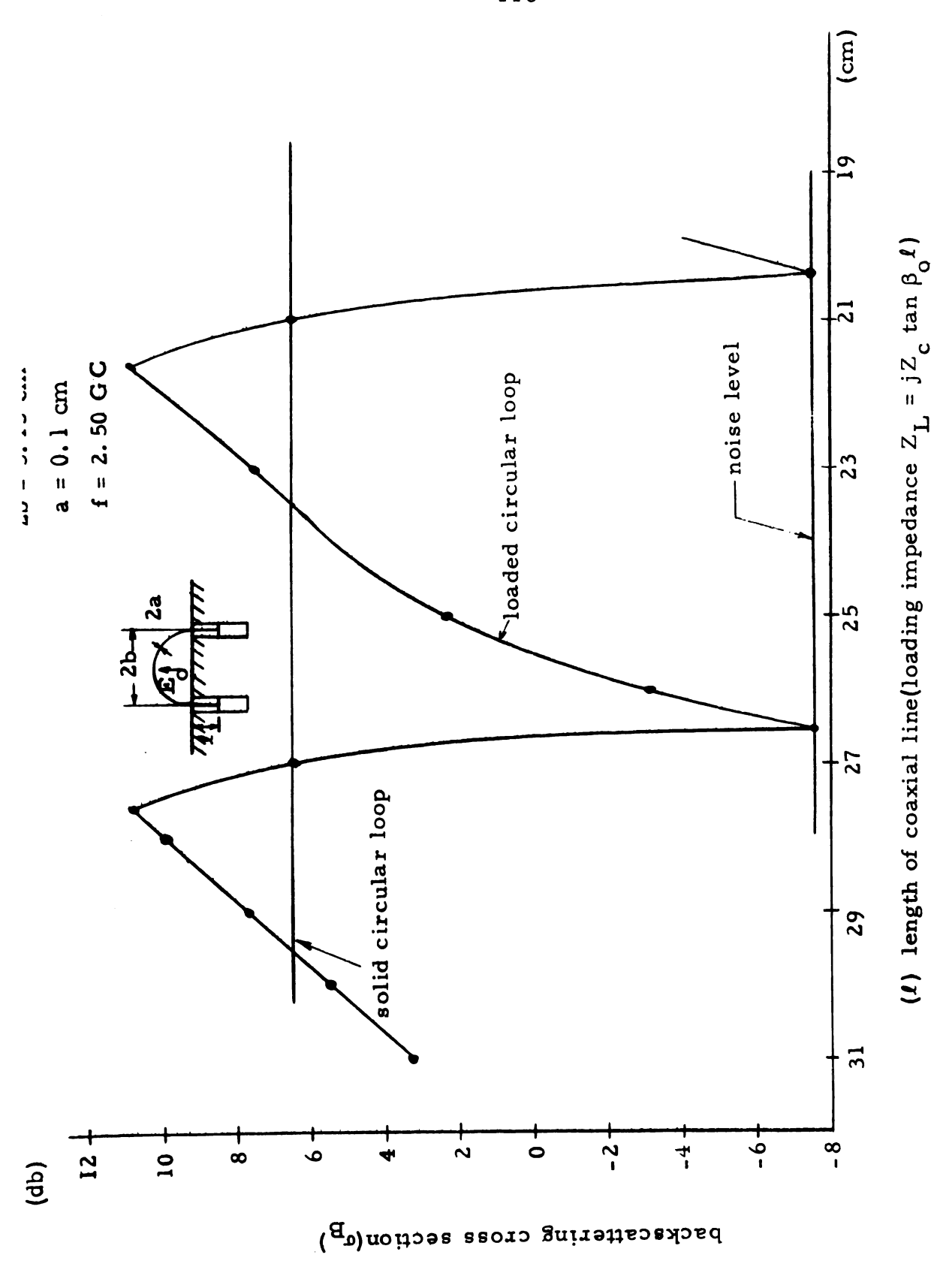
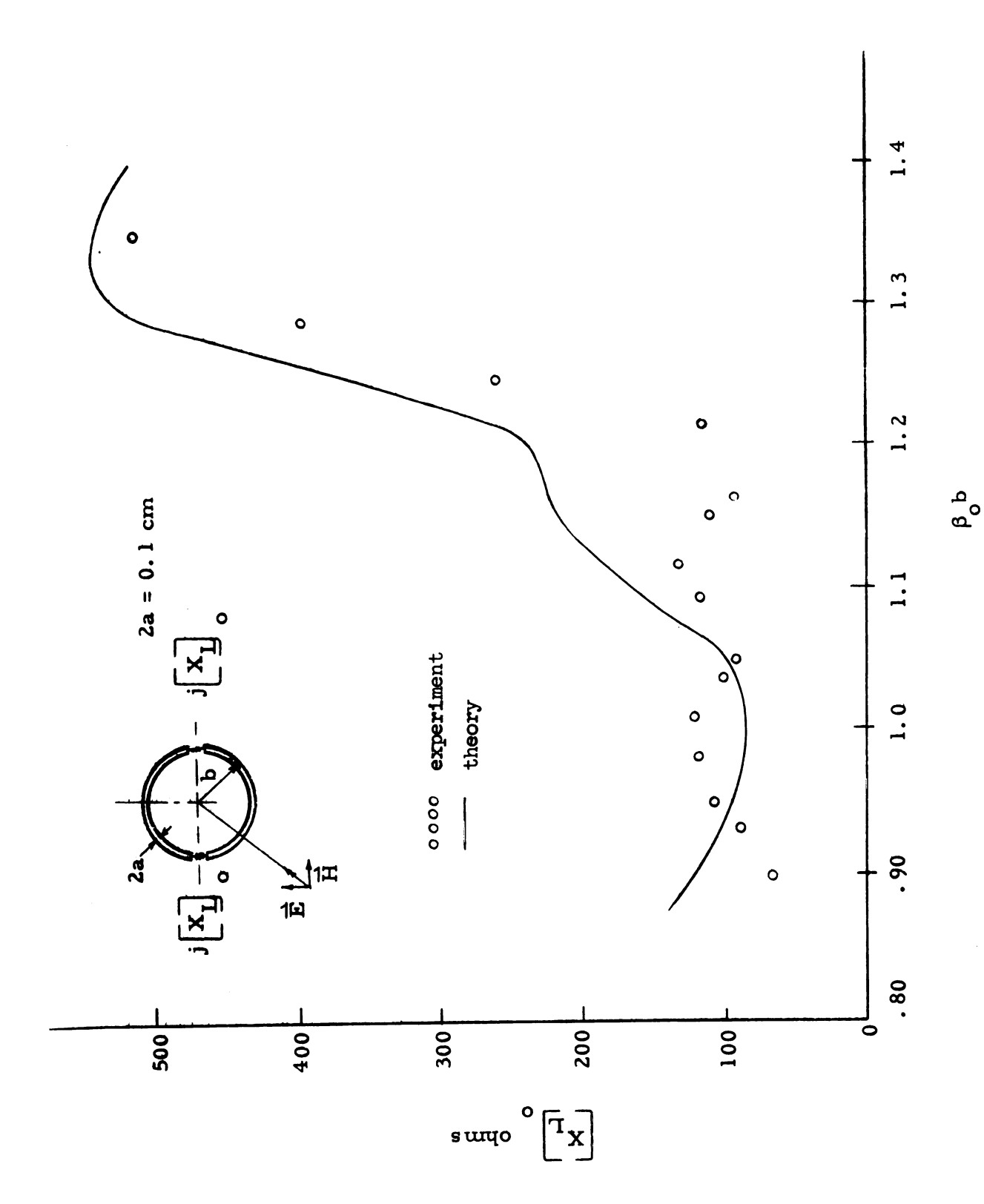


Figure 2.19. Backscattering cross section of a loaded loop as a function of loading impedance ( $f=2.40\,\text{GC}$ )



Backscattering cross section of a loaded loop as a function of loading impedance (f = 2.50 GC) Figure 2.20.



circular loop illuminated by a plane wave at normal incidence. Optimum impedance for minimum backscattering from a Figure 2.21.

#### CHAPTER III

# MINIMIZATION OF BACKSCATTERING OF A LOADED RECTANGULAR LOOP

#### 3.1. Introduction

A theory of the minimization of the backscatter of a metallic rectangular loop by impedance loading method is developed in this chapter. A rectangular loop loaded symmetrically with two identical lumped impedances at the centers of the long sides of the loop is assumed to be illuminated by a plane wave at normal incidence. The induced current on the loaded loop is determined as a function of the loop dimensions and the loading impedance. Based on the induced current, the backscattered field can be calculated. It is then possible to find an optimum impedance which leads to zero backscattering from the loop as a function of loop dimensions. Some numerical examples are included.

# 3.2. Theory

Based on the principle of superposition, the problem of the scattering from a loaded loop illuminated by a plane wave at normal incidence can be considered as the combination of the scattering of a solid loop and the radiation of a driven loop as described in Chapter II. Thus the following two cases will be considered separately and the results will then be combined to yield the final solution for the scattering from loaded loop:

(A) A solid rectangular loop illuminated by a normally incident plane wave.

(B) A rectangular loop driven by two identical voltages at the centers of the long sides.

The situation is illustrated in Figure 3.1. In fact, case (A) is the scattering of a solid rectangular loop and case (B) is the radiation of a rectangular loop antenna. Case (A) has already been solved in Chapter 1 and its results are quoted here for further theoretical development. Case (B) will be considered in this section. The results of Case (B) will be superposed upon those of case (A) to obtain the solution for an illuminated, loaded rectangular loop.

3.2.1. Scattering from a Solid Rectangular Loop

The following expressions from Chapter 1 are needed for further development:

$$\begin{bmatrix}
I_{4y}^{s}(y)
\end{bmatrix}_{11} = \frac{j4\pi}{\zeta_{o}\Phi_{s}} \quad \frac{E_{o}}{\beta_{o}} \chi$$

$$\frac{\cos \beta_{0}h_{1} \cos \beta_{0}y - \cos \beta_{0}(h_{1} + h_{2}) + \frac{1}{\Phi_{s}} P_{41}^{s}(y) + \frac{1}{\Phi_{s}^{2}} P_{42}^{s}(y)}{\cos \beta_{0}(h_{1} + h_{2}) + \frac{1}{\Phi_{s}} G}$$

$$(1.167)$$

$$\begin{bmatrix}
I_{1x} & \mathbf{x} \\
\end{bmatrix}_{11} = \frac{-j4\pi}{\zeta_0 \Phi_x} \quad \frac{E_0}{\beta_0} \chi$$

$$\frac{\left[\sin \beta_{0}h_{2} \sin \beta_{0}x + \frac{1}{\Phi_{s}} P_{11}^{s}(x) + \frac{1}{\Phi_{s}^{2}} P_{12}^{s}(x)\right]}{\cos \beta_{0}(h_{1} + h_{2}) + \frac{1}{\Phi_{s}} G}$$
(1.170)

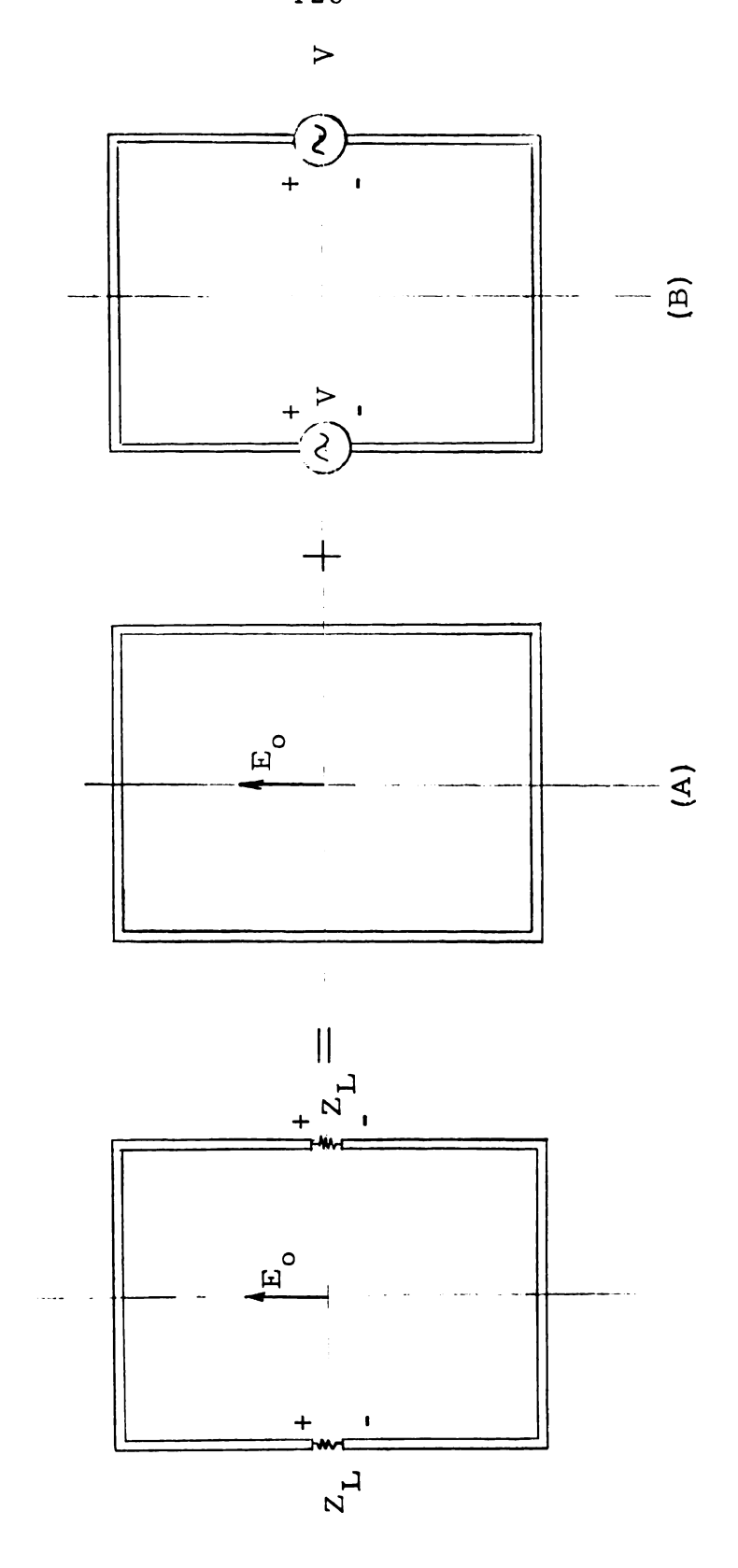


Figure 3.1. A loaded loop is the sum of a scattering loop and a radiating loop.

$$\begin{bmatrix}
I_{4y}^{s}(y) \\
I_{0}
\end{bmatrix}_{10} = \frac{j4\pi}{\zeta_{0}\Phi_{s}} \quad \frac{E_{0}}{\beta_{0}} \times$$

$$\frac{\left[2\left[\cos\beta_{0}h_{1}\cos\beta_{0}y-\cos\beta_{0}(h_{1}+h_{2})\right]+\frac{1}{\Phi_{s}}U_{41}^{s}(y)+\frac{1}{\Phi_{s}^{2}}U_{42}^{s}(y)\right]}{\cos\beta_{0}(h_{1}+h_{2})+\frac{1}{\Phi_{s}}G}$$
(1.173)

$$\begin{bmatrix} I_{1x}^{s}(x) \end{bmatrix}_{10} = \frac{-j4\pi}{\zeta_{0}\Phi_{s}} \quad \frac{E_{o}}{\beta_{0}} \times$$

$$\frac{\left[2 \sin \beta_{0} h_{2} \sin \beta_{0} x + \frac{1}{\Phi_{s}} g_{11}^{s}(x) + \frac{1}{\Phi_{s}^{2}} g_{12}^{s}(x)\right]}{\cos \beta_{0}(h_{1} + h_{2}) + \frac{1}{\Phi_{s}} G}$$
(1.176)

$$\left[E^{s}\right]_{11} = 2 E_{o} \frac{e^{-j\beta_{o}R_{o}}}{R_{o}} \frac{J_{1}}{\Phi_{s}\left[\cos\beta_{o}(h_{1} + h_{2}) + \frac{1}{\Phi_{s}} G\right]}$$
(1.183)

$$\left[ E^{s} \right]_{10} = 2 E_{o} \frac{e^{-j\beta_{o}R_{o}}}{R_{o}} \frac{J_{2}}{\Phi_{s} \left[ \cos \beta_{o}(h_{1} + h_{2}) + \frac{1}{\Phi_{s}} G \right]}$$
(1.188)

where  $I_{4y}^{s}(y)$  and  $I_{1x}^{s}(x)$  are the induced current on side 4 and side 1 of the rectangular loop respectively.  $E^{s}$  is the backscattered field on the axis and in the far zone of the loop maintained by the induced

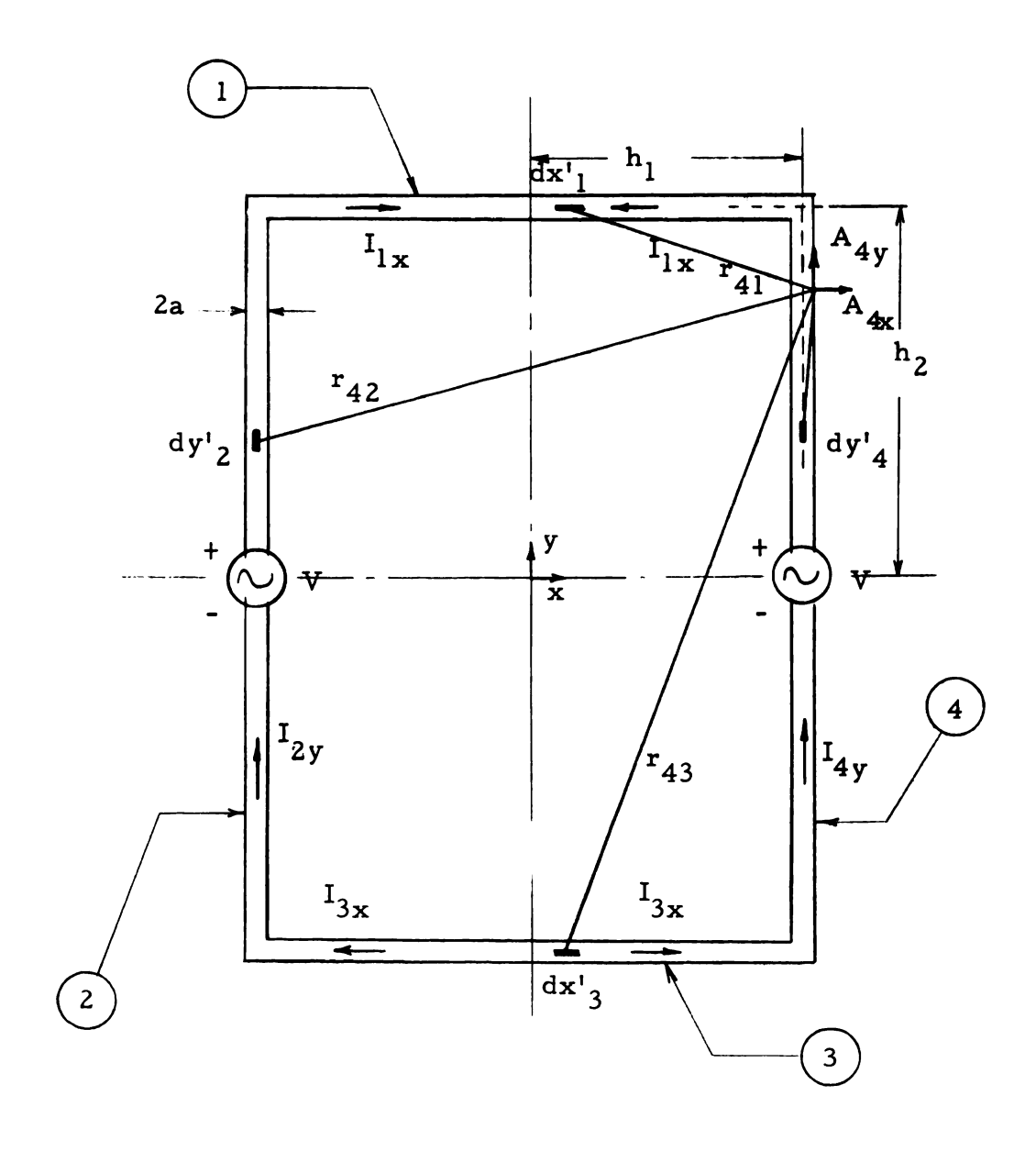


Figure 3.2. Geometry of a radiating loop.

currents. The subscripts outside the brackets in the above expressions are referred to the order of solutions.

## 3.2.2. Radiation from a Rectangular Loop

## (A) Geometry of Problem

The geometry of the problem is as shown in Figure 3.2. A rectangular loop with short side  $2h_1$  and large side  $2h_2$  is assumed to be made of perfectly conducting wire of radius a. Two identical voltages V are connected across the gaps at the centers of the long sides of the loop. The dimensions of interest are

$$a^2 << h_1^2$$
 and  $h_2^2$  ,  $\beta_0^2 a^2 << 1$ 

where  $\beta_0$  is the wave number. We assume that the wire is thin enough so that only the tangential component of current is induced.

## (B) Integral Equations for Loop Currents

The tangential electric field should vanish at the surface of the loop except at the gaps at the centers of the long sides where voltages of V are maintained. Assuming that the gaps are very small, we obtain the following equation:

For side 4

$$E_{4t}^{a} = -V \delta(y)$$
 (3.1)

where  $E_{4t}^{\ a}$  is the tangential electric field at the surface of side 4 and  $\delta(y)$  is a Dirac delta function. Due to symmetrical configuration, if follows that

$$I_{2y}^{r}(y) = I_{4y}^{r}(y)$$
 (3.2)

$$I_{1x}^{r}(x) = -I_{3x}^{r}(x)$$
 (3.3)

$$q_2^{r}(y) = q_4^{r}(y)$$
 (3.4)

$$q_1^r(x) = -q_3^r(x)$$
 (3.5)

where  $I_{4y}^{r}(y)$  is the induced current on side 4 and  $I_{1x}^{r}(x)$  is that on side 1, etc.  $q_i^{r}$  denotes the induced charge on side i, i = 1, 2, 3, and 4.  $E_{4t}^{a}$  can be expressed as

$$E_{4t}^{a} = - (\nabla \phi_{4}^{r}) \qquad \qquad - j \omega (\overline{A}_{4}^{r}) \qquad \qquad (3.6)$$

where  $\overrightarrow{A}_4^r$  is the vector potential at the surface of side 4 contributed by the currents in the loop;  $\phi_4^r$  is the scalar potential at the surface of side 4 maintained by the induced charges on the loop.

In symbols,  $A_4^{\phantom{4}r}$  and  $\phi_4^{\phantom{4}r}$  can be expressed as

$$\overrightarrow{A}_{4}^{r} = A_{4x}^{r} + A_{4y}^{r}$$

$$\phi_4^r = \phi_{41}^r + \phi_{42}^r + \phi_{43}^r + \phi_{44}^r$$
 (3.8)

where  $A_{4x}^{r}$  is the vector potential at the surface of side 4 contributed by the currents in sides 1 and 3. The currents in sides 2 and 4 do not contribute to  $A_{4x}^{r}$  because they do not have x component.

Similarly,  $A_{4y}^{r}$  has the same meaning as  $A_{4x}^{r}$  except that the contribution is made by the currents in sides 2 and 4.  $\phi_{4i}^{r}$  is the scalar potential at the surface of side 4 maintained by the charges on side i, i = 1, 2, 3, and 4.

 $A_{4y}^{r}$  can be expressed in terms of current as

$$A_{4y}^{r}(y) = \frac{\mu_{o}}{4\pi} \int_{-h_{2}}^{h_{2}} I_{4y}^{r}(y') = \frac{e^{-j\beta_{o}r_{44}}}{r_{44}} dy'$$

$$+\frac{\mu_{o}}{4\pi}\int_{-h_{2}}^{h_{2}}I_{2y}^{r}(y')\frac{e^{-j\beta_{o}r_{42}}}{r_{42}}dy'$$

$$= \frac{\mu_{o}}{4\pi} \int_{-h_{2}}^{h_{2}} I_{4y}^{r}(y') K_{1A}(y, y') dy'$$
 (3.9)

where

$$K_{1A}(y, y') = \frac{e^{-j\beta_0 r_{44}}}{r_{44}} + \frac{e^{-j\beta_0 r_{42}}}{r_{42}}$$
 (3.10)

$$r_{44} = \sqrt{(y' - y)^2 + a^2}$$
 (3.11)

$$r_{42} = \sqrt{(y' - y)^2 + 4h_1^2}$$
 (3.12)

With (3.7) and (3.8), (3.6) can be rewritten as

$$E_{4t}^{r} = -\frac{\partial}{\partial y} (\phi_{42}^{r} + \phi_{44}^{r}) - j\omega A_{4y}^{r} - \frac{\partial}{\partial y} (\phi_{41}^{r} + \phi_{43}^{r})$$
(3.13)

By the Lorentz condition, it follows that

$$\phi_{42}^{\mathbf{r}} + \phi_{44}^{\mathbf{r}} = \frac{j\omega}{\beta_0^2} \quad \nabla \cdot \left( \overrightarrow{A}_{42}^{\mathbf{r}} + \overrightarrow{A}_{44}^{\mathbf{r}} \right) = \frac{j\omega}{\beta_0^2} \quad \frac{\partial A_{4y}^{\mathbf{r}}(y)}{\partial y}$$
(3.14)

After substituting (3.14) in (3.13) and after rearranging, (3.13) becomes

$$E_{4t}^{a} = -\frac{j\omega}{\beta_{0}^{2}} \left( \frac{\partial^{2}}{\partial y^{2}} + \beta_{0}^{2} \right) A_{4y}^{r}(y) - \frac{\partial}{\partial y} \left( \phi_{41}^{r} + \phi_{43}^{r} \right) \qquad (3.15)$$

The substitution of (3.15) in (3.1) gives

$$\left(\frac{\partial^{2}}{\partial y^{2}} + \beta_{o}^{2}\right) A_{4y}^{r}(y) = -\frac{j\beta_{o}^{2}V}{\omega} \delta(y) + \frac{j\beta_{o}^{2}}{\omega} \frac{\partial}{\partial y} \left(\phi_{41}^{r} + \phi_{43}^{r}\right)$$
(3.16)

$$\phi_{41}^{r} + \phi_{43}^{r} = \frac{1}{4\pi\epsilon_{o}} \int_{-h_{1}}^{h_{1}} q_{1}^{r}(x') \frac{e^{-j\beta_{o}r_{41}}}{r_{41}} dx'$$

$$+ \frac{1}{4\pi\epsilon_{o}} \int_{-h_{1}}^{h_{1}} q_{3}^{r}(x') \frac{e^{-j\beta_{o}r_{43}}}{r_{43}} dx'$$

$$= \frac{1}{4\pi\epsilon_{o}} \int_{-h_{1}}^{h_{1}} q_{1}^{r}(x') K_{1B}(y, x') dx'$$
(3.17)

$$K_{1B}(y, x') = \frac{e^{-j\beta_0 r_{41}}}{r_{41}} - \frac{e^{-j\beta_0 r_{43}}}{r_{42}}$$
 (3.18)

$$r_{41} = \sqrt{(h_2 - y)^2 + (h_1 - x^1)^2}$$
 (3.19)

$$r_{43} = \sqrt{(h_2 + y)^2 + (h_1 - x')^2}$$
 (3.20)

Similarly, the differential equation for the vector potential at side 1 can be obtained as follows:

Since the tangential electric field should vanish at the surface of side 1, we have

$$E_{1t}^{a} = 0$$
 (3.21)

where E<sub>lt</sub> a is the tangential E field at the surface of side 1 maintained by the current and charge on the loop.

E<sub>lt</sub> a can be expressed as

$$E_{1t}^{a} = - (\nabla \phi_{1}^{r})_{x} - j\omega (\overrightarrow{A}_{1}^{r})_{x}$$
 (3.22)

where  $\phi_1^{\ r}$  is the scalar potential at the surface of side 1 maintained by the induced charges on the loop and  $\overrightarrow{A}_1^{\ r}$  is the vector potential at the surface of side 1 contributed by the currents in the loop. In symbols,  $\overrightarrow{A}_1^{\ r}$  and  $\phi_1^{\ r}$  can be expressed as

$$\overrightarrow{A}_{1}^{r} = A_{1x}^{r} \hat{x} + A_{1y}^{r} \hat{y}$$
 (3.23)

$$\phi_1^r = \phi_{11}^r + \phi_{12}^r + \phi_{13}^r + \phi_{14}^r$$
 (3.24)

where  $A_{lx}^{r}$  is the vector potential at the surface of side 1 contributed by the currents in sides 1 and 3; while  $A_{ly}^{r}$  is that contributed by the currents in sides 2 and 4.  $\phi_{li}^{r}$  is the scalar potential at the surface of side 1 maintained by the induced charges on side i, i = 1, 2, 3 and 4.  $A_{lx}^{r}$  can be expressed in terms of current as

$$A_{1x}^{r} = \frac{\mu_{o}}{4\pi} \int_{-h_{1}}^{h_{1}} I_{1x}^{r}(x') \frac{e^{-j\beta_{o}r_{11}}}{r_{11}} dx'$$

$$+ \frac{\mu_{o}}{4\pi} \int_{-h_{1}}^{h_{1}} I_{3x}^{r}(x') \frac{e^{-j\beta_{o}r_{13}}}{r_{13}} dx'$$

$$= \frac{\mu_{o}}{4\pi} \int_{-h_{1}}^{h_{1}} I_{1x}^{r}(x') K_{2A}(x, x') dx'$$

$$= \frac{\mu_{o}}{4\pi} \int_{-h_{1}}^{h_{1}} I_{1x}^{r}(x') K_{2A}(x, x') dx'$$

where

$$K_{2A}(x, x') = \frac{e^{-j\beta_0 r_{11}}}{r_{11}} - \frac{e^{-j\beta_0 r_{13}}}{r_{13}}$$
 (3.26)

$$r_{11} = \sqrt{(x^1 - x)^2 + a^2}$$
 (3.27)

(3.25)

$$r_{13} = \sqrt{(x' - x)^2 + 4h_2^2}$$
 (3.28)

With (3.23) and (3.24), (3.22) can be rewritten as

$$E_{1t}^{a} = -\frac{\partial}{\partial x} \left( \phi_{11}^{r} + \phi_{13}^{r} \right) - j\omega A_{1x}^{r} - \frac{\partial}{\partial x} \left( \phi_{12}^{r} + \phi_{14}^{r} \right)$$
 (3.29)

By the Lorentz condition, we have

$$\phi_{11}^{r} + \phi_{13}^{r} = \frac{j\omega}{\beta_{0}^{2}} \quad \nabla \cdot \left(\overrightarrow{A}_{11}^{r} + \overrightarrow{A}_{13}^{r}\right) = \frac{j\omega}{\beta_{0}^{2}} \quad \frac{\partial A_{1x}^{r}}{\partial x}$$
(3.30)

Substituting (3.30) in (3.29), we can rearrange (3.29) as

$$E_{1t}^{a} = -\frac{j\omega}{\beta_{0}^{2}} \left(\frac{\partial^{2}}{\partial x^{2}} + \beta_{0}^{2}\right) A_{1x}^{r} - \frac{\partial}{\partial x} \left(\phi_{12}^{r} + \phi_{14}^{r}\right)$$
(3.31)

$$\phi_{12}^{r} + \phi_{14}^{r} = \frac{1}{4\pi\epsilon_{0}} \int_{-h_{2}}^{h_{2}} q_{2}^{r}(y') \frac{e^{-j\beta_{0}r_{12}}}{r_{12}} dy'$$

$$+\frac{1}{4\pi\epsilon_0}\int_{-h_2}^{h_2} q_4^{r}(y') \frac{e^{-j\beta_0 r_{14}}}{r_{14}} dy'$$

$$= \frac{1}{4\pi\epsilon_0} \int_{-h_2}^{h_2} q_4^{r}(y') K_{2B}(x, y') dy'$$
(3.32)

where

$$K_{2B}(x, y') = \frac{e^{-j\beta_0 r_{12}}}{r_{12}} + \frac{e^{-j\beta_0 r_{14}}}{r_{14}}$$
 (3.33)

$$r_{12} = \sqrt{(h_2 - y')^2 + (h_1 + x)^2}$$
 (3.34)

$$r_{14} = \sqrt{(h_2 - y')^2 + (h_1 - x)^2}$$
 (3.35)

With (3.31), (3.21) can be rewritten as

$$\left(\frac{\partial^{2}}{\partial \mathbf{x}^{2}} + \beta_{0}^{2}\right) A_{1x}^{r}(\mathbf{x}) = \frac{j\beta_{0}^{2}}{\omega} \frac{\partial}{\partial \mathbf{x}} \left(\phi_{12}^{r} + \phi_{14}^{r}\right)$$
(3.36)

Due to symmetrical configuration, we note that

$$A_{4v}^{r}(y) = A_{4v}^{r}(-y)$$
 (3.37)

$$A_{1x}^{r}(x) = -A_{1x}^{r}(-x)$$
 (3.38)

(3.37) implies that  $A_{4y}^{r}(y)$  is an even function of y and, therefore, the general solution for  $A_{4y}^{r}(y)$  in (3.16) can be expressed as

$$A_{4y}^{r}(y) = \frac{-j}{v_0} \left[ C_4^{r} \cos \beta_0 y + \theta_4^{r}(y) \right]$$
 (3.39)

where  $C_4^{\ r}$  is an arbitrary constant, and  $\theta_4^{\ r}(y)$  is a particular integral which can be found to be

$$\theta_4^{r}(y) = \frac{V}{2} \sin \beta_0 |y| - \int_0^y \frac{\partial}{\partial s} \left[ \phi_{41}^{r}(s) + \phi_{43}^{r}(s) \right] \sin \beta_0 (y-s) ds$$
(3.40)

Similarly, (3.38) implies that  $A_{lx}^{r}(x)$  is an odd function of x and, therefore, the general solution for  $A_{lx}^{r}(x)$  in (3.36) can be expressed as

$$A_{1x}^{r}(x) = \frac{-j}{v_0} \left[ C_1^{r} \sin \beta_0 x + \theta_1^{r}(x) \right]$$
 (3.41)

where  $C_1^{\ r}$  is an arbitrary constant and  $\theta_1^{\ r}(x)$  is a particular integral which is found as

$$\theta_1^{\mathbf{r}}(\mathbf{x}) = -\int_0^{\mathbf{x}} \frac{\partial}{\partial \mathbf{s}} \left[ \phi_{12}^{\mathbf{r}}(\mathbf{s}) + \phi_{14}^{\mathbf{r}}(\mathbf{s}) \right] \sin \beta_0(\mathbf{x} - \mathbf{s}) d\mathbf{s}$$
 (3.42)

With (3.9) and (3.39), it follows that

$$\frac{4\pi}{\mu_0} A_{4y}^{r}(y) = \int_{-h_2}^{h_2} I_{4y}^{r}(y') K_{1A}(y, y') dy'$$

$$= \frac{-j4\pi}{\zeta_0} \left[ C_4^r \cos \beta_0 y + \theta_4^r (y) \right]$$
 (3.43)

Meanwhile, with (3.25) and (3.41) we obtain

$$\frac{4\pi}{\mu_0} A_{1x}^{r}(x) = \int_{-h_1}^{h_1} I_{1x}^{r}(x') K_{2A}(x, x') dx'$$

$$= \frac{-j4\pi}{\zeta_0} \left[ C_1^r \sin \beta_0 x + \theta_1^r (x) \right]$$
 (3.44)

(C) Zeroth Order Solutions for Loop Currents

At the first approximation, we assume that

$$\frac{A_{4y}^{r}(y)}{I_{4y}^{r}(y)} = \frac{\mu_{0}}{4\pi} \quad \Phi_{r}(y)$$
 (3.45)

$$\frac{A_{1x}^{r}(x)}{I_{1x}(x)} = \frac{\mu_{0}}{4\pi} \quad \Phi_{r}(x)$$
 (3.46)

where  $\Phi_{\mathbf{r}}(\mathbf{y})$  and  $\Phi_{\mathbf{r}}(\mathbf{x})$  are defined respectively as

$$\Phi_{r}(y) = \frac{4\pi}{\mu_{o}} \frac{A_{4y}^{r}(y)}{I_{4y}^{r}(y)}$$
 (3.47)

$$\Phi_{\mathbf{r}}(\mathbf{x}) = \frac{4\pi}{\mu_{0}} \frac{\mathbf{A_{1x}}^{\mathbf{r}}(\mathbf{x})}{\mathbf{I_{1x}}^{\mathbf{r}}(\mathbf{x})}$$
(3.48)

Substituting (3.45) in (3.39), we obtain

$$I_{4y}(y) = \frac{-j4\pi}{\zeta_0 \Phi_{\mathbf{r}}(y)} \left[ C_4^{\mathbf{r}} \cos \beta_0 y + \theta_4^{\mathbf{r}}(y) \right]$$
 (3.49)

Similarly, the substitution of (3.48) in (3.43) gives

$$I_{1x}^{r}(x) = \frac{-j4\pi}{\zeta_0 \Phi_r(x)} \left[ C_1^{r} \sin \beta_0 x + \theta_1^{r}(x) \right]$$
 (3.50)

As we can see from (3.9) and (3.25) respectively that  $A_{4y}^{r}(y)$  is primarily contributed by the current elements in the neighborhood of y and that  $A_{1x}^{r}(x)$  is mainly due to the current elements located

nearby x. It is, therefore, quite reasonable to assume that  $\Phi_{\mathbf{r}}(\mathbf{y})$  in (3.47) is independent of y and  $\Phi_{\mathbf{r}}(\mathbf{x})$  in (3.48) independent of x. For simplicity, we assume that

$$\Phi_{\mathbf{r}}(\mathbf{y}) = \Phi_{\mathbf{r}}(\mathbf{x}) = \Phi_{\mathbf{r}} \tag{3.51}$$

The boundary conditions for determining  $C_4^{\ r}$  and  $C_1^{\ r}$  are

(a) Current at the corners being continuous.

i.e., 
$$I_{4y}^{r}(y = h_2) = -I_{1x}^{r}(x = h_1)$$
 (3.52)

(b) Charge around the corners being continuous.

i.e., 
$$q_4^r(y = h_2) = q_1^r(x = h_1)$$
 (3.53)

The substitution of (3.49), (3.50) and (3.51) in (3.52) yields

$$C_4^r \cos \beta_0 h_2 + \theta_4^r (h_2) = -C_1 \sin \beta_0 h_1 - \theta_1^r (h_1)$$
 (3.54)

 $q_4^r(y)$  and  $q_1^r(x)$  can be found as follows by making use of the equation of continuity.

$$q_4^r(y) = \frac{j}{\omega} \frac{\partial}{\partial y} I_{4y}^r(y)$$

$$= \frac{j}{\omega} \frac{-j4\pi}{\zeta_0 \Phi_r} \left[ -C_4^r \beta_0 \sin \beta_0 y + \frac{\partial \theta_4^r(y)}{\partial y} \right]$$
(3.55)

$$q_1^r(x) = \frac{j}{\omega} \frac{\partial}{\partial x} I_{1x}^r(x)$$

$$= \frac{j}{\omega} \frac{-j4\pi}{\zeta_0 \Phi_r} \left[ C_1^r \beta_0 \cos \beta_0 x + \frac{\partial \theta_1^r(x)}{\partial x} \right]$$
 (3.56)

Combining (3.55) and (3.56) with boundary condition (3.53), we have

$$-C_{4}^{r}\beta_{0}\sin\beta_{0}h_{2} + \frac{\partial\theta_{4}^{r}(y)}{\partial y} \bigg|_{y=h_{2}} = C_{1}^{r}\beta_{0}\cos\beta_{0}h_{1} + \frac{\partial\theta_{1}^{r}(x)}{\partial x} \bigg|_{x=h_{1}}$$
(3.57)

Solving (3.56) and (3.57) for  $C_4^r$  and  $C_1^r$ , we obtain

$$C_4^{r} = \frac{1}{\beta_0 \left[\cot \beta_0 h_1 \cos \beta_0 h_2 - \sin \beta_0 h_2\right]} \left[\frac{\partial \theta_1^{r}(x)}{\partial x}\right|_{x=h_1} - \frac{\partial \theta_4^{r}(y)}{\partial y}\bigg|_{y=h_2}$$

$$+ \frac{1}{\tan \beta_0 h_1 \sin \beta_0 h_2 - \cos \beta_0 h_2} \left[ \theta_1^{\mathbf{r}} (h_1) + \theta_4^{\mathbf{r}} (h_2) \right]$$

$$C_1^{\mathbf{r}} = \frac{1}{\beta_0 \left[ \sin \beta_0 h_1 \tan \beta_0 h_2 - \cos \beta_0 h_1 \right]} \times$$
(3.58)

$$\cdot \left\{ \frac{\partial \theta_{1}^{r}(x)}{\partial x} \middle|_{x = h_{1}} - \frac{\partial \theta_{4}^{r}(y)}{\partial y} \middle|_{y = h_{2}} - \beta_{0} \tan \beta_{0}^{h_{2}} \left[ \theta_{1}^{r}(h_{1}) + \theta_{4}^{r}(h_{2}) \right] \right\}$$

$$(3.59)$$

For zeroth order solution, we assume that  $\theta_4^{\ r}(y)$  in (3.40) and  $\theta_1^{\ r}(x)$  in (3.42) can be approximated respectively as

$$\left[\theta_4^{r}(y)\right]_0 = \frac{V}{2} \sin \beta_0 |y| \qquad (3.60)$$

$$\begin{bmatrix} \theta_1 & (x) \\ 0 \end{bmatrix} = 0 \tag{3.61}$$

With (3.60) and (3.61) substituted in (3.58) and (3.59), it follows that

$$\begin{bmatrix} C_4 \\ \end{bmatrix}_0 = \frac{-V}{2} \tan \beta_0 (h_1 + h_2)$$
 (3.62)

$$\begin{bmatrix} C_1^4 \end{bmatrix}_0 = \frac{V}{2} \frac{1}{\cos \beta_0 (h_1 + h_2)}$$
 (3.63)

Consequently, zeroth order solution of currents are obtained as

$$\left[ I_{4y}^{r}(y) \right]_{0} = \frac{-j4\pi}{\zeta_{0} \Phi_{r}} \left[ -\frac{V}{2} \tan \beta_{0}(h_{1} + h_{2}) \cos \beta_{0} y + \theta_{4}^{y}(y) \right]$$
 (3.64)

$$\begin{bmatrix} I_{1x}^{r}(x) \end{bmatrix}_{0} = \frac{-j4\pi}{\zeta_{0}\Phi_{r}} \begin{bmatrix} \frac{V}{2} \frac{\sin\beta_{0}^{x}}{\cos\beta_{0}(h_{1}+h_{2})} + \theta_{1}^{r}(x) \end{bmatrix}$$
(3.65)

If (3.60) and (3.61) are applied to (3.64) and (3.65), we have

$$I_{4y}^{r}(y) = \frac{j2\pi V}{\zeta_{o}\Phi_{r}} \frac{\sin \beta_{o}(h_{1} + h_{2} - |y|)}{\cos \beta_{o}(h_{1} + h_{2})}$$
(3.66)

$$\begin{bmatrix} I_{1x}^{r}(x) \end{bmatrix}_{00} = \frac{-j2\pi V}{\zeta_{0}\Phi_{r}} \frac{\sin \beta_{0}x}{\cos \beta_{0}(h_{1} + h_{2})}$$
(3.67)

## (D) First Order Solutions for Loop Currents

To obtain first order solutions of currents, the following equations are needed:

From (3.39) and (3.41)

$$A_{4y}^{r}(y) = \frac{-j}{v_0} \left[ C_4^{r} \cos \beta_0 y + \theta_4^{r} (y) \right]$$

$$A_{1x}^{r}(x) = \frac{-j}{v_0} \left[ C_1^{r} \sin \beta_0 x + \theta_1^{r}(x) \right]$$

From (3.49), (3.50) and (3.51), it follows that

$$\begin{bmatrix} I_{4y}(y) \end{bmatrix}_0 = \frac{-j4\pi}{\zeta_0 \Phi_r} \begin{bmatrix} C_4^r \cos \beta_0 y + \theta_4^y(y) \end{bmatrix}$$

$$\begin{bmatrix} I_{1x}^{r}(x) \end{bmatrix}_{0} = \frac{-j4\pi}{\zeta_{0}\Phi_{r}} \begin{bmatrix} C_{1}^{r} \sin \beta_{0}x + \theta_{1}^{r}(x) \end{bmatrix}$$

From (3.55) and (3.56)

$$\left[q_4^{r}(y)\right]_0 = \frac{4\pi}{\omega \zeta_0 \Phi_r} \left[ -C_4^{r} \beta_0 \sin \beta_0 y + \frac{\partial \theta_4^{r}(y)}{\partial y} \right]$$

$$\left[q_1^{r}(x)\right]_0 = \frac{4\pi}{\omega \zeta_0 \Phi_r} \left[C_1^{r} \beta_0 \cos \beta_0 x + \frac{\partial \theta_1^{r}(x)}{\partial x}\right]$$

First order currents are formulated as follows:

$$\begin{bmatrix} I_{4y}^{r}(y) \end{bmatrix}_{1} = \begin{bmatrix} I_{4y}^{r}(y) \end{bmatrix}_{0} + \frac{4\pi}{\mu \frac{\Phi}{\Phi}} \left\{ A_{4y}^{r} - \frac{\mu_{\Phi}}{4\pi} \right\}$$

$$\cdot \int_{-h_1}^{h_1} \left[ I_{4y}^{r}(y') \right]_{0} K_{1A}(y, y') dy'$$
(3.68)

$$\begin{bmatrix} I_{1x}^{r}(x) \end{bmatrix}_{1} = \begin{bmatrix} I_{1x}^{r}(x) \end{bmatrix}_{0} + \frac{4\pi}{\mu_{0}\Phi_{r}} \left\{ A_{1x} - \frac{\mu_{0}}{4\pi} \right\}$$

$$\cdot \int_{-h_1}^{h_1} \left[ I_{1x}^{r}(x') \right]_{0}^{K_{2A}}(x, x') dx'$$
(3.69)

In fact, (3.68) and (3.69) can be rewritten as

$$\begin{bmatrix} I_{4y}^{r}(y) \end{bmatrix}_{1} \stackrel{\text{def}}{=} 2 \begin{bmatrix} I_{4y}^{r}(y) \end{bmatrix}_{0} - \frac{1}{\Phi_{r}} \int_{-h_{2}}^{h_{2}} I_{4y}^{r}(y') \end{bmatrix}_{0} K_{1A}(y, y') dy' \tag{3.70}$$

$$\begin{bmatrix} \mathbf{I}_{1\mathbf{x}}^{\mathbf{r}}(\mathbf{x}) \end{bmatrix}_{1} \approx 2 \begin{bmatrix} \mathbf{I}_{1\mathbf{x}}^{\mathbf{r}}(\mathbf{x}) \end{bmatrix}_{0} - \frac{1}{\Phi_{\mathbf{r}}} \int_{-h_{1}}^{h_{1}} [\mathbf{I}_{1\mathbf{x}}^{\mathbf{r}}(\mathbf{x}')] \int_{0}^{\mathbf{K}_{2A}} (\mathbf{x}, \mathbf{x}') d\mathbf{x}'$$
(3.71)

Substituting zeroth order solutions in (68) and (69) yields

$$\begin{split} \left[I_{4y}^{r}(y)\right]_{1} &= \frac{-j4\pi}{\zeta_{o}\Phi_{r}} \left\{ 2 \left[C_{4}^{r} \cos \beta_{o} y + \theta_{4}^{r}(y)\right] \right. \\ &\left. - \frac{C_{4}^{r}}{\Phi_{r}} \int_{-h_{2}}^{h_{2}} \cos \beta_{o} y' K_{1A}(y, y') dy' \right. \\ &\left. - \frac{1}{\Phi_{r}} \int_{-h_{2}}^{h_{2}} \theta_{4}^{r}(y') K_{1A}(y, y') dy' \right\} \\ &\left. = \frac{-j4\pi}{\zeta_{o}\Phi_{r}} \left\{ C_{4}^{r} \left[2 \cos \beta_{o} y - \frac{T_{ca}(y)}{\Phi_{r}}\right] + 2\theta_{4}^{r}(y) - \frac{n_{1}^{r}(y)}{\Phi_{r}} \right\} \end{split}$$

$$= \frac{-j4\pi}{\zeta_0 \Phi_r} \left[ C_4^r L_1^r(y) + 2\theta_4^r(y) - N_1^r(y) \right]$$
(3.72)

$$L_1^{r}(y) = 2 \cos \beta_0 y - \frac{T_{ca}(y)}{\Phi_r}$$
 (3.73)

$$N_1^{r}(y) = \frac{n_1^{r}(y)}{\Phi_r}$$
 (3.74)

$$T_{ca}(y) = \int_{-h_2}^{h_2} \cos \beta_0 y' K_{lA}(y, y') dy'$$
 (3.75)

$$n_1^r(y) = \int_{-h_2}^{h_2} \theta_4^r(y') K_{1A}(y, y') dy'$$
 (3.76)

$$\begin{bmatrix}
I_{1x}^{r}(x)
\end{bmatrix}_{1} = \frac{-j4\pi}{\zeta_{0}\Phi_{r}} \left\{ 2 \left[C_{1}^{r} \sin \beta_{0} + \theta_{1}^{r}(x)\right]\right\}$$

$$-\frac{C_1^r}{\Phi_r} \int_{-h_1}^{h_1} \sin \beta_0 x' K_{2A}(x, x') dx'$$

$$-\frac{1}{\Phi_{\mathbf{r}}} \int_{-h_1}^{h_1} \theta_1^{\mathbf{r}}(\mathbf{x}') K_{2\mathbf{A}}(\mathbf{x}, \mathbf{x}') d\mathbf{x}'$$

$$= \frac{-j4\pi}{\zeta_0 \Phi_r} \left\{ C_1^r \left[ 2 \sin \beta_0 x - \frac{T_{s*d}(x)}{\Phi_r} \right] + 2\theta_1^r(x) - \frac{d_1^r(x)}{\Phi_r} \right\}$$

$$= \frac{-j4\pi}{\zeta_0 \Phi_r} \left[ C_1^r M_1^r(x) + 2\theta_1^r(x) - D_1^r(x) \right]$$
 (3.77)

$$M_1^{r}(x) = 2 \sin \beta_0 x - \frac{T_{s*d}(x)}{\Phi_r}$$
 (3.77)

$$D_1^{r}(x) = \frac{d_1^{r}(x)}{\Phi_r}$$
 (3.78)

$$T_{s*d}(x) = \int_{-h_1}^{h_1} \sin \beta_0 x' K_{2A}(x, x') dx'$$
 (3.79)

$$d_1^r(x) = \int_{-h_1}^{h_1} \theta_1^r(x') K_{2A}(x, x') dx'$$
 (3.80)

With (3.14) and (3.17), (3.8) can be rewritten as

$$\phi_4^{\mathbf{r}}(y) = \frac{j\omega}{\beta_0^2} \frac{\partial A_{4y}^{\mathbf{r}}(y)}{\partial y} + \frac{1}{4\pi\epsilon_0} \int_{-h_1}^{h_1} q_1^{\mathbf{r}}(\mathbf{x}') K_{1B}(y, \mathbf{x}') d\mathbf{x}' \qquad (3.81)$$

Similarly, with (3.30) and (3.32), (3.24) can be rewritten as

$$\phi_1^{r}(x) = \frac{j\omega}{\beta_0^2} \frac{\partial A_{1x}^{r}(x)}{\partial x} + \frac{1}{4\pi\epsilon_0} \int_{-h_2}^{h_2} q_4^{r}(y') K_{2B}(x, y') dy'$$
 (3.82)

If the zeroth order solutions are substituted in (3.81) and (3.82) respectively, we obtain

$$\phi_4^{\mathbf{r}}(y) = \frac{j\omega}{\beta_0^2} \frac{-j}{v_0} \left[ -C_4^{\mathbf{r}} \beta_0 \sin \beta_0 y + \frac{\partial \theta_4^{\mathbf{r}}(y)}{\partial y} \right]$$

$$+ \frac{1}{4\pi\epsilon_0} \int_{-h_1}^{h_1} \left[ q_1^{r}(x') \right]_{0} K_{1B}(y, x') dx'$$

$$= -C_4^r \sin \beta_0 y + \frac{1}{\beta_0} \frac{\partial \theta_4^r(y)}{\partial y} + \frac{C_1^r}{\Phi_r} \int_{-h_1}^{h_1} \cos \beta_0 x' K_{1B}(y,x') dx'$$

$$+ \frac{1}{\Phi_{\mathbf{r}}\beta_{0}} \int_{-h_{1}}^{h_{1}} \frac{\partial \theta_{1}^{\mathbf{r}}(\mathbf{x}')}{\partial \mathbf{x}'} K_{1B}(\mathbf{y}, \mathbf{x}') d\mathbf{x}'$$

$$= -C_4^r \sin \beta_0 y + \frac{1}{\beta_0} \frac{\partial \theta_4^r(y)}{\partial y} + C_1^r \frac{T_{cd}(y)}{\Phi_r} + \frac{f_1^r(y)}{\Phi_r}$$

$$= -C_4^r \sin \beta y + \frac{1}{\beta_0} \frac{\partial \theta_4^r(y)}{\partial y} + C_1^r L_2^r(y) + F_1^r(y)$$
(3.83)

$$L_2^{r}(y) = \frac{T_{cd}(y)}{\Phi_r}$$
 (3.84)

$$F_1^{r}(y) = \frac{f_1^{r}(y)}{\Phi_r}$$
 (3.85)

$$T_{cd}(y) = \int_{-h_1}^{h_1} \cos \beta_0 x' K_{lB}(y, x') dx'$$
 (3.86)

$$f_1^r(y) = \frac{1}{\beta_0} \int_{-h_1}^{h_1} \frac{\partial \theta_1^r(\mathbf{x}')}{\partial \mathbf{x}'} K_{1B}(y, \mathbf{x}') d\mathbf{x}'$$
 (3.87)

$$\phi_1^{\mathbf{r}}(\mathbf{x}) = \frac{j\omega}{\beta_0^2} \frac{-j}{v_0} \left[ C_1^{\mathbf{r}} \beta_0 \cos \beta_0 \mathbf{x} + \frac{\partial \theta_1^{\mathbf{r}}(\mathbf{x})}{\partial \mathbf{x}} \right]$$

$$+ \frac{1}{4\pi\epsilon_0} \int_{-h_2}^{h_2} \left[ q_4^{\mathbf{r}}(y') \right]_0 K_{2B}(\mathbf{x}, y') dy'$$

$$= C_1^r \cos \beta_0 x + \frac{1}{\beta_0} \frac{\partial \theta_1^r(x)}{\partial x} - \frac{C_4^r}{\Phi_r} T_{s*a}(x) + \frac{f_2^r(x)}{\Phi_r}$$

$$= C_1^r \cos \beta_0 x + \frac{1}{\beta_0} \frac{\partial \theta_1^r(x)}{\partial x} - C_4^r M_2^r(x) + F_2^r(x)$$
(3.88)

$$M_2^{r}(x) = \frac{T_{s*a}(x)}{\Phi_r}$$
 (3.89)

$$F_2^{r}(x) = \frac{f_2^{r}(x)}{\Phi_r}$$
 (3.90)

$$T_{s*a}(x) = \int_{-h_2}^{h_2} \sin \beta_0 y' K_{2B}(x, y') dy'$$
 (3.91)

$$f_2^{r}(x) = \frac{1}{\beta_0} \int_{-h_2}^{h_2} \frac{\partial \theta_4^{r}(y')}{\partial y'} K_{2B}(x, y') dy'$$
 (3.92)

The boundary conditions to be used for the first order solutions are:

(a) Current at the corners is continuous

i.e., 
$$I_{4v}^{r}(y = h_2) = -I_{1x}^{r}(x = h_1)$$
 (3.93)

(b) Scalar potential at the corners is continuous

i.e., 
$$\phi_4^r(y = h_2) = \phi_1^r(x = h_1)$$
 (3.94)

The substitution of (3.72) and (3.77) in (3.93) gives

$$C_4^{r}L_1^{r}(h_2) + 2\theta_4^{r}(h_2) - N_1^{r}(h_2)$$

$$= - \left[C_1^{r}M_1^{r}(h_1) + 2\theta_1^{r}(h_1) - D_1^{r}(h_1)\right] \qquad (3.95)$$

With (3.83) and (3.88), (3.94) becomes

$$-C_{4}^{r} \sin \beta_{0}h_{2} + \frac{1}{\beta_{0}} \frac{\partial \theta_{4}^{r}(y)}{\partial y} + C_{1}^{r}L_{2}^{r}(h_{2}) + F_{1}^{r}(h_{2})$$

$$y = h_{2}$$

$$= C_{1}^{r} \cos \beta_{0}h_{1} + \frac{1}{\beta_{0}} \frac{\partial \theta_{1}^{r}(\mathbf{x})}{\partial \mathbf{x}} - C_{4}^{r}M_{2}^{r}(h_{2}) + F_{2}^{r}(h_{1})$$

$$\mathbf{x} = h_{1}$$
(3.96)

Solving (3.95) and (3.96) for  $C_4^r$  and  $C_1^r$ , we obtain

$$C_{4}^{r} = \frac{\begin{bmatrix} 2\theta_{4}^{r}(h_{2}) + 2\theta_{1}^{r}(h_{1}) - N_{1}^{r}(h_{2}) - D_{1}^{r}(h_{1}) \end{bmatrix} \begin{bmatrix} \cos \beta_{0}h_{1} - L_{2}^{r}(h_{2}) \end{bmatrix}}{+ M_{1}^{r}(h_{1}) \begin{bmatrix} \frac{1}{\beta_{0}} \frac{\partial \theta_{4}^{r}(y)}{\partial y} \\ y = h_{2} \end{bmatrix}} - \frac{1}{\beta_{0}} \frac{\partial \theta_{1}^{r}(x)}{\partial x} + F_{1}^{r}(h_{2}) - F_{2}^{r}(h_{1}) \end{bmatrix}}{+ K_{1}^{r}(h_{2}) - K_{2}^{r}(h_{2})}$$

$$= \frac{M_{1}^{r}(h_{1}) \begin{bmatrix} \sin \beta_{0}h_{2} - M_{2}^{r}(h_{1}) \end{bmatrix} - L_{1}^{r}(h_{2}) \begin{bmatrix} \cos \beta_{0}h_{1} - L_{2}^{r}(h_{2}) \end{bmatrix}}{(3.97)}$$

$$C_{1}^{r} = \frac{\begin{bmatrix} 2\theta_{4}^{r}(h_{2}) + 2\theta_{1}^{r}(h_{1}) - N_{1}^{r}(h_{2}) - D_{1}^{r}(h_{1}) \end{bmatrix} \begin{bmatrix} \sin \beta_{0}h_{2} - M_{2}^{r}(h_{1}) \end{bmatrix}}{ + L_{1}^{r}(h_{2}) \begin{bmatrix} \frac{1}{\beta_{0}} \frac{\partial \theta_{4}^{r}(y)}{\partial y} \\ y = h_{2} \end{bmatrix}} - \frac{1}{\beta_{0}} \frac{\partial \theta_{1}^{r}(x)}{\partial x} + F_{1}^{r}(h_{2}) - F_{2}^{r}(h_{1}) \end{bmatrix}}{ \times = h_{1}}$$

$$C_{1}^{r} = \frac{M_{1}^{r}(h_{1}) \begin{bmatrix} \sin \beta_{0}h_{2} + M_{2}^{r}(h_{1}) \end{bmatrix} - L_{1}^{r}(h_{2}) \begin{bmatrix} \cos \beta_{0}h_{1} - L_{2}^{r}(h_{2}) \end{bmatrix}}{ \times = h_{1}}$$

$$\frac{\mathbf{L}_{1}^{r} = -\mathbf{L}_{1}^{r}(\mathbf{h}_{1}) \left[ \sin \beta_{0} \mathbf{h}_{2} - \mathbf{M}_{2}^{r}(\mathbf{h}_{1}) \right] - \mathbf{L}_{1}^{r}(\mathbf{h}_{2}) \left[ \cos \beta_{0} \mathbf{h}_{1} - \mathbf{L}_{2}^{r}(\mathbf{h}_{2}) \right]}{(3.98)}$$

For our first approximation, we assume that

$$\theta_4^{r}(y) \cong \left[\theta_4^{r}(y)\right]_0 = \frac{V}{2} \sin \beta_0 |y|$$
 (3.99)

$$\theta_1^{\mathbf{r}}(\mathbf{x}) \cong \left[\theta_1^{\mathbf{r}}(\mathbf{x})\right]_0 = 0$$
 (3.100)

Then (3.74), (3.78), (3.85) and (3.90) can be rewritten as

$$N_1^{r}(y) = \frac{\frac{V}{2}}{\Phi_r} \int_{-h_2}^{h_2} \sin \beta_0 |y'| K_{1A}(y, y') dy' = \frac{\frac{V}{2}}{\Phi_r} T_{sa}(y)$$
 (3.101)

$$T_{sa}(y) = \int_{-h_2}^{h_2} \sin \beta_0 |y'| K_{lA}(y, y') dy'$$
 (3.102)

$$D_1^{r}(x) = 0 (3.103)$$

$$F_1^{r}(y) = 0$$
 (3.104)

$$F_2^r(x) = \frac{\frac{V}{2}}{\Phi_r} \int_{-h_2}^{h_2} \pm \cos \beta_0 y' K_{2B}(x, y') dy'$$
 + for  $y' > 0$ 

$$= \frac{\frac{V}{2}}{\Phi_r} T_{ba}(x) \tag{3.105}$$

$$T_{ba}(x) = \int_{-h_2}^{h_2} \pm \cos \beta_0 y' K_{2B}(x, y') dy' - \text{for } y' < 0$$
(3.106)

Using (3.99) to (3.106),  $C_4^r$  in (3.97) and  $C_1^r$  in (3.98) can be obtained as follows if only the terms with the order of  $\frac{1}{\Phi_r}$  are retained in both numerator and denominator:

$$\begin{bmatrix} C_4^r \end{bmatrix}_1 = -\frac{\frac{V}{2} \left[ \sin \beta_0 (h_1 + h_2) + \frac{B^r}{\Phi_r} \right]}{\cos \beta_0 (h_1 + h_2) + \frac{G}{\Phi_r}}$$
(3.107)

$$\begin{bmatrix} C_1^T \end{bmatrix}_1 = \frac{\frac{V}{2} \begin{bmatrix} 1 + \frac{H^T}{\Phi_r} \end{bmatrix}}{\cos \beta_0 (h_1 + h_2) + \frac{G}{\Phi_r}}$$
(3.108)

$$B^{r} = -\frac{1}{2} \left[ T_{sa}(h_{2}) \cos \beta_{o} h_{1} + 2 T_{cd}(h_{2}) \sin \beta_{o} h_{2} + T_{s*d}(h_{1}) \cos \beta_{o} h_{2} + 2 T_{ba}(h_{1}) \sin \beta_{o} h_{1} \right]$$

$$(3.109)$$

$$G = \frac{1}{2} \left[ T_{s*d}(h_1) \sin \beta_0 h_2 + 2T_{s*a}(h_1) \sin \beta_0 h_1 \right]$$

$$-T_{ca}(h_2) \cos \beta_0 h_1 - 2T_{cd}(h_2) \cos \beta_0 h_2$$
(3.110)

$$H^{r} = -\frac{1}{2} \left\{ \sin \beta_{0} h_{2} \left[ T_{sa}(h_{2}) + 2T_{s*a}(h_{1}) \right] + \cos \beta_{0} h_{2} \left[ T_{ca}(h_{2}) + 2T_{ba}(h_{1}) \right] \right\}$$
(3.111)

With (3.51), (3.107) and (3.108), (3.49) and (3.50) can be rewritten as

$$\left[I_{4y}^{r}(y)\right]_{1} = \frac{-j4\pi}{\zeta_{o}\Phi_{r}} \left\{ -\frac{\frac{V}{2}\left[\sin\beta_{o}(h_{1} + h_{2}) + \frac{B^{r}}{\Phi_{r}}\right]}{\cos\beta_{o}(h_{1} + h_{2}) + \frac{G}{\Phi_{r}}} \cos\beta_{o}y + \theta_{4}^{r}(y) \right\} \tag{3.112}$$

$$\begin{bmatrix}
I_{1x}^{\mathbf{r}}(\mathbf{x})
\end{bmatrix}_{1} = \frac{-j4\pi}{\zeta_{0}\Phi_{\mathbf{r}}} \left\{ \frac{\frac{V}{2}\left[1 + \frac{H^{\mathbf{r}}}{\Phi_{\mathbf{r}}}\right]}{\cos\beta_{0}(h_{1} + h_{2}) + \frac{G}{\Phi}} \sin\beta_{0}\mathbf{x} + \theta_{1}^{\mathbf{r}}(\mathbf{x}) \right\}$$
(3.113)

(E) Evaluation of Particular Integrals  $\theta_4^r(y)$  and  $\theta_1^r(x)$ :

Integrating by parts, we can rewrite  $\theta_4^{\ r}(y)$  and  $\theta_1^{\ r}(x)$  in (3.40) and (3.42) as

$$\theta_{4}^{\mathbf{r}}(y) = \frac{V}{2} \sin \beta_{0} |y| - \int_{0}^{y} \frac{\partial}{\partial s} \left[ \phi_{41}^{\mathbf{r}}(x) + \phi_{43}^{\mathbf{r}}(s) \right] \sin \beta_{0}(y-s) ds$$

$$= \frac{V}{2} \sin \beta_{0} |y| + \left[ \phi_{41}^{\mathbf{r}}(0) + \phi_{43}^{\mathbf{r}}(0) \right] \sin \beta_{0} y$$

$$+ \beta_{0} \int_{0}^{y} \left[ \phi_{41}^{\mathbf{r}}(s) + \phi_{43}^{\mathbf{r}}(s) \right] \cos \beta_{0}(y-s) ds$$

$$= \frac{V}{2} \sin \beta_{0} |y| + \beta_{0} \int_{0}^{y} \left[ \phi_{41}^{\mathbf{r}}(s) + \phi_{43}^{\mathbf{r}}(s) \right] \cos \beta_{0}(y-s) ds$$

$$= \frac{V}{2} \sin \beta_{0} |y| + \beta_{0} \int_{0}^{y} \left[ \phi_{41}^{\mathbf{r}}(s) + \phi_{43}^{\mathbf{r}}(s) \right] \cos \beta_{0}(y-s) ds$$

$$= \frac{V}{2} \sin \beta_{0} |y| + \beta_{0} \int_{0}^{y} \left[ \phi_{41}^{\mathbf{r}}(s) + \phi_{43}^{\mathbf{r}}(s) \right] \cos \beta_{0}(y-s) ds$$

$$= \frac{V}{2} \sin \beta_{0} |y| + \beta_{0} \int_{0}^{y} \left[ \phi_{41}^{\mathbf{r}}(s) + \phi_{43}^{\mathbf{r}}(s) \right] \cos \beta_{0}(y-s) ds$$

$$= \frac{V}{2} \sin \beta_{0} |y| + \beta_{0} \int_{0}^{y} \left[ \phi_{41}^{\mathbf{r}}(s) + \phi_{43}^{\mathbf{r}}(s) \right] \cos \beta_{0}(y-s) ds$$

$$= \frac{V}{2} \sin \beta_{0} |y| + \beta_{0} \int_{0}^{y} \left[ \phi_{41}^{\mathbf{r}}(s) + \phi_{43}^{\mathbf{r}}(s) \right] \cos \beta_{0}(y-s) ds$$

$$= \frac{V}{2} \sin \beta_{0} |y| + \beta_{0} \int_{0}^{y} \left[ \phi_{41}^{\mathbf{r}}(s) + \phi_{43}^{\mathbf{r}}(s) \right] \cos \beta_{0}(y-s) ds$$

$$= \frac{V}{2} \sin \beta_{0} |y| + \beta_{0} \int_{0}^{y} \left[ \phi_{41}^{\mathbf{r}}(s) + \phi_{43}^{\mathbf{r}}(s) \right] \cos \beta_{0}(y-s) ds$$

(3.114) is derived based on the relation of

$$\phi_{41}^{r}(0) = -\phi_{43}^{r}(0)$$
 (3.115)

Similarly,

$$\theta_{1}^{\mathbf{r}}(\mathbf{x}) = -\int_{0}^{\mathbf{x}} \frac{\partial}{\partial \mathbf{s}} \left[ \phi_{12}^{\mathbf{r}}(\mathbf{s}) + \phi_{14}^{\mathbf{r}}(\mathbf{s}) \right] \sin \beta_{0}(\mathbf{x} - \mathbf{s}) d\mathbf{s}$$

$$= \left[ \phi_{12}^{\mathbf{r}}(\mathbf{o}) + \phi_{14}^{\mathbf{r}}(\mathbf{o}) \right] \sin \beta_{0}\mathbf{x} + \beta_{0} \int_{0}^{\mathbf{x}} \left[ \phi_{12}^{\mathbf{r}}(\mathbf{s}) + \phi_{14}^{\mathbf{r}}(\mathbf{s}) \right]$$

$$\cdot \cos \beta_{0}(\mathbf{x} - \mathbf{s}) d\mathbf{s}$$

$$= 2 \phi_{12}^{\mathbf{r}}(\mathbf{o}) \sin \beta_{0}\mathbf{x} + \beta_{0} \int_{0}^{\mathbf{x}} \left[ \phi_{12}^{\mathbf{r}}(\mathbf{s}) + \phi_{14}^{\mathbf{r}}(\mathbf{x}) \right] \cos \beta_{0}(\mathbf{x} - \mathbf{s}) d\mathbf{s}$$

$$= 2 \phi_{12}^{\mathbf{r}}(\mathbf{o}) \sin \beta_{0}\mathbf{x} + \beta_{0} \int_{0}^{\mathbf{x}} \left[ \phi_{12}^{\mathbf{r}}(\mathbf{s}) + \phi_{14}^{\mathbf{r}}(\mathbf{x}) \right] \cos \beta_{0}(\mathbf{x} - \mathbf{s}) d\mathbf{s}$$

$$= 3 \phi_{12}^{\mathbf{r}}(\mathbf{o}) \sin \beta_{0}\mathbf{x} + \beta_{0} \int_{0}^{\mathbf{x}} \left[ \phi_{12}^{\mathbf{r}}(\mathbf{s}) + \phi_{14}^{\mathbf{r}}(\mathbf{x}) \right] \cos \beta_{0}(\mathbf{x} - \mathbf{s}) d\mathbf{s}$$

$$= 3 \phi_{12}^{\mathbf{r}}(\mathbf{o}) \sin \beta_{0}\mathbf{x} + \beta_{0} \int_{0}^{\mathbf{x}} \left[ \phi_{12}^{\mathbf{r}}(\mathbf{s}) + \phi_{14}^{\mathbf{r}}(\mathbf{x}) \right] \cos \beta_{0}(\mathbf{x} - \mathbf{s}) d\mathbf{s}$$

$$= 3 \phi_{12}^{\mathbf{r}}(\mathbf{o}) \sin \beta_{0}\mathbf{x} + \beta_{0} \int_{0}^{\mathbf{x}} \left[ \phi_{12}^{\mathbf{r}}(\mathbf{s}) + \phi_{14}^{\mathbf{r}}(\mathbf{x}) \right] \cos \beta_{0}(\mathbf{x} - \mathbf{s}) d\mathbf{s}$$

$$= 3 \phi_{12}^{\mathbf{r}}(\mathbf{o}) \sin \beta_{0}\mathbf{x} + \beta_{0} \int_{0}^{\mathbf{x}} \left[ \phi_{12}^{\mathbf{r}}(\mathbf{s}) + \phi_{14}^{\mathbf{r}}(\mathbf{s}) \right] \cos \beta_{0}(\mathbf{x} - \mathbf{s}) d\mathbf{s}$$

$$= 3 \phi_{12}^{\mathbf{r}}(\mathbf{o}) \sin \beta_{0}\mathbf{x} + \beta_{0} \int_{0}^{\mathbf{x}} \left[ \phi_{12}^{\mathbf{r}}(\mathbf{s}) + \phi_{14}^{\mathbf{r}}(\mathbf{s}) \right] \cos \beta_{0}(\mathbf{x} - \mathbf{s}) d\mathbf{s}$$

$$= 3 \phi_{12}^{\mathbf{r}}(\mathbf{o}) \sin \beta_{0}\mathbf{x} + \beta_{0} \int_{0}^{\mathbf{x}} \left[ \phi_{12}^{\mathbf{r}}(\mathbf{s}) + \phi_{14}^{\mathbf{r}}(\mathbf{s}) \right] \cos \beta_{0}(\mathbf{x} - \mathbf{s}) d\mathbf{s}$$

based on the relation of

$$\phi_{12}^{r}(0) = \phi_{14}^{r}(0)$$
 (3.117)

For the first approximation, we substitute (3.99) and (3.100) in (3.55) and (3.56). This leads to

$$q_4^{r}(y) = +\frac{4\pi\epsilon_0}{\Phi_r} \left[ -C_4^{r} \sin\beta_0 y \pm \frac{V}{2} \cos\beta_0 y \right] - \text{for } y < 0$$
(3.118)

$$q_1^{r}(x) = + \frac{4\pi\epsilon_0}{\Phi_r} C_1^{r} \cos \beta_0 x \qquad (3.119)$$

The substitution of (3.119) in (3.17) gives

$$\phi_{41}^{r}(y) + \phi_{43}^{r}(y) = + \frac{C_{1}^{r}}{\Phi_{r}} \int_{-h_{1}}^{h_{1}} \cos \beta_{0} x' K_{1B}(y, x') dx'$$

$$= \frac{C_1^r}{\Phi_r} T_{cd}(y)$$
 (3.120)

Similarly, with (3.118), (3.32) can be rewritten as

$$\phi_{12}^{r}(x) + \phi_{14}^{r}(x) = -\frac{C_4^{r}}{\Phi_r} \int_{-h_2}^{h_2} \sin \beta_0 y' K_{2B}(x, y') dy'$$

$$+ \frac{\frac{V}{2}}{\Phi_{r}} \int_{-h}^{h_{2}} \pm \cos \beta_{o} y' K_{2B}(x, y') dy' + \text{for } y' > 0$$

$$- \text{ for } y' < 0$$

$$= -\frac{C_4^r}{\Phi_r} T_{s*a}(x) + \frac{\frac{V}{2}}{\Phi_r} T_{ba}(x)$$
(3.121)

With (3.117), (3.121) yields

$$2\phi_{12}^{r}(o) = -\frac{C_4^{r}}{\Phi_r} T_{s*a}(o) + \frac{\frac{V}{2}}{\Phi_r} T_{ba}(o)$$
 (3.122)

Substituting (3.120) in (3.114), we obtain

$$\theta_4^{r}(y) = \frac{V}{2} \sin \beta_0 |y| + \frac{C_1^{r} \beta_0}{\Phi_r} \int_0^y T_{cd}(s) \cos \beta_0(y-s) ds$$
 (3.123)

Similarly, with (3.121) and (3.122), (3.116) becomes

$$\theta_{1}^{r}(x) = \frac{1}{\Phi_{r}} \left\{ \left[ -C_{4}^{r} T_{s*a}(o) + \frac{V}{2} T_{ba}(o) \right] \sin \beta_{o} x \right.$$

$$\left. -C_{4}^{r} \int_{0}^{x} T_{s*a}(s) \cos \beta_{o}(x-s) ds + \frac{V}{2} \right.$$

$$\left. \cdot \int_{0}^{x} T_{ba}(s) \cos \beta_{o}(x-s) ds \right\}$$

(3.124)

With (3.108), (3.123) becomes

$$\left[\theta_4^{r}(y)\right] = \frac{V}{2} \sin \beta_0 |y|$$

$$+ \frac{-\frac{V}{2}\left[\sin\beta_{o}(h_{1}+h_{2})+\frac{B^{r}}{\Phi_{r}}\right]}{\cos\beta_{o}(h_{1}+h_{2})+\frac{G}{\Phi_{r}}} \frac{\beta_{o}}{\Phi_{r}} \int_{0}^{y} T_{cd}(s)\cos\beta_{o}(y-s)ds$$

$$= \frac{V}{2} \frac{\sin \beta_{0} |y| \left[\cos \beta_{0} (h_{1} + h_{2}) + \frac{G}{\Phi_{r}}\right] - \frac{\beta_{0}}{\Phi_{r}} \left[\sin \beta_{0} (h_{1} + h_{2}) + \frac{B^{r}}{\Phi_{r}}\right] t_{cd}(y)}{\cos \beta_{0} (h_{1} + h_{2}) + \frac{G}{\Phi_{r}}}$$

$$(3.125)$$

$$t_{cd}(y) = \int_{0}^{y} T_{cd}(s) \cos \beta_{o}(y - s) ds$$
 (3.126)

Similarly, the substitution of (3.107) in (3.124) gives

$$\begin{bmatrix} \theta_1^{\mathbf{r}}(\mathbf{x}) \\ 1 \end{bmatrix}_1 = \frac{1}{\Phi_{\mathbf{r}}} \frac{\mathbf{v}}{2} \left\{ \begin{bmatrix} \sin \beta_0(\mathbf{h}_1 + \mathbf{h}_2) + \frac{\mathbf{B}^{\mathbf{r}}}{\Phi_{\mathbf{r}}} \\ \cos \beta_0(\mathbf{h}_1 + \mathbf{h}_2) + \frac{\mathbf{G}}{\Phi_{\mathbf{r}}} \end{bmatrix} \right. \mathbf{T}_{\mathbf{s}*\mathbf{a}}(\mathbf{o}) + \mathbf{T}_{\mathbf{b}\mathbf{a}}(\mathbf{o}) \right\} \sin \beta_0 \mathbf{x}$$

$$+ \frac{\sin \beta_{0}(h_{1} + h_{2}) + \frac{B^{r}}{\Phi_{r}}}{\cos \beta_{0}(h_{1} + h_{2}) + \frac{G}{\Phi_{r}}} t_{s*a}(x) + t_{ba}(x)$$
(3.127)

where

$$t_{s*a}(x) = \int_{0}^{x} T_{s*a}(s) \cos \beta_{o}(x - s) ds$$
 (3.128)

$$t_{ba}(x) = \int_{0}^{x} T_{ba}(s) \cos \beta_{0}(x - s) ds$$
 (3.129)

With (3.125), (3.112) becomes

$$\begin{bmatrix}
I_{4y}^{\mathbf{r}}(y)
\end{bmatrix}_{11} = \frac{j2\pi V}{\zeta_0 \Phi_{\mathbf{r}}} \quad \mathbf{x}$$

$$= \frac{j2\pi V}{\zeta_{o}\Phi_{r}} \frac{\sin \beta_{o}(h_{1} + h_{2} - |y|) + \frac{1}{\Phi_{r}} P_{41}^{r}(y) + \frac{1}{\Phi_{r}^{2}} P_{42}^{r}(y)}{\cos \beta_{o}(h_{1} + h_{2}) + \frac{1}{\Phi_{r}} G}$$
(3.130)

$$P_{41}^{r}(y) = B^{r} \cos \beta_{0} y - G \sin \beta_{0} |y| + \beta_{0} \sin \beta_{0} (h_{1} + h_{2}) t_{cd}(y)$$
(3.131)

$$P_{42}^{r}(y) = \beta_0 B^r t_{cd}(y)$$
 (3.132)

Similarly, with (3.127), (3.113) becomes

$$\begin{bmatrix} I_{1x}^{r}(x) \end{bmatrix}_{11} = \frac{-j2\pi V}{\zeta_{0}\Phi_{r}} \times$$

$$\sin \beta_{0} x + \frac{1}{\Phi_{r}} \left\{ H^{r} \sin \beta_{0} x + \left[ \sin \beta_{0} (h_{1} + h_{2}) T_{s*a}(o) \right] \right.$$

$$+ \cos \beta_{0} (h_{1} + h_{2}) T_{ba}(o) \left[ \sin \beta_{0} x + \sin \beta_{0} (h_{1} + h_{2}) t_{s*a}(x) \right]$$

$$+ \cos \beta_{0} (h_{1} + h_{2}) t_{ba}(x) \left. \right\}$$

$$+ \frac{1}{\Phi_{r}^{2}} \left\{ \left[ B^{r} T_{s*a}(o) + G T_{ba}(o) \right] \sin \beta_{0} x + B^{r} t_{s*a}(x) + G t_{ba}(x) \right\}$$

$$\cos \beta_0(h_1 + h_2) + \frac{G}{\Phi_r}$$

$$= \frac{-j2\pi V}{\zeta_{o}\Phi_{r}} \frac{\sin \beta_{o}x + \frac{1}{\Phi_{r}} P_{11}^{r}(x) + \frac{1}{\Phi_{r}^{2}} P_{12}^{r}(x)}{\cos \beta_{o}(h_{1} + h_{2}) + \frac{G}{\Phi_{r}}}$$
(3.133)

$$P_{11}^{r}(x) = H^{r} \sin \beta_{o}x + \left[\sin \beta_{o}(h_{1} + h_{2}) T_{s*a}(o) + \cos \beta_{o}(h_{1} + h_{2}) T_{ba}(o)\right]$$

$$\cdot \sin \beta_{o}x + \sin \beta_{o}(h_{1} + h_{2}) t_{s*a}(x) + \cos \beta_{o}(h_{1} + h_{2}) t_{ba}(x)$$
(3.134)

$$p_{12}^{r}(x) = \left[B^{r}T_{s*a}(o) + GT_{ba}(o)\right] \sin \beta_{o}x$$

$$+ B^{r}t_{s*a}(x) + Gt_{ba}(x)$$
(3.135)

$$\begin{bmatrix} I_{4y}^{r} & (y) \end{bmatrix}_{11}$$
 and  $\begin{bmatrix} I_{1x}^{r} & (x) \end{bmatrix}_{11}^{r}$  involve the doubel integrals which in

turn complicate the problem. In order to avoid double integral, the following method is presented at the expense of sacrificing the accuracy of the theory:

Substituting (3.99) to (3.105) in (3.72), we obtain

$$\begin{bmatrix} I_{4y}^{\mathbf{r}}(y) \\ I_{0}^{\mathbf{r}} \end{bmatrix} = \frac{-j4\pi}{\zeta_{0}\Phi_{\mathbf{r}}}$$

$$\left\{-\frac{\frac{V}{2} \left[\sin \beta_{0}(h_{1} + h_{2}) + \frac{B^{r}}{\Phi_{r}}\right]}{\cos \beta_{0}(h_{1} + h_{2}) + \frac{G}{\Phi_{r}}}\right[2 \cos \beta_{0}y - \frac{T_{ca}(y)}{\Phi_{r}}\right]$$

$$+ V \sin \beta_{o} |y| - \frac{\frac{V}{2} T_{sa}(y)}{\Phi_{r}}$$

$$= \frac{j 2\pi V}{\zeta_{o} \Phi_{r}} \times \frac{2 \sin \beta_{o} ((h_{1} + h_{2}) - |y|) + \frac{1}{\Phi_{r}} U_{41}^{r}(y) + \frac{1}{\Phi_{r}^{2}} U_{42}^{r}(y)}{\cos \beta_{o} (h_{1} + h_{2}) + \frac{G}{\Phi_{r}}}$$

(3.136)

$$U_{41}^{r}(y) = 2B^{r} \cos \beta_{0} y - \sin \beta_{0}(h_{1} + h_{2}) T_{ca}(y) - G \sin \beta_{0} |y|$$

$$+ \cos \beta_{0}(h_{1} + h_{2}) T_{sa}(y)$$

$$U_{42}^{r}(y) = -B^{r}T_{ca}(y) + GT_{sa}(y)$$
 (3.138)

Similarly, the substitution of (3.99) to (3.105) in (3.77) yields

(3.137)

$$\begin{bmatrix}
I_{1x}^{r}(x)
\end{bmatrix}_{10} = \frac{-j4\pi}{\zeta_{0}\Phi_{r}} \left\{ \frac{\frac{V}{2}\left[1 + \frac{H^{r}}{\Phi_{r}}\right]}{\cos\beta_{0}(h_{1} + h_{2}) + \frac{G}{\Phi_{r}}} \left( 2 \sin\beta_{0}x - \frac{T_{s*d}(x)}{\Phi_{r}} \right) \right\}$$

$$= \frac{-j2\pi V}{\zeta_{o}\Phi_{r}} \frac{2 \sin \beta_{o}x + \frac{1}{\Phi_{r}} g_{11}^{r}(x) + \frac{1}{\Phi_{r}^{2}} g_{12}^{r}(x)}{\cos \beta_{o}(h_{1} + h_{2}) + \frac{G}{\Phi_{r}}}$$
(3.139)

$$g_{11}^{r}(x) = 2H^{r} \sin \beta_{0} x - T_{s*d}(x)$$
 (3.140)

$$g_{12}^{r}(x) = -H^{r} T_{s*d}(x)$$
 (3.141)

# (F) Expansion Parameter, $\Phi_{r}$

With zeroth order current in (3.66),  $\Phi_{\mathbf{r}}(\mathbf{y})$  in (3.45) can be rewritten as

$$\Phi_{\mathbf{r}}(y) = \frac{\int_{-h_2}^{h_2} \sin \beta_0(h_1 + h_2 - |y'|) K_{1A}(y, y') dy'}{\sin \beta_0(h_1 + h_2 - |y|)}$$

$$= \frac{\sin \beta_0! (h_1 + h_2) T_{ca}(y) - \cos \beta_0 (h_1 + h_2) T_{sa}(y)}{\sin \beta_0 (h_1 + h_2 - |y|)}$$

For a loop with  $\beta_0(h_1 + h_2) \le \frac{\pi}{2}$ , the point of maximum current is at y = 0, so

$$\Phi_{\mathbf{r}} = \left[ \Phi_{\mathbf{r}}(y) \right]_{y=0} = T_{ca}(0) - \cot \beta_{o}(h_{1} + h_{2}) T_{sa}(0)$$
(3.142)

For a loop with  $\beta_0(h_1+h_2)\geq \frac{\pi}{2}$ , the point of maximum current is at  $y=(h_1+h_2)-\frac{\lambda}{4}$ , so

$$\Phi_{\mathbf{r}} = \Phi_{\mathbf{r}}(\mathbf{y})$$

$$\mathbf{y} = (\mathbf{h}_1 + \mathbf{h}_2) - \frac{\lambda}{4}$$

$$= \sin \beta_0 (h_1 + h_2) T_{ca} (h_1 + h_2 - \frac{\lambda}{4}) - \cos \beta_0 (h_1 + h_2) T_{sa} (h_1 + h_2 - \frac{\lambda}{4})$$
(3.143)

#### 3.3. Total Loop Currents

By the principle of superposition we note that

$$I_{y}(y) = I_{4y}^{r}(y) + I_{4y}^{s}(y)$$
 (3.144)

$$I_{x}(x) = I_{1x}^{r}(x) + I_{1x}^{s}(x)$$
 (3.145)

$$V = -I_{y}(0)Z_{L} = -\left[I_{4y}^{r}(0) + I_{4y}^{s}(0)\right]Z_{L}$$
 (3.146)

(A) Considering the first order solutions of currents

$$\begin{bmatrix} I_{4y}^{\mathbf{r}}(y) \end{bmatrix}$$
 in (3.130),  $\begin{bmatrix} I_{4y}^{\mathbf{s}}(y) \end{bmatrix}$  in (1.167),  $\begin{bmatrix} I_{1x}^{\mathbf{r}}(x) \end{bmatrix}$  in

(3.133) and 
$$I_{1x}(x)$$
 in (1.170), V in (3.146) can be solved as

$$V = \frac{-j4\pi Z_{L} \frac{E_{o}}{\beta_{o}} \Phi_{r} \left[\cos \beta_{o}(h_{1} + h_{2}) + \frac{G}{\Phi_{r}}\right]}{\Phi_{s} \left[\cos \beta_{o}(h_{1} + h_{2}) + \frac{G}{\Phi_{s}}\right]} \times$$

$$\left[\cos \beta_{0}h_{1} - \cos \beta_{0}(h_{1} + h_{2}) + \frac{1}{\Phi_{s}}P_{41}^{s}(o) + \frac{1}{\Phi_{s}^{2}}P_{42}^{s}(o)\right]$$

$$\left[\zeta_{0}\Phi_{r}\left[\cos \beta_{0}(h_{1} + h_{2}) + \frac{G}{\Phi_{r}}\right] + j2\pi Z_{L}\left[\sin \beta_{0}(h_{1} + h_{2})\right]$$

$$+ \frac{1}{\Phi_{r}}P_{41}^{r}(o) + \frac{1}{\Phi_{r}^{2}}P_{42}^{r}(o)\right]$$
(3.147)

With (3.147), (3.130) can be rewritten as

$$\begin{split} & \left[ I_{4y}^{\mathbf{r}}(y) \right]_{11} = \frac{8\pi^{2} Z_{L}}{\zeta_{o}} \frac{E_{o}}{\beta_{o}} x \\ & \left[ \cos \beta_{o} h_{1} - \cos \beta_{o} (h_{1} + h_{2}) + \frac{1}{\Phi_{s}} P_{41}^{s}(o) + \frac{1}{\Phi_{s}^{2}} P_{42}^{s}(o) \right] x \\ & \left[ \sin \beta_{o} (h_{1} + h_{2} - |y|) + \frac{1}{\Phi_{r}} P_{41}^{\mathbf{r}}(y) + \frac{1}{\Phi_{r}^{2}} P_{42}^{\mathbf{r}}(y) \right] \\ & \left[ \Phi_{s} \left[ \cos \beta_{o} (h_{1} + h_{2}) + \frac{G}{\Phi_{s}} \right] \left\{ \zeta_{o} \Phi_{r} \left[ \cos \beta_{o} (h_{1} + h_{2}) + \frac{G}{\Phi_{r}} \right] \right. \\ & \left. + j 2\pi Z_{L} \left[ \sin \beta_{o} (h_{1} + h_{2}) + \frac{1}{\Phi_{r}} P_{41}^{\mathbf{r}}(o) + \frac{1}{\Phi_{r}^{2}} P_{42}^{\mathbf{r}}(o) \right] \right\} \end{split}$$

$$\begin{bmatrix} \Phi_{s} \left[ \cos \beta_{o}(h_{1} + h_{2}) + \frac{G}{\Phi_{s}} \right] \left\{ \zeta_{o} \Phi_{r} \left[ \cos \beta_{o}(h_{1} + h_{2}) + \frac{G}{\Phi_{r}} \right] \right. \\ + j 2\pi Z_{L} \left[ \sin \beta_{o}(h_{1} + h_{2}) + \frac{1}{\Phi_{r}} P_{41}^{r}(o) + \frac{1}{\Phi_{r}^{2}} P_{42}^{r}(o) \right] \right\}$$

Similarly, (3.133) can also be rewritten as

$$\begin{bmatrix} I_{1x}^{r}(x) \end{bmatrix}_{11} = -\frac{8\pi^{2}Z_{L}}{\zeta_{o}} \frac{E_{o}}{\beta_{o}} \times$$

$$= \int_{0}^{2\pi} \left[ \int_{0}^{2\pi}$$

(3.149)

(3.148)

Thus, the total loop currents in (3.144) and (3.145) can be expressed as the functions of the loop dimensions and the loading impedance  $Z_{I}$ .

(B) If consideration is given to the sub-first order solutions of currents  $\begin{bmatrix} I_{4y}^{r}(y) \end{bmatrix}$  in (3.136),  $\begin{bmatrix} I_{1x}^{r}(x) \end{bmatrix}$  in (3.139),  $\begin{bmatrix} I_{4y}^{s}(y) \end{bmatrix}$  in (1.173)

and  $I_{1x}(x)$  in (1.176), V in (3.146) is obtained as

$$V = \frac{-j4\pi Z_{L} \frac{E_{o}}{\beta_{o}} \Phi_{r} \left[\cos \beta_{o}(h_{1} + h_{2}) + \frac{G}{\Phi_{r}}\right]}{\Phi_{s} \left[\cos \beta_{o}(h_{1} + h_{2}) + \frac{G}{\Phi_{s}}\right]} \times$$

$$\frac{\left[2 \cos \beta_{0} h_{1} - 2 \cos \beta_{0} (h_{1} + h_{2}) + \frac{1}{\Phi_{s}} U_{41}^{s}(o) + \frac{1}{\Phi_{s}^{2}} U_{42}^{s}(o)\right]}{\left[\zeta_{0} \Phi_{r} \left[\cos \beta_{0} (h_{1} + h_{2}) + \frac{G}{\Phi_{r}}\right]\right]} + j2\pi Z_{L} \left[2 \sin \beta_{0} (h_{1} + h_{2}) + \frac{1}{\Phi_{r}} U_{41}^{r}(o) + \frac{1}{\Phi_{r}^{2}} U_{42}^{r}(o)\right] \qquad (3.150)$$

With (3.150), (3.136) can be rewritten as

$$\left[I_{4y}^{r}(y)\right]_{10} = \frac{8\pi^{2}Z_{L}}{\zeta_{0}} \frac{E_{0}}{\beta_{0}} \times$$

$$\begin{bmatrix}
2 \cos \beta_{0} h_{1} - 2 \cos \beta_{0} (h_{1} + h_{2}) + \frac{1}{\Phi_{s}} U_{41}^{s}(o) + \frac{1}{\Phi_{s}^{2}} U_{42}^{s}(o) \end{bmatrix} \times \\
\begin{bmatrix}
2 \sin \beta_{0} (h_{1} + h_{2} - y) + \frac{1}{\Phi_{r}} U_{41}^{r}(y) + \frac{1}{\Phi_{r}^{2}} U_{42}^{r}(y)
\end{bmatrix} \times \\
\Phi_{s} \begin{bmatrix}
\cos \beta_{0} (h_{1} + h_{2}) + \frac{G}{\Phi_{s}} \end{bmatrix} \times \left\{ \zeta_{0} \Phi_{r} \begin{bmatrix}
\cos \beta_{0} (h_{1} + h_{2}) + \frac{G}{\Phi_{r}} \end{bmatrix} + j2\pi Z_{L} \begin{bmatrix}
2 \sin \beta_{0} (h_{1} + h_{2}) + \frac{1}{\Phi_{r}} U_{41}^{r}(o) + \frac{1}{\Phi_{r}^{2}} U_{42}^{r}(o)
\end{bmatrix} \right\}$$
(3.151)

Similarly, (3.139) can be rewritten as

$$\begin{bmatrix} I_{1x}^{r}(x) \end{bmatrix}_{10} = -\frac{8\pi^{2}Z_{L}}{\zeta_{0}} \frac{E_{0}}{\beta_{0}} \times$$

$$\frac{\left[2 \sin \beta_{0} x + \frac{1}{\Phi_{r}} U_{11}^{r}(x) + \frac{1}{\Phi_{r}^{2}} U_{12}^{r}(x)\right]}$$

$$\frac{\Phi_{s} \left[\cos \beta_{o}(h_{1} + h_{2}) + \frac{G}{\Phi_{s}}\right] \left\{\zeta_{o}\Phi_{r} \left[\cos \beta_{o}(h_{1} + h_{2}) + \frac{G}{\Phi_{r}}\right] + j2\pi Z_{L}\left[2\sin \beta_{o}(h_{1} + h_{2}) + \frac{1}{\Phi_{r}}U_{41}^{r}(o) + \frac{1}{\Phi_{r}^{2}}U_{42}^{r}(o)\right]}{(3.152)}$$

#### 3.4. Total Backscattered Field

The vector potential, maintained by the induced current in the radiating loop, at an arbitrary point on the axis of the loop and in the far zone of the loop (Fig. 3.3) can be expressed as

$$A^{r} = A_{y}^{r} = \frac{\mu_{o}}{4\pi} \int_{-h_{2}}^{h_{2}} 2I_{4y}^{r}(y') \frac{e^{-j\beta_{o}R}}{R} dy'$$

$$\approx \frac{\mu_{o}}{2\pi} \frac{e^{-j\beta_{o}R_{o}}}{R_{o}} \int_{-h_{2}}^{h_{2}} I_{4y}^{r}(y') dy'$$
(3.153)

where

$$R = \sqrt{R_0^2 + y'^2 + h_1^2} \approx R_0$$
 (3.154)

# 3.4.1. Total Backscattered Field Based on First Order Currents

With (3.148), (3.153) can be rewritten as

$$\begin{bmatrix} A^{T} \end{bmatrix}_{11} = \begin{bmatrix} A^{T} \\ y \end{bmatrix}_{11} = \frac{4\pi\mu_{o}^{Z}L}{\zeta_{o}\beta_{o}} \quad E_{o} \quad \frac{e^{-j\beta_{o}^{R}o}}{R_{o}} \quad x$$

$$\begin{bmatrix} \cos\beta_{o}h_{1} - \cos\beta_{o}(h_{1} + h_{2}) + \frac{1}{\Phi_{s}} P_{41}^{s}(o) + \frac{1}{\Phi_{s}^{2}} P_{42}^{s}(o) \end{bmatrix} K_{1}$$

$$\frac{\Phi_{s} \left[\cos \beta_{o}(h_{1} + h_{2}) + \frac{G}{\Phi_{s}}\right] \left[\zeta_{o}\Phi_{r} \left[\cos \beta_{o}(h_{1} + h_{2}) + \frac{G}{\Phi_{r}}\right] + j2\pi Z_{L} \left[\sin \beta_{o}(h_{1} + h_{2}) + \frac{1}{\Phi_{r}} P_{41}^{r}(o) + \frac{1}{\Phi_{r}^{2}} P_{42}^{r}(o)\right]\right]}$$
(3. 155)

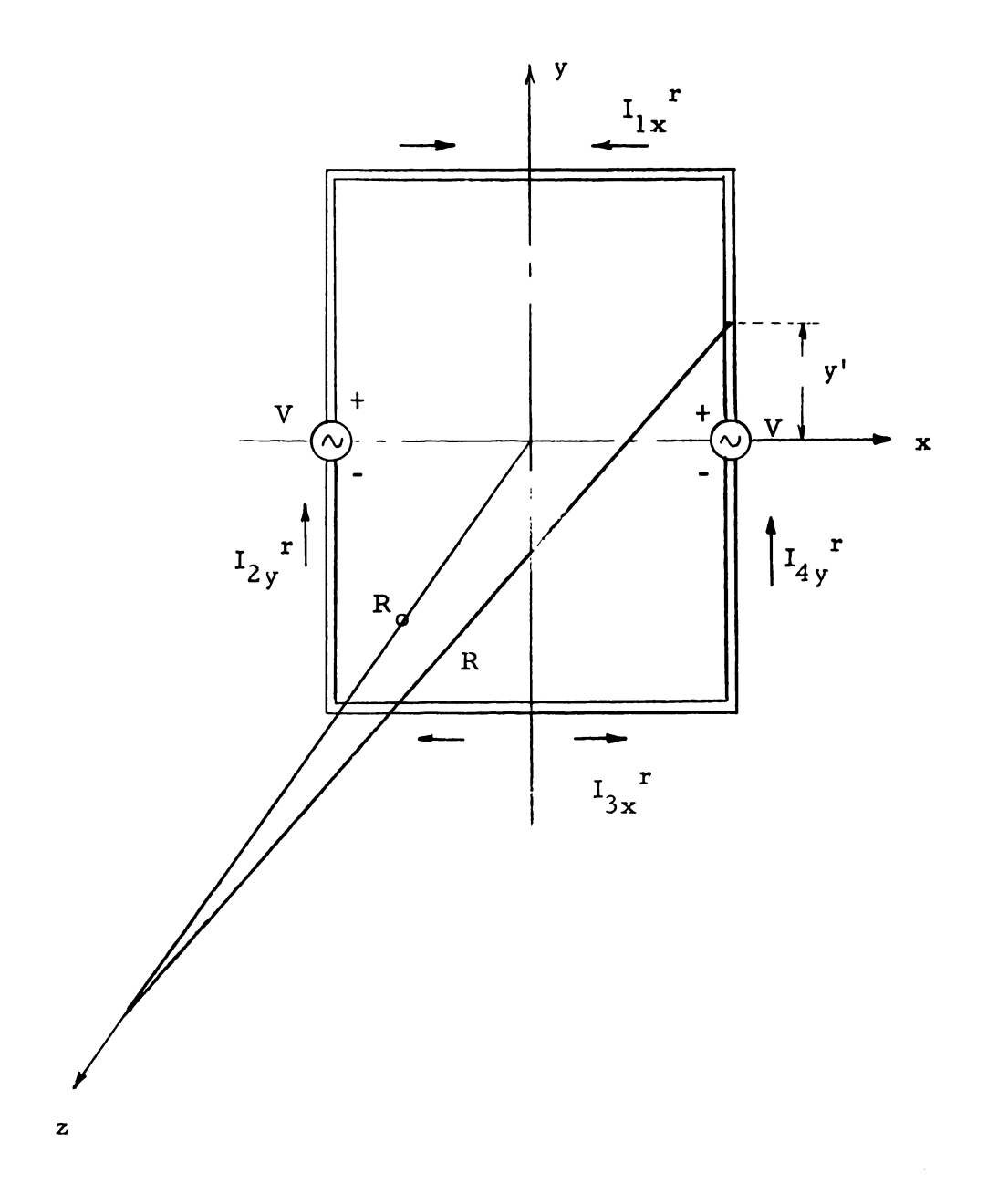


Figure 3.3 Geometry for the calculation of the radiation field of a radiating rectangular loop.

where
$$K_{1} = \int_{-h_{2}}^{h_{2}} \left[ \sin \beta_{0}(h_{1} + h_{2} - |y'|) + \frac{P_{41}^{r}(y')}{\Phi_{r}} + \frac{P_{42}^{r}(y')}{\Phi_{r}^{2}} \right] dy'$$
(3.156)

K, will be evaluated in a following section.

The backscattered electric field due to the radiating loop is

$$\begin{bmatrix} \mathbf{E}_{\mathbf{y}}^{\mathbf{r}} \end{bmatrix}_{11} = -j \omega \begin{bmatrix} \mathbf{A}_{\mathbf{y}}^{\mathbf{r}} \end{bmatrix}_{11} = -j 4\pi \mathbf{E}_{\mathbf{o}} \mathbf{Z}_{\mathbf{L}} \frac{e^{-j\beta_{\mathbf{o}} \mathbf{R}_{\mathbf{o}}}}{\mathbf{R}_{\mathbf{o}}} \mathbf{x}$$

$$\frac{\left[\cos \beta_{0}h_{1} - \cos \beta_{0}(h_{1} + h_{2}) + \frac{1}{\Phi_{s}} P_{41}^{s}(o) + \frac{1}{\Phi_{s}^{2}} P_{42}^{s}(o)\right] K_{1}}{\left[\Phi_{s} \left[\cos \beta_{0}(h_{1} + h_{2}) + \frac{G}{\Phi_{s}}\right] \left\{\zeta_{0}\Phi_{r} \left[\cos \beta_{0}(h_{1} + h_{2}) + \frac{G}{\Phi_{r}}\right]\right\} + j2\pi Z_{L} \left[\sin \beta_{0}(h_{1} + h_{2}) + \frac{1}{\Phi_{r}} P_{41}^{r}(o) + \frac{1}{\Phi_{r}^{2}} P_{42}^{r}(o)\right]} \right]$$
(3.157)

The total backscattered field from a loaded rectangular loop is obtained with (1.183) and (3.157)

$$\begin{bmatrix} E_{y} \end{bmatrix}_{11} = \begin{bmatrix} E_{y}^{s} \end{bmatrix}_{11} + \begin{bmatrix} E_{y}^{r} \end{bmatrix}_{11}$$

$$= 2E_{o} \frac{e^{-j\beta_{o}R_{o}}}{R_{o}} \frac{1}{\Phi_{s} \begin{bmatrix} \cos \beta_{o}(h_{1} + h_{2}) + \frac{G}{\Phi_{s}} \end{bmatrix}} \times \begin{cases} J_{1} - j_{2}\pi Z_{L}X \\ J_{1} - j_{2}\pi Z_{L}X \end{cases}$$

$$\begin{bmatrix} \cos \beta_{o}h_{1} - \cos \beta_{o}(h_{1} + h_{2}) + \frac{1}{\Phi_{s}} P_{41}^{s}(o) + \frac{1}{\Phi_{s}^{2}} P_{42}^{s}(o) \end{bmatrix} K_{1}$$

$$\begin{bmatrix} \zeta_{o}\Phi_{r} \begin{bmatrix} \cos \beta_{o}(h_{1} + h_{2}) + \frac{G}{\Phi_{r}} \end{bmatrix} + j2\pi Z_{L} \begin{bmatrix} \sin \beta_{o}(h_{1} + h_{2}) \\ + \frac{1}{\Phi_{r}} P_{41}^{r}(o) + \frac{1}{\Phi_{r}^{2}} P_{42}^{r}(o) \end{bmatrix}$$

$$(3.158)$$

3.4.2. Total Backscattered Field Based on Sub-first Order Currents
With (3.151), (3.153) can be rewritten as

$$\begin{bmatrix} A^{r} \\ 10 \end{bmatrix} = \begin{bmatrix} A_{y}^{r} \\ 10 \end{bmatrix} \approx \frac{\mu_{o}}{2\pi} \frac{e^{-j\beta_{o}R_{o}}}{R_{o}} \int_{-h_{2}}^{h_{2}} \left[ I_{4y}^{r}(y') \right]_{10} dy'$$

$$= \frac{4\pi\mu_{o}Z_{L}}{\zeta_{o}\beta_{o}} \quad E_{o} \quad \frac{e^{-j\beta_{o}R_{o}}}{R_{o}}$$

$$\begin{bmatrix} 2\cos\beta_{o}h_{1} - 2\cos\beta_{o}(h_{1} + h_{2}) + \frac{1}{\Phi_{s}} U_{41}^{s}(o) + \frac{1}{\Phi_{s}^{2}} U_{42}^{s}(o) \right] K_{2}$$

$$\boxed{\Phi_{s} \left[ \cos\beta_{o}(h_{1} + h_{2}) + \frac{G}{\Phi_{s}} \right] \left\{ \zeta_{o}\Phi_{r} \left[ \cos\beta_{o}(h_{1} + h_{2}) + \frac{1}{\Phi_{r}} G \right] \right\}$$

$$+ j2\pi Z_{L} \left[ 2\sin\beta_{o}(h_{1} + h_{2}) + \frac{1}{\Phi_{r}} U_{41}^{r}(o) + \frac{1}{\Phi_{r}^{2}} U_{42}^{r}(o) \right] \right\}$$

$$(3.159)$$

where
$$K_{2} = \int_{-h_{2}}^{h_{2}} \left[ 2 \sin \beta_{0}(h_{1} + h_{2} - |y'|) + \frac{1}{\Phi_{r}} U_{41}^{r}(y') + \frac{1}{\Phi_{r}^{2}} U_{42}^{r}(y') \right] dy'$$
(3.160)

Then, the backscattered electric field due to the radiating loop is obtained as

$$\begin{bmatrix} \mathbf{E}^{\mathbf{r}} \end{bmatrix}_{10} = \begin{bmatrix} \mathbf{E}_{\mathbf{y}} \end{bmatrix}_{10} = -\mathrm{j} \, \omega \begin{bmatrix} \mathbf{A}_{\mathbf{y}} \end{bmatrix}_{10} = -\mathrm{j} \, 4\pi \, \mathbf{E}_{\mathbf{o}} \mathbf{Z}_{\mathbf{L}} \frac{\mathrm{e}^{-\mathrm{j} \beta_{\mathbf{o}} \mathbf{R}_{\mathbf{o}}}}{\mathbf{R}_{\mathbf{o}}} \quad \mathbf{x}$$

$$\frac{\left[2\cos\beta_{0}h_{1}-2\cos\beta_{0}(h_{1}+h_{2})+\frac{1}{\Phi_{s}}U_{41}^{s}(o)+\frac{1}{\Phi_{s}^{2}}U_{42}^{s}(o)\right]K_{2}}{\Phi_{s}\left[\cos\beta_{0}(h_{1}+h_{2})+\frac{G}{\Phi_{s}}\right]\left\{\zeta_{0}\Phi_{r}\left[\cos\beta_{0}(h_{1}+h_{2})+\frac{G}{\Phi_{r}}\right]\right\} +j2\pi Z_{L}\left[2\sin\beta_{0}(h_{1}+h_{2})+\frac{1}{\Phi_{r}}U_{41}^{r}(o)+\frac{1}{\Phi_{r}^{2}}U_{42}^{r}(o)\right]\right\}} (3.161)$$

The total backscattered electric field due to the loaded rectangular loop can be calculated by superposing  $\begin{bmatrix} E^{\overline{S}} \end{bmatrix}$  in (1.188) upon  $\begin{bmatrix} E^{\overline{T}} \end{bmatrix}$ 

in (3.160) as

$$\begin{bmatrix} \mathbf{E}_{\mathbf{y}} \end{bmatrix}_{10} = \begin{bmatrix} \mathbf{E}_{\mathbf{y}} \end{bmatrix}_{10} + \begin{bmatrix} \mathbf{E}_{\mathbf{y}} \end{bmatrix}_{10}$$

$$= 2E_o \frac{e^{-j\beta_o R_o}}{R_o} \frac{1}{\Phi_s \left[\cos \beta_o (h_1 + h_2) + \frac{1}{\Phi_s} G\right]} \times$$

$$\left\{J_2 - j2\pi Z_L X\right\}$$

$$\frac{\left[2\cos\beta_{0}h_{1}-2\cos\beta_{0}(h_{1}+h_{2})+\frac{1}{\Phi_{s}}U_{41}^{s}(o)+\frac{1}{\Phi_{s}^{2}}u_{42}^{s}(o)\right]K_{2}}{\left[\zeta_{0}\Phi_{r}\left[\cos\beta_{0}(h_{1}+h_{2})+\frac{1}{\Phi_{r}}G\right]+j2\pi Z_{L}\left[2\sin\beta_{0}(h_{1}+h_{2})\right]} + \frac{1}{\Phi_{r}}U_{41}^{r}(o)+\frac{1}{\Phi_{r}^{2}}U_{42}^{r}(o)\right]}$$

$$\frac{\left[\zeta_{0}\Phi_{r}\left[\cos\beta_{0}(h_{1}+h_{2})+\frac{1}{\Phi_{r}}G\right]+j2\pi Z_{L}\left[2\sin\beta_{0}(h_{1}+h_{2})\right]}{\left[\zeta_{0}\Phi_{r}\left[\cos\beta_{0}(h_{1}+h_{2})+\frac{1}{\Phi_{r}}G\right]+j2\pi Z_{L}\left[2\sin\beta_{0}(h_{1}+h_{2})\right]\right]} + \frac{1}{\Phi_{r}}U_{41}^{r}(o)+\frac{1}{\Phi_{r}^{2}}U_{42}^{r}(o)\right]}$$

$$\frac{\left[\zeta_{0}\Phi_{r}\left[\cos\beta_{0}(h_{1}+h_{2})+\frac{1}{\Phi_{r}}G\right]+j2\pi Z_{L}\left[2\sin\beta_{0}(h_{1}+h_{2})\right]}{\left[\zeta_{0}\Phi_{r}\left[\cos\beta_{0}(h_{1}+h_{2})+\frac{1}{\Phi_{r}}G\right]+j2\pi Z_{L}\left[2\sin\beta_{0}(h_{1}+h_{2})\right]\right]}$$

$$\frac{\left[\zeta_{0}\Phi_{r}\left[\cos\beta_{0}(h_{1}+h_{2})+\frac{1}{\Phi_{r}}G\right]+j2\pi Z_{L}\left[2\sin\beta_{0}(h_{1}+h_{2})\right]}{\left[\zeta_{0}\Phi_{r}\left[\cos\beta_{0}(h_{1}+h_{2})+\frac{1}{\Phi_{r}}G\right]+j2\pi Z_{L}\left[2\sin\beta_{0}(h_{1}+h_{2})\right]}$$

# 3.4.3. Evaluations of $K_1$ and $K_2$

From (3.156) we note that

$$K_{1} = \int_{-h_{2}}^{h_{2}} \left[ \sin \beta_{0}(h_{1} + h_{2} - |y'|) + \frac{1}{\Phi_{r}} P_{41}^{r}(y') + \frac{1}{\Phi_{2}^{2}} P_{42}^{r}(y') \right] dy'$$

where

$$P_{41}^{r}(y) = B^{r} \cos \beta_{0} y - G \sin \beta_{0} |y| + \sin \beta_{0} (h_{1} + h_{2}) t_{cd}(y)$$

$$P_{42}^{r}(y) = \beta_{0} B^{r} t_{cd}(y)$$

then

$$K_1 = \frac{2}{\beta_0} \left[ \cos \beta_0 h_1 - \cos \beta_0 (h_1 + h_2) \right]$$

$$+\frac{1}{\Phi_{\mathbf{r}}}\left\{2B^{\mathbf{r}}\sin\beta_{0}h_{2}-G\left[1-\cos\beta_{0}h_{2}\right]+\beta_{0}\sin\beta_{0}(h_{1}+h_{2})b_{cd}\right\}$$

$$+\frac{1}{\Phi_{r}^{2}}$$
  $\beta_{o} B^{r} b_{cd}$  (3.163)

where

$$b_{cd} = \int_{-h_2}^{h_2} t_{cd}(y')dy' = \int_{-h_2}^{h_2} \left[ \int_{0}^{y'} T_{cd}(s) \cos \beta_0(y'-s) ds \right] dy'$$
(3.164)

Similarly, from (3.160), we have

$$K_{2} = \int_{-h_{2}}^{h_{2}} \left[ 2 \sin \beta_{0}(h_{1} + h_{2} - |y'|) + \frac{1}{\Phi_{r}} U_{41}^{r}(y') + \frac{1}{\Phi_{r}^{2}} U_{42}^{r}(y') \right] dy'$$

where

$$U_{41}^{r}(y) = 2B^{r} \cos \beta_{0} y - \sin \beta_{0}(h_{1} + h_{2}) T_{ca}(y) - G \sin \beta_{0}|y|$$

$$+ \cos \beta_{0}(h_{1} + h_{2}) T_{sa}(y)$$

$$U_{42}^{r}(y) = -B^{r} T_{ca}(y) + G T_{sa}(y)$$

Then

$$K_2 = \frac{4}{\beta_0} \left[ \cos \beta_0 h_1 - \cos \beta_0 (h_1 + h_2) \right]$$

$$+\frac{1}{\Phi_{\mathbf{r}}} \left[ \frac{4B^{\mathbf{r}}}{\beta_{0}} \quad \sin \beta_{0} h_{2} - \sin \beta_{0} (h_{1} + h_{2}) t_{ca} - \frac{2G\left[1 - \cos \beta_{0} h_{2}\right]}{\beta_{0}} \right]$$

+ 
$$\cos \beta_0(h_1 + h_2) t_{sa}$$
 +  $\frac{1}{\Phi_r^2} \left[ G t_{sa} - B^r t_{ca} \right]$  (3.165)

where

$$t_{ca} = \int_{-h_2}^{h_2} T_{ca}(y') dy'$$
 (3.166)

$$t_{sa} = \int_{-h_2}^{h_2} T_{sa}(y') dy'$$
 (3.167)

# 3.5. Optimum Impedance for Zero Backscattering

The optimum impedance for zero backscattering can be obtained by letting total backscattered field equal to zero.

3.5.1. First Order Optimum Impedance for Zero Backscattering

Letting  $\begin{bmatrix} E \\ y \end{bmatrix}_{11}$  in (3.158) equal to zero and solving for  $Z_L$ ,

we have

$$\begin{bmatrix} Z_{L} \\ 0 \end{bmatrix} = \frac{-jJ_{1}\zeta_{o}\Phi_{r} \left[\cos\beta_{o}(h_{1} + h_{2}) + \frac{1}{\Phi_{r}} G\right]}{\left[K_{1}\left[\cos\beta_{o}h_{1} - \cos\beta_{o}(h_{1} + h_{2}) + \frac{1}{\Phi_{s}} P_{41}^{s}(o) + \frac{1}{\Phi_{s}^{2}} P_{42}^{s}(o)\right]} - J_{1}\left[\sin\beta_{o}(h_{1} + h_{2}) + \frac{1}{\Phi_{r}} P_{41}^{r}(o) + \frac{1}{\Phi_{r}^{2}} P_{42}^{r}(o)\right]}$$

$$(3.168)$$

3.5.2. Sub-first Order Optimum Impedance for Zero Backscattering Letting  $\begin{bmatrix} E \\ y \end{bmatrix}_{10}$  in (3.161) equal to zero and solving for  $Z_L$ , we get

$$\begin{bmatrix} Z_{L} \\ 0 \end{bmatrix} = \frac{-jJ_{2}\zeta_{o}\Phi_{r} \left[\cos\beta_{o}(h_{1} + h_{2}) + \frac{1}{\Phi_{r}} G\right]}{\left[K_{2}\left[2\cos\beta_{o}h_{1} - 2\cos\beta_{o}(h_{1} + h_{2}) + \frac{1}{\Phi_{s}} U_{41}^{s}(o) + \frac{1}{\Phi_{s}^{2}} U_{42}^{s}(o)\right]} - J_{2}\left[2\sin\beta_{o}(h_{1} + h_{2}) + \frac{1}{\Phi_{r}} U_{41}^{r}(o) + \frac{1}{\Phi_{r}^{2}} U_{42}^{r}(o)\right]}$$

$$(3.169)$$

# 3.6. Numerical Examples

The numerical results are obtained for a square loop with  $\frac{a}{h} = 0.0388$ .  $\Phi_r$  is numerically calculated as functions of  $\beta_0 h$  and is plotted in Figure 3.4. The optimum loading for zero backscattering  $Z_L$  in (3.168) is then calculated as a function of

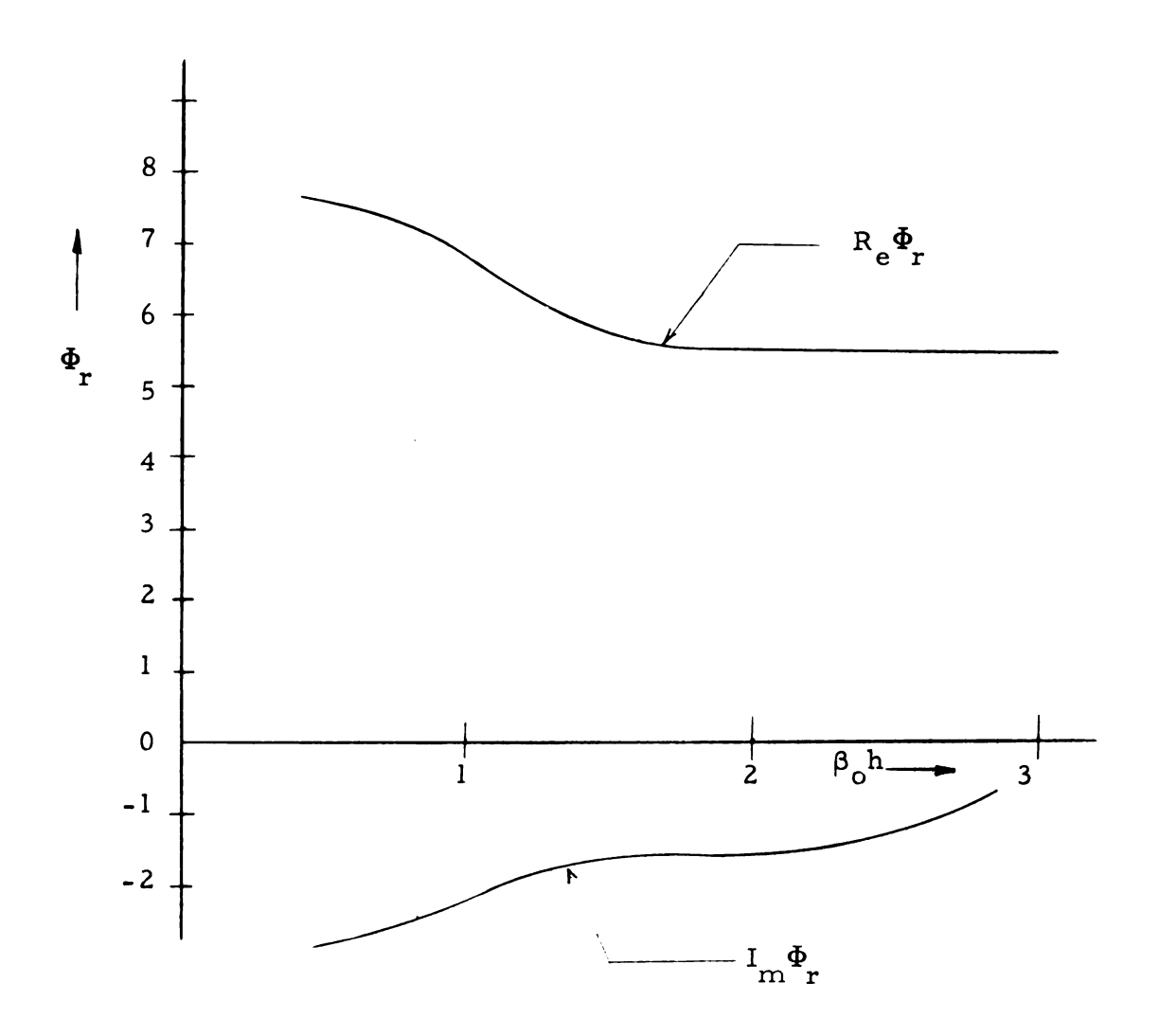


Figure 3.4.  $\Phi_r$  as a function of  $\beta_0 h$  (a/h = 0.0388).

 $\beta_0$ h for the case of  $\frac{a}{h} = 0.0388$ . Numerical results of  $Z_L$  are shown in Figure 3.5.

### 3.7. Experiment

The optimum impedance for zero backscattering from a rectangular loop requires both the resistive part and the reactive part shown in Figure 3.5. To simplify the problem, an experiment was conducted for a conducting square loop loaded with two identical reactive impedances. Experimentally, this reactive loading method proved to be quite adequate in reducing the backscattering cross section of a square loop.

## 3.7.1. Experimental Arrangement and Measuring Technique

The experimental setup and measuring technique were identical to the case of the circular loop mentioned in Chapter 2 and no further description seems to be necessary.

### 3.7.2. Experimental Results

A square loop (side length = 5.15 cm) were constructed as an experimental model using cylindrical wire of 0.1 cm radius. The experiments were conducted at various frequencies. The experimental results are shown in Figure 3.6 to Figure 3.16 in which the backscattering cross sections of the square loop were plotted as functions of loading impedances at each particular frequency. The solid curve represents the backscattering cross section of a loaded square loop



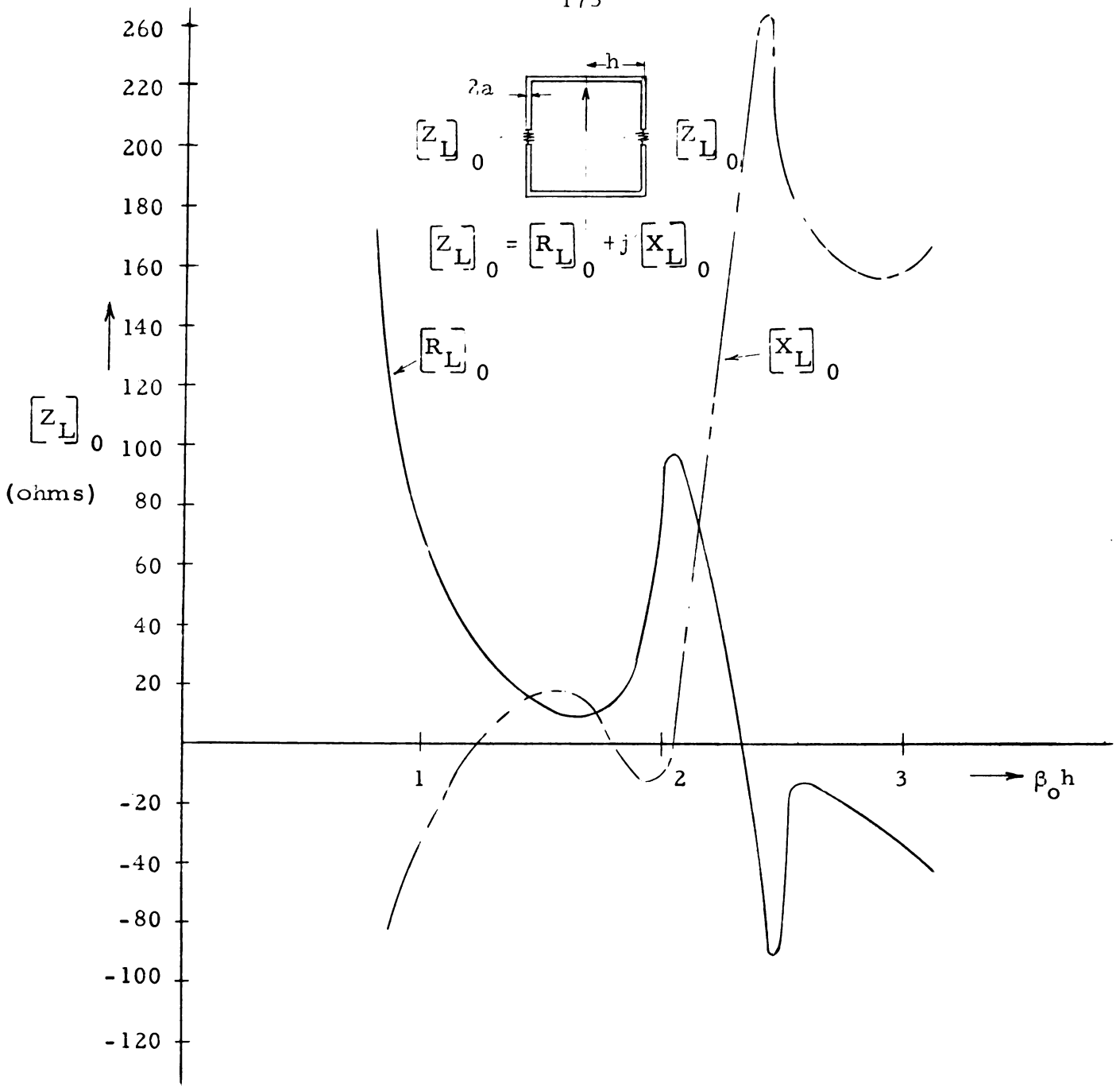


Figure 3.5. Optimum impedance for zero backscattering from a square loop (a/h = 0.0388).

and the solid straight line represents that of the solid quare loop. It is observed that if the loading impedance (or the length of the coaxial line) is properly adjusted, the backscatters of the square loops can be minimized to the noise level. About 15 db reduction in the backscattering cross section was obtained in the experiments. In Figure 3.17, the optimum reactive impedances for minimum backscattering are plotted as a function of  $\beta_0$ h.

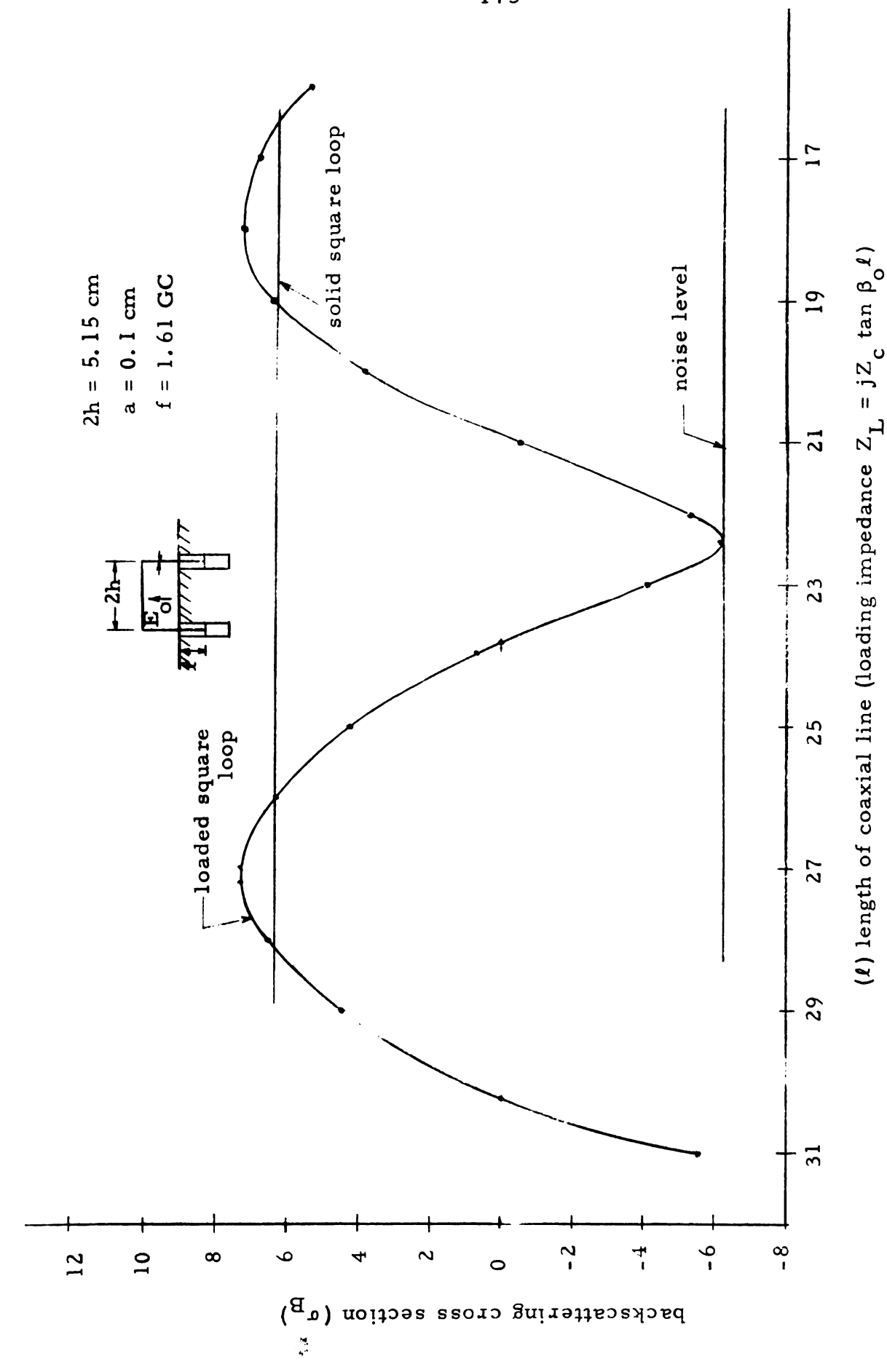


Figure 3.6. Backscattering cross section of a loaded square loop as a function of loading impedance  $(f = 1.61 \, \text{GC})$ .

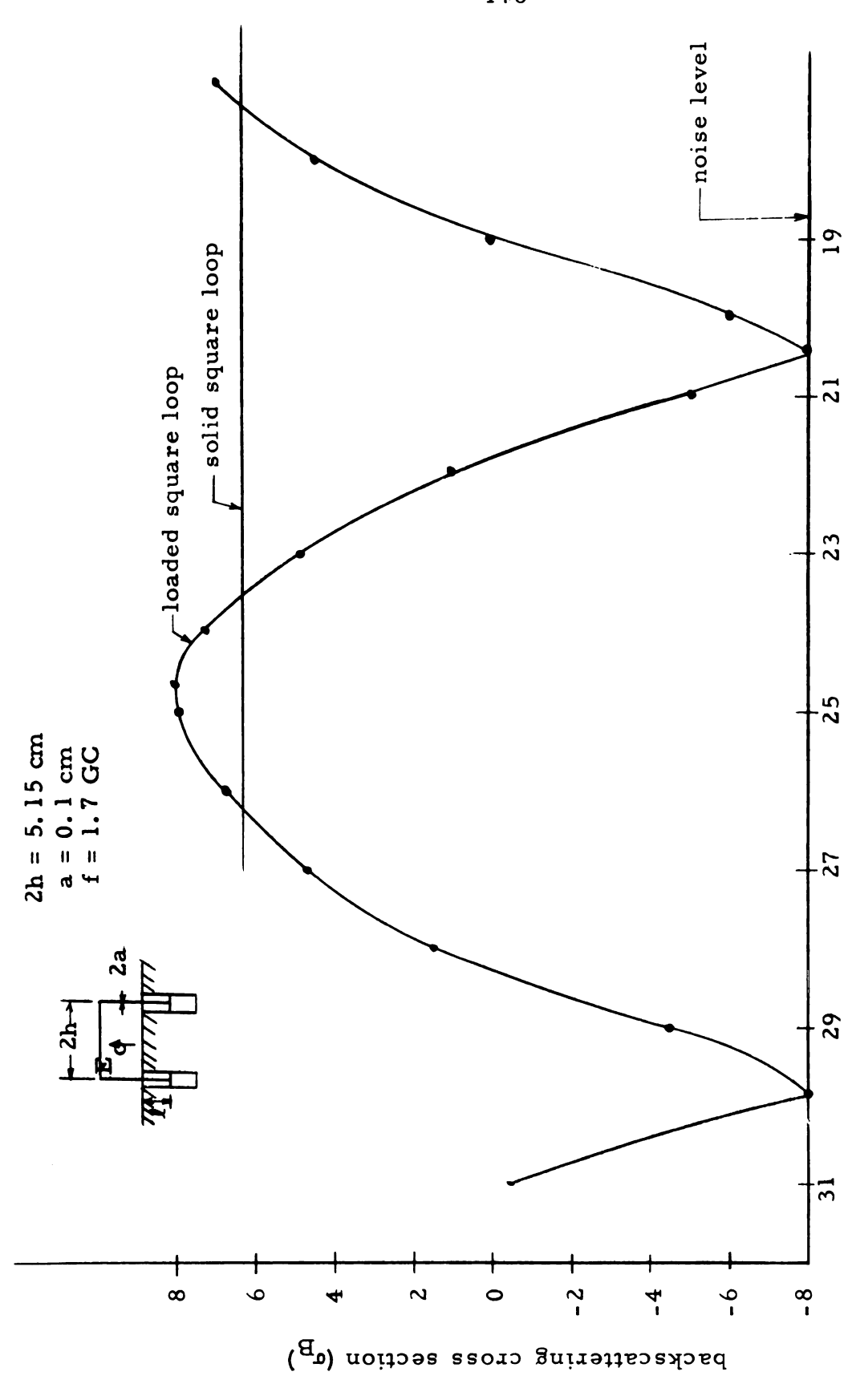
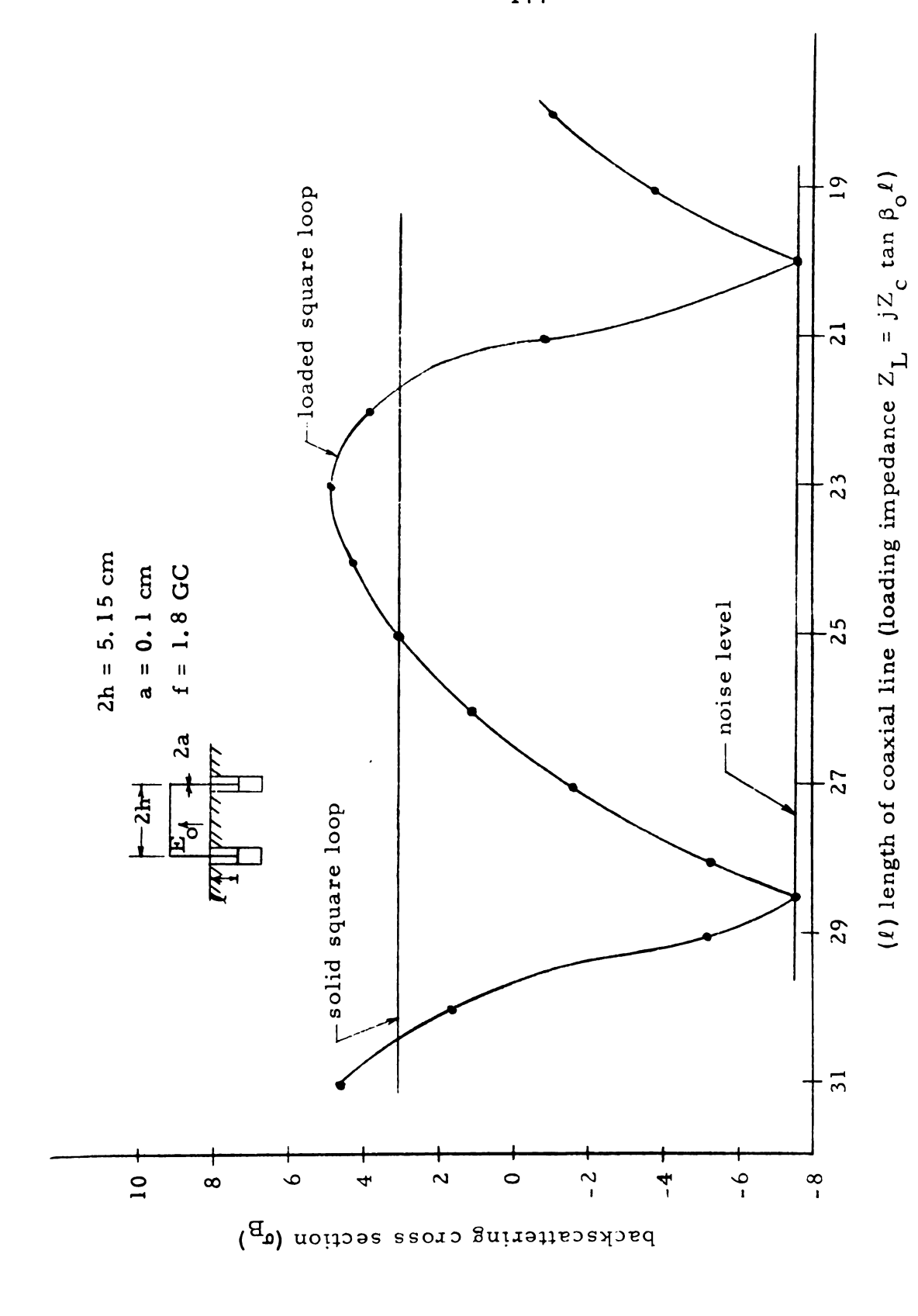
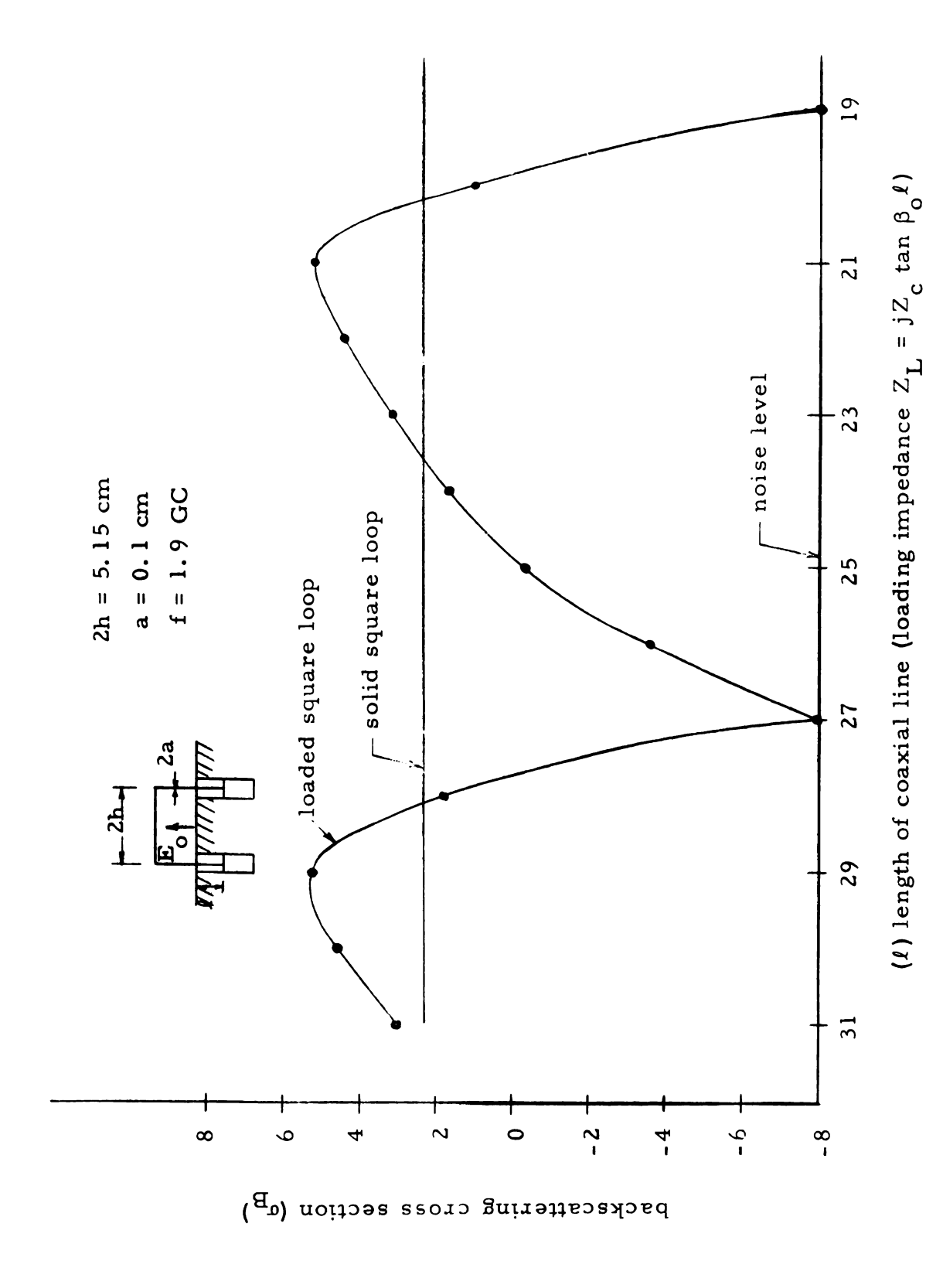


Figure 3.7. Backscattering cross section of a loaded sqare loop as a function of loading impedance (f = 1.7 GC.)(1) length of coaxial line (loading impedance  $Z_L = jZ_c \tan \beta_0 I$ )



Backscattering cross section of a loaded square loop as a function of loading impedance  $(f=1.8\ GC)$ . Figure 3.8.



Backscattering cross section of a loaded square loop as a function of loading impedance (f = 1.9 GC). Figure 3.9.

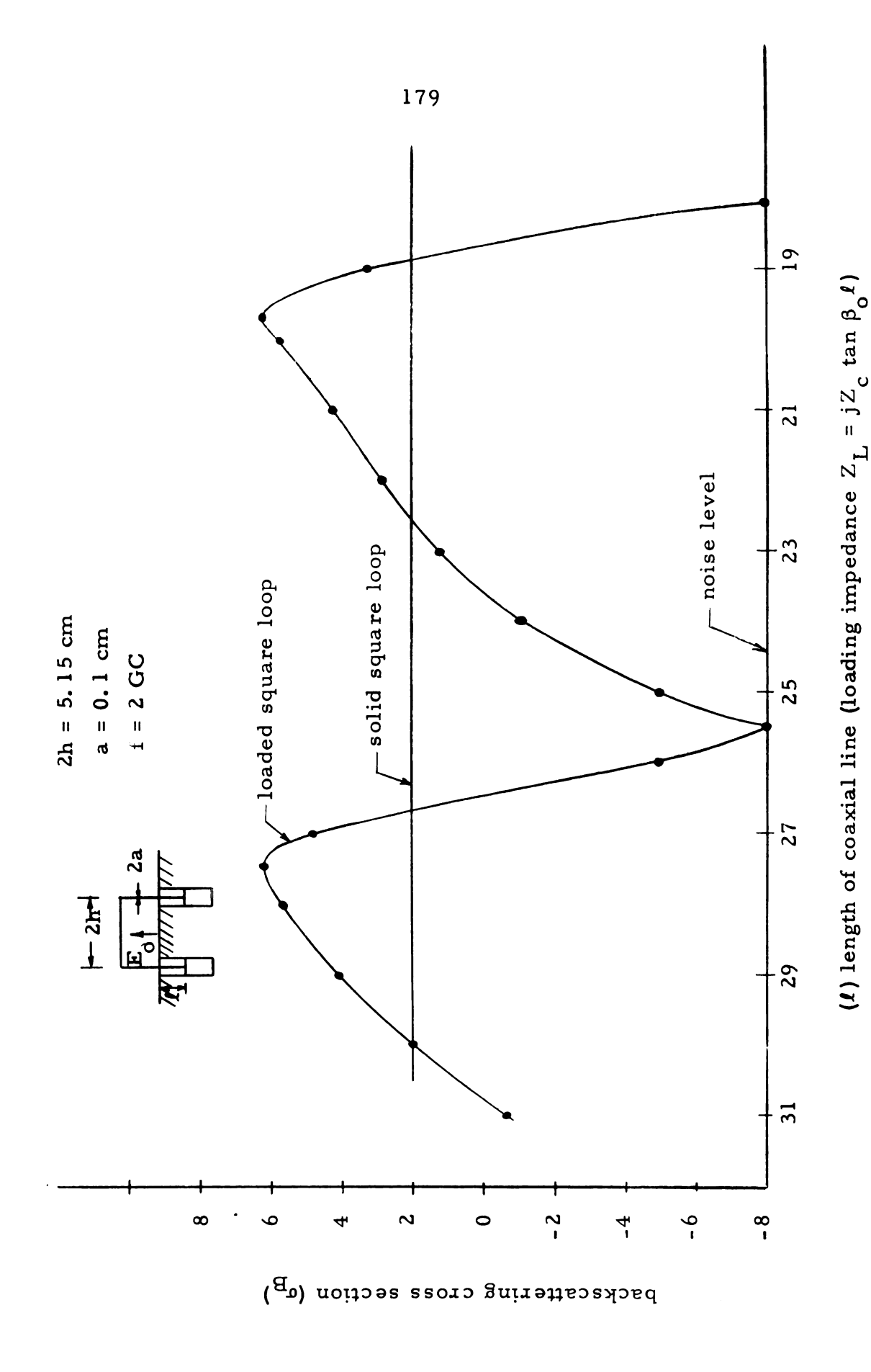


Figure 3.10. Backscattering cross section of a loaded square loop as a function of loadgin impedance (f = 2 GC).

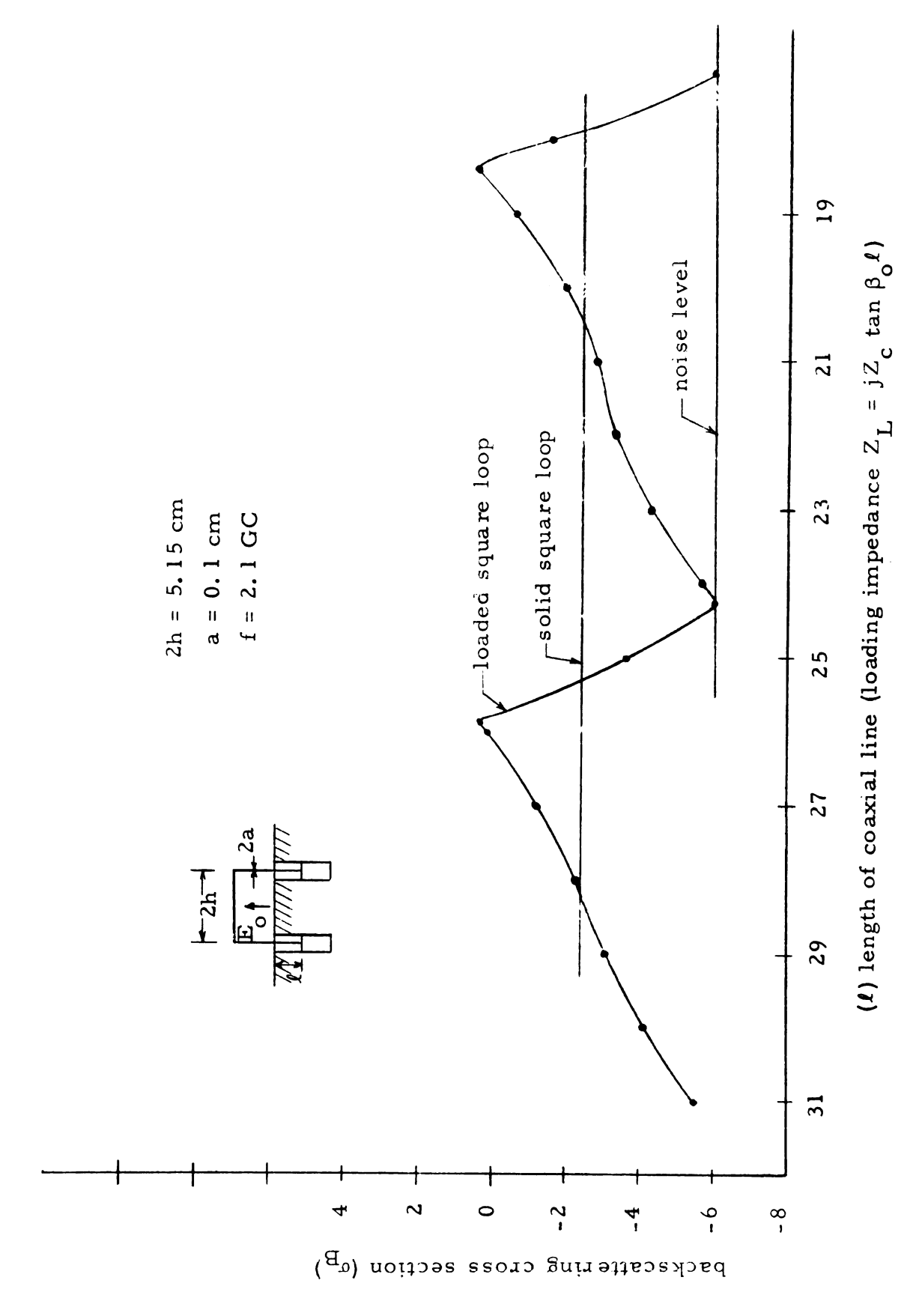


Figure 3.11. Backscattering cross section of a loaded square loop as a function of loading impedance (f = 2.1 GC).

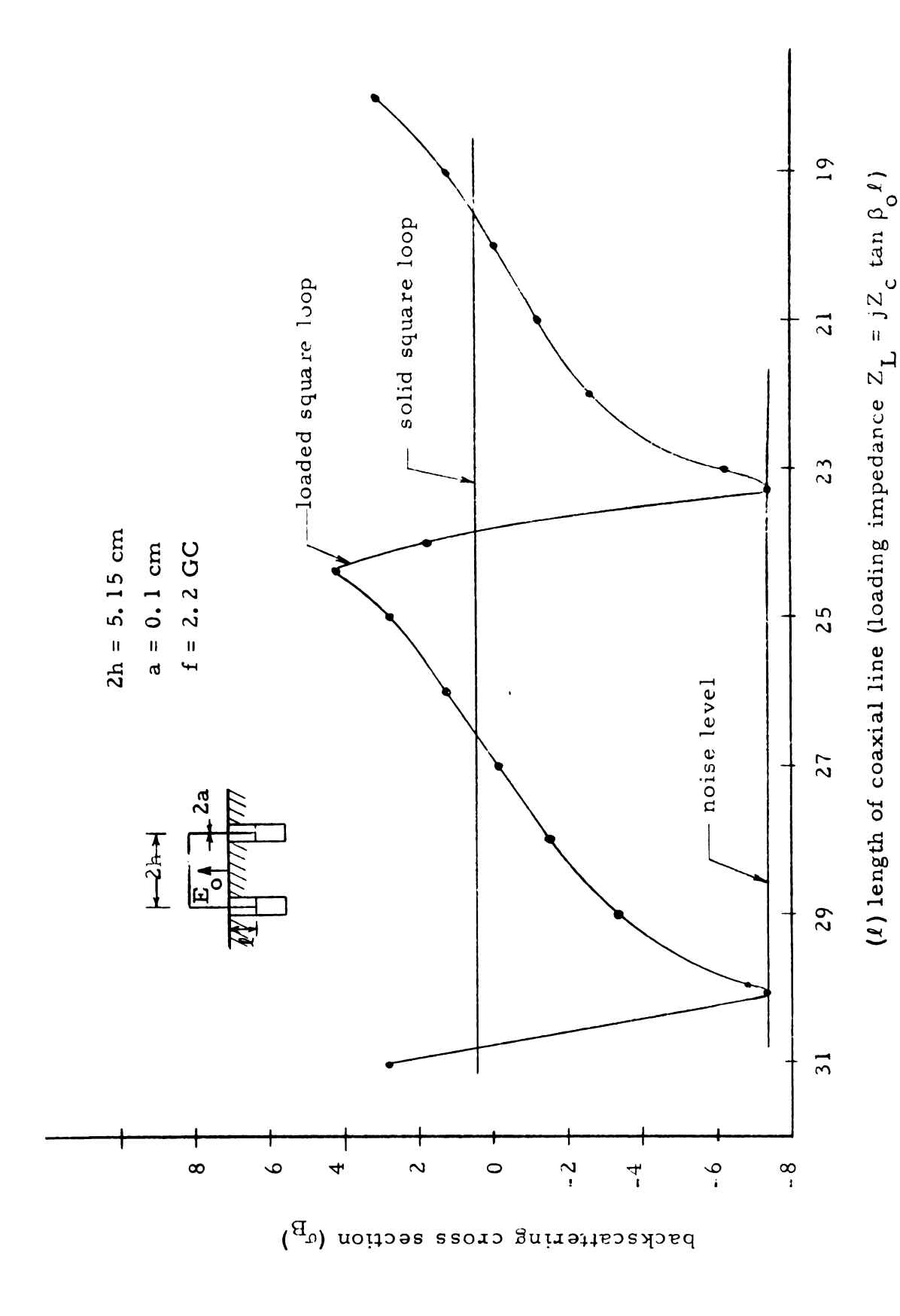
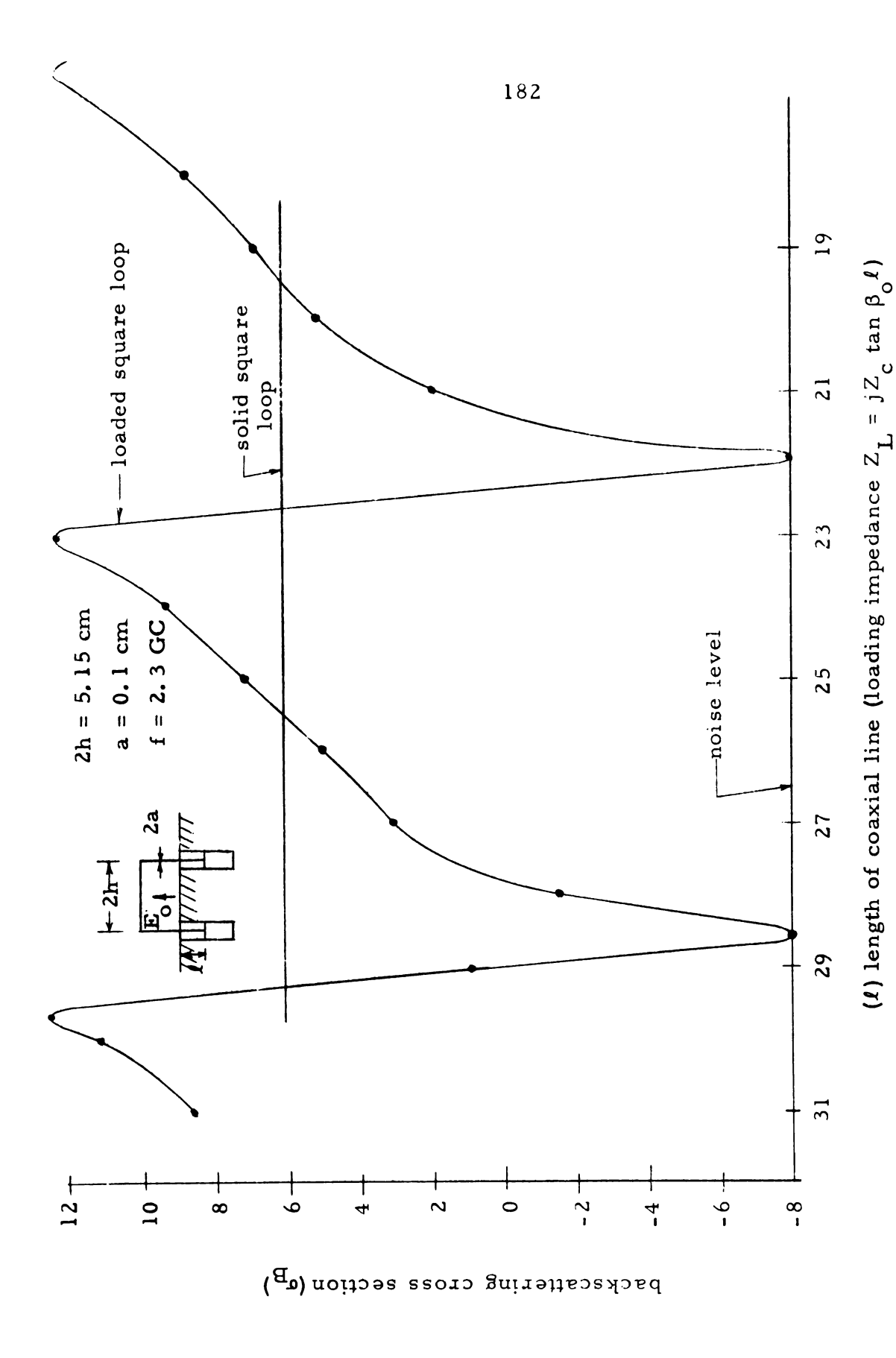
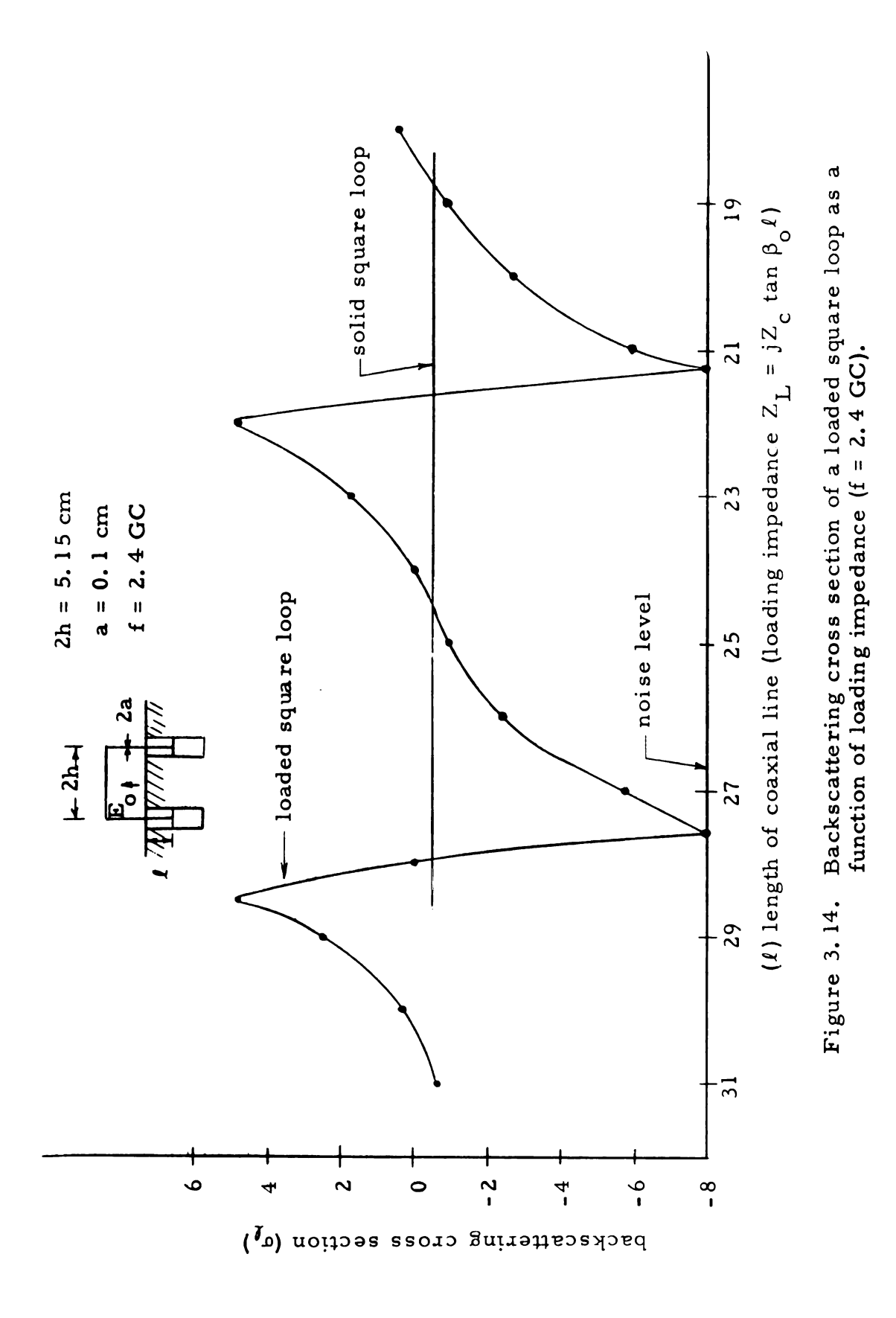


Figure 3.12. Backscattering cross section of a loaded square loop as a function of loading impedance (f = 2.2 GC).



Backscattering cross section of a loaded square loop as a function of loading impedance ( $f = 2.3 \, \text{GC}$ ). Figure 3.13.



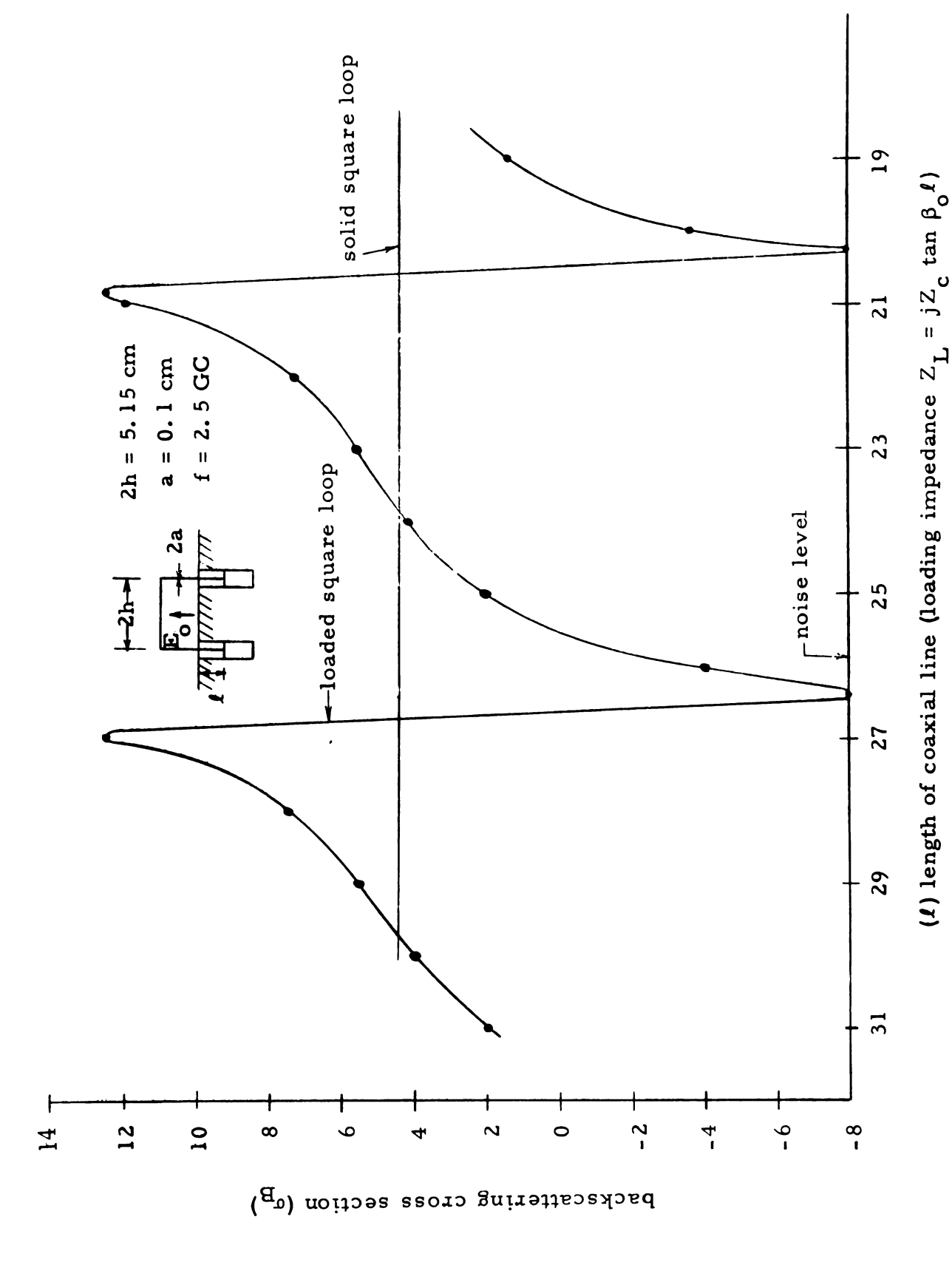


Figure 3.15. Backscattering cross section of a loaded square loop as a function of loading impedance (f = 2.5 GC).

		•
		· . · · · · :

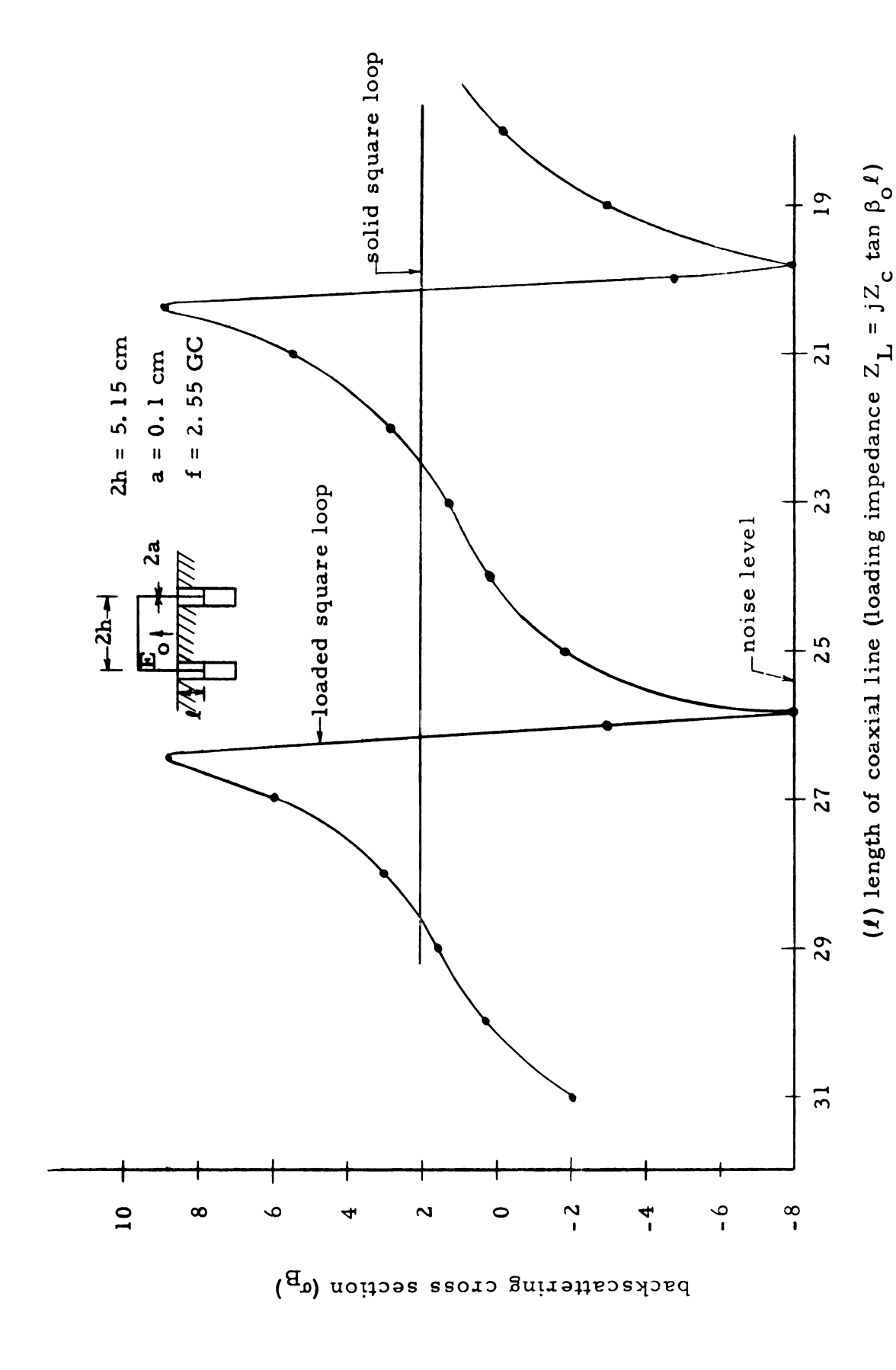
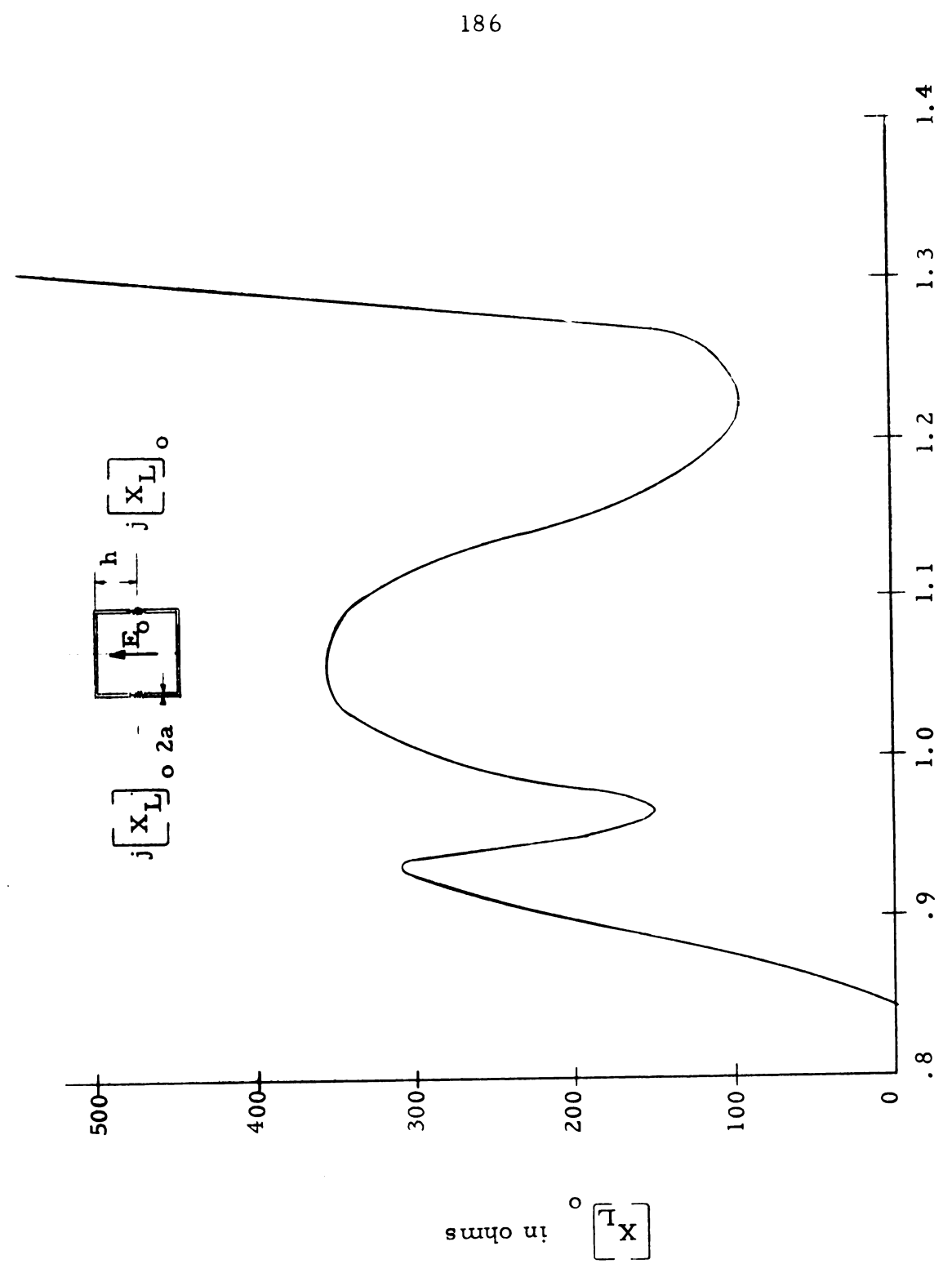


Figure 3.16. Backscattering cross section of a loaded square loop as a function of loading impedance ( $f = 2.55 \, \text{GC}$ ).



Optimum reactive impedance for minimum backscattering from a square loop. Figure 3.17.

 $\beta_{o}$ h

#### REFERENCES

- 1. Kouyoumjian, R. G., "Back-Scattering from a Circular Loop," Ohio State University Engineering Experiment Station, Bulletin No. 162 (November 1956).
- 2. Weston, V. H., "Scattering from a Circular Loop," University of Toronto (1957).
- 3. Chen, K. M., and King, R. W. P., "A Loop Antenna Coupled Electromagnetically tota Four-Wire Transmission Line," Scientific Report 5, Cruft Lab., Harvard University, Cambridge, Mass. (January 1960).
- 4. Chen, K. M., and Liepa, V., "Minimization of the back scattering of a cylinder by a central loading," IEEE Trans.

  Antennas Propagation AP-12, 576 (1964).
- 5. Chen, K. M., "Minimization of backscattering of a cylinder by double loading," IEEE Trans. Antennas Propagation

  AP-13, 262 (1965).
- 6. Chen, K. M., "Reactive loading of arbitrarily illumined cylinders to minimize microwave backscatter," J. Res. Nat'l. Bur. Std. 690, 1481 (1965).
- 7. Hu, Y. Y., "Backscattering cross section of a center-loaded cylinder antenna," IRE Trans. Antennas Propagation AP-6, 140 (1958).
- 8. As, B. O., and Schmitt, H. J., "Backscattering cross section of reactively loaded cylindrical antennas," Scientific Report 18, Cruft Lab., Harvard University, Cambridge, Mass. (August 1958).
- 9. Liepa, V., and Senior, T. B. A., "Modification of the scattering behavior of a sphere by reactive loading," Proc. IEEE 53, 1004 (1965).
- 10. Storer, J. E., "Impedance of thin-wire loop antennas," Trans.

  AIEE (Communication and Electronics) 75, 606 (1956).

MICHIGAN STATE UNIVERSITY LIBR